Mikołaj Kocikowski

Of Dogs and Men. Tracing Immune Checkpoint Signatures Across Cancers and Unleashing the Potential of Canine PD-1 Antibodies

PhD Thesis

Of Dogs and Men. Tracing Immune Checkpoint Signatures Across Cancers and Unleashing the Potential of Canine PD-1 Antibodies
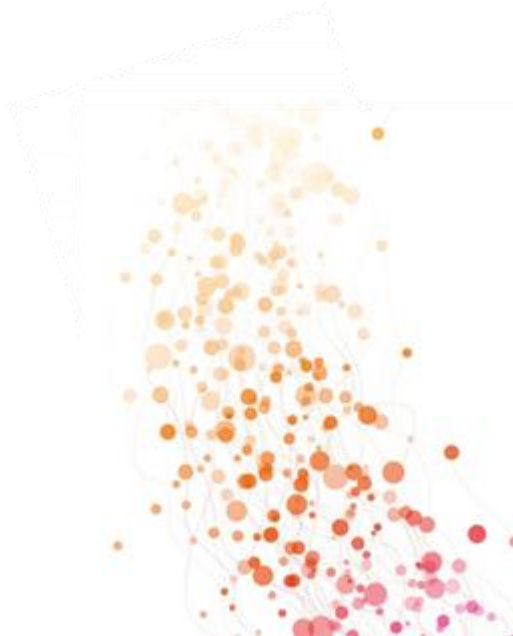
By **Mikołaj Kocikowski**

PhD Thesis

Supervisors

Prof. Theodore Hupp

Dr. Javier Alfaro

Dr. Maciej Parys

International Centre for Cancer Vaccine Science (ICCVS)

Intercollegiate Faculty of Biotechnology (IFB) UG & MUG

Presented to the Scientific Council of Biotechnology in Partial Fulfillment of the Requirements for the Degree of Doctor of Philosophy.

University of Gdansk, October 2023

ORCID ID: 0000-0001-7396-9005

This project was conducted within a joint programme

between the University of Gdansk and The University of Edinburgh

Funding and Support

Preface

I hereby declare that I am the author of this thesis. The work described is my own, with specific contributions from others detailed in the 'methods' sections of each experimental chapter. Throughout the thesis, the first-person plural ('we') is used to reflect the collaborative nature of scientific research, with a switch to the first-person singular ('I') in latter sections where personal reflection and commentary are presented. No part of this thesis has been previously submitted for any other degree or professional qualification.

Mikołaj Kocikowski

09 Oct 2023

Lay Summary

In a time thousands of years before the dawn of civilization, a curious wolf hesitated at the edge of flickering shadows, entranced by the tongues of fire dancing in the night. As the flames surged and waned, so did the allure of discarded scraps near an evening bonfire. Since that night we and our four-legged companions hunted, migrated, and adapted together, co-evolving at the genetic level. Today, dogs suffer from similar cancers as humans. Through studying them we can understand cancer more and devise better treatments for both species.

Both us and dogs have immune cells patrolling our bodies in search of threats like cancer. To avoid friendly fire, these 'warrior' cells have 'brake pedals' - proteins that can put them to 'sleep'. Unfortunately, cancer cells can 'push the brakes', effectively disabling our defense. Drugs can block some 'brakes,' but multiple 'brake', 'pusher' and also 'gas' proteins can be involved, complicating the treatment landscape. My work aims to untangle this complexity.

Here, I analyze 44 such proteins across 41 human and dog cancer types, identifying clinically important patterns. Remarkably, certain brain cancer and sarcoma types in dogs closely mirror their human counterparts. These cancers can be excellent research models for advancing human and veterinary medicine together.

Moreover, I find that some types of cancer display consistent 'braking' patterns among patients, suggesting a universal treatment might work. Others show individual patterns, pointing to the need for personalized therapies. This information may also help us understand why some cancers develop resistance to treatment.

For dogs, however, no drugs exist to tackle the immune "braking" problem. This limits our ability to treat dog patients and advance research. Thus, I develop antibodies that block PD-1, a key 'brake pedal' in dogs. Next, I computationally modify the antibodies to make them dog-safe, paving the way for future clinical trials.

The key to the next breakthrough in human health may well be awaiting at the crossroads between medicine and other scientific disciplines. Sometimes it's in helping others that we find solutions for ourselves. Every step we take in understanding and treating dog cancers not only honors our millennia-old alliance but brings us closer to helping humans. In Dog we Trust.

Abstract (English)

Dogs, sharing genetic similarities and lifestyle factors with us, develop cancers mimicking human ones, yet lack access to the most advanced treatments. Here, I present a canine 'research toolbox,' featuring antibodies, data, and methods to bolster studies into spontaneous canine cancers as a comparative oncology model.

Human immunotherapy employs monoclonal antibodies (mAbs) to block immune checkpoints (ICs) – immuno-modulatory proteins and downstream pathways that are hijacked by cancer cells as a means of immune evasion. Despite the increasing interest in the development of similar drugs for dogs, little was known about the abundance of ICs – the very targets – in canine malignancies. My study bridges that gap by profiling 44 IC genes across 14 canine cancers. Utilizing correlation-driven distance and hierarchical clustering, I identify gliomas and certain sarcomas as prospective research models characterized by strikingly similar IC landscapes across both species. Additionally, I pinpoint IC genes driving inter-species differences.

Human ICs and their impacts are studied deeply - typically in isolation. Here I introduce a broader perspective through characterizing comprehensive IC abundance patterns of particular diagnostic labels and individual human patients alike. In this study I reveal those patterns reflect cancer's histological type, primary site, and inter-patient variation. In certain cancer types the patterns are highly diverse across individuals, pointing to the need for personalized treatment selection and offering clues into the mechanisms underpinning therapy resistance.

To further enable IC-focused studies in dogs, I also characterize two novel mAbs against canine PD-1 receptor – a prominent IC; both exhibit sub-nanomolar affinity, effectively block the key PD-1/PD-L1 interaction and prove useful in a palette of key molecular assays. These antibodies represent valuable research and diagnostic tools as much as potential veterinary therapeutics.

To address the risk of severe immune reactions to murine-derived antibodies if used in dog patients, I develop a specialized set of 'caninization' methods and canine mAb sequence libraries, resulting in de-immunized, dog-like PD-1 antibody constructs. These advancements can pave the way for canine clinical trials and streamline veterinary antibody development.

Streszczenie (Polish)

Psy, dzieląc z nami genetyczne podobieństwa i warunki życiowe, rozwijają nowotwory przypominające ludzkie w kluczowych aspektach klinicznych. Onkologia porównawcza – równoległe badania nad leczeniem nowotworów u ludzi i innych zwierząt – może usprawnić leczenie obu gatunków. Niestety, najnowsze leki – przeciwciała monoklonalne przeciwko punktom kontrolnym układu immunologicznego (ang. immune checkpoint - IC) – nie są dostępne w weterynarii. W tej pracy prezentuję 'zestaw narzędzi' dla badań immunologii psów.

Mimo rosnącego zainteresowania immunoterapią psów, brakuje danych o obecności u nich celów molekularnych - białek IC. Moje badania wypełniają tę lukę, profilując ekspresję 44 genów IC w 14 typach psich nowotworów. W wyniku międzygatunkowej analizy porównawczej odkryłem uderzające podobieństwo między glejakami i niektórymi mięsakami obu gatunków. Predestynuje ono ww. nowotwory do roli modeli badawczych.

W medycynie punkty kontrolne są badane intensywnie, jednak zazwyczaj jednostkowo. W tej pracy proponuję szersze spojrzenie na krajobraz mechanizmów IC poprzez charakteryzację wzorców ekspresji obejmujących 44 geny naraz, przy użyciu macierzy odległości opartych na korelacji oraz klastrowania hierarchicznego. Tymi metodami wykryłem, iż wzorce ekspresji IC są charakterystyczne dla poszczególnych typów histologicznych i lokalizacji nowotworów. Co kluczowe, w niektórych typach nowotworów, wzorce te mogą różnić się znacznie pomiędzy pacjentami z ta samą diagnozą. Wskazuje to na potrzebę spersonalizowanego doboru terapii i potencjalny kierunek badań nad przyczynami rozwoju lekooporności.

W kolejnym badaniu scharakteryzowałem dwa nowe przeciwciała przeciwko psiemu receptorowi PD-1 – białku kluczowemu w immunoterapii u ludzi. Oba wykazały sub-nanomolowe powinowactwo i efektywnie blokowały receptor PD-1. Ponadto, zostały zwalidowane w kluczowych zastosowaniach laboratoryjnych.

Wreszcie, by zminimalizować ryzyko ciężkich reakcji immunologicznych na przeciwciała mysie w potencjalnych badaniach klinicznych u psów, rozwinąłem metody, które pozwoliły na de-immunizację opisanych przeciwciał. Opracowany zestaw cząsteczek obejmuje wszechstronne narzędzia badawcze, diagnostyczne, jak i konstrukty przeciwciał o potencjale leczniczym.

Acknowledgements

Ewa, Magda, Tsabieh. Your resilience and life philosophies have been inspirational. Each of you deserves a sword. Here's to my current team - the main reason I keep going many a time: Javier, Alexander, Ashwin, Emilia, Michał, Georges, Marysia – thank you for everything!

But... It all starts much earlier. I would not be here if not for my ancestors who had to leave behind the houses they built, to fight for our freedom. As they had to surrender their aspirations to rebuild our country, they passed their hopes, talents and fascinations on to me. I thank my parents, who gifted me curiosity, critical thinking and love of nature, and Marysia and Kuba - for the love and coaching.

On the long way to here, I have been blessed with great teachers who selflessly fed my passion for knowledge and questioning; it makes me enormously happy that I have this avenue to thank Ms Anna Helmin, Mr Paweł Lęcki, and Ms Anita Wrzeszcz, who ensured I understood more than biology, and helped me follow my path in their own unique ways. Additional thanks to my chemistry teachers, whose unique teaching styles reinforced my decision not to venture into this dark territory.

Heartful thanks to Lila Serafin, the gifted artist who has enchanted the various threads of this thesis, hopes of this project and my personal longings into one artful cover.

I am truly grateful to my friends, who have injected adventure, inspiration, and joy into these last few years, provided a listening ear, space to decompress, and helped me persevere through the Covid-19 pandemic isolation far from home. I am sorry for all the times I have had to say no to your invitations - they were priceless to me nevertheless! Here's to you - Andrzej, Paulina, Kasia, Ania, Piotr and all of the "Kocioł"; Sabina, Jacek, Dagmara, Piotr, Patryk, Marta, Ela from my home city; Magda and Jarek for „adopting" me after I came back to Poland; good souls from other realms: Dorota, Sasha, Wiesław and the warrior gang. Endless gratitude to Ms Ewa whose support on many paths of this realm has been too invaluable to me to be adequately conveyed with human words.

To (Dr) Marta – your unparalleled understanding, wisdom, and belief in me at the last miles of this marathon were indispensable. Thank you for teaching me to celebrate and for bringing the applewood smoked cheddar crumpets into my life. You've arrived like a beautiful, nocturnal butterfly on a concrete floor, or like happiness which only comes when one stays still.

Writing this feels like processing one lifetime that has come to an end. A lifetime of discovery and getting lost, inspiration and sacrifice, adventure and loss, blood and wine. It is most precious that you all walked this path with me and that many of you are still here now, when a new chapter begins. Thank you, Gracias, Obrigado, Dziękuję.

Finally, thank you, Dear Reader, for taking the time to dive into this thesis. If you happen to be a fellow student tracing some of my experimental footsteps, please know you are very welcome to contact me with any questions. Also, take a look at Appendix 8.1.

PS huge thanks to everyone who warned me about doing a PhD!

Dla Moich Babć, Wandy i Zdzisławy

For My Grandmothers

Index of Contents

1. INTRODUCTION

1.1 Cancer

Cancer is a major issue by any measure, indiscriminately affecting individuals and families across all continents. Discussions on cancer often commence with a statistical analysis of patient numbers and the associated burden of healthcare costs. While these are undeniably important aspects of its societal impact, cancer is not primarily an economic problem; it's a profoundly human one that brings about a tremendous amount of suffering, robbing many of their full potential. It's a battle fought in labs and clinics, but most of all in the daily lives of patients and their loved ones, whose resilience and participation often catalyzes advancements in the field.

1.2 One name, many diseases

'Cancer' is an umbrella term covering numerous distinct sub-diseases, all unified by the uncontrolled proliferation of cells, local invasive growth, and often, the ability to spread (metastasize) within the body. Typically, cancers are classified based on the cell type from which they originate and the organ they affect. Yet, even within a so defined cancer type, various subtypes can be distinguished using molecular methods. Furthermore, no two cancers within a subtype are identical. A single tumor itself can comprise a myriad of heterogeneous cancer cells. This heterogeneity is one of the key factors in why finding effective treatments is challenging and achieving complete eradication even more so [1,2].

1.3 Intrinsic evolution of cancer

The profoundly dysregulated cancer cells override most of the intrinsic safety mechanisms encoded in the DNA of every cell. The resulting rapid cell division and accelerated mutation, together with the increasing heterogeneity of the cell population, catalyze a peculiar, selection-based process, akin to Darwinian evolution [3]. Consequently, cancer cells chance upon new metabolic adaptations and methods to evade immune recognition. Thanks to the survival advantage, such cells give rise to new populations. Through similar means, those populations attain the ability to influence their immediate cellular environment, co-opt nearby cells for support, and even remotely manipulate distant tissues [4,5]. These fascinating yet ominous features are collectively known as Cancer Hallmarks [6–8]. Perhaps the most critical is the

ability of some solid tumor cells to metastasize, traveling through blood or lymphatic routes to establish new, genetically distinct colonies in other body sites [9].

1.4 The genesis of cancer

Cancer's initiation is an ongoing subject of study. What appears clear is that the process involves disruptions in multiple tumor suppressor genes - key guardians preventing uncontrolled proliferation. These disruptions can occur through mutations, deletions, or 'epigenetic silencing', a process where a gene's function is suppressed without altering its DNA sequence [10–12]. Similarly, these mechanisms can lead to the abnormal activation of oncogenes - genes that promote uncontrolled cell growth when not properly regulated. Therefore, cancer is often referred to as a disease of the genome - despite its downstream impact on all facets of the cell phenotype. The exact mechanisms and timings required for the genomic alterations to precipitate cancer, however, remain elusive [13,14].

Investigating the earliest stages of cancer is nearly impossible. At this point, cancer is virtually undetectable within the body. In vitro experiments using immortalized cell lines, while extremely useful for specialized purposes, emerge as poorly replicable and struggle to authentically reproduce the conditions within a living organism [15–18]. A key consideration is the cancer's interaction with the immune cells, naturally equipped to identify and destroy malignant cells. The reasons why the immune system sometimes falls short in this task remain unclear. As cancer evolves, the immune cells keep interacting with the mutating cells, creating a form of selection pressure. This process, known as 'immunoediting', leads to the emergence of cancer cells that can effectively camouflage their aberrant nature, disable immune cells in the tumor microenvironment, or suppress the immune response when identified [19].

More broadly, cancer is a challenge bequeathed to us by evolution, which optimized our genetic makeup for early reproductive success over long, healthy lives [20–22]. Environmental pollution, demanding lifestyles, dietary shifts, and the overall impact of rapid societal and technological change further exacerbate the prevalence of many cancer types (*diet* [23–25]*, refined sugar* [26,27]*, obesity* [28]*, alcohol consumption* [29]*, stress* [30]*, loneliness* [31]*, sedentary lifestyle* [32,33]*, smoking* [34]*, circadian*

rhythm disruption [35]*, phone-related radiation* [36–38]*, plastic pollution* [39–41]*).* While preventive measures hold immense value, it's clear that lifestyle choices alone can't fully shield a person from the risk of cancer. Genetic predispositions and other factors beyond one's control remain a significant causative factor [42].

1.5 Cancer treatment

Depending on the type and location of the malignancy, as well as other factors determining feasibility, cancer is commonly treated using modalities such as surgery, radiotherapy, and chemotherapy. Surgery seeks to excise the malignantly transformed tissue, often including a small margin of surrounding healthy tissue to ensure complete removal. Radiotherapy leverages different forms of ionizing radiation to damage cell DNA. Cancer cells, due to their aberrant growth, struggle to mend this damage, leading to halted growth and ultimately cell destruction. Chemotherapy involves various classes of drugs targeting the cancer's biochemistry, and this approach can be broadly categorized into two primary strategies.

One method is to target cell traits generally shared by cancers of many patients - such as rapid proliferation. However, such treatment adversely affects some healthy cell subtypes that divide fast. Additionally, some cancer cells, regarded as 'cancer stem cells', can enter a dormant state, where they halt their divisions for periods of time. Thus, some of them remain unaffected, exhibiting a functionality not unlike bacterial spores [7]. The above method is central to the action of many traditional chemotherapies. Despite the limitations, these chemotherapies form the cornerstone of oncological treatment and remain a crucial tool in the fight against many types of cancer.

An alternative strategy is to target the unique vulnerabilities of each cancer instance. Although complex, demanding, and challenging to evaluate in clinical trials, this approach offers a more precise strike against the cancer's weak points. Such a personalized strategy, rooted in advanced diagnostics, encompasses treatments like small molecule inhibitors that interrupt specific molecular pathways involved in cancer progression, and to an extent, also the immunotherapies discussed later in this thesis.

1.6 Progress and challenges in cancer research

The tireless dedication and creativity of scientific teams worldwide has transformed some of the cancer types into manageable, chronic conditions. However, with the most apparent cancer targets already addressed, the development of each novel therapeutic incurs escalating costs. This, in combination with other factors common to many scientific disciplines, risks decelerating the research progress [43]. Fortunately, recent years brought about the development of immunotherapeutics, often heralded as breakthroughs. As a single thread within the complex tapestry of cancer immunology, this study explores the intricacies of these novel treatments, with the ultimate aim of contributing to innovative therapeutic strategies.

1.7 Immune checkpoints (ICs)

Immune checkpoints (ICs) are signaling pathways that play a key role in regulating immune responses by modulating the activity of immune cells. They can be categorized as inhibitory, stimulatory, or complex based on their effect on the immune cells. ICs rely on IC receptors present on the surface of the immune cells, in particular the cytotoxic lymphocytes. In this context, auxiliary immune cells can produce protein ligands that bind inhibitory or stimulatory receptors, which adjusts cytotoxicity levels. Healthy stromal cells can also express inhibitory ligands, a mechanism instrumental for maintaining self-tolerance.

1.8 Immune checkpoint blockade (ICB)

Cancer cells mimic this immune-inhibitory mechanism to avoid detection and destruction by the host's cytotoxic cells. They can express inhibitory IC ligands on their surface and 'recruit' otherwise healthy cells from their environment to provide further assistance [44]. Immune checkpoint blockers (ICB; also known as inhibitors - ICI) are drugs that aim to inhibit the interaction between the IC receptors of the immune cells and the IC ligands of the cancerous or cancer-recruited cells. Antibody-based ICB therapeutics induce remarkable remissions in some cancer cases [45,46].

1.9 Antibodies as tools and drugs

Antibodies (immunoglobulins) are specialized glycoproteins produced by the immune system to identify and neutralize foreign objects, in particular pathogens. Structurally, they consist of protein chains and attached carbohydrate molecules (glyco-), which can influence an antibody's stability, impact its half-life in circulation, and assist in its proper folding. Furthermore, they can modulate the antibody's function and offer protection from enzymatic degradation. Beyond their natural physiological roles, antibodies have been instrumental in biomedical research. Their unique ability to bind specifically to virtually any target makes them invaluable as detection tools in a range of biochemical assays. Therapeutically, monoclonal antibodies (mAbs), which are antibodies derived from a single cell lineage, have revolutionized treatment in areas like oncology, autoimmunity, and infectious diseases. Yet, it's crucial to remember that while antibodies offer specificity, their therapeutic use can be limited by factors such as delivery, immunogenicity, and potential off-target effects, necessitating meticulous design and optimization. For a comprehensive discussion on the structure, classes, and features of antibodies, please refer to the introduction section of Chapter 4.

1.10 Antibody epitopes and paratopes

An epitope is a specific region of an antigen that is targeted by a particular antibody. Epitopes are categorized into two main types: linear epitopes, which involve continuous sequences of amino acids, and conformational epitopes, in which protein folding brings key amino acid residues into proximity [47]. Conformational epitopes are advantageous for applications where the protein target is in its native state, such as therapeutic use or flow cytometry. On the other hand, antibodies targeting linear epitopes are better suited for assays that require protein denaturation, such as in Western blot or immunohistochemistry (IHC). Complementing the epitopes are the paratopes, which are the specific regions on the antibody's structure responsible for binding to an epitope. The "lock and key" fit between an epitope and a paratope is crucial for the specificity of an antibody-antigen interaction.

1.11 Generation of monoclonal antibodies

Monoclonal antibodies can be generated through two primary methods: Hybridoma technology and Phage Display. Hybridoma technology involves immunizing an animal and then fusing its spleen-derived B cells with cultured myeloma cells. This well-established, robust method produces antibodies with natural post-translational modifications, reducing the risk of protein aggregation. However, the process can be time-consuming, often requiring several months and the use of animals. Typically, the animals are immunized with a complete target protein domain, limiting control over specific epitope targeting. However, precise epitope targeting can be achieved in certain cases by using peptides for immunization. Outside the scope of this thesis, but within my doctoral studies, I contributed to work on a canine mAb that recognizes both human and canine CD20. The antibody was generated using a peptide from a cross-species conserved section of the CD20 sequence [48,49]. Antibodies generated through murine hybridoma typically require further modification, such as humanization, for therapeutic applications. The present work will describe antibodies obtained using murine hybridoma technology utilizing whole-protein immunization.

Phage Display technology employs bacteriophages to hold extensive libraries of antibody fragment sequences. These phages link the surface presentation of an encoded protein with its corresponding genetic information, allowing efficient screening for high-affinity binders. This approach allows for working with toxic or non-immunogenic antigens. While conceptually straightforward, Phage Display is labor-intensive and often yields antibodies with moderate affinities and propensity for aggregation. It can also result in suboptimal heavy and light chain pairing. The products are frequently antibody fragments requiring further engineering steps to achieve full functionality. Adalimumab was the first approved therapeutic antibody generated through phage display. Despite its fully human sequence it induces marked immune responses in patients [50,51]. Following its approval, several other therapeutics were developed through phage display [52].

Within my doctoral studies, extensive efforts were made to generate a canine PD-1 antibody using this method. Although unsuccessful, these endeavors provided critical learning experiences. The idea of using a canine scFv phage display library for

generating antibodies against canine targets offers the hypothetical advantage of producing fully canine antibodies that bypass the need for deimmunization. However, antibodies against self-proteins are rare in healthy individuals due to immune tolerance mechanisms, making it unlikely to find a high-affinity, specific antibody in a library originating from the same species as the target protein.

There are mammalian display technologies emerging which offer a compelling synthesis of features from both aforementioned methods. They allow for the high-throughput screening of diverse antibody libraries, albeit usually not as vast as in phage display. By using mammalian cells for expression, they capture the physiological relevance of post-translational modifications, akin to hybridoma. Additionally, mammalian display enables screening and isolation of the best binders through flow cytometry techniques. Resulting antibodies have good affinity for real biological targets and do not require modifications for further use.

1.12 Programmed cell death protein 1 (PD-1)

In the ICB treatment of cancers, therapeutic antibodies most commonly prevent interaction between Programmed cell death protein 1 (PD-1) inhibitory receptor of the immune cells and the better studied one of its two known ligands, Programmed cell death ligand 1 (PD-L1) [53,54]. PD-L1 expression by multiple human cancer types is well-documented and sufficient to induce an immunosuppressive tumor microenvironment [55]. The ICB monoclonal antibodies (mAbs) Nivolumab and Pembrolizumab significantly increase survival of cancer patients in multiple cancer types. Treatment response is especially marked in cases with high tumor PD-L1 expression [56].

1.13 The dark side of immunotherapy

Despite major improvement in the management of some cancer types, the efficacy of ICB therapeutics is limited to a subset of patients, many must be excluded from treatment, and adverse effects affect over 60% of the treated individuals [57–59]. These effects range from mild and transient to severe autoimmune reactions manifesting long after the treatment ends [58,60].

1.14 Hyperprogressive disease (HPD)

Owing to its different mechanism of action compared to conventional chemotherapy, ICB immunotherapy frequently induces atypical response patterns. These patterns encompass the desired long-term remissions, the misleading pseudoprogression, and a detrimental adverse effect known as disease hyperprogression. As we wrote in a prior publication dedicated to this phenomenon [61], "The concept of hyperprogression (HP) or Hyperprogressive Disease (HPD) was introduced by Champiat et al. in 2016, based on the observation that a subset of patients receiving ICB experiences extremely rapid disease progression that leads to fast patient deterioration" [62]. Estimating the frequency of HPD is fraught with challenges. Data on pre-therapy tumor growth kinetics are infrequently collected and available, standardized definitions and protocols are lacking, and in some studies, patients who deteriorated most rapidly could not be thoroughly evaluated. The incidence of HPD, depending on the methodology and specific cancer type, is estimated to range from 5% to 37% of cases [61]. However, HPD only came to light three years after the first two ICB treatments, pembrolizumab and nivolumab, were approved [62–64]. Potential causes of HPD and factors associated with successful treatment are being investigated [61,65–68], but the mechanisms underlying different responses remain undefined.

1.15 Cancer models

The extent of the failure to anticipate and mitigate severe adverse effects in the drug development process necessitates a more robust approach to immunotherapy development. This is particularly urgent amid the current surge in immunotherapy development. Experimental ICB compounds frequently target underexplored ICs and their combinations, making the outcomes even less predictable. For this reason there is a dire need for preclinical models more adequate than those currently employed [69,70].

1.16 Drawbacks of the murine model

We, as well as others, have described the shortcomings of laboratory mice for immunological studies [61,71]. ICB immunotherapy, unlike conventional chemotherapy, modulates a complex signaling network to reactivate the patient's

immune cells, so they can recognize and combat immune-edited cancer [72]. The curative and toxic outcomes of this intricate process cannot be thoroughly evaluated in rodent models such as xenografts injected into immunocompromised animals or artificially induced syngeneic tumors. While a fully developed immune system is necessary to recapitulate human treatment response, laboratory mice live in artificial habitats, lacking natural antigenic stimulation. The composition of the microbiome is known to influence immunotherapy outcomes [73], yet laboratory mice do not possess a natural one. Their artificially induced tumors mimic neither the real cancer heterogeneity nor the complex mutational history or the mutual cancer-host immunoediting, all characteristics of human cancer. Furthermore, syngeneic strains lack the genetic diversity characterizing human population [74]. Some authors go as far as to state that mice are 'poor models for the majority of human diseases' in general [75]. They further argue that reliance on predominantly murine animal models leads to at least 90% failure rate in translating research from animal studies to clinical trials. This failure rate may be significantly underestimated, as these observations focused on a limited selection of highly cited research [75,76]. While some researchers see increasingly engineered rodent models as a solution [69], others, including us, propose a comparative oncology approach to drug development that involves naturally occurring dog cancers in cancer research [77,78].

1.17 Canine cancer model

By contrast to the murine cancer model, canine cancers, spontaneous, heterogeneous, developing along with a fully functional immune system, often mirror their human counterparts on a histological, clinical and genetic level [79]. Consequently, they rise as prospective research models, uniquely suited for immunotherapy evaluation [61,77,78,80,81]. Canine cancers are not rare either, with approximately 25% of all dogs dying of cancer [82]. Dogs resemble humans in terms of their body size, and their tumors present similar immune infiltration features [83]. In certain types of cancer, such as osteosarcoma, the canine patient pool outnumbers the human patient population by a ratio of 10 to 1. This significant difference presents an opportunity for otherwise improbable, statistically robust studies of such malignancies [83–85]. Unlike laboratory animals, dogs live in similar environments to humans, share many aspects of our lifestyles, and consequently, develop

spontaneous tumors that have striking parallels to human malignancies. Moreover, dogs have shorter life spans compared to humans, which means their disease progression occurs at a faster rate. This enables the study of real cancer evolution, response to treatments, and long-term outcomes within a shorter timeframe.

1.18 Comparative oncology

Comparative oncology is a research approach that draws on naturally occurring cancers in animals to understand and treat human cancer. As explained earlier, within this discipline, dogs hold unique potential. Furthermore, the close bond between humans and their canine companions emphasizes the ethical importance of offering them the best available treatments. In fact, dogs with cancer are treated in advanced medical settings, using the modalities known from oncology: surgery, radiotherapy and the same chemotherapeutic drugs. Yet, they lack access to contemporary treatments [86,87]. Canine clinical trials could facilitate thorough immunotherapy evaluation, leading to higher drug success rates and safer human therapeutics while offering a pragmatic, financially viable way to develop lacking veterinary treatments. The cost angle is important: introducing new immunotherapeutic drugs is an extremely costly process at every stage, from initial R&D and optimization, through clinical trials, to the production of molecules that adhere to rigorous regulatory standards. Returns from veterinary drug sales are unlikely to recoup these significant investments, possibly explaining why some promising canine treatments gain media traction or achieve patenting, yet never make it to the clinics. Crucially, in this pursuit, we regard dogs as patients deserving of care, not mere experimental subjects.

1.19 Canine genetics

Traditionally, phylogenetic analyses have classified humans (Primates) and mice (Rodentia) within the same clade, Euarchontoglires, while placing dogs (Carnivora) in a separate clade, Laurasiatheria. However, more recent molecular studies challenge this view, proposing that humans and dogs share a closer evolutionary relationship [88,89]. In the context of comparative immunology, it's crucial to note that the human antigen receptor locus is more akin to canine than to murine one [89].

There's a rich body of work examining dog (wolf) domestication, believed to have occurred between 20-400 thousand years ago [79,90–92]. The discrepancy is due to differing definitions: more recent estimates come from researchers who define dog domestication as the point at which dogs became a distinct species, easily distinguishable from wolves based on recovered genetic material. However, some of the aforementioned studies demonstrate that wolves were domesticated much earlier. First, some wolves integrated into human groups and began cohabiting with them - essentially, domestication - well before clear genetic divergence from wild wolves could occur. Second, these early domesticated wolves likely engaged in crossbreeding with wild wolves for an extended period, thus retaining a predominantly wolf-like genetic makeup [90]. Lastly, the scarcity of ancient genetic material complicates efforts to peer further back into history.

Research on dog domestication encompasses behavioral, morphological, archaeological, genetic, and paleogenomic studies [90,92]. Its outcomes led some scholars to question whether we domesticated wolves, or wolves made us human [91,93]. What is more certain, is that as humans and dogs lived, worked, migrated and adapted to new conditions together, they have co-evolved on the level of genetics. A major study in this field found an "extraordinary amount of parallel evolution", including co-evolving human-dog ortholog genes. Many of those genes were involved in diseases present in both species, in particular, neurological disorders and cancer [94]. Finally, dogs exhibit genetic uniformity within roughly 450 distinct breeds and variety across them. This characteristic is deemed invaluable for biomedical research involving genetics [95].

1.20 Why not cats?

While cats also belong to the Carnivora order and provide valuable contributions in fields such as virology, immunology, and cancer research, they don't quite rival the utility of dogs in biomedical studies. Cats entered the human sphere considerably later, likely drawn in by the appeal of addressing rodent issues in agrarian societies [96]. This specific benefit made them welcome guests rather than chosen partners. The extent to which cats are truly domesticated remains a matter of debate; they might simply tolerate human interaction for mutual convenience. Unlike dogs, which

originally have been bred for a variety of functional traits affecting a broad range of genes relevant to complex diseases, cats have mostly been bred for aesthetic qualities, thereby limiting the genetic diversity useful for disease research. While cats naturally hold the upper paw over mice in the natural world, it's the canine model that's stepping in to address the limitations of rodent models in cancer research.

1.21 Aims of this thesis

The previously discussed context highlights several research gaps:

1) The landscape of immune checkpoints (ICs) in canine cancers and its relation to human cancer: the potential of canine model for cancer immunotherapy research is clear, yet the expression of immune checkpoints – the targets – remains virtually unknown across canine cancers. Existing literature offers isolated insights into the few most common ICs in selected cancer types. Without comprehensive studies, no comparison of the C abundance patterns between cancers of both species had been possible. The knowledge of similarities between particular dog and human cancer types is necessary for developing canine immunotherapy within a comparative oncology framework. While many studies exist on ICs in human cancers, they predominantly focus on particular ICs in isolation. A canine-human comparison would require analyzing comprehensive IC expression patterns of human cancers as well.

2) Antibodies targeting canine PD-1: while two teams published on antibodies targeting the canine PD-1, none were available as research or therapeutic agents at the time of this research. It is prudent to build the foundations of canine immunotherapy starting with the most extensively researched and successfully targeted human IC. This necessitates developing new, versatile antibodies against canine PD-1.

3) Canine cancer ICB therapeutics: no IC-blocking antibodies were developed, approved and made available as canine therapeutics. Antibodies, typically generated in mice, must undergo de-immunizing modifications for a safe therapeutic application in another species. For dogs, such engineered antibodies would be "caninized". While the literature occasionally references "caninized" ICB antibodies, a closer examination reveals these are mostly chimeric proteins, merging significant portions of canine and

murine protein. Caninizing antibodies requires the creation of specialized methods and canine immunoglobulin datasets, both of which are currently missing.

This thesis endeavors to bridge the identified gaps.

1.22 The structure of this document

The aforementioned objectives are addressed in three self-contained experimental chapters that follow, each culminating in a synthesis of results, discussion and associated supplementary information. These core chapters are succeeded by an overarching summary ("Conclusions and Implications") and a "Perspectives" section offering a more exploratory and personal commentary. The document concludes with additional appendices and the bibliography.

2. IMMUNE CHECKPOINT LANDSCAPES OF HUMAN AND CANINE CANCERS

2.1 Introduction

More than 40 immune checkpoints have been identified in humans, but the presence of these potential immunotherapy targets in canine cancers remains mostly unknown [87]. The feasibility of canine immunotherapy hinges upon comprehensive characterization of the canine IC landscape. Only canine cancers that show immune checkpoint patterns similar to those found in human cancers can serve as valuable models for immunotherapy studies.

In contrast to dogs, much is known about the abundance of individual ICs in most human cancers [97]. Expression signatures encompassing a few ICs at a time have been linked to treatment responses and prognosis in several cancers, which supports the clinical value of considering multi-IC patterns [98–101]. However, comprehensive IC signatures have not been investigated. Clinically important, yet unanswered questions include the influence of the cancer's histological type on its IC abundance patterns, the existence of immunologically related cancer clusters, and the similarity of signatures among patients with the same cancer type.

In this study we pursued three objectives: first, to assess the abundance of immune checkpoints across the canine cancer types; second, to compare these IC profiles with those found in human cancers; and third, to analyze the IC patterns of human cancer subtypes and individual patients.

2.2 Results

2.2.1 Immune checkpoints' expression across canine cancer types

Diving into the largely uncharted territory of canine cancer immunology, we set out to explore whether spontaneous canine cancers express immune checkpoints (ICs) relevant to human cancers. To probe this, we harnessed publicly accessible raw RNA sequencing data that met our inclusion criteria (see: methods). That yielded a robust dataset from 418 canine patients spanning 14 distinct cancer types (**Tab. 3**, Methods). Additionally, we compiled a comprehensive list of both established and emerging ICs (**Tab. 4**, Methods). We quantified gene-level expression and visualized the normalized median abundances of those IC genes in **Fig. 1A**, along with their impact on the immune response and best-known interactions. Importantly, all ICs were expressed in at least some canine cancers. While SIRPA-CD47 and TIM-3-GAL-9 inhibitory receptor-ligand pairs were universally highly expressed, the abundance of others, like B7-H4 (inhibitory), NECTIN4 (inhibitory) and GITR (complex role) varied greatly. Interestingly, in the case of the commonly drugged PD-1 / PD-L1 inhibitory pair, oral squamous cell carcinoma (OSCC) and meningioma exhibited low PD-1 receptor expression, while OSCC displayed elevated PD-L1 ligand levels alongside undetectable PD-1. The distribution of normalized abundances for each IC across canine cancer types can be found in **Fig. S4**. The standard deviation and median absolute deviation/median (MADm) plot to match Fig. 1A is available as **Fig S2**.

Figure 1: Immune environment across canine cancer types. (A) Normalized median abundances of immune checkpoints (ICs). Notable is the universal expression of ICs like TIM-3 and GAL-9, while others, such as GITR, B7-H4, and NECTIN4, show variability. The gray accessory plots summarize the gene expression per cancer and per IC, with lymphomas showing the strongest total IC expression and SIRPA/CD47 exhibiting the highest total expression. (B) This heatmap displays abundance scores for IC categories. The bar plot above illustrates the ratio between inhibitory and stimulatory scores, with a ratio of 1 indicating an equal balance. Noteworthy are MC, UC, LC, GLM, and HSA (see: abbreviations), which have a high ratio, suggesting a potentially more inhibitory environment. (C) A heatmap of standardized scores for various immune cell populations, showing the diversity in immune infiltration across different cancer types.
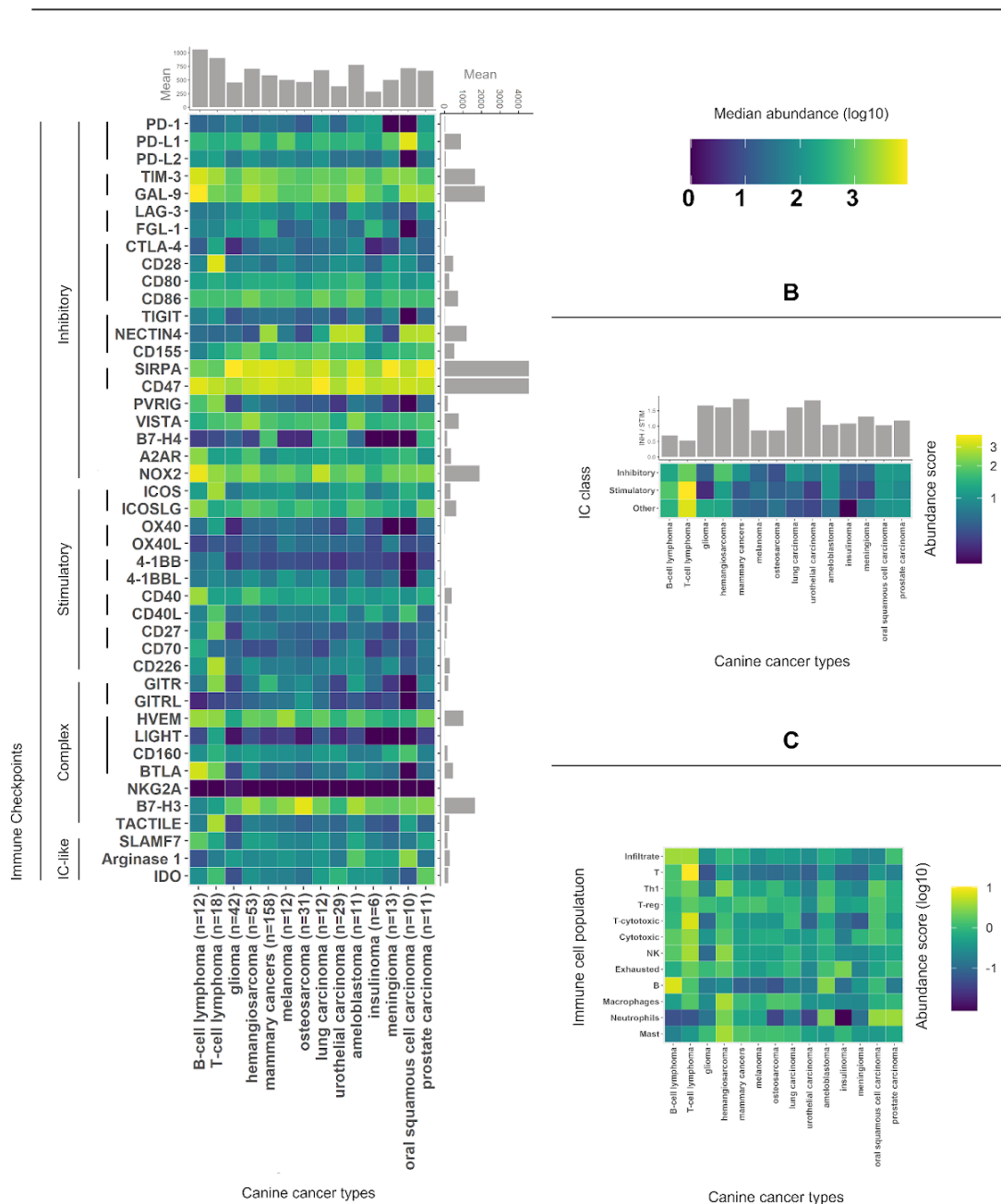
2.2.2 The extent of immune inhibition varies across canine cancer types

How does the IC landscape of each cancer influence the resident immune cells? Single ICs such as PD-1 do not reflect the general level of immune inhibition within the tumor microenvironment [102]. This complexity is underscored by the compensatory role of other ICs like TIM-3/GAL-9, which can drive resistance to PD-1 blockade immunotherapy [103,104]. In an attempt to assess the level of immune inhibition in the tumor environment, we categorized the ICs under study into inhibitory, stimulatory, or complex groups, and summarized the abundance of each category into an inhibitory and stimulatory IC scores (see Methods section - calculating immune inhibition score). We then computed the ratio of inhibitory to stimulatory score (**Fig. 1B**). MC, UC, LC, GLM, and HSA showcased a notably high ratio (putatively more inhibitory environment), while BCL, TCL, MEL, and OS exhibited low values.

2.2.3 Diverse immune infiltrates characterize canine cancers

To contextualize IC abundance within each cancer's immune cell population, we turned to the expression of immune cell markers. Advanced methods for deconvoluting immune infiltrate from sequencing data - for example CiberSort - were not yet available for the canine model; hence, we quantified the expression of marker genes characteristic for each cell population and summarized them into population estimate scores (**Fig. 1C**; see methods: immune infiltrate estimation). We found a particularly high estimated immune infiltration in prostate carcinoma and lymphomas (artifact expected due to the immune nature of lymphoma cells). Estimated scores for T- and cytotoxic T-cells were high in T-cell lymphoma, while scores for B-cells were high in B-cell lymphoma, which was expected due to the nature of these cancers. Additionally, B-cells score appeared high in ameloblastoma. Macrophage and mast cell scores appeared on a high level in hemangiosarcoma. Neutrophil score appeared high in hemangiosarcoma, ameloblastoma, prostate carcinoma and oral squamous cell carcinoma. Additionally, we observed a relatively high score for exhausted immune cells in insulinoma. Glioma appeared low in most immune cell types, save for T-reg and exhausted lymphocytes. Intriguingly, glioma had a particularly low score for NK cells, while being the only canine cancer with considerable abundance of NKG2A - the NK cell receptor (**Fig. 1 A & C, Fig. S4**). Other low scores included neutrophils in osteosarcoma, urothelial carcinoma and especially, insulinoma. Our findings reveal a

broad variation in the estimated composition of immune infiltrates across canine tumors.

2.2.4 Cancer IC signatures cluster by species

After discovering variations in the immune environment of canine tumors, we set out to find if these canine cancers mirror their human equivalents in terms of immunotherapy targets, specifically, immune checkpoints. Accordingly, we decided to compare cancer IC signatures within and between the human and canine species. We combined our data on IC abundance in canine cancer types (n=14) with human data (n=27) supplied by the PanCancer Analysis of Whole Genomes (PCAWG) and sourced from EBI [105]. Subsequently, we quantified the median abundance of each IC in each cancer type and created a vector of these medians for every cancer type (see methods). We assessed the similarity of these vectors, using a Pearson correlation-based distance matrix. The dendrogram resulting from the hierarchical clustering of the matrix showed that cancer types predominantly clustered within their respective species, as seen in **Fig. 2** below. In other words, when cancers were grouped based on IC expression similarity, canine cancers primarily clustered with other canine types, while human cancers largely grouped together as well.

Figure 2: Dendrogram representing the hierarchical clustering of a distance matrix which compared canine and human cancers in respect to their immune checkpoint (IC) expression levels. Cancers grouped predominantly within their respective species (**bold** font - canine, normal font - human). However, notable interspecies similarities emerged, particularly between canine and human gliomas and between canine osteosarcoma and human sarcoma. The figure also illustrates that human cancers tend to cluster according to their histological subtype and primary cancer site. Colors distinguish 14 different clusters. For detailed distance values, refer to Table S4.
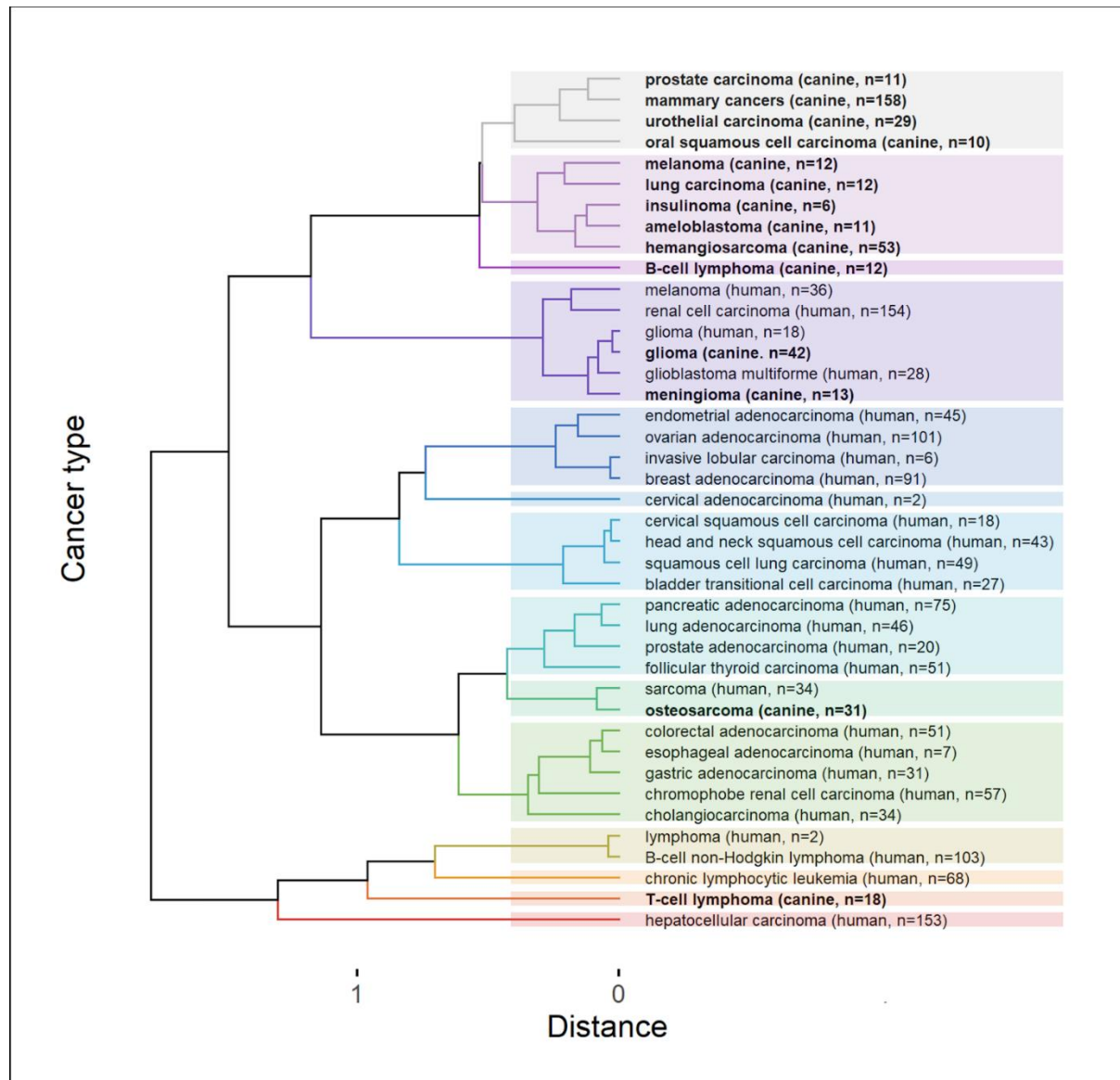
2.2.5 Transcending species lines: brain cancers and sarcomas

Remarkably, there were two interspecies groups that did not follow the trend of clustering within species. Canine glioma and meningioma, along with human glioma and glioblastoma, displayed striking relatedness. Our analysis of the distance table (**Tab. S4**) revealed that the interspecies glioma distance (0.025) was remarkably

smaller than any distance found within the same species for humans or dogs, where the lowest recorded distances were 0.032 and 0.083, respectively. In addition, canine osteosarcoma and human sarcoma demonstrated exceptional correlation, even though sarcoma represents a broad category (0.086). Delving further into **Tab. S4**, we observed that many human-canine pairs displayed a distance that was lower than the median intraspecies distances (0.344 for dogs and 0.541 for humans, shown in **Tab. S4**, violet and green), thus illustrating a broad similarity.

2.2.6 IC signatures reflect histology and primary site in human cancers

For a more granular view of type-specific patterns, we inspected human cancers, as these were categorized into more precise diagnostic subtypes. Human cancers appeared to cluster by histological type and subtype (e.g., distinct clustering of squamous cell carcinomas vs adenocarcinomas). Clustering also appeared to follow physiologically related primary sites, evident in the grouping of endometrial, ovarian, invasive lobular and breast adenocarcinomas, vs gastric, esophageal, and colorectal adenocarcinomas (**Fig. 3**).

Curious to see whether these clustering tendencies were driven by the abundances of any specific ICs, we investigated median-based IC differential expression between the clusters of interest and the remaining cancer types, or in between particular clusters. The statistically significant results as defined by p < 0.05 were sorted by decreasing fold change and presented in **Table 1** below. Additionally, the outcomes of a mean-based analysis were attached in **Table S1**. ICs found significant in both analyzes were marked in bold.

Uncharacteristically, the levels of Nectin4 and/or B7-H4 featured as significant in almost all clusters. Carcinomas were characterized by upregulated B7-H4 and NECTIN4 as compared to non-epithelial cancers. SCC and TCC carcinomas, which clustered together, additionally displayed elevated GITR. On the other hand, another type of carcinoma, adenocarcinomas, distinguished itself by slightly elevated ICOS. Within adenocarcinomas, we assessed two separate clusters: gynecological and gastric ones. Compared to all adenocarcinomas, the gynecological ones featured upregulated IDO, while gastric adenocarcinomas had severely down-regulated B7-H4. Brain cancers had down-regulated NECTIN4 - consistent with their non-epithelial

character - and down-regulated IDO. When the whole cluster was considered - glioma and glioblastoma with their close HC neighbors melanoma and renal cell carcinoma - elevated SIRPA became a statistically significant feature. Down-regulation of Nectin4 and B7-H4 was the strongest characteristic of human sarcoma vs all other human cancers. However, the same was true for melanoma. This highlights the limitation of differential-expression based methods. The expression analysis of individual genes does not identify features unique to clusters identified with more comprehensive methods. Arginase 1 and FGL-1 levels were extremely elevated in hepatocellular carcinoma, as they are in healthy liver tissues [106]. Differential expression against healthy samples would be necessary to put their levels into the right context.

Table 1: Median-based differential IC expression between human cancer type clusters. Genes that were found significant in both median- and mean-based analysis were marked in bold for denoting increased confidence. Fc - fold change, log2fc - Log of fc, pval - p value, HCC - hepatocellular carcinoma, MEL - melanoma, RCC - renal cell carcinoma, SCC - squamous cell carcinoma, TCC - transitional cell carcinoma.

Comparison	ID	median tpm	reference tpm	fc	log2_fc	zscore	pval	regulation
Sarcoma vs other	**NECTIN4**	0.40	22.50	0.02	-5.81	-4.01	2.9894E-05	down
	B7-H4	0.10	1.50	0.07	-3.91	-2.63	4.2311E-03	down
	CD70	6.00	1.00	6.00	2.58	2.07	1.9363E-02	up
Melanoma vs other human	**NECTIN4**	0.50	22.50	0.02	-5.49	-4.30	8.5662E-06	down
	B7-H4	0.10	1.50	0.07	-3.91	-3.02	1.2592E-03	down
HCC vs other	**FGL-1**	530.00	0.10	5300.00	12.37	4.23	1.1564E-05	up
	Arginase 1	335.00	0.20	1675.00	10.71	3.68	1.1883E-04	up
	NECTIN4	0.20	22.50	0.01	-6.81	-2.20	1.3918E-02	down
Gynecological vs other	**B7-H4**	86.50	1.50	57.67	5.85	5.30	5.9158E-08	up
Gastric cluster vs other	**B7-H4**	0.40	1.50	0.27	-1.91	-3.14	8.3576E-04	down
	NECTIN4	10.00	22.50	0.44	-1.17	-1.88	3.0173E-02	down
	GAL-9	68.00	31.50	2.16	1.11	2.04	2.0919E-02	up
	CD70	2.00	1.00	2.00	1.00	1.85	3.2445E-02	up
Lymphomas vs other	BTLA	29.00	0.40	72.50	6.18	1.66	4.8874E-02	up
	NECTIN4	0.50	22.50	0.02	-5.49	-3.24	5.8839E-04	down
	CD155	4.50	36.50	0.12	-3.02	-2.21	1.3671E-02	down
	B7-H3	7.00	55.00	0.13	-2.97	-2.19	1.4359E-02	down
Brain cancers vs other	**NECTIN4**	0.15	22.50	0.01	-7.23	-3.17	7.5006E-04	down
	IDO	0.20	7.50	0.03	-5.23	-2.12	1.7039E-02	down
Brain cancers cluster with MEL and RCC vs other	**NECTIN4**	0.20	22.50	0.01	-6.81	-5.08	1.8943E-07	down
	SIRPA	153.50	48.50	3.16	1.66	1.68	4.6889E-02	up
SCC and TCC vs other	GITR	27.00	4.50	6.00	2.58	2.78	2.6858E-03	up
	NECTIN4	105.50	22.50	4.69	2.23	2.33	9.9524E-03	up
	B7-H4	6.00	1.50	4.00	2.00	2.03	2.0954E-02	up
Carcinomas vs other	B7-H4	7.00	1.50	4.67	2.22	5.09	1.7518E-07	up
	NECTIN4	43.50	22.50	1.93	0.95	2.05	2.0195E-02	up
Adenocarcinomas vs other	B7-H4	9.00	1.50	6.00	2.58	4.61	2.0487E-06	up
	ICOS	2.00	0.90	2.22	1.15	1.77	3.8458E-02	up
Gynecological adenocarcinomas vs other adenocarcinomas	IDO	30.50	9.00	3.39	1.76	3.89	4.9942E-05	up
Gastric adenocarcinomas vs other adenocarcinomas	**B7-H4**	0.40	66.00	0.01	-7.37	-5.73	4.9198E-09	down

2.2.7 A2AR and six other ICs are possible drivers of the species divide

What were the roots of the differences between human and canine IC signatures? Are these distinctions due to complex, species-specific characteristics, or are a handful of IC genes the main influencers? To shed light on these questions, we first performed a differential IC expression analysis - like above - comparing the human and canine cancer type clusters (**Tab. 2** - below). Five ICs appeared to distinguish canine from human cancer types.

Table 2: Median-based differential IC expression comparing the human vs canine cancer types. Genes that were found significant in both median- and mean-based analysis were marked in bold for denoting increased confidence. Fc - fold change, log2fc - Log of fc, pval - p value.

Comparison	ID	median tpm	reference tpm	fc	log2_fc	zscore	pval	regulation
Canine vs Human	FGL-1	4.78	0.10	47.75	5.58	2.61	4.5128E-03	up
	Arginase 1	5.21	0.20	26.04	4.70	2.18	1.4554E-02	up
	NECTIN4	0.77	18.00	0.04	-4.55	-2.36	9.2459E-03	down
	A2AR	**4.27**	**0.20**	**21.33**	**4.41**	**2.04**	**2.0641E-02**	**up**
	OX40L	0.32	3.00	0.11	-3.24	-1.71	4.3182E-02	down

However, only A2AR was indicated in both median- and mean-based analysis (**Tab. 2 & S1**). Hence, aware of the aforementioned limitations of this method, we decided to answer the question of the species divide by performing a principal component analysis (PCA) on the IC signatures (refer to **Fig. 3**).

Principal Component Analysis (PCA) is a method that reduces the complexity of high-dimensional data, while retaining key patterns. In the original dataset, each variable or sample can be considered a dimension. PCA generates as many 'principal components' (PCs) as there are dimensions - 44 in our case, because there are 44 genes (variables), but only 41 cancers (samples). These PCs are, essentially, new 'dimensions' that are combinations of the original ones. However, PCs are ranked (PC1-PC44) based on their contribution to the overall variability. The first few PCs usually encapsulate a significant portion of this variability, thus by focusing on these, we simplify further analyses and enable meaningful data visualization.

We decided the optimal number of PCs to retain using a scree plot, which visualizes the proportion of the total data variance that is captured by each PC (**Fig. 3A**). We visualized the top 10 PCs, marked the threshold capturing at least 80% of the data variability, and analyzed the optimal number of PCs to consider with Horn's and Elbow methods. The Elbow method identifies an 'elbow' point at which the addition of more

PCs provides diminishing returns in terms of explained variability. Based on the more conservative Elbow estimate we chose to retain the 6 top PCs. Following the selection of the top six PCs, we proceeded to investigate their interplay (**Fig. 3B**). Studying combinations of PCs, rather than each individually, provides a more comprehensive understanding of the dataset as it allows us to explore the simultaneous effect of multiple components on the variability. Strikingly, the PC2 alone delineated a clear separation between human and canine groups (**Fig. 3C**).

For deeper insight, we scrutinized the 'component loadings' for PC1 to PC3 (**Fig. 3D**). Component loadings represent the weight by which each initial variable (in this case, each gene) contributes to the principal component. By investigating these loadings, we can identify the key players driving the differences captured by each PC. We pinpointed the four most influential ICs contributing to PC2, while noting that these ICs were not the primary contributors to the variability along PC1 and PC3 (**Fig. 3D**).

These ICs - CD160, A2AR, NKG2A, and OX40 - were further examined for potential enrichment in various categories using StringDB, but they appeared to share only their immuno-regulatory function. We visualized the StringDB-based relationships between all the analyzed IC genes (**Fig. 3E**), which made the weak links between four genes of interest clear. Subsequently, we repeated hierarchical clustering like before, but with signatures consisting solely of the four identified genes only or four random genes for comparison (VISTA, ICOSLG, 4-1BBL, TACTILE). Remarkably, clustering the signatures consisting solely of the 4 identified genes resulted in a nearly complete separation of cancers by species (**Fig. 3F**), while clustering by 4 random genes made the cancer types of both species intermingle freely (**Fig. S7**). Broadly speaking, in canine versus human cancers, abundances of CD160 and A2AR were higher, while those of NKG2A and OX40 were lower (Tab. S2). Importantly, these trends should not be assumed to apply universally to all individual cancer cases or cancer types - as exemplified by canine glioma's NKG2A expression, isolated amongst canine malignancies (**Fig. S4**).

Figure 3: Principal component analysis (PCA) of immune checkpoint (IC) signatures in human and canine cancers. (A) Optimal dimensionality determination (B) Top five principal components (PCs). (C) Clear species separation along the second principal component (PC2). (D) Component loadings for PC1 to PC3, highlighting influential ICs contributing to PC2. (E) StringDB-based analysis showing the immuno-regulatory function as the only shared feature among the four influential ICs. (F) Dendrogram resulting from clustering of signatures consisting solely of the 4 identified genes, demonstrating nearly complete separation of cancers by species.
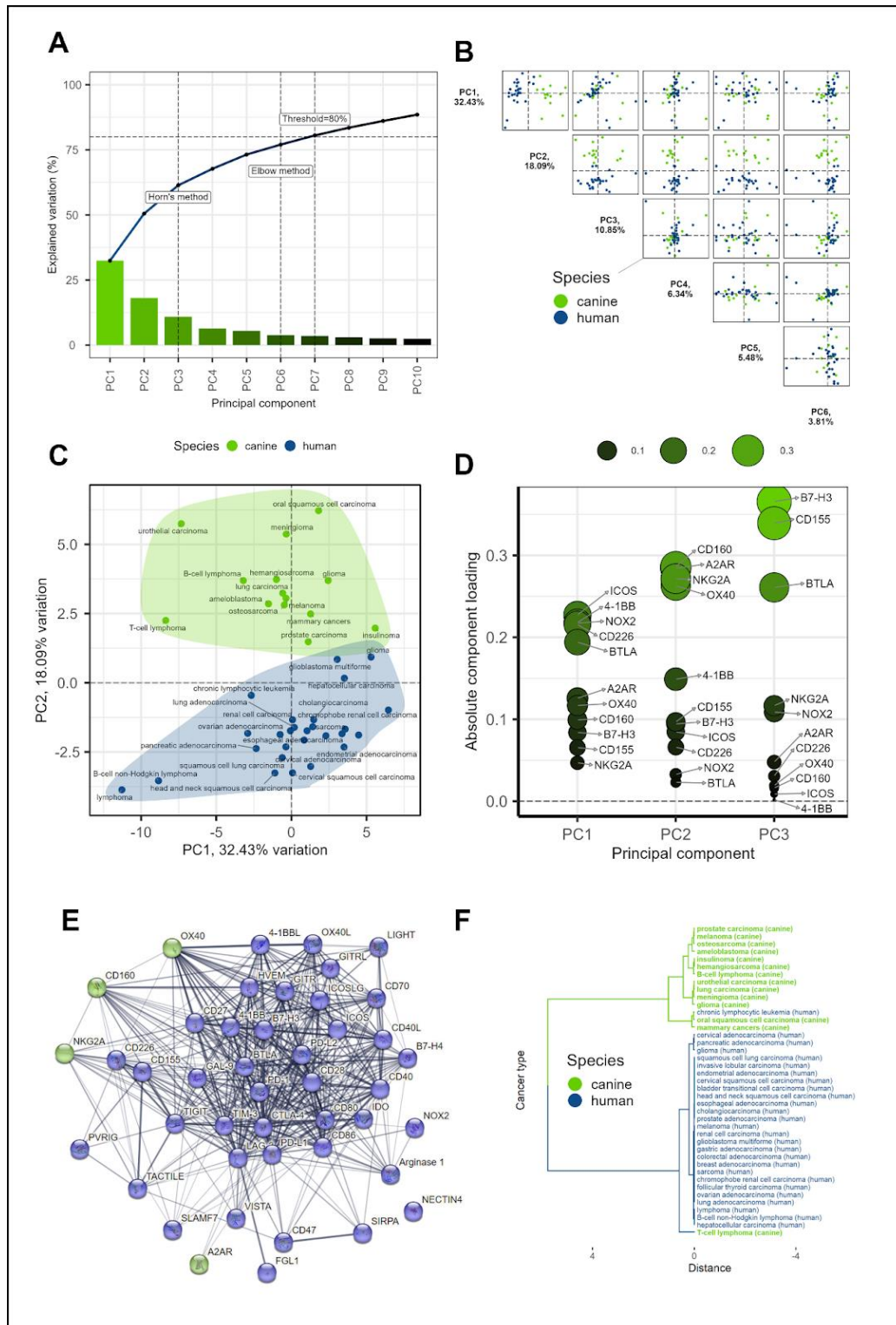
Summarizing the results of the two experimental approaches, our confidence is predominantly anchored in A2AR's role as a determinant of the interspecies divide. Given the very low median values for NKG2A in both species (see **Tab. S2**) and considering that the majority of canine expression is attributable to glioma alone, we infer that the influence of NKG2A is likely statistical rather than biological. The quartet of ICs identified through differential expression analysis did not converge with the two other ICs isolated by PCA, a finding consistent with the disparate nature of these methodologies. This discrepancy, coupled with the constraints of TPM normalization used in the input data, limits our confidence in these six other ICs. In conclusion, the species divide appears to be primarily driven by A2AR, possibly in concert with one or more of the following immune checkpoints: FGL-1, Arginase 1, NECTIN4, OX40L, CD160, OX40. From a comparative oncology perspective, immune checkpoints with notable abundance variability within or between species may not be optimal treatment targets.

2.2.8 Key IC genes driving non-species-related differences in cancer types

During the PCA analysis we also observed that the IC genes ICOS, 4-1BB, NOX2, CD226 and BTLA had the highest loadings on PC-1 and not PC-2 (**Fig. 3D**). Between PC-1 and PC-2, 4-1BB, an inducible costimulatory IC receptor of T-cells, was the only one unique to PC-1. Given that PC-1 captures the most variability in the dataset, the abundances of these five ICs, especially the 4-1BB, may strongly contribute to the non-species-related differences between the analyzed cancer types. 4-1BB is considered a promising immunotherapy target [107].

2.2.9 Case-by-case: individual tumors unveil heterogeneity of IC signatures

At the outset, we used gene expression medians to discern patterns across cancers. To expose the internal heterogeneity of IC signatures within each cancer type, we decided to turn our attention to individual cases. We sought to see if cases of the same cancer type share associated IC signatures or if the signatures are unique to each case, irrespective of the diagnosis. We were also interested in outliers that would defy their classification by aligning with cases of other cancer types. We processed individual IC abundance signatures with UMAP for its ability to capture the complex and potentially non-linear relationships among the expression levels of analyzed

genes in each patient's profile. This is important because gene expression levels often interact in intricate ways that linear methods can overlook. The use of UMAP allowed us to maintain both the broader patterns and the finer details in our data (**Fig. 4**). This method is especially effective for revealing significant insights in individual cases and outliers where nuanced patterns can have substantial implications. Our findings echo previous observations at the cancer type-level; individual canine and human cancer cases formed distinguishable clusters (**Fig. 4A**). Gliomas in both species were closely situated, demonstrating highly uniform signatures (**Fig. 4B**). In fact, all brain cancer cases presented a high degree of proximity (**Fig. 4C**). Sarcomas in both species also exhibited clustering, albeit less tight (**Fig. 4D**). Hemangiosarcoma, a predominantly canine cancer, did not cluster as closely with human sarcomas, as did canine osteosarcoma. Certain cancer types, such as human cholangiocarcinoma, presented a high degree of dispersion in their individual case signatures, thereby co-localizing with other cancers (**Fig. 4E**). This precludes meaningful interpretation of averaged trends for such cancer types. In line with hierarchical clustering earlier, certain human-canine cancer sets, such as prostate carcinomas, did not exhibit similar signatures (**Fig. 4F**).

Figure 4: Individual IC abundance signatures via UMAP representation underscore cancer type-specific patterns and intrinsic heterogeneity. (A) Global overview of the signatures distinguishes two primary clusters: canine and human, highlighting species-dependent variation. (B) Glioma cases from both species are closely situated, signifying a shared IC signature landscape. (C) Inspection of brain cancer cases from both species reveals not only mutual proximity but also a marked uniformity within each cancer type. (D) Examination of sarcoma cases unveils a proximity between human sarcoma and canine osteosarcoma, while canine hemangiosarcoma exhibits a more distant relationship. (E) Human cholangiocarcinoma displays a notable case dispersion, indicative of a high degree of IC signature heterogeneity. (F) A cross-species comparison of prostate cancer evidences a lack of co-clustering, suggesting distinct IC signatures for these species-specific prostate cancers.
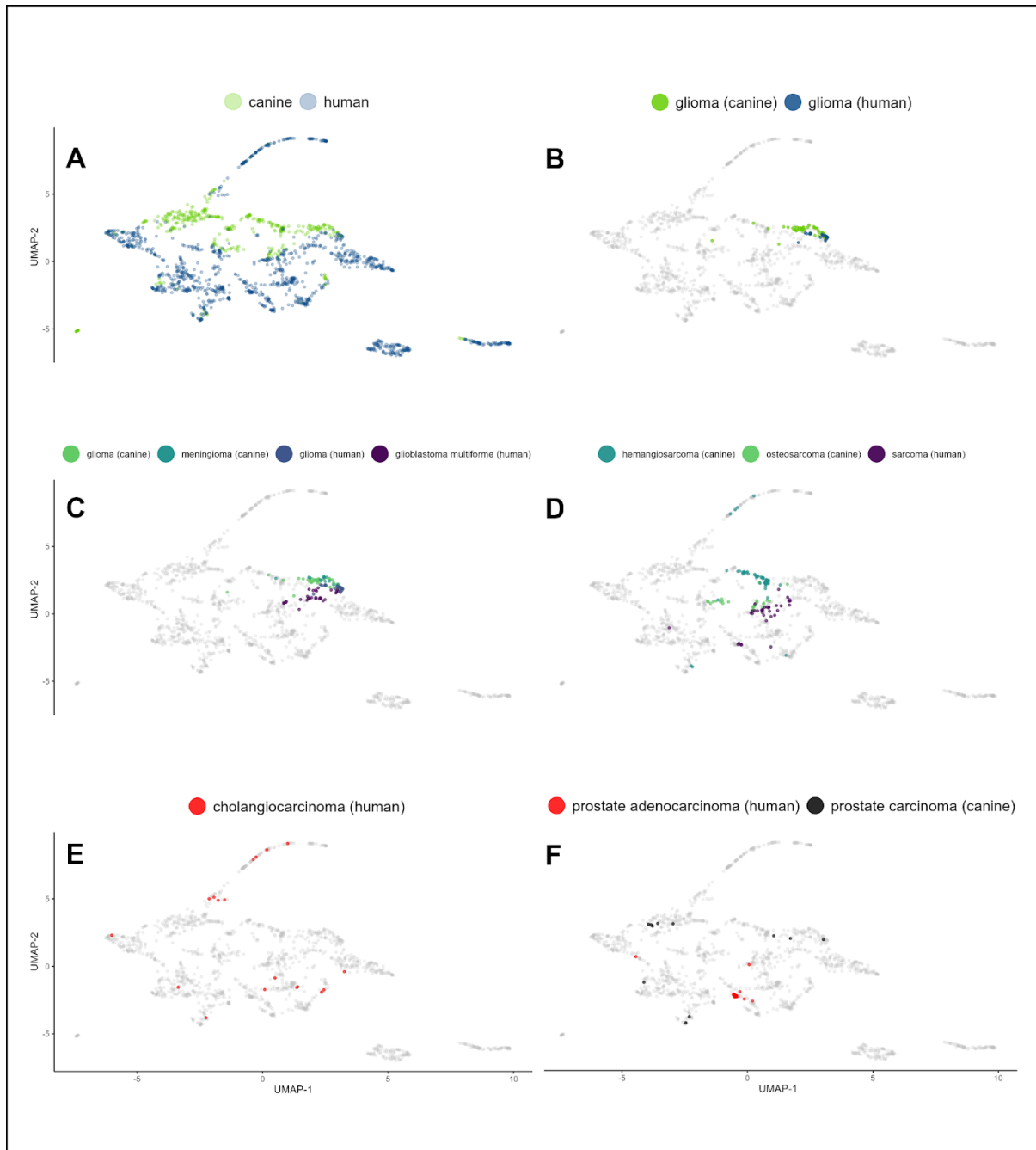
2.2.10 Confirmations and surprises: revisiting patient data with PCA

To complement our UMAP analysis, we applied PCA to the same dataset, providing a linear perspective to validate and expand the non-linear UMAP insights. **Figure 5** displays PCA plots of log-normalized IC signature data of individual patients. Consistency in primary trends between UMAP and PCA strengthens our findings and provides a robust analysis framework. **Figure 5A** provides a global overview of the PCA analysis, distinguishing two primary clusters representing canine and human cases. The plot reinforces the species-dependent variation observed in the UMAP analysis and in the earlier, cancer type-focused PCA analysis. In line with the UMAP results, the PCA analysis confirms that brain cancers, particularly gliomas, of both species exhibit close proximity (**Fig. 5C**), indicating a shared immune checkpoint signature landscape. Sarcomas, characterized by a less homogeneous distribution of patient signatures, demonstrate somewhat more separation along the species-distinguishing PC-2 axis, while still exhibiting a reasonably similar distribution along the PC-1 axis, which captures the most variability in the dataset (**Fig. 5D**). Prostate carcinomas, on the other hand, do not appear well aligned along the PC-1 axis, affirming their distinct IC signatures and serving as an example of human-dog cancer pair with low potential for comparative immunotherapy (**Fig. 5F**). Similarly to UMAP, the PCA analysis confirms that human cholangiocarcinoma displays a wide distribution of data points along the PC-1 axis, reflecting a high degree of intratumoral IC signature heterogeneity within this cancer type (**Fig. 5E**). Interestingly, the PCA analysis reveals a novel finding that was not observed in the previous approaches. A cluster of human patients with signatures uniquely positioned within the plot area belonging to the canine cancer patients was identified (**Fig. 5B**). Notably, all these patients belong to the human chronic lymphocytic leukemia (CCL), a B-cell based blood cancer. While no equivalent leukemia was present in our canine dataset for direct comparison, the clustering of these human CCL patients with canine cancer cases along the PC-2 axis, previously identified as species-distinguishing, suggests a unique resemblance between the IC landscapes of human CCL and canine malignancies in general (**Fig. 5B**). In the earlier UMAP analysis CCL cases formed a very distinct cluster only neighboring some canine B-cell lymphoma cases (**Fig. S6**). CCL is the only leukemia included in our study, and it is important to acknowledge that the differential sample preparation methods employed for leukemia versus solid tumors could have

influenced the observed results. Nevertheless, this unexpected finding highlights the value of multi-method analysis and warrants future exploration. In summary, the PCA analysis validates and expands upon the UMAP findings, while highlighting the unique nature of human CCL within the context of canine cancers.

Figure 5: PCA representation of individual IC signatures validates and augments the insights from UMAP analysis, uncovering unexpected similarities between human chronic lymphocytic leukemia (CCL) and canine cancers. (A) Consistent with UMAP findings, the global overview reveals two primary clusters: canine and human. (B) Patient signatures of human CCL, a B-cell blood cancer, exhibit a striking similarity to canine cancers along PC2. This suggests a resemblance between human CCL and canine malignancies in the context of the identified key immune checkpoint genes. (C) Further examination of brain cancer cases reaffirms the mutual proximity observed in UMAP, particularly evident in gliomas, and the overall uniformity of signatures within each cancer type. (D) Human sarcoma and canine osteosarcoma, while displaying variability along PC-1, demonstrate alignment with each other, further supporting the concordance between species. (E) Similar to UMAP, human cholangiocarcinoma exhibits notable case dispersion, reflecting the high degree of heterogeneity in IC signatures. (F) Consistent with previous observations, PCA confirms that human and dog prostate carcinomas display distinct IC signatures, as they do not align along PC-1. The findings reinforce the significance of our multimethod approach in uncovering both expected patterns and intriguing surprises within the dataset.
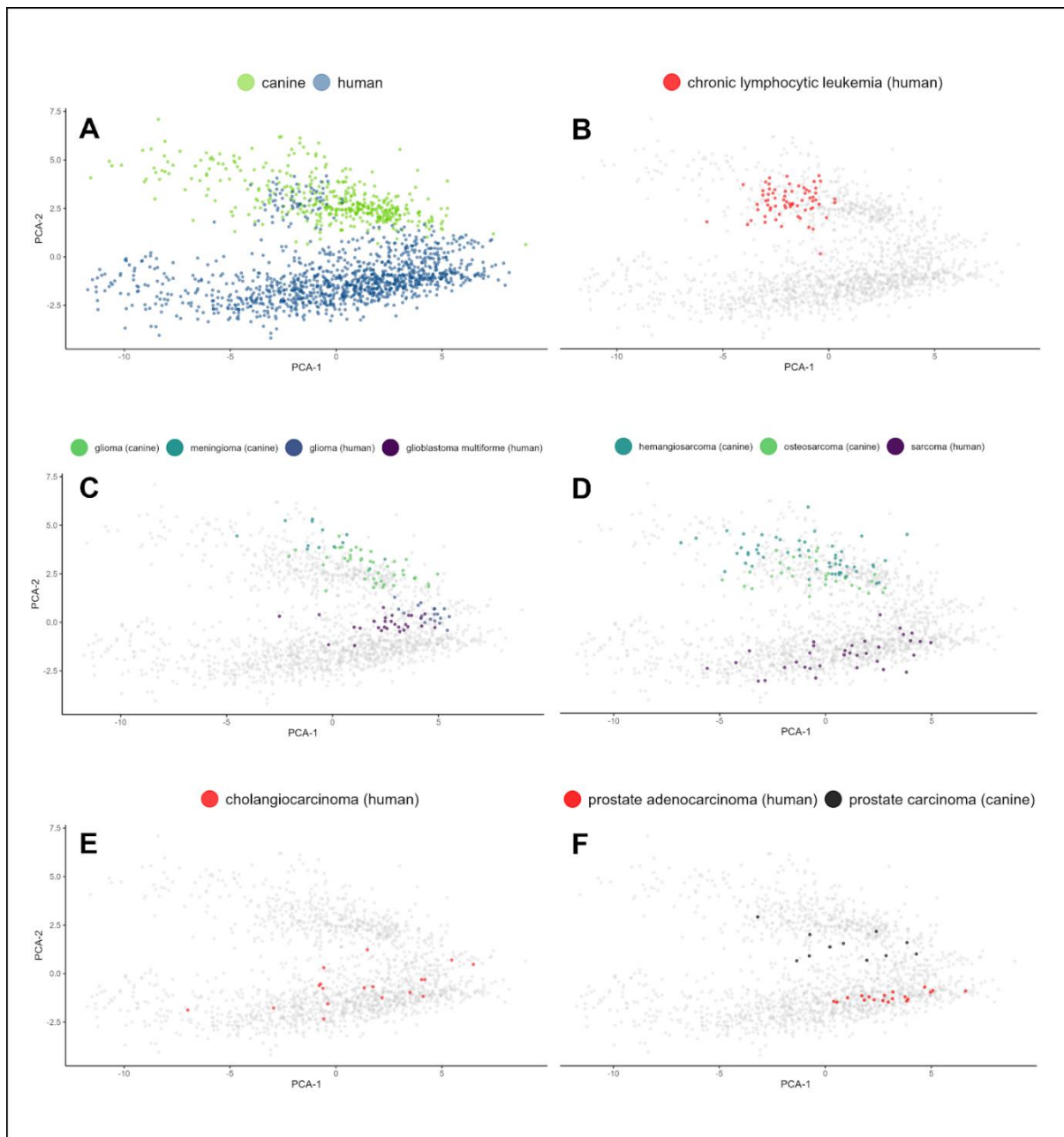
2.2.11 Distinguishing cancer and healthy tissue through IC signatures

Our primary goal was to compare IC signatures between various cancers, both within and across species. Thus, we concentrated on the baseline IC expression in cancer, rather than a differential expression between cancerous and healthy tissues. Regardless of the IC status in healthy tissues, the target abundance in cancer alone offers valuable insights for immunotherapy. However, five human cancers had at least nine healthy references available, so we took the opportunity to evaluate whether cancer IC signatures mirror the characteristics of their healthy tissues of origin, or if they exhibit an independent character. To this end, we visualized the diseased samples compared to healthy adjacent tissues, as assessed by UMAP and PCA. This time the analyses were extended to include all 150 normal samples present in the PCAWG dataset (**Tab. S3**).

In UMAP, small sample size limited the interpretations for cholangiocarcinoma and hepatocellular carcinoma, but renal cell carcinoma and chromophobe renal cell carcinoma samples presented a very distinct shift between normal and cancerous (**Fig. 5A-E**). Lung adenocarcinoma also exhibited a notable contrast in the immune checkpoint profiles of tightly clustered normal samples and the more diverse set of cancer samples. It's important to acknowledge that the 'normal' reference samples from PCAWG RNAseq study were obtained from areas adjacent to primary tumors [105]. The potential sharing of features between tumor and nearby stroma could downplay the observed differences.

Figure 6: Immune Checkpoint Expression Patterns Differ Between Cancers and Their Corresponding Normal Samples. UMAP visualizations of IC gene expression patterns in individual samples of five different cancer types along with corresponding healthy tissues. (A) Renal cell carcinoma, (B) Chromophobe renal cell carcinoma, (C) Lung adenocarcinoma, (D) Cholangiocarcinoma, and (E) Hepatocellular carcinoma. Distributions provide insights into differential IC landscapes between cancerous and normal tissues, with a notable shift in the case of renal carcinomas and lung adenocarcinoma.
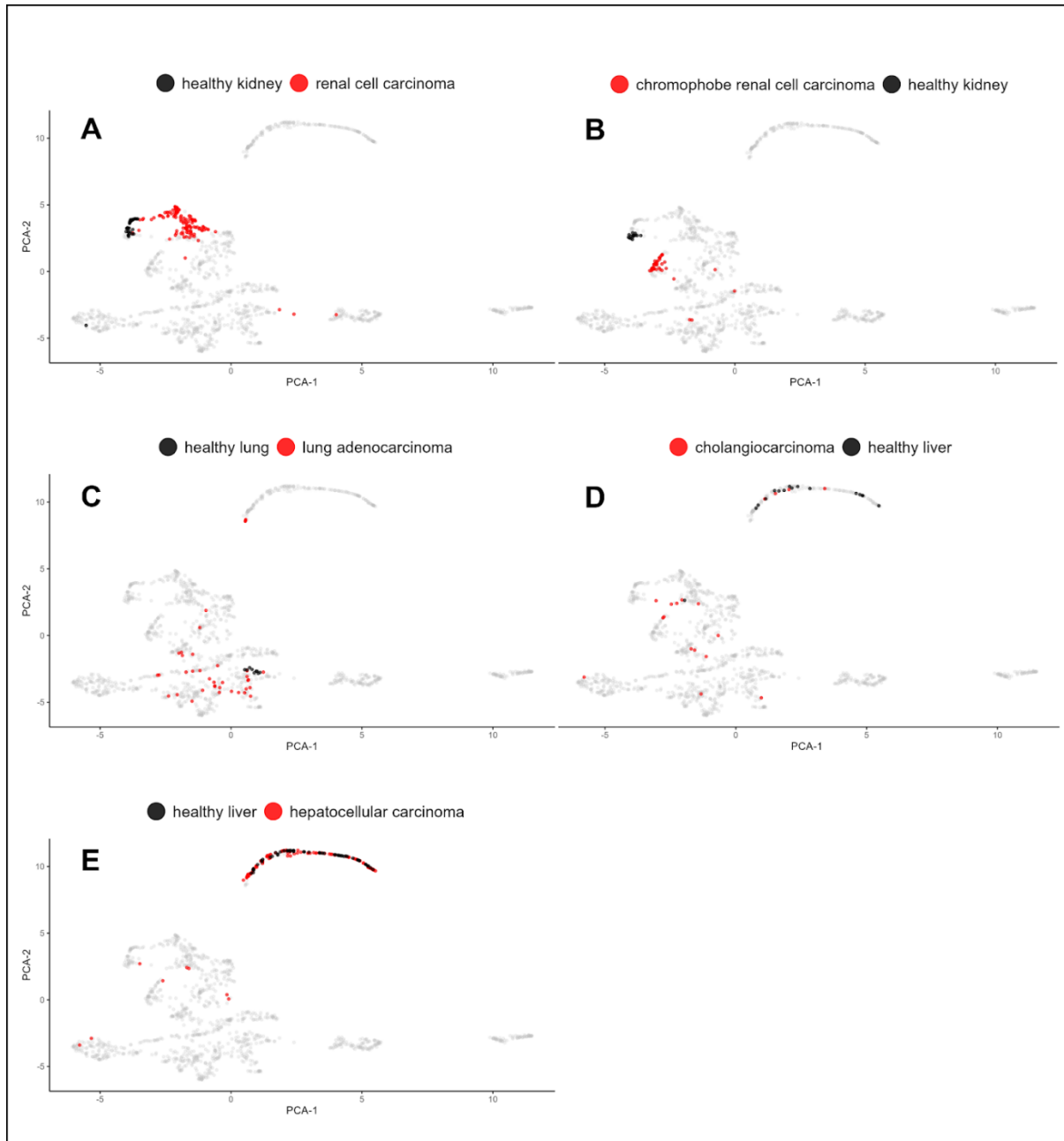
The PCA mirrored these findings (**Fig. 7A-E**), particularly with the renal carcinomas demonstrating an observable shift in the distribution of healthy and cancer samples along the PC-1 axis. CD86, TIGIT, ICOS, and BTLA emerged as genes with the highest contributions to the PC-1 component loadings (**Fig. 7F**). As such, these IC genes merit further exploration for their possible differential expression in cancer and

their potential as immunotherapy targets in renal cell carcinomas, which are currently addressed with PD-1 and CTLA-4 blocking therapeutics [108].

Figure 7: Differential Immune Checkpoint Expression Patterns Between Cancers and Normal Samples Unveiled Through PCA and Component Loadings Analysis. PCA biplots (PC-1 vs PC-2) present the IC expression distributions for the same cancer types and corresponding healthy tissues as in **Figure 6**. (A) Renal cell carcinoma, (B) Chromophobe renal cell carcinoma, (C) Lung adenocarcinoma, (D) Cholangiocarcinoma, and (E) Hepatocellular carcinoma. (F) A plot of component loadings for PC-1 to PC-3, emphasizing genes CD86, TIGIT, ICOS, and BTLA, which show the most substantial contributions to the PC-1 component. These genes deserve further scrutiny for their potential roles in cancer immunotherapy, particularly in renal cell carcinomas.
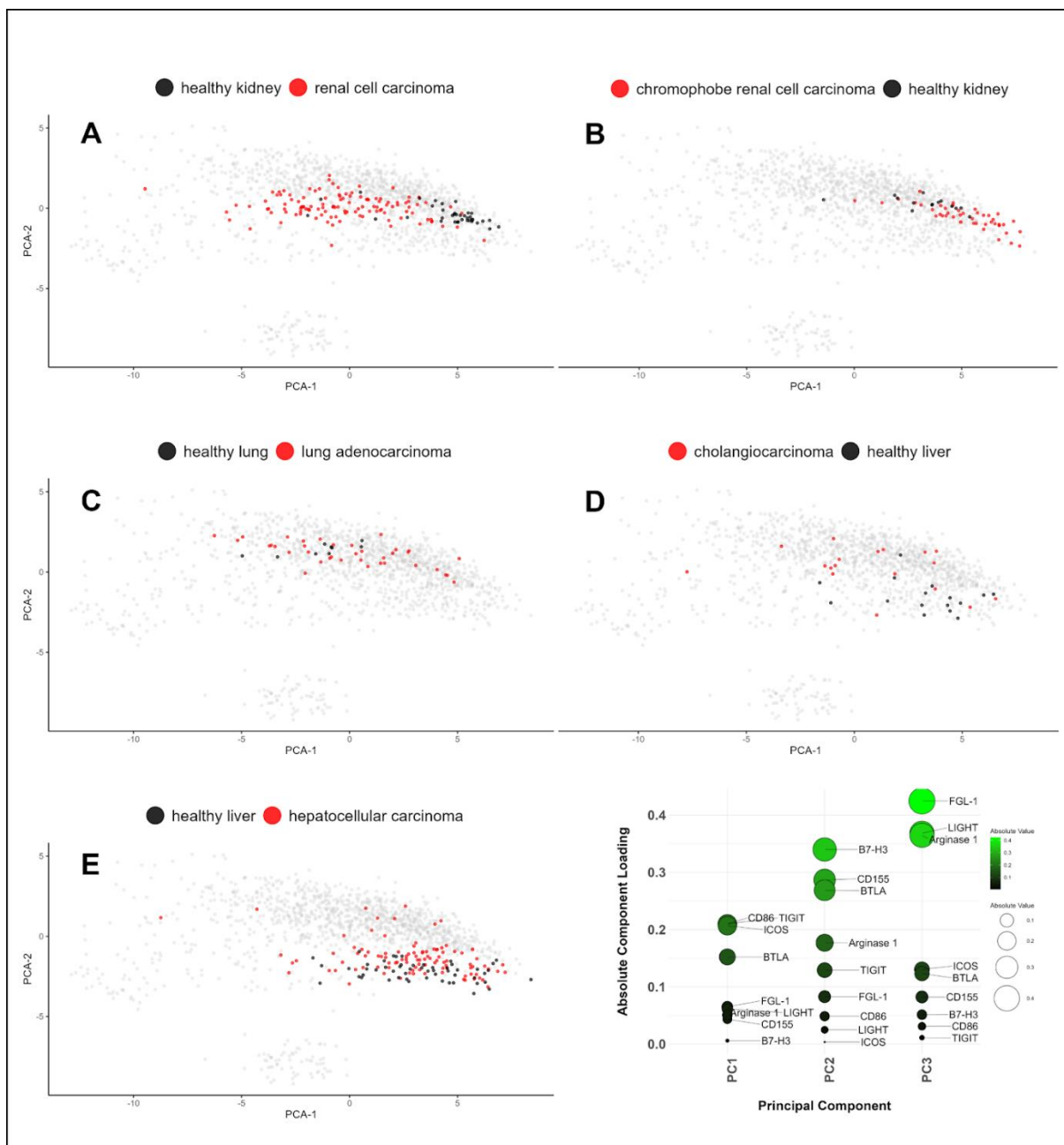
2.3 Discussion

The domain of immune checkpoint (IC) expression has been largely untouched in canine cancers. Here, we provide a comprehensive overview of IC expression patterns in both human and canine cancers. We unveil potential canine models for human cancer immunotherapy and identify prospective IC targets that intersect both species. By comparing the 'IC signatures' encompassing 44 IC genes in 27 human and 14 canine cancer types, we uncover distinct and shared patterns across species, cancer types, and individual patients. Our findings progress the fields of human cancer immunology, canine immunology and fill a knowledge gap in comparative oncology.

2.3.1 Prior studies

The veterinary part of our investigation builds upon prior studies, which identified PD-1 receptors on canine T-cells and observed PD-L1 in various canine cancer types using immunohistochemistry [109–112]. Other authors reported on the presence of CTLA-4 and IDO in specific canine cancer types such as B-cell lymphoma and melanoma [113,114], and found overexpression of B7-H4 in bladder cancer [112]. Murakami et al. advanced the field with their RT-qPCR investigation of 20 immune-regulating molecules in fresh samples [115], yet their study was constrained by a small sample size covering a wide range of cancer subtypes. Our study expands the scope and depth of the investigation with a larger sample size and comprehensive IC profiling.

2.3.2 The immune environment of canine cancers

Our study reveals the expression of 44 ICs in the majority of the 14 analyzed canine cancers. Their abundance varied across the cancer types, highlighting the potential for both universal and cancer type-specific treatment targets. Additionally, we observed diverse levels of immune cell infiltration and varied levels of estimated immune inhibition, thus characterizing the tumor microenvironment in aspects crucial for successful immunotherapy.

2.3.3 Immune checkpoint signatures that link human and dog cancers

We used hierarchical clustering to compare IC signatures between canine and human cancers. This allowed us to discover remarkable similarities between canine glioma and human glioma, as well as between canine osteosarcoma and human sarcoma, highlighting them as potential models for immunotherapy development. Intriguingly, this analysis also suggested a close relationship between brain cancers, human melanoma and human renal cell carcinoma in the IC context. Given the successful treatment of melanoma with ICB, this association could provide some rationale for exploring similar approaches in brain cancers. Furthermore, using PCA, we found unexpected similarity between human chronic lymphocytic leukemia cases and canine malignancies at large. Further research is needed to validate the meaning of these findings.

2.3.4 Brain Cancers, immunotherapy and comparative oncology

The striking similarities in immune checkpoint expression by human and canine glioma were evidenced through UMAP, PCA, and hierarchical clustering analysis. In fact, this similarity was unparalleled by any other pair of cancers in this study, including the intra-species pairs. Canine gliomas also exhibited high immune inhibition scores, increased T-reg infiltration, and exhausted lymphocytes, mirroring the immunologically 'cold' nature of human gliomas. One notable finding was the significant expression of SIRPA, an inhibitory receptor on macrophages, and its ligand CD47, often overexpressed in cancers. SIRPA is also prevalent in healthy brain tissues, nevertheless, its high level in brain cancers suggests the SIRPA-CD47 interaction may be of high importance in gliomas across both species. By highlighting the shared IC landscape in human and canine gliomas, our findings lend further support to the suitability of canine gliomas as models for human gliomas and point to SIRPA as a promising target for glioma immunotherapy. While many have doubted the feasibility of immunotherapy for glioma, this challenging cancer offers an opportunity to explore the key innovative treatment approaches: novel animal models, personalized therapies, combinatorial treatments, and targeting of immune populations beyond T-cells. Although we observed close similarity between canine glioma and human meningioma - another brain cancer - we prioritized gliomas and glioblastomas due to their aggressive nature and lower operability. Insights from our glioma analysis may

extend to meningiomas. For an in-depth discussion on glioma, please see the supplementary materials.

2.3.5 NKG2A levels vs NK cells in canine glioma

We have observed an apparent anomaly in canine glioma infiltrate. Unlike other canine cancers, glioma presented detectable expression of NKG2A, a known receptor of NK cells. However, it appeared to simultaneously present with the lowest expression of NK marker genes of all analyzed cancers. Although we have no definitive explanation of this phenomenon, we propose a hypothesis based on alternative NKG2A roles in humans. It has been reported that NKG2A can be expressed by Natural Killer T (NKT) cells, a unique group of T lymphocytes that possess characteristics of both T cells and NK cells. Further, a subset of CD8+ $\alpha\beta$ T-cells, particularly $\gamma\delta$ T-cells, is also known to express NKG2A [116,117]. NKG2A is additionally present in some T-cells that infiltrate peripheral nerves [118]. Therefore, the unexpected relationship between comparatively high NKG2A abundance and low NK cell score in canine glioma could be attributed to the involvement of the non-canonical NKG2A carrier cells. This, however, would require dedicated research to prove.

2.3.6 Notes on osteosarcoma

Osteosarcoma may be unlikely to benefit from targeting inhibitory ICs like CTLA-4, PD-1 and OX40 alone [83]. Based on our canine IC expression heatmap and human literature we suggest B7-H3, a complex function IC molecule associated with bad prognosis [119], appearing highly expressed in both human and canine OS, could be an interesting target to study on the human-canine intersection.

2.3.7 IC signatures clustered

In hierarchical clustering analysis most cancer signatures aggregated based on species, cancer histological type and primary site. These findings shed light on the links between cancer's characteristics and its immune checkpoint landscape. Within human cancer subtypes, further research should explore the underlying molecular mechanisms driving these trends, particularly in regard to optimizing treatment. In exploring the species-specific IC differences, we identified four functionally unrelated IC genes (CD160, A2AR, NKG2A, OX40) that drove the divide between canine and

human IC signatures in PCA. Since the human and canine datasets were differently sourced, further research needs to validate these findings. However, as most IC genes did not exhibit statistically significant differential expression between species, bias is an unlikely explanation.

2.3.8 IC signatures of healthy and malignant tissues

In this investigation, we utilized UMAP and PCA visualizations to compare IC signatures of cancer tissues and corresponding healthy tissues in a few human cancer types. In UMAP, renal cell carcinoma and chromophobe renal cell carcinoma exhibited a distinct shift between healthy and diseased states. In addition, we observed a significant contrast between consistent signatures of healthy lung samples and highly diverse signatures of adenocarcinoma cases. These results suggest the transition of a healthy tissue into a cancerous one involves a broad shift in the immune checkpoint expression. The diversity observed in lung adenocarcinoma sheds light on the heterogeneity of IC-based immune evasion strategies within one cancer type. On the other hand, these trends were not clear in cholangiocarcinoma and hepatocarcinoma, but low numbers of healthy reference samples limited the interpretability in these cases. PCA mirrored the above patterns, especially in renal carcinomas. In renal cancers, the main contributors to PC-1 - the axis separating healthy and sick - were CD86, TIGIT, ICOS, and BTLA genes. Further exploration could focus on their role in cancer development and potential as immunotherapy targets. Importantly, the healthy reference samples are typically derived from tumor-adjacent tissues, which might share certain features with nearby cancer. Consequently, this issue may downplay the real differences between healthy and cancerous tissues in this experimental setup.

2.3.9 The IC signatures of individual patients

Our analysis revealed that human patients with the same cancer type tended to exhibit similar IC signatures. For example, we noted a close alignment of IC signatures among glioma cases within species, indicative of conserved immune characteristics. However, in some cancers, like sarcoma, the case signatures were more heterogeneous, hinting at greater variability. Cancers displaying uniform IC signatures across patients offer promise for more consistent treatment success with a single therapeutic strategy. In contrast, the observation of cancers with high signature

variability underscores the need for personalized choice of a therapy attuned to the unique immune landscape of each patient. Therefore, our comprehensive characterization of IC signatures complements individualized therapy approaches like the cancer immunogram [120]. Further investigation is needed to understand the factors behind IC signature differences and their implications for treatment outcomes.

2.3.10 Differential gene expression between identified clusters

When we calculated differential IC gene expression between the previously defined clusters of human cancers, many trends were observed, which require further validation. Particularly interesting, B7-H4 was characteristically upregulated in female cancers, consistent with studies of ovarian, cervical, breast cancers [121–126]. Gynecological adenocarcinomas appeared to differentiate themselves from other adenocarcinomas by a higher IDO expression. These findings showcase both shared traits and unique IC characters of gynecological adenocarcinomas.

The results of canine-human clusters comparison by differential expression and PCA did not converge, except for A2AR, highlighting it as the most confident species-related gene. In humans, A2AR can be upregulated in response to anti-PD-1 treatment, and its blockade increases treatment efficacy [127]. While we observed trends in cancer type clusters, the IC signature heterogeneity across individual patients with the same diagnosis appears to be a crucial research direction to explore.

2.3.11 Cross-species target conservation

As we assessed the conservation of IC amino acid sequences between dog and human (**Tab. 4**), TIM-3 was the least (24/100) and B7-H4 together with NECTIN-4 were the most (94/100) conserved of analyzed proteins. While these scores do not specifically describe extracellular domains holding the potential epitopes, the observation suggests some canine ICs may be druggable with caninized human antibodies. Others will likely require the development of canine-specific antibodies. While the cross-reactivity of human antibody therapeutics is disputed, Pantelyushin et al. convincingly described ipilimumab, nivolumab, atezolizumab and avelumab (targeting CTLA-4, PD-1 and PD-L1 respectively) as cross-reactive, with various levels of functionality [128]. In this context Nectin-4 stands as a particularly interesting target, combining high conservation, IC inhibition and tumor specificity [129].

2.3.12 Limitations

The limitations of our study were primarily dictated by the available data. While the selected human dataset did not include osteosarcoma, it provided 27 other precisely-diagnosed cancer types including some closely related ones. In contrast, we could only analyze 14 distinct types of canine cancer. This discrepancy is due to a paucity of canine studies and the less precise diagnostic categorization of canine cancers. We anticipate that future subdivisions of canine cancers into discrete subtypes will allow for more precise comparison with human equivalents, thus revealing higher interspecies similarity. The study focused on 44 ICs, but many have likely not been identified yet, which precludes capturing the full complexity of immune checkpoint landscapes. Further, we could not analyze several ICs due to their apparent absence in the CanFam6 reference transcriptome; these included SIGLEC7/9, SLAMF3/4, LILRB1-5, BTN2A1, and KIRs. Multiple gene markers of immune cell populations were also excluded due to their absence or misrepresentation in the reference transcriptome (see: supplementary methods). These research limitations will diminish as the canine model becomes more widespread.

A common challenge in transcriptomic and proteomic studies of solid tumors, including ours, is identifying the cell type responsible for the analyte presence. IC ligands, in particular, can be expressed by multiple cell types within the tumor microenvironment. However, the source of ICs doesn't significantly impact our evaluation of the IC landscape. Regardless of the source, inhibitory ligands interact with immune effector cells and are potential ICB targets. One caveat is the possibility of cancer cells themselves expressing functional IC receptors, a hypothesis lacking consistent evidence. We followed the common assumption that comparatively high IC expression indicates a promising target.

The functional equivalence of ICs in canines and humans isn't guaranteed. Interspecies variations in IC functionality, as seen in GITR between mice and humans, may bolster the canine model's relevance, yet warrant caution in studying isolated ICs [130]. Moreover, genetic and metabolic differences between the two species may limit the applicability of the findings to humans. Despite promising results, it is essential to validate the functional equivalence of human and canine ICs.

Transcript abundance, as measured by RNAseq, does not perfectly correlate with the production and membrane presence of the associated protein [131–134]. However, transcriptomics provides a snapshot of the cell's signaling frozen in time, offering invaluable insights. Flow cytometry and immunohistochemistry can help validate our findings as more antibodies against canine ICs become available.

2.3.13 Future perspectives

One important aspect of the immune checkpoint signatures that remained beyond the scope of this study is their interplay with therapy response, as well as emergence of resistance, especially via upregulation of undrugged ICs. Additionally, the possibility of predicting hyperprogressive disease based on those signatures is a promising question. In light of the escalating development costs of novel immunotherapeutics and challenges in thoroughly evaluating their effects before approval, streamlining the preclinical drug screening and development is critical. Here, we unveil key similarities in canine and human immune checkpoint expression patterns of cancer, thereby reinforcing the argument for comparative oncology. Our analysis of individual human cancer IC signatures can pave the way for more personalized treatment decisions and monitoring. Ultimately, we hope these insights will catalyze advancements in both veterinary and human oncology leading to the generation of more accessible, effective, and safer immunotherapies.

2.4 Methods

2.4.1 Acquisition of canine gene expression data

Study selection

Openly available canine RNA sequencing data were utilized for this analysis. A comprehensive literature search was conducted on PubMed on 2022-05-15, employing the search query: '((rnaseq) OR (rna-seq) OR (rna sequencing) OR (transcriptomics)) AND ((dog) OR (canine) OR (canis)) AND cancer'. Of the 413 identified articles, 15 studies representing 8 cancer types met the inclusion criteria outlined below:

1. Pertinence to canine cancer.
2. Inclusion of original data.
3. Data source: data originated from tumor tissues as opposed to cell cultures, single cells or exosomes; cell lines are notoriously different from their tumors of origin, and data for single cells or extracellular vesicles is not comparable with bulk tumor.
4. Accessibility: RNAseq data was declared openly available, actually linked to and accessible.
5. Data format: raw data was provided as FASTQ, SRA or BAM (complete) files so that raw reads from all datasets could be analyzed together consistently.
6. Adequate description: the samples and methods were sufficiently described, ensuring the used protocols make the data reliable and comparable.
7. Sample preservation method: samples were preserved by snap-freezing or RNAlater infusion and freezing - known to maintain RNA quality better than the FFPE method.
8. mRNA enrichment: Samples were mRNA-enriched through poly-A selection or rRNA depletion, as total RNA and mRNA sequencing would not be fully comparable.
9. Sequencing method: Paired-end (PE) sequencing was conducted, providing higher accuracy and more dependable data using contemporary sequencing technology.

10. Treatment status: None of the animals appeared to have received chemotherapy or radiation therapy before tissue sampling, as this could alter the transcriptome of the tumors, including IC expression. This study focused on treatment-naive tumors.

If multiple studies of the same cancer type passed the criteria, the one with maximum sample number was included. Additionally, pulmonary neoplasm and oral melanoma datasets unavailable elsewhere were obtained from ICDC canine commons. We strived to have no less than 10 samples per cancer type where possible, hence an additional T-cell lymphoma dataset was downloaded from ICDC. All ICDC data pass our inclusion criteria. In the originally chosen HSA study, 15 of 23 samples were rejected because of very short (length: 25) reads incongruent with the other samples (length: 38) and not compatible with the quantification settings. To achieve a sufficient number of samples, we used data from an additional Hemangiosarcoma publication (of the 51 samples found at SRA database, 6 appeared to come from cell lines and were rejected, leaving out 45 samples, 2 less that described in the paper).

Exceptions made

We made the following exceptions to get insight into cancer types unavailable otherwise: OSCC (FFPE samples), ameloblastoma (SE sequencing), meningioma (SE + FFPE), prostate cancer (Total RNA library). In case of insulinoma the type of sequenced RNA library was unknown, the reads were pre-trimmed with an unknown method, and the shared bam files were based on an older canine reference genome (CanFam3.1). Hence, insulinoma analysis must be considered purely exploratory. One of the 12 Ameloblastoma samples was not downloadable at the time of the analysis. In the BCL study 4 of 16 were either T-cell or undefined lymphomas. In glioma study, of the 83 samples, 38 came from FFPE, and of the 45 frozen ones, 42 were available for download. The samples not satisfying the inclusion criteria were rejected. A summary of the cancer types, their abbreviations, data sources and articles of origin can be found in **Table 3** below.

Table 3: Data sources for the RNAseq analysis; FFPE – formalin-fixed paraffin-embedded; SE - single-end sequencing; na – not applicable, ns - not specified; if the dataset contained more samples but only a subset passed the criteria or was available, the total number was put in brackets.

Study ID	Cancer type	Short	# of dogs	Exception	Dataset access	REF
PMID: 29674676	B-cell lymphoma	BCL	12(16)	-	GSE112474	[135]
PMID: 30684308	T-cell lymphoma	TCL	6	-	GSE122347	[136]
NCATS-COP01	T-cell lymphoma	TCL	12	-	caninecommons. cancer.gov/	[137]
PMID: 32049048	Glioma	Glioma	42(83)	-	PRJNA579792	[138]
PMID: 31570656	Hemangiosarcoma	HSA	8(23)	-	PRJNA562916	[139]
PMID: 24525151	Hemangiosarcoma	HSA	45(51)	Data not shared in the paper	PRJNA376380	[140]
PMID: 30089113	Invasive urothelial carcinoma	iUC	29	-	GSE110661	[141]
PMID: 31413331	Mammary tumors	Breast	158	-	GSE119810	[142]
NCATS-COP01	Oral melanoma	OM	12	-	caninecommons. cancer.gov/	[137]
PMID: 29066513	Osteosarcoma	OS	31	-	GSE87649	[143]
NCATS-COP01	Pulmonary neoplasm	Lung	12	-	caninecommons. cancer.gov/	[137]
PMID: 31041834	Ameloblastoma	AM	11(12)	SE	PRJNA533473	[144]
PMID: 32665562	Insulinoma	INS	6	Ns RNA library	PRJNA574196	[145]
PMID: 29073243	Meningioma	MEN	13	SE + FFPE	GSE95048	[146]
PMID: 33142242	Oral squamous cell carcinoma	OSCC	10	FFPE	PRJEB34234	[147]
PMID: 31519932	Prostate cancer	Prostate	11	Total RNA library	GSE122916	[148]

2.4.2 Acquisition of human gene expression data

Quantified expression of the IC genes of interest was sourced from the PanCancer Analysis of Whole Genomes (PCAWG) dataset and obtained from the European Bioinformatics Institute (EBI) Expression Atlas. The dataset encompassed 1200 samples from 27 human cancer types. Detailed descriptions of the data acquisition, ethical considerations, and primary sequencing techniques can be found in their accompanying publication [105].

45

2.4.3 Processing of canine RNA sequencing data

Raw canine RNAseq data was pre-processed from BAM or SRA files into fastq format, has undergone quality control with FastQC v0.11.6 [149] and MultiQC v1.12 [150], and was quantified without trimming on a PLGrid Prometheus computational cluster. Reads were quantified with Kallisto v0.45.0 [151], using a Kallisto-generated index based on an Ensembl canine reference transcriptome release 106 (Canis_lupus_familiarisboxer.Dog10K_Boxer_Tasha.cdna.all.fa file version). Parameters for PE data were default (K-mer length of 31). The setting for SE samples was "-l 200 -s 20" as bioanalyzer reports for sequencing libraries were not available. The resulting abundance data was imported to the R/Rstudio using the following libraries: GenomicFeatures [152], tximport, tximportData [153]. Technical replicates were collapsed, the entire dataset was normalized with DESeq2 [154] and results were visualized using ggplot2 [155] combined with *Viridis* colorblind-friendly color map [156]. DESeq2 performs normalization in regard to the size and composition of sequencing libraries created in each experiment, which allows for a comparison of different sample groups (cancer types in our case). When combined with tximport, it also normalizes the abundance data in regard to average transcript length of each gene. This in turn allows for comparison of expression between different genes. For all canine (single-species) analyses, DESeq-2 normalized counts were used as the most appropriate for combining sequencing data obtained with different protocols and from different tissues. The relation between gene expression and particular dog breeds was not assessed due to inconsistent quality of provided sample metadata.

2.4.4 Integration of human and canine data

To compare cross-species datasets, the dataset representing the abundance of IC expression in canine cancers was transformed into transcripts per million (TPM) units. This version of the dataset will be referred to as "TPM data" throughout the remainder of this section. This transformation was carried out to ensure compatibility between the canine data and the PCAWG human dataset, which was already quantified in TPM. Canine and human datasets were merged and standardized (scaled and centered) using the 'scale' function in R. Standardized dataset was used for subsequent analyses unless otherwise stated.

2.4.5 The choice of immune checkpoints

The research on immune checkpoints is dynamically evolving, and new ICs emerge. A list of IC receptors and ligands was performed based on literature, including well known (PD-1) and emerging (SLAMF7) ones [157]. ICs that were available in the canine reference transcriptome of choice were selected for the study (**Tab. 4 below**).

2.4.6 Conservation of the IC amino acid sequence

Identity [%] and coverage [%] were calculated with NCBI BlastP alignment of canine and human amino acid sequences of the top canonical protein-coding Ensembl transcripts. Conservation score was calculated as identity*coverage/100. One caveat of this approach is that it does not prioritize the extracellular, exposed domains (potential antibody epitopes).

Table 4: We analyzed the transcript expression for established and emerging immune checkpoints (ICs). ICs were classified by their impact on the immune reaction: inhibitory, stimulatory, or complex. Identity [%] and coverage [%] were calculated by BlastP alignment of canine and human proteins; conservation was calculated as identity*coverage/100. Receptors and their canonical ligands were marked with the same shades of gray.

	Gene	Protein name	Description	Canine Ensembl ID	Identity	Coverage	Conservation
Inhibitory ICs	PDCD1	PD-1	Programmed cell death 1	ENSCAFG00000013184	72	39	28
	PDCD1LG1	PD-L1	Programmed cell death 1 ligand 1	ENSCAFG00000002120	76	100	76
	PDCD1LG2	PD-L2	Programmed cell death 1 ligand 2	ENSCAFG00000002121	67	95	64
	HAVCR1	TIM-3	Hepatitis A virus cellular receptor 1	ENSCAFG00000023455	40	59	24
	LGALS9	GAL-9	Galectin 9	ENSCAFG00000018641	72	91	66
	LAG3	LAG-3	Lymphocyte Activation Gene 3	ENSCAFG00000014675	79	95	75
	FGL1	FGL-1	Fibrinogen like 1	ENSCAFG00000032313	88	100	88
	CTLA4	CTLA-4	Cytotoxic T-lymphocyte associated protein 4	ENSCAFG00000012876	87	100	87
	CD28	CD28	CD28 molecule	ENSCAFG00000012872	80	82	66
	CD80	CD80	CD80 molecule	ENSCAFG00000010997	54	100	54
	CD86	CD86	CD86 molecule	ENSCAFG00000011751	62	83	51
	TIGIT	TIGIT	T cell immunoreceptor with Ig and ITIM domains	ENSCAFG00000010817	67	100	67
	NECTIN4	NECTIN4	Nectin Cell Adhesion Molecule 4	ENSCAFG00000012722	94	100	94
	PVR	CD155	Poliovirus receptor	ENSCAFG00000004666	57	96	55
	SIRPA	SIRPA	Signal-regulatory protein alpha	ENSCAFG00000025524	74	100	74
	CD47	CD47	Integrin associated protein	ENSCAFG00000009587	66	91	60
	PVRIG	PVRIG	Poliovirus receptor-related immunoglobulin domain-containing	ENSCAFG00000014498	58	98	57
	VSIR	VISTA	V-domain Ig suppressor of T-cell activation	ENSCAFG00000014354	82	100	82
	VTCN1	B7-H4	V-set domain-containing T-cell activation inhibitor 1	ENSCAFG00000009858	94	100	94
	ADORA2A	A2AR	Adenosine A2A receptor	ENSCAFG00000013828	93	100	93
	CYBB	NOX2	NADPH oxidase 2	ENSCAFG00000013933	93	100	93
Stimulatory ICs	ICOS	ICOS	Inducible T cell costimulator	ENSCAFG00000012880	70	99	69
	ICOSLG	ICOSLG	Inducible T cell costimulator ligand	ENSCAFG00000010718	62	50	31
	TNFRSF4	OX40	TNF receptor superfamily member 4	ENSCAFG00000019328	64	64	41
	TNFSF4	OX40L	TNF superfamily member 4	ENSCAFG00000014587	68	99	67
	TNFRSF9	4-1BB	TNF receptor superfamily member 9	ENSCAFG00000019673	78	100	78
	TNFSF9	4-1BBL	TNF superfamily member 9	ENSCAFG00000030400	66	58	38
	CD40	CD40	CD40 molecule	ENSCAFG00000009994	68	90	61
	CD40LG	CD40L	CD40 ligand	ENSCAFG00000018945	83	100	83
	CD27	CD27	CD27 molecule	ENSCAFG00000015149	72	98	71
	CD70	CD70	CD70 molecule	ENSCAFG00000030308	69	100	69
	CD226	CD226	CD226 molecule	ENSCAFG00000000038	65	100	65
Complex ICs	TNFRSF18	GITR	Glucocorticoid-induced TNFR-related protein	ENSCAFG00000019329	65	86	56
	TNFSF18	GITRL	GITR ligand	ENSCAFG00000014590	72	100	72
	TNFRSF14	HVEM	Herpesvirus entry mediator	ENSCAFG00000019422	58	80	46
	TNFSF14	LIGHT	Homologous to lymphotoxin	ENSCAFG00000018627	82	100	82
	CD160	CD160	CD160 molecule	ENSCAFG00000055618	73	64	47
	BTLA	BTLA	B- and T-lymphocyte attenuator	ENSCAFG00000010480	62	100	62
	KLRC1	NKG2A	Killer cell lectin like receptor C1	ENSCAFG00000028587	55	69	38
	CD276	B7-H3	CD276 molecule	ENSCAFG00000017820	94	60	56
	CD96	TACTILE	T cell activation, increased late expression	ENSCAFG00000010358	69	100	69
IC-like	SLAMF7	SLAMF7	SLAM Family Member 7	ENSCAFG00000012598	60	98	59
	ARG1	Arginase 1	Arginase 1	ENSCAFG00000000386	92	100	92
	IDO1	IDO	indoleamine 2,3-dioxygenase 1	ENSCAFG00000005750	68	97	66

47

2.4.7 The choice of cell marker genes

Our list of immune cell markers was inspired by the NanoString panels [158]. The list was adapted based on the reference transcriptome and gene specificity in Human Protein Atlas [159]. TNFRSF17 gene was rejected as it was absent in quantification results and CPA3 gene was rejected as misleading upon inspecting the results (see: Supplementary Methods).

2.4.8 Immune infiltrate composition

For each of the chosen marker genes, a mean value was calculated based on its means in all cancer types. Subsequently, expression levels for individual cancer types were normalized by dividing them by this mean. This normalization approach was adopted to ensure equal contributions from each marker to the overall analysis, independent of their inherent abundance. In the absence of precise information regarding canine cell markers, this strategy was deemed most appropriate. For each cell type category, means of normalized values were computed for marker genes. These averaged values were then visualized.

2.4.9 Immune inhibition score

The Immune Inhibition Score was calculated in a manner analogous to how the estimation of immune infiltrate composition was performed. Immune checkpoints (ICs) were categorized as 'inhibitory', 'stimulatory', or 'other'. For each IC, mean expression value was calculated across cancer types. Subsequently, means for individual cancer types were divided by this mean. This step was taken to account for the wide variations in expression and the absence of specific signaling impact weights for each IC molecule. Data were then averaged within each category. For each cancer type, the derived inhibitory score was divided by the stimulatory score, resulting in a singular estimate that represented the immune environment character for that particular cancer.

2.4.10 Hierarchical clustering (HC)

Hierarchical clustering was conducted in R based on standardized cross-species TPM data. For each cancer type, a distinct vector was created to encapsulate the median

expression of all ICs. Those vectors were compared in a distance matrix created with the 'amap::Dist' package employing Pearson's correlation as the distance metric. The resulting matrix was subjected to hierarchical clustering using the 'hclust' function with the 'ward.D2' Ward linkage method. The clustered output was visualized as a dendrogram with the aid of the 'factoextra' package in R.

2.4.11 Different transcript abundance between clusters

An exploratory analysis of differential transcript abundance between cancer type clusters was performed in R, based on the TPM data.

2.4.12 Functional network analysis of immune checkpoints

The potential functional relationships between ICs were analyzed and visualized as a network using STRING (Search Tool for the Retrieval of Interacting Genes/Proteins; https://string-db.org/), a robust database and computational resource that offers comprehensive information on protein-protein interactions from diverse sources, including experimental data, computational predictions, and literature [160].

2.4.13 Uniform manifold approximation and projection (UMAP)

The UMAP analysis was conducted using the 'umap' function in R and standardized data. The default configuration was set with a n_neighbors value of 15, n_components set to 2, and min_dist set at 0.1. UMAP was chosen for its capability to capture the nuances of high-dimensional data and effectively project them onto a two-dimensional space, highlighting potential clusters or patterns within the data.

2.4.14 Principal component analysis (PCA)

PCA is sensitive to the scale of variables and performs best with normally distributed data. Variables vastly different in the order of magnitude can lead to biased principal components that reflect the larger scale variables more. However, transcriptomic data often exhibits a wide range of abundance values and is not typically normally distributed. To address these issues, the data was first log2-normalized. This transformation compressed the scale of the data and approximated a normal distribution. Subsequently, the normalized data was standardized (centered and scaled) within the 'prcomp' or 'PCAtools::pca' R functions. This step involved

subtracting the mean and dividing by the standard deviation of each variable, which ensured all variables contribute equally to the analysis. Next, PCA was performed with the aforementioned functions.

2.4.15 Healthy vs. cancerous tissue comparison

Healthy reference samples originated from areas adjacent to primary tumors as described in [105].

2.4.16 Computational environment

Below, detailed information on the computational environment used for this study is presented. The raw data pre-processing and read quantification was performed on a Prometheus cluster, and the detailed data analysis was conducted in R 4.2.3 (2023-03-15 ucrt), using RStudio 2022.07.0 (Build 548) on a platform x86_64-w64-mingw32/x64 (64-bit), running under Windows 10 x64 (build 22621). Detailed information about the versions of all directly used R packages, and their recursively defined dependencies, is provided in **Table 5** below.

Table 5: R configuration: versions of the R packages directly used in the projects as well as their dependencies

package	version		package	version		package	version
askpass	1.1		grDevices	4.2.3		RColorBrewer	1.1.3
backports	1.4.1		grid	4.2.3		readr	2.1.4
base64enc	0.1.3		gtable	0.3.2		readxl	1.4.2
bit	4.0.5		haven	2.5.2		rematch	1.0.1
bit64	4.0.5		highr	0.10		rematch2	2.1.2
blob	1.2.4		hms	1.1.2		reprex	2.0.2
broom	1.0.4		htmltools	0.5.4		rlang	1.1.0
bslib	0.4.2		httr	1.4.5		rmarkdown	2.20
cachem	1.0.7		ids	1.0.1		rstudioapi	0.14
callr	3.7.3		isoband	0.2.7		rvest	1.0.3
cellranger	1.1.0		jquerylib	0.1.4		sass	0.4.5
cli	3.6.0		jsonlite	1.8.4		scales	1.2.1
clipr	0.8.0		knitr	1.42		selectr	0.4.2
colorspace	2.1.0		labeling	0.4.2		splines	4.2.3
conflicted	1.2.0		lattice	0.20.45		stats	4.2.3
cpp11	0.4.3		lifecycle	1.0.3		stringi	1.7.12
crayon	1.5.2		lubridate	1.9.2		stringr	1.5.0
curl	5.0.0		magrittr	2.0.3		sys	3.4.1
data.table	1.14.8		MASS	7.3.58.3		systemfonts	1.0.4
DBI	1.1.3		Matrix	1.5.3		textshaping	0.3.6
dbplyr	2.3.1		memoise	2.0.1		tibble	3.2.1
digest	0.6.31		methods	4.2.3		tidyr	1.3.0
dplyr	1.1.0		mgcv	1.8.42		tidyselect	1.2.0
dtplyr	1.3.0		mime	0.12		tidyverse	2.0.0
ellipsis	0.3.2		modelr	0.1.10		timechange	0.2.0
evaluate	0.20		munsell	0.5.0		tinytex	0.44
fansi	1.0.4		nlme	3.1.162		tools	4.2.3
farver	2.1.1		openssl	2.0.6		tzdb	0.3.0
fastmap	1.1.1		pillar	1.8.1		utf8	1.2.3
forcats	1.0.0		pkgconfig	2.0.3		utils	4.2.3
fs	1.6.1		prettyunits	1.1.1		uuid	1.1.0
gargle	1.3.0		processx	3.8.0		vctrs	0.6.0
generics	0.1.3		progress	1.2.2		viridisLite	0.4.1
ggplot2	3.4.1		ps	1.7.2		vroom	1.6.1
glue	1.6.2		purrr	1.0.1		withr	2.5.0
googledrive	2.0.0		R6	2.5.1		xfun	0.39
googlesheets4	1.0.1		ragg	1.2.5		xml2	1.3.3
graphics	4.2.3		rappdirs	0.3.3		yaml	2.3.7

2.5 Supplementary Materials

2.5.1 Supplementary methods

2.5.1.1 Marker gene choice

The CPA3 (mast cell carboxypeptidase A) gene was removed from the results as misleading. We observed an uncharacteristically high CPA3 apparent abundance in insulinoma (a pancreatic cancer), unlikely to originate from mast cells, while pancreatic carboxypeptidase B (CPB2) - a CPA3 paralogue gene - did not exhibit similarly high expression. We performed an Ensembl blast of the canonical CPA3 transcript (ENSCAFT00000071516.2) cDNA sequence against cDNA (transcripts/splice variants) of all Ensembl dog breeds (German Shepherd , ROS_Cfam_1.0, Basenji_breed-1.1. Great Dane and the Boxer itself). In all breeds except the Boxer, the top hits belonged to CPB2. Additionally, we observed similarly high expression of CPA1 and CPA5 in insulinoma. Suspecting a confusion in the reference genome/transcriptome annotation we contacted the Ensembl support. They have kindly checked and confirmed the issue stems from inaccurate annotation of the locus encoding for both CPA3 and CPB2 in the Ensembl dog breeds. In our case readthrough transcripts (ENSCAFT00000071516.2 and ENSCAFT00000087051.2) reportedly joined both transcript sets because of overlapping protein-coding regions. Until the locus is reviewed, we resigned from analyzing CPA3 and CPB expression, which would require modification of the reference used at the fastq files quantification stage.

2.5.2 Supplementary discussion

2.5.2.1 Glioma vs immunotherapy

The parallels between human and canine glioma (and to a large extent canine meningioma and human glioblastoma) necessitate a deeper discussion. The IC signatures of these cancers of the two species presented remarkable similarity in 3 different analyses: UMAP, PCA, and hierarchical clustering of distances. This we consider very strong evidence for the canine glioma resemblance of human glioma in terms of immune checkpoint expression.

Consistent with the rather immunologically 'cold' character of human gliomas, in canine gliomas we observed a high immune inhibition score, as well as high score for T-reg cells and exhausted lymphocytes. The IC expression was relatively low, barring the notably abundant SIRPA - an inhibitory receptor found predominantly on macrophages. Its ligand, CD47 - a broadly expressed membrane protein often overexpressed by cancers - was present at a considerable level.

Our IC-focused findings support canine gliomas as a suitable model for human gliomas, which has in the past been backed on the level of genomic events, methylation and immune infiltration [138]. In the cited study, canine gliomas appeared to recapitulate human pediatric gliomas particularly well. In our analysis of the IC landscape, the similarity in gliomas of both species was pronounced despite the fact that the median patient age was 40.5 years in the glioma dataset we used (calculated based on Table S1 from [105] and patient IDs from EBI PCAWG experiment design table). The human-canine glioma similarity has been exploited in pilot drug studies [161–164] and precipitated more clinical assessments [164]. One team investigated peptide-based inhibition of a CD200 purported IC in high-grade canine gliomas with promising outcomes [165]. However, antibody-based blockade of the major checkpoints has not been studied in the canine model yet.

The lack of such studies can likely be traced to the limited success of the ICB interventions in human glioma and glioblastoma. However, one could argue these unsatisfactory results only call for more investment in innovative research approaches. Moreover, new studies begin to challenge the notion of glioma as untreatable with immunotherapy [166–168].

Still, there is no shortage of challenges in studying and treating gliomas, unique as they are. These issues have been elegantly set in the wider theme of cancer immunology and comprehensively synthesized by Khasraw and colleagues [169]. To name a few, the availability and volume of the samples is limited and repeated biopsies are not possible due to the tumor location. These factors limit the statistical power of studies and the range of assays that can be run. The unique brain environment, with its specific immune features, hypoxia, and other unusual physiological conditions, is particularly difficult to mimic realistically in animal models, both syngeneic and in xenografts. What's more, the knowns established in other cancers, become unknowns

in glioma. For instance, tumor mutational burden (TMB), commonly considered a proxy for tumor immunogenicity and a predictor of ICB success, does not hold the same predictive power in glioma as in other tumors [170,171]. The limited understanding of glioma led the field to try treatments that were promising in other cancers rather than based on glioma-specific rationale. Researchers do call for novel preclinical animal models for studying glioma and glioblastoma [169]. This is where the canine model has a special role to play.

Yet another troublesome characteristic of gliomas is the myeloid character of infiltrating immune cells, which discourages the PD-1 ICB and similar therapeutic approaches that are theoretically aimed at T-cells. It is worthwhile mentioning that the theoretical assumptions of ICB do not cover all its effects - it is becoming clear that B, NK and other immune cells meaningfully react to those treatments and contribute to its success or failure [172,173]. More importantly, the prevalence of immune cells of myeloid lineage - such as macrophages, neutrophils and dendritic cells - in gliomas may be the key to treat these cancers successfully.

SIRPA, the inhibitory IC receptor that we detected on a comparatively high level in canine glioma, is a critical mediator of immune responses in myeloid cells. Its interaction with CD47 plays a significant role in cancer immune evasion. SIRPA is naturally highly expressed in the brain [174]. However, elevated levels of SIRPA and CD47 correlate with decreased survival in human glioma and glioblastoma [175]. The CD47/SIRPA interaction in glioblastoma broadly inhibits immune cells, rendering ICB a promising treatment strategy [176,177].

Targeting SIRPA - rather than its ligand CD47 - may be beneficial, reaching the immune cells of interest similarly, rather than the wide array of cells expressing CD47. Targeting SIRPA has been made difficult by SIRPA's low conservation between species (**Tab. 4** - Methods) and high polymorphism within the CD47-binding domain. However, one team has developed pan-allelic, 'pan-mammal' antibodies targeting human, monkey and mouse SIRPA and blocking its interaction with CD47 [178,179]. The team has utilized another unusual animal model for expanding the capabilities of cancer research. Uniquely, they raised the antibodies in chickens. The high phylogenetic distance between chickens and humans, together with low homology of their SIRPA sequences, became a captured opportunity in this case. These chicken

traits allowed for raising antibodies against unique and pan-mammalian epitopes that would not be accessible, were the antibodies raised in mice or rabbits [179]. This is to say that antibodies raised in mice would likely not recognize epitopes of murine SIRPA or many similar mammalian epitopes. While these researchers did not aim at antibodies cross-reactive with canine SIRPA and did not seem to evaluate their activity against the canine protein variant, their elegant approach seems to hold promise of developing such antibodies.

Despite many unique opportunities for immunotherapy development, many still believe glioma and glioblastoma are not treatable with such modality. We propose the high-grade glioma is both a cancer of high unmet need and a chance for cancer immunology to progress through the application of novel animal models. It is also fertile ground for testing key paradigm changes, such as targeting of checkpoints beyond PD-1, personalized therapy recognizing tumor heterogeneity, combinatorial treatments involving appropriate methods for their evaluation, and targeting all of the relevant immune cell populations.

2.5.3 Supplementary tables

Table S1: Mean-based differential IC expression comparing human and canine cancer types and clusters.
Genes that were found significant in both median- and mean-based analysis were marked in bold for denoting increased confidence. Fc - fold change, log2fc - Log of fc, pval - p value, HCC - hepatocellular carcinoma, MEL - melanoma, RCC - renal cell carcinoma, SCC - squamous cell carcinoma, TCC - transitional cell carcinoma.

Comparison	gene_id	mean TPM	reference TPM	fc	log2_fc	zscore	pval	regulation
Canine vs Human	PVRIG	11.07	0.54	20.33	4.35	2.09	1.82E-02	up
	A2AR	8.96	0.51	17.40	4.12	1.98	2.38E-02	up
Sarcoma vs other (human)	B7-H4	0.10	33.92	0.00	-8.41	-2.94	1.64E-03	down
	FGL-1	0.10	24.58	0.00	-7.94	-2.74	3.11E-03	down
	NECTIN4	0.40	43.96	0.01	-6.78	-2.23	1.30E-02	down
	Arginase 1	0.30	14.84	0.02	-5.63	-1.72	4.28E-02	down
	BTLA	0.20	9.07	0.02	-5.50	-1.66	4.81E-02	down
Melanoma vs other (human)	B7-H4	0.10	33.92	0.00	-8.41	-3.65	1.33E-04	down
	NECTIN4	0.50	43.96	0.01	-6.46	-2.62	4.35E-03	down
	Arginase 1	0.20	14.84	0.01	-6.21	-2.49	6.30E-03	down
HCC vs other (human)	NECTIN4	0.20	43.96	0.00	-7.78	-2.66	3.86E-03	down
	B7-H4	0.30	33.92	0.01	-6.82	-2.24	1.24E-02	down
	BTLA	0.20	9.07	0.02	-5.50	-1.67	4.79E-02	down
	Arginase 1	335.00	14.84	22.58	4.50	2.72	3.26E-03	up
	FGL-1	530.00	24.58	21.57	4.43	2.69	3.56E-03	up
	LIGHT	16.00	3.01	5.31	2.41	1.80	3.56E-02	up
Gynecological cancers vs other (human)	FGL-1	0.08	24.58	0.00	-8.20	-4.28	9.55E-06	down
	Arginase 1	0.22	14.84	0.01	-6.10	-3.07	1.06E-03	down
Gastric cluster vs other (human)	BTLA	0.30	9.07	0.03	-4.92	-3.28	5.13E-04	down
	B7-H4	3.36	33.92	0.10	-3.34	-1.90	2.86E-02	down
	Arginase 1	1.50	14.84	0.10	-3.31	-1.88	3.03E-02	down
	CD70	1.34	13.00	0.10	-3.28	-1.85	3.20E-02	down
	CD155	68.40	34.15	2.00	1.00	1.88	2.97E-02	up
	LIGHT	5.80	3.01	1.93	0.95	1.84	3.32E-02	up
Lymphomas vs other (human)	NECTIN4	0.50	43.96	0.01	-6.46	-3.54	2.00E-04	down
	Arginase 1	0.35	14.84	0.02	-5.41	-3.04	1.18E-03	down
	B7-H3	7.00	56.71	0.12	-3.02	-1.91	2.81E-02	down
	CD155	4.50	34.15	0.13	-2.92	-1.87	3.11E-02	down
Human brain cancers vs other human	NECTIN4	0.15	43.96	0.00	-8.20	-2.22	1.33E-02	down
	B7-H4	0.30	33.92	0.01	-6.82	-1.67	4.78E-02	down
	SIRPA	180.00	60.75	2.96	1.57	1.70	4.48E-02	up
Brain cancers with melanoma and RCC vs other (human)	NECTIN4	0.25	43.96	0.01	-7.46	-2.78	2.69E-03	down
	FGL-1	0.15	24.58	0.01	-7.36	-2.73	3.12E-03	down
	B7-H4	0.30	33.92	0.01	-6.82	-2.48	6.61E-03	down
	Arginase 1	0.25	14.84	0.02	-5.89	-2.03	2.11E-02	down
SCC and TCC vs other (human)	FGL-1	0.03	24.58	0.00	-9.94	-4.67	1.52E-06	down
	Arginase 1	0.20	14.84	0.01	-6.21	-2.70	3.51E-03	down
	BTLA	0.43	9.07	0.05	-4.42	-1.75	4.05E-02	down
Carcinomas vs other (human)	BTLA	0.55	9.07	0.06	-4.06	-3.97	3.65E-05	down
	CTLA-4	2.44	17.79	0.14	-2.87	-2.61	4.54E-03	down
	CD27	6.34	26.73	0.24	-2.08	-1.70	4.42E-02	down
Adenocarcinomas vs other (human)	Arginase 1	0.22	14.84	0.01	-6.08	-3.55	1.93E-04	down
	FGL-1	0.40	24.58	0.02	-5.94	-3.46	2.71E-04	down
	BTLA	0.59	9.07	0.07	-3.94	-2.13	1.68E-02	down
Gynecological adenocarcinomas vs other adenocarcinomas (human)	GITRL	0.35	1.04	0.34	-1.58	-2.61	4.54E-03	down
Gastric adenocarcinomas vs other adenocarcinomas (human)	B7-H4	2.53	93.29	0.03	-5.20	-4.01	3.09E-05	down
	CD70	2.00	21.54	0.09	-3.43	-2.48	6.49E-03	down

Table S2: Median abundance of the four species-dividing genes quantified in TPM units; values provided only as an illustration of the general trends.

	CD160	A2AR	NKG2A	OX40
MEDIAN DOG TPM:	2.29	4.27	0.00	0.87
MEDIAN HUMAN TPM:	0.30	0.20	0.40	6.00

Table S3: The number of malignant and healthy samples available in the analyzed human cancers.

Human cancer type	Cancer samples	Normal samples
B-cell non-Hodgkin lymphoma	103	0
bladder transitional cell carcinoma	23	4
breast adenocarcinoma	85	6
cervical adenocarcinoma	2	0
cervical squamous cell carcinoma	18	0
cholangiocarcinoma	18	16
chromophobe renal cell carcinoma	43	14
chronic lymphocytic leukemia	68	0
colorectal adenocarcinoma	51	0
endometrial adenocarcinoma	44	1
esophageal adenocarcinoma	7	0
follicular thyroid carcinoma	47	4
gastric adenocarcinoma	29	2
glioblastoma multiforme	28	0
glioma	18	0
head and neck squamous cell carcinoma	42	1
hepatocellular carcinoma	100	53
invasive lobular carcinoma	6	0
lung adenocarcinoma	37	9
lymphoma	2	0
melanoma	36	0
ovarian adenocarcinoma	101	0
pancreatic adenocarcinoma	75	0
prostate adenocarcinoma	19	1
renal cell carcinoma	117	37
sarcoma	34	0
squamous cell lung carcinoma	47	2
TOTAL:	**1200**	**150**

Table S4: The distance matrix comparing IC signatures between human and canine cancer types; the values are a measure of distance, hence lower numbers equal higher similarity between the two cancer types.

2.5.4 Supplementary figures

Figure S1: IC abundance plot with values normalized to mean expression of each gene, corresponding to Fig. 1A; each value was divided by the mean of the abundances of the respective gene across all cancer types to obtain the visualized abundance score. This way the relative up- or down-regulation of each IC in between the cancer types can be inspected without the confusion caused by transcript abundances characterized by different orders of magnitude depending on the IC; gray color - lack of information due to undetectable expression.
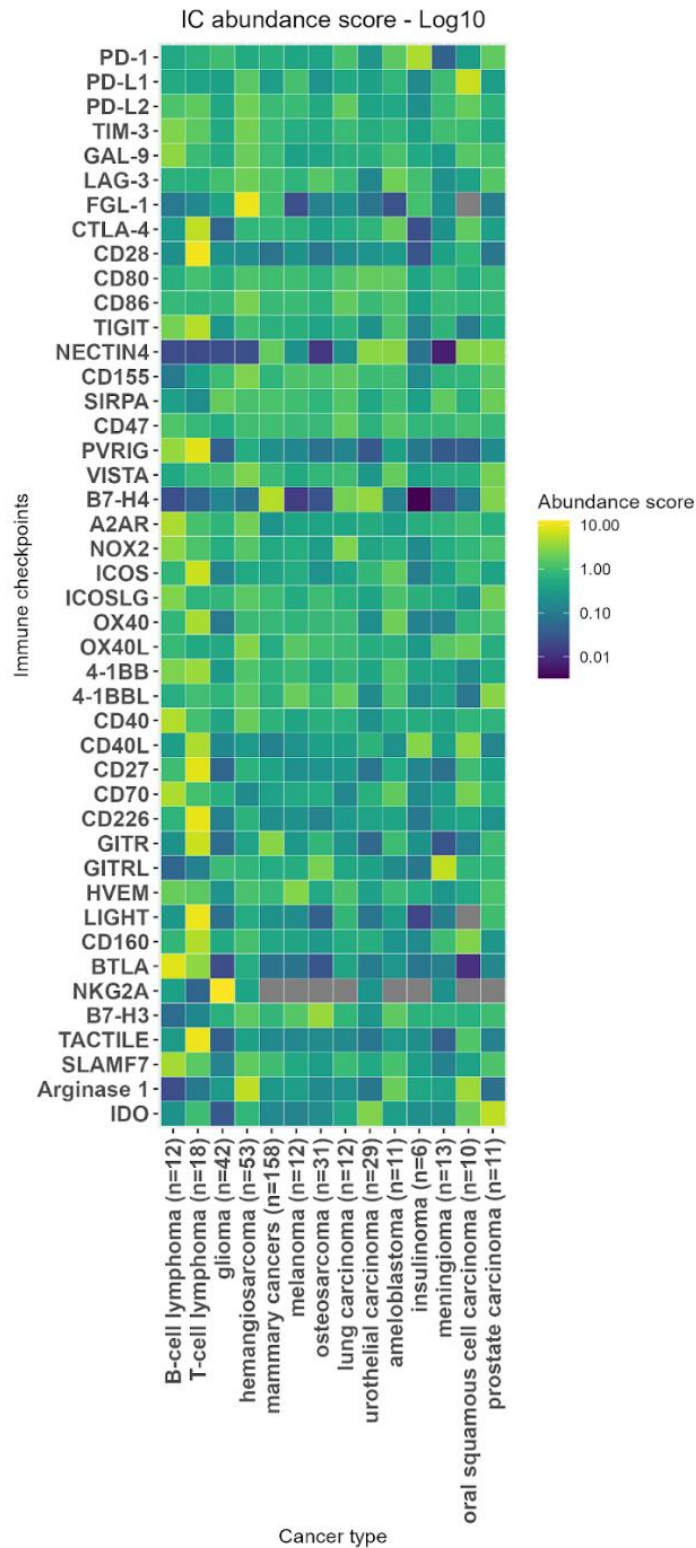
Figure S2: Variance control plot corresponding to the median IC abundance plot (Fig. 1A): Median Absolute Deviation divided by median (MAD/m); grey color - lack of information due to undetectable expression.
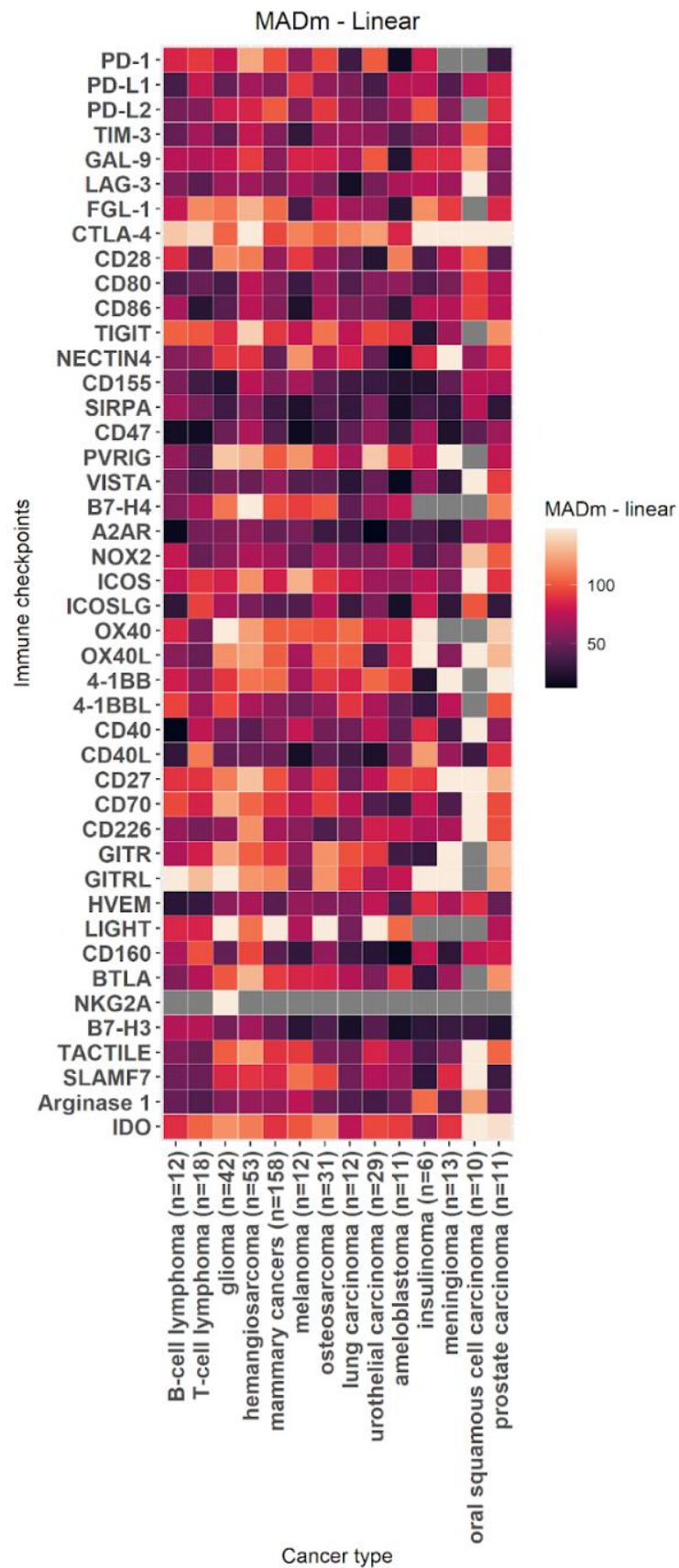
Figure S3: Median TPM-quantified expression of ICs across human cancers based on EBI-obtained human data; gray color - lack of information due to undetectable expression.

Human Median TPM of ICs - Log10
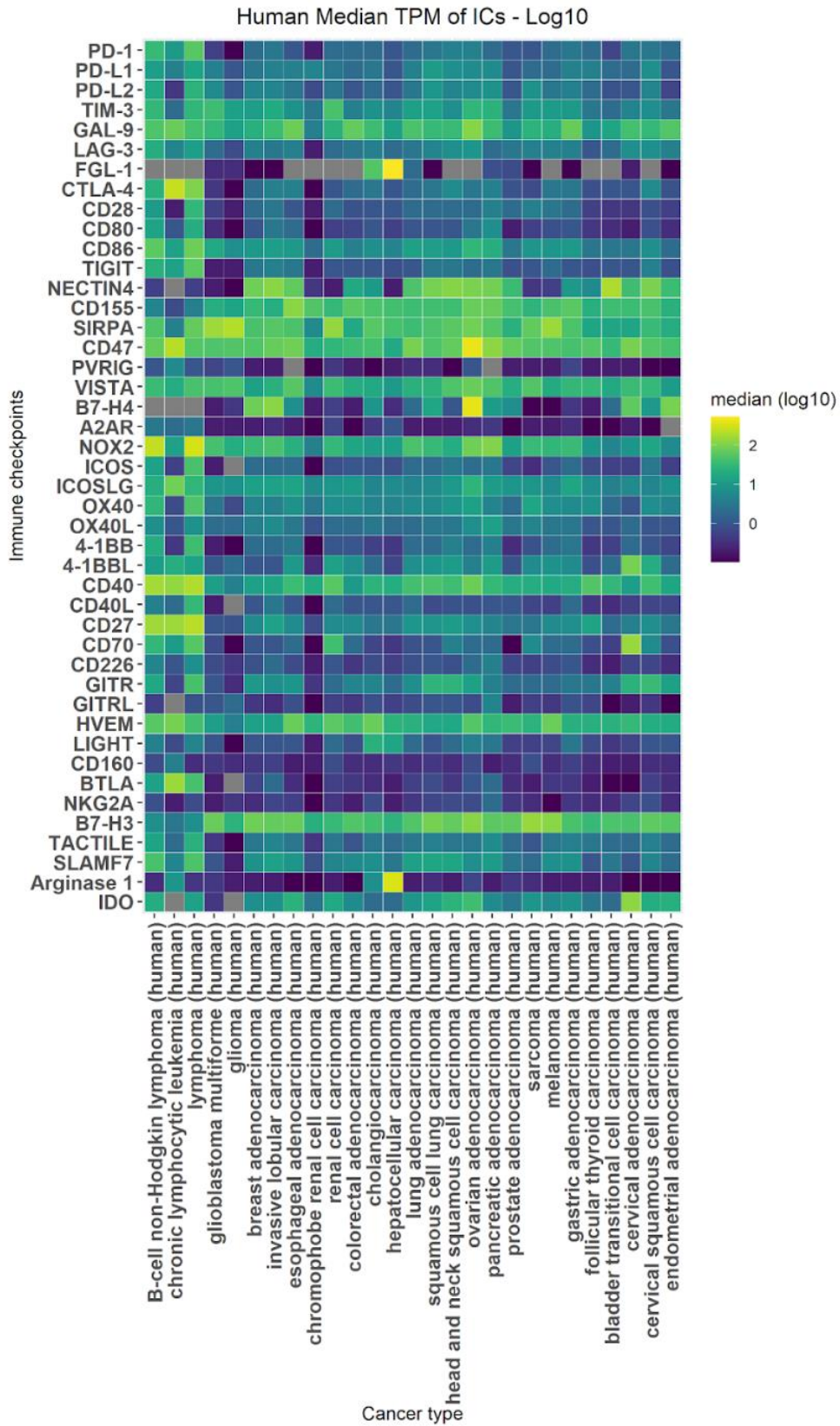
Figure S4: Boxplots representing the distribution of IC expression across individual samples of each canine cancer type.
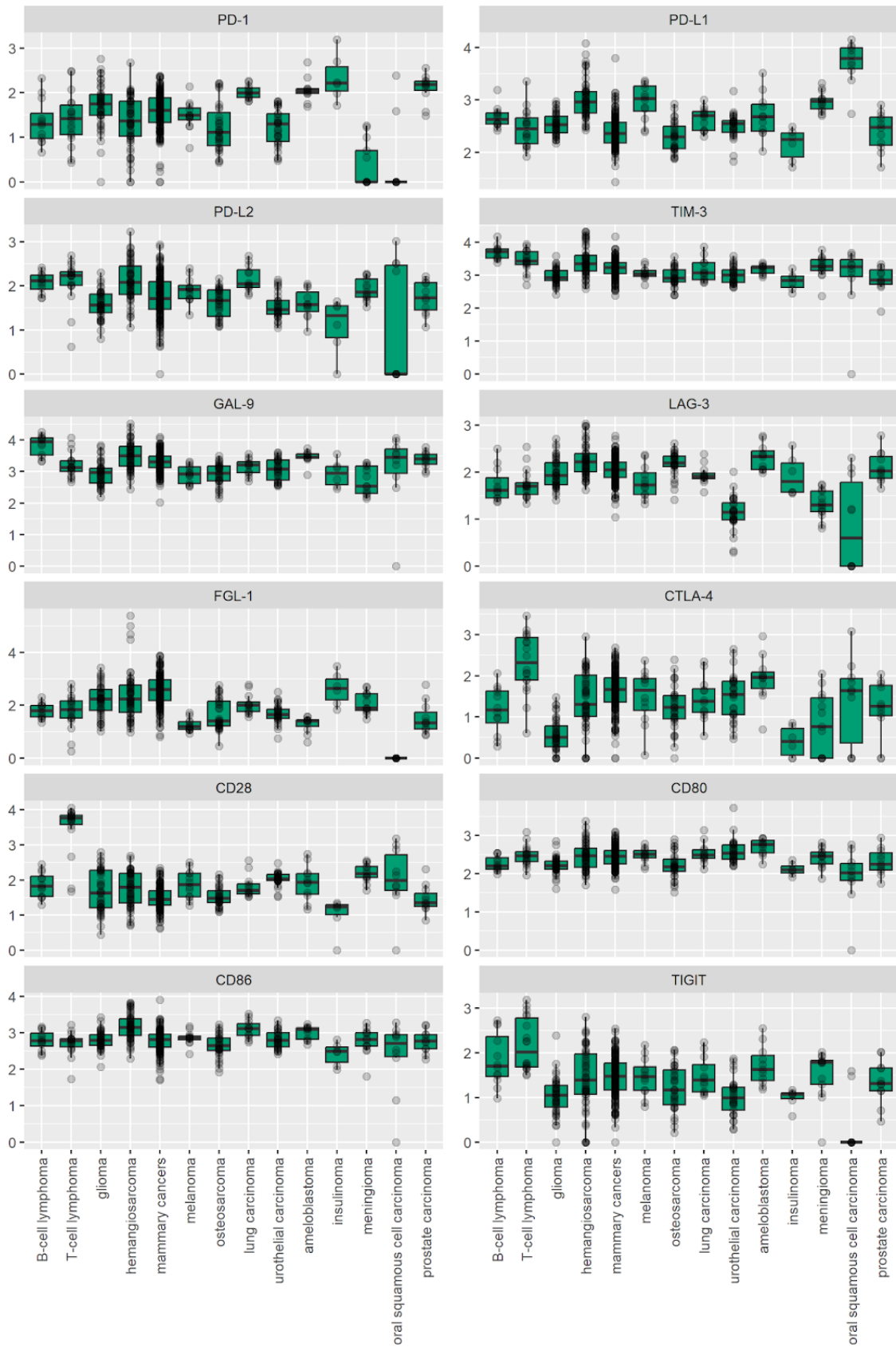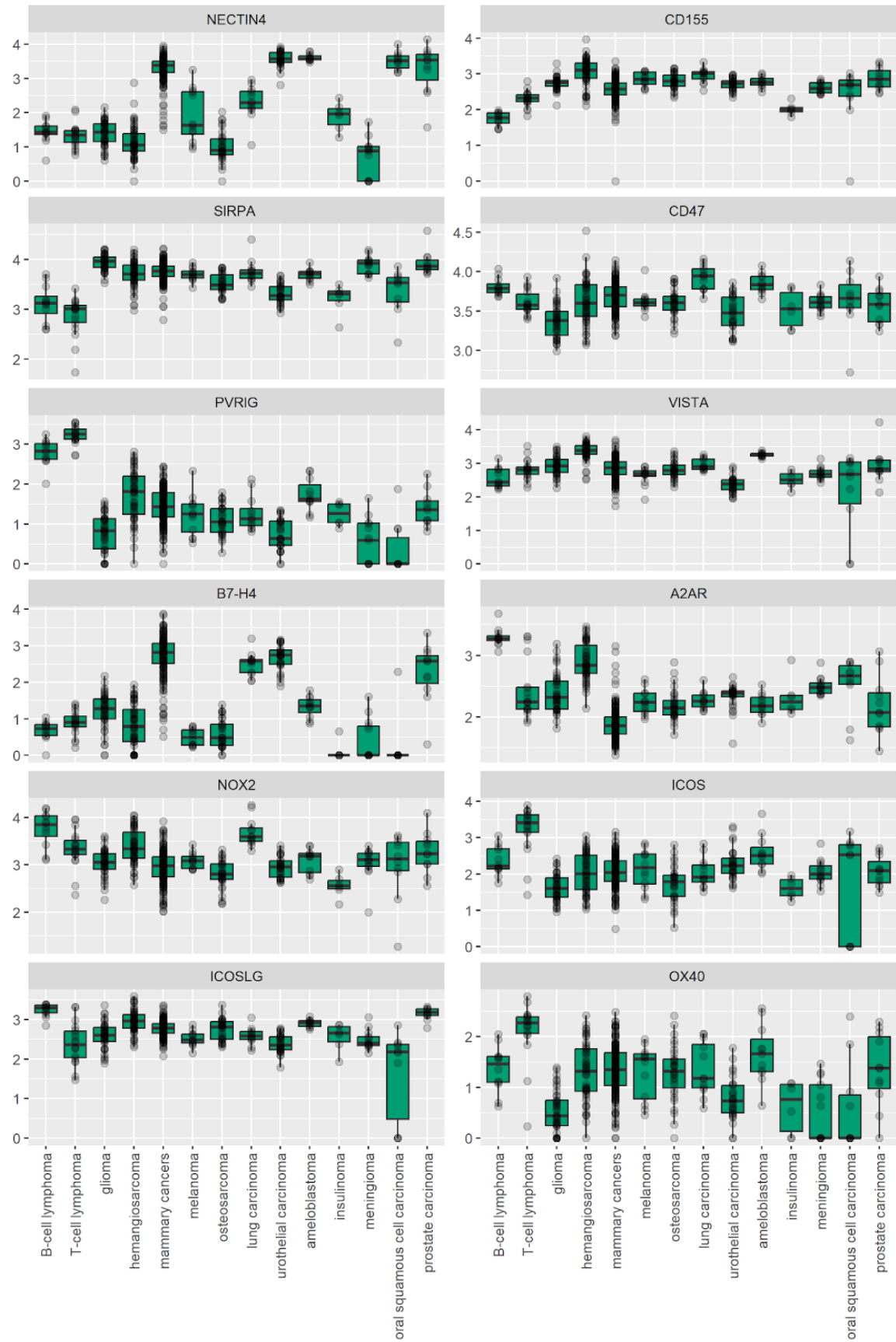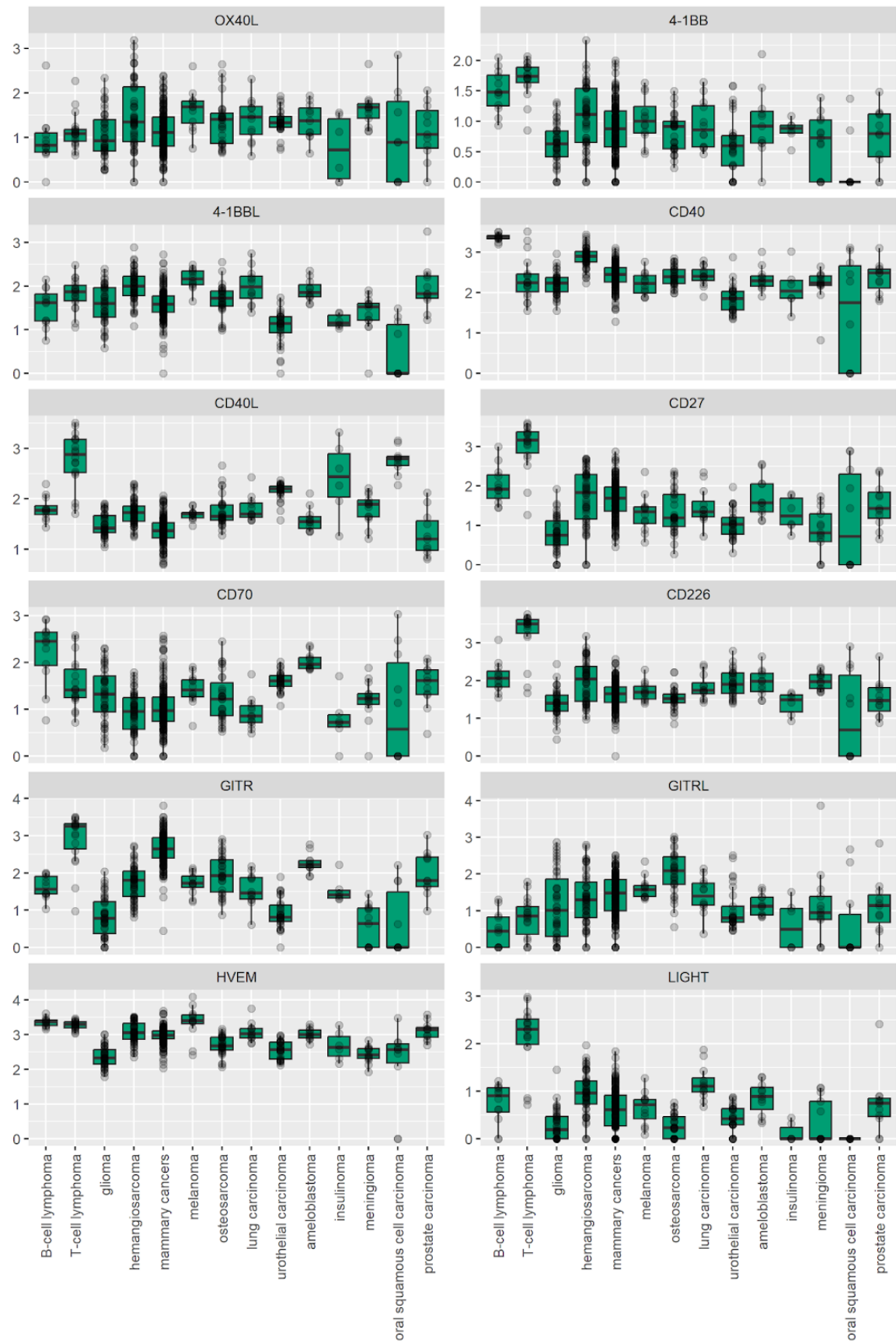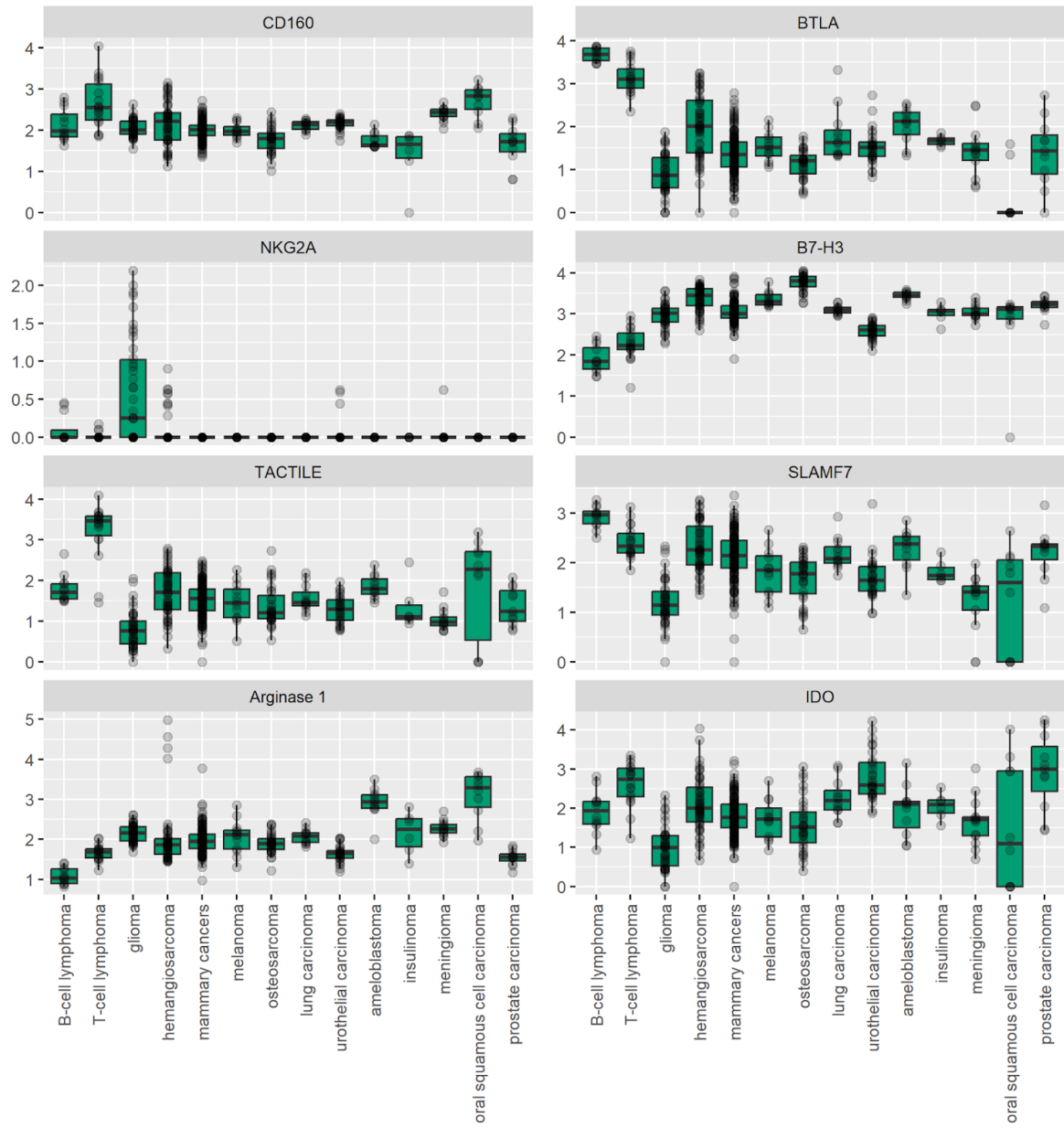
Figure S5: Normalized expression of the markers of immune cell populations infiltrating tumors.
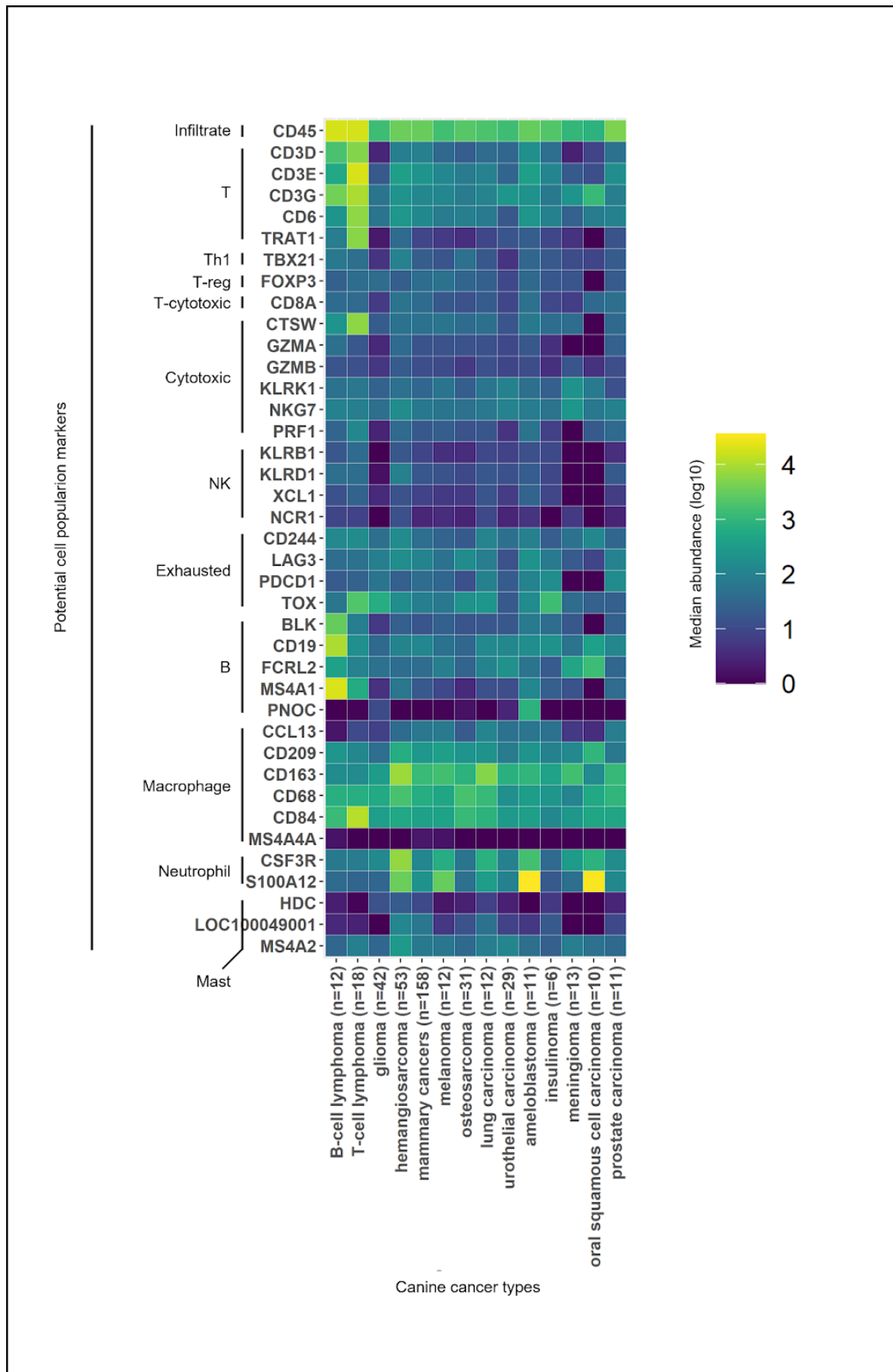
Figure S6: UMAP representation of individual patient IC signatures across the human/canine cancers.

colorectal adenocarcinoma (human)

endometrial adenocarcinoma (human)

esophageal adenocarcinoma (human)

follicular thyroid carcinoma (human)

gastric adenocarcinoma (human)

glioblastoma multiforme (human)

glioma (canine)

glioma (human)

head and neck squamous cell carcinoma (human)

hemangiosarcoma (canine)

UMAP-1

UMAP-2

UMAP-1

UMAP-2

71

urothelial carcinoma (canine)
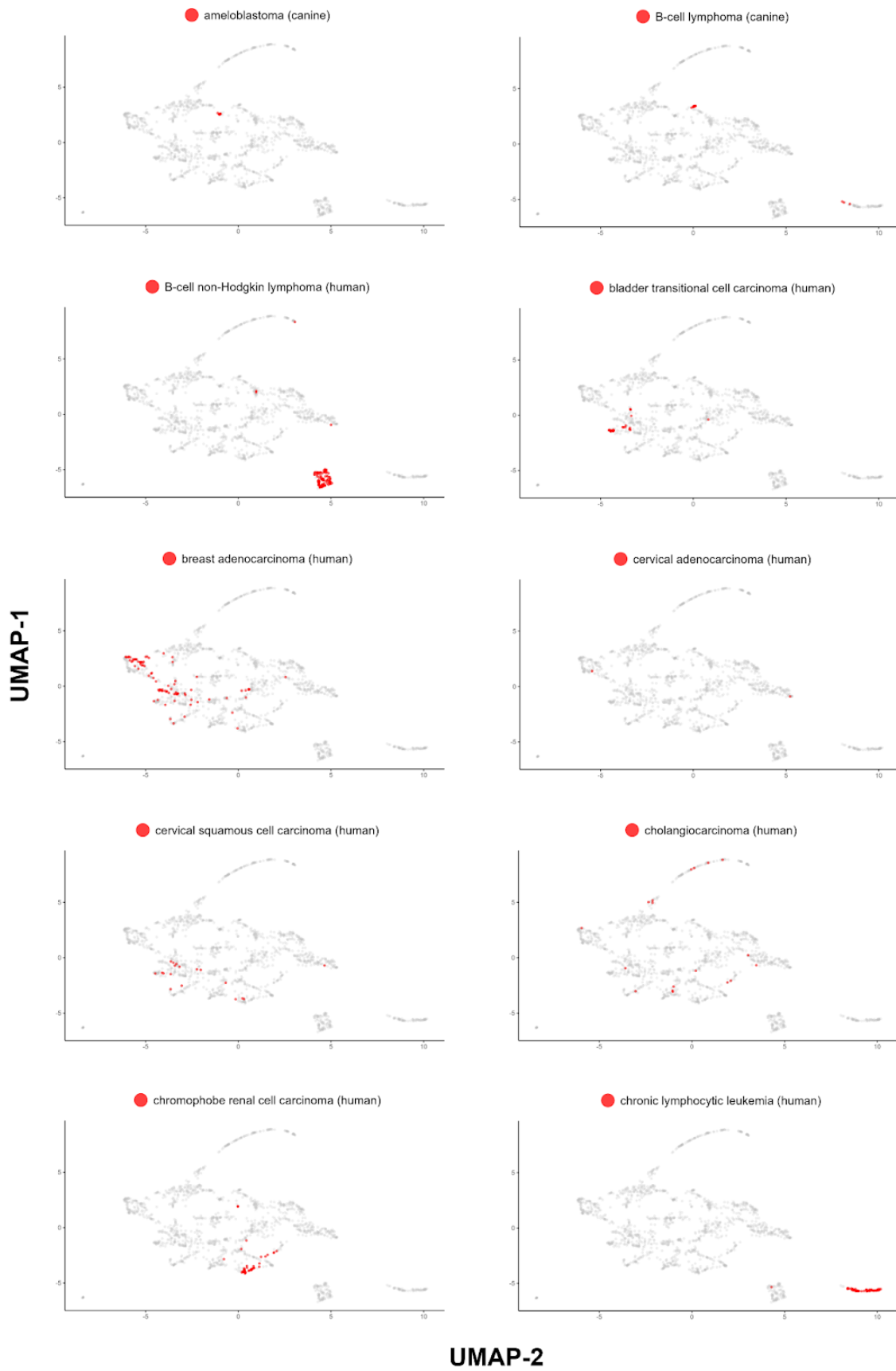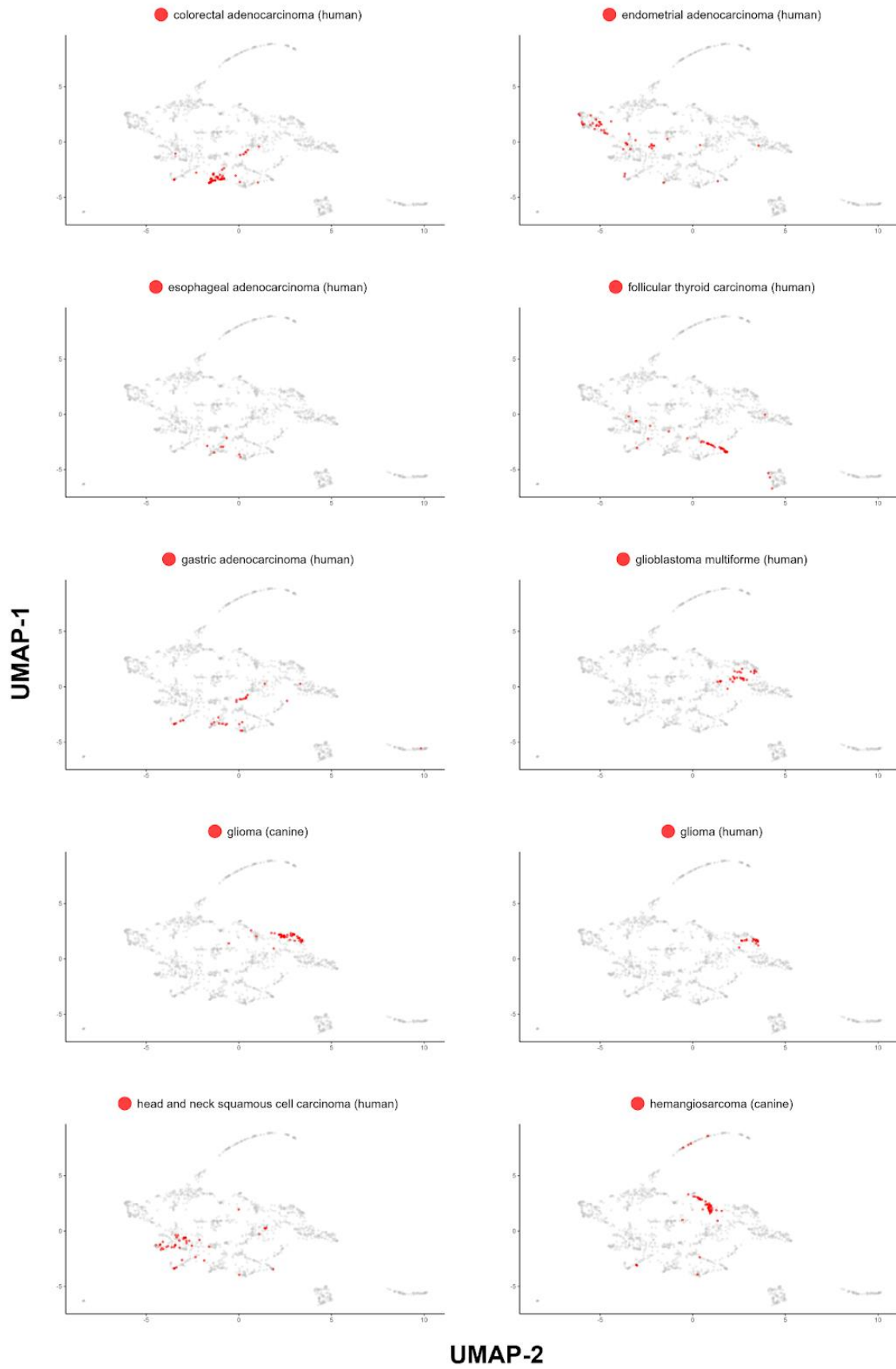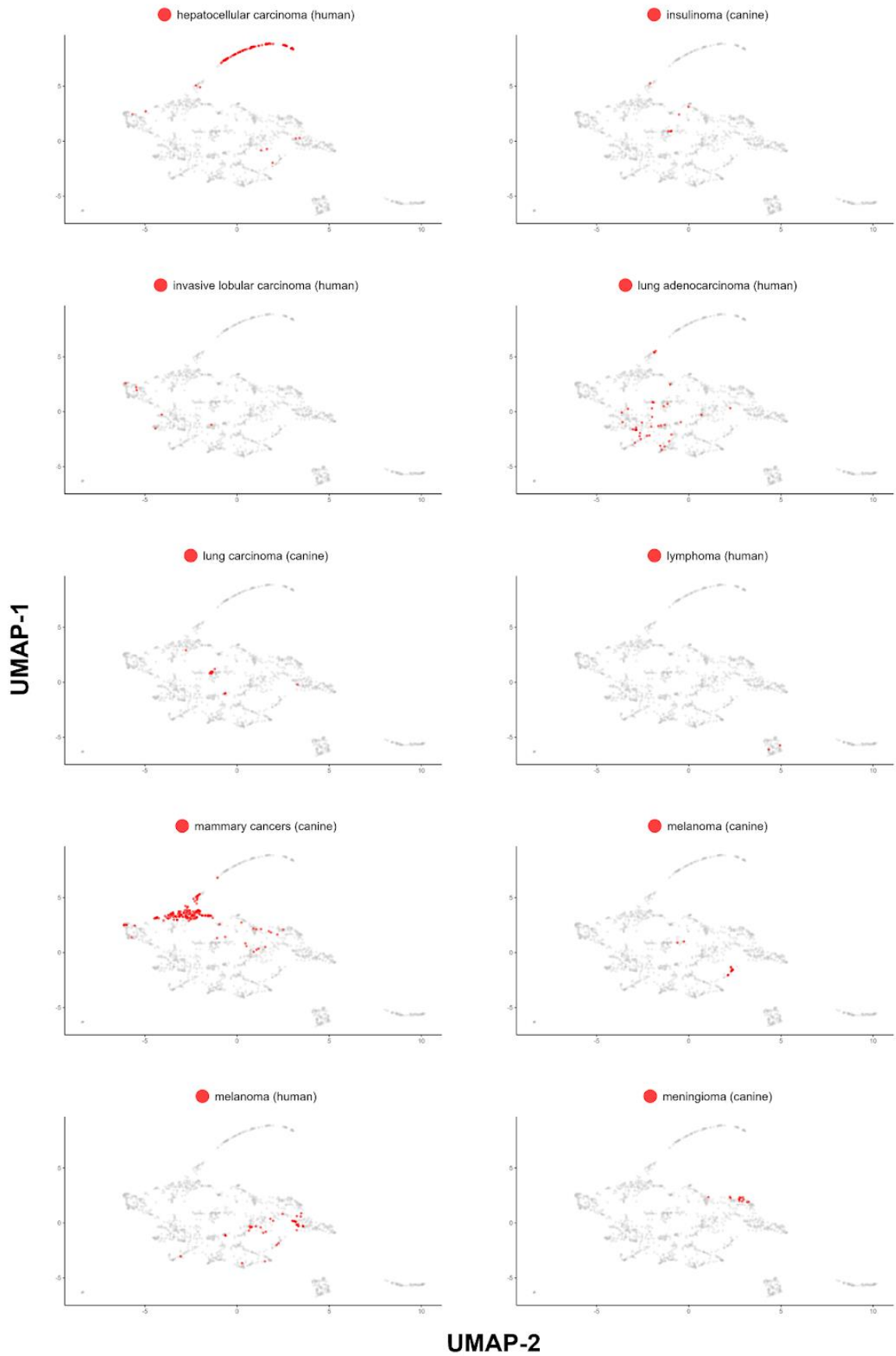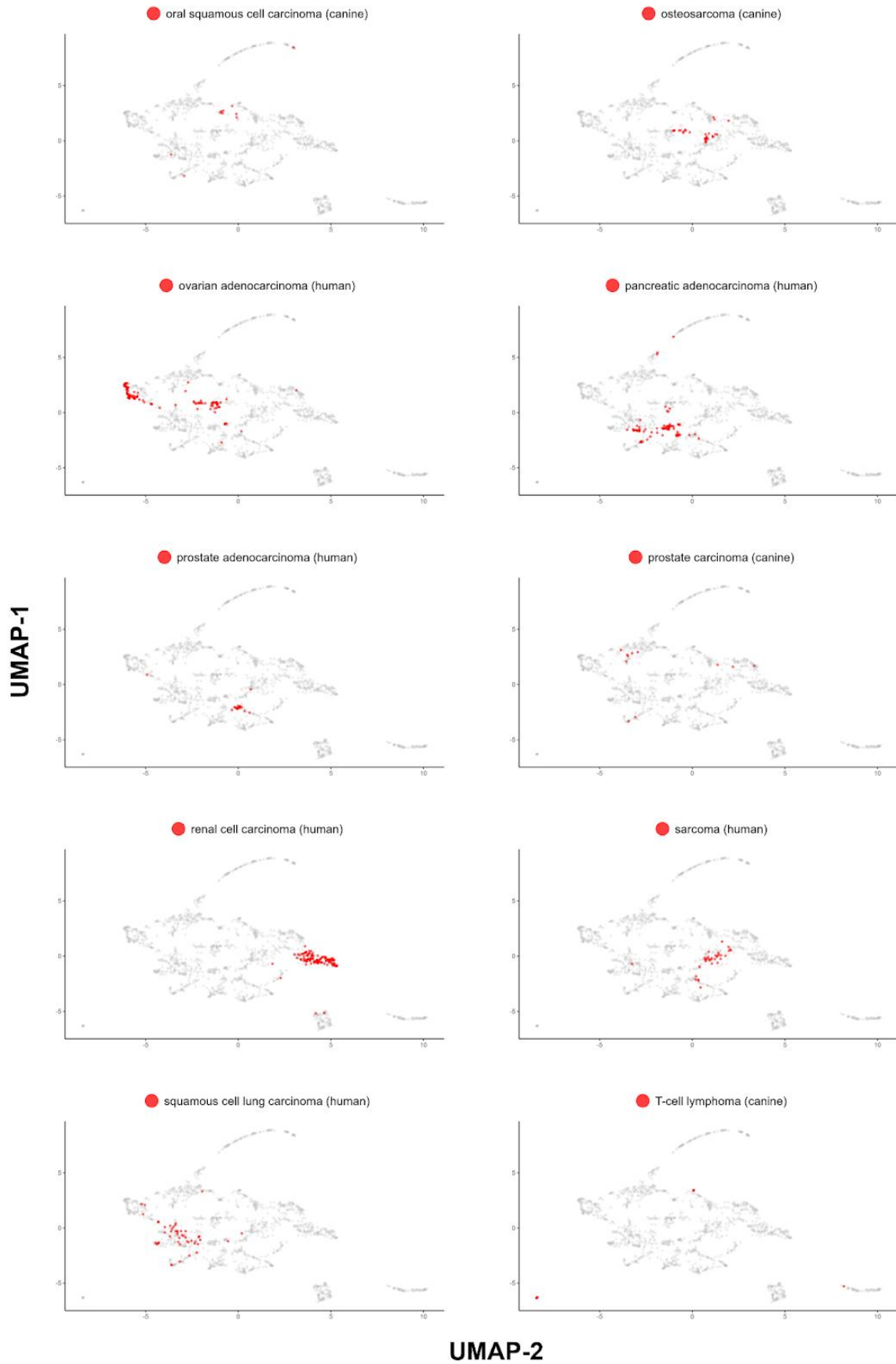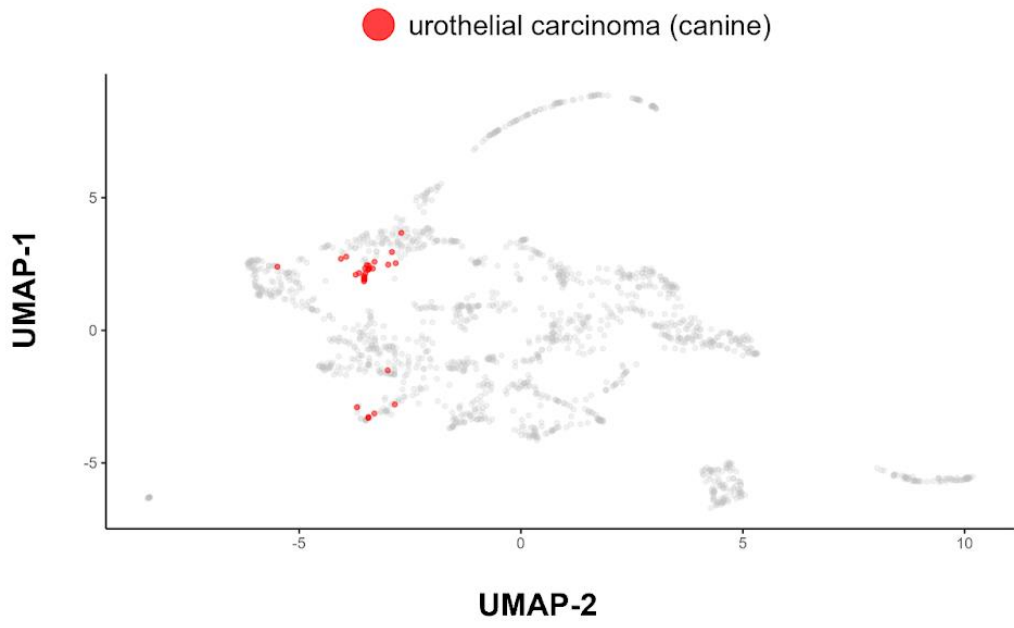
Figure S7: A dendrogram of human and canine cancer types corresponding to Fig. 4F but prepared by clustering the data by 4 randomly chosen IC genes only; blue - human and green - canine cancers.
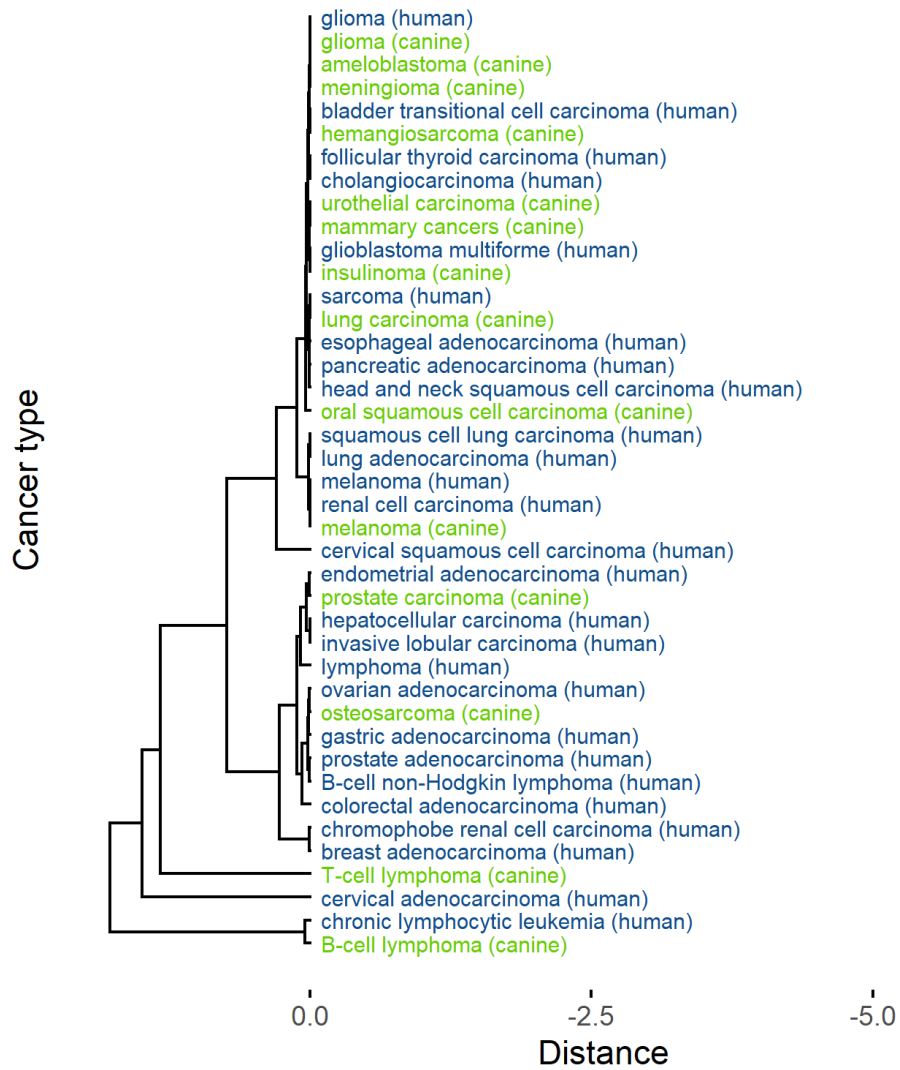
3. COMPARATIVE CHARACTERIZATION OF TWO NOVEL ANTIBODIES AGAINST CANINE PD-1

3.1 Introduction

Given the profound impact and comprehensive research surrounding the PD-1 receptor in human immunotherapy, it is a strategic starting point for laying the groundwork in canine immunotherapy. The expression of the PD-1 receptor was observed in canine immune cells [109] as was PD-L1 in cancers of companion animals including dogs [111,180,181]. These observations have been further corroborated by the findings presented in the preceding chapter of this thesis.

To date, a few groups have developed monoclonal antibodies targeting the canine PD-1 checkpoint. Choi et al. developed an anti-canine PD-L1 antibody that blocked PD-1 checkpoint in vitro [182]. Maekawa et al. identified rat anti-bovine PD-L1 antibodies that recognized canine PD-L1 and also blocked its interaction with PD-1 [180]. The antibody was recombined to create a canine-rat chimera and subsequently tested in seven dogs with cancers. In this study, exploratory in nature, responses were observed in two of the dogs [183]. Most recently, Oh and colleagues developed a blocking antibody against canine PD-L1, which was comprehensively tested through with in vitro, ex vivo and in vivo assays. The authors described its therapeutic potential, pharmacokinetics and safety profile in dogs [184]. Regarding the PD-1 itself, Coy et al. developed a panel of murine antibodies against this canine receptor [109]. Nemoto and colleagues developed rat antibodies targeting canine PD-1 and PD-L1 and demonstrated their blocking ability, but a commercial effort to caninize them has not resulted in any new products [185]. At the time of this research, the niche for successful veterinary IC blockers remains empty, and there are no available diagnostic antibodies against canine ICs.

In this chapter, we introduce two novel monoclonal antibodies targeting canine PD-1 (cPD-1) - PD1-1.1 [186] and PD1-2.1. The antibodies are characterized in respect to their performance in key molecular assays and in regard to the therapeutically crucial checkpoint blocking ability.

3.2 Results

3.2.1 Generation of monoclonal antibodies against canine PD-1

We used murine hybridoma technology to generate monoclonal antibodies (mAbs) against the canine PD-1 protein. We chose two clones for characterization, designated PD1-1.1 and PD1-2.1. First, we isotoped the antibodies, revealing PD1-1.1 belonged to IgG2a isotype and PD1-2.1 did to IgG2b. Both antibodies possessed kappa light chains. Additionally, the RNA sequences from antibody-producing hybridomas were sequenced. Given that over 30% of hybridomas can produce additional chains with different specificity, thus degrading the antibody properties, isotyping and sequencing of PD1-1.1 and PD1-2.1 offered critical validation of their monoclonal integrity and functional specificity [187,188].

3.2.2 Detection of cPD-1 in western blot

To confirm the binding of cPD-1 by PD1-1.1 and PD1-2.1 mAbs, we conducted a Western Blot analysis using a lysate of a human osteosarcoma U2OS cell line transfected with an expression plasmid encoding canine PD-1. Lysate from an empty vector-transfected cell line was used as negative control. Both antibodies successfully detected the target protein, evidenced by a distinct band at approximately 60kDa (Fig. 1). While the predicted molecular weight of cPD-1 is approximately 32kDa, it is known to migrate at around 60kDa, which is attributed to protein glycosylation [185]. This band was absent in the negative control.

Figure 1: Western blot analysis of PD1-1.1 and PD1-2.1 mAbs binding to cPD-1. U2OS cells were transfected with a cPD-1 encoding plasmid or an empty vector as a negative control. Panels A (PD1-1.1) and B (PD1-2.1) show distinct bands at ~60kDa in cPD-1 transfected cells, confirming specific binding of both antibodies to their target. No bands are observed in the negative controls. B-actin blots beneath serve as loading controls. Molecular weight markers are displayed on the right side of each blot. A faint additional band around 70 kDa may be due to non-specific reactivity of our anti-canine or secondary anti-mouse antibodies with human proteins. This artifact is absent in HEK cells (Fig. 1, S1).
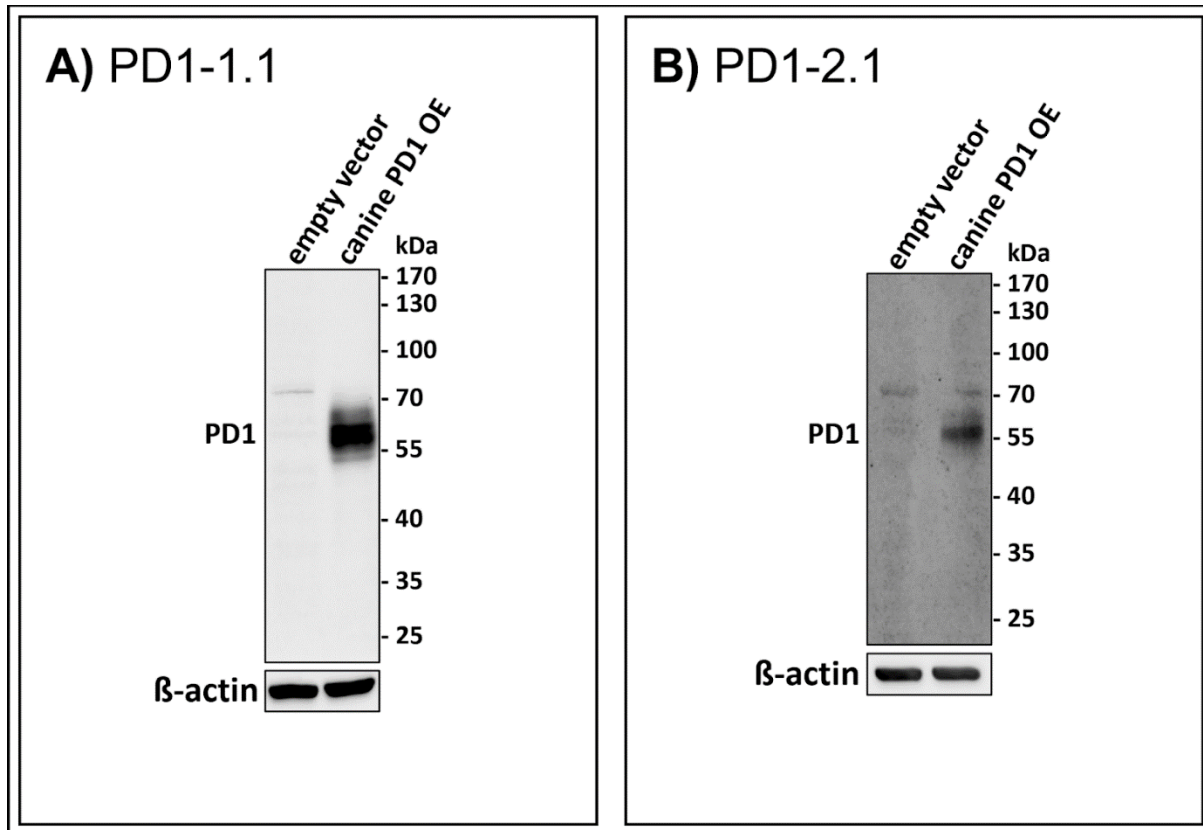
3.2.3 Testing antibody cross-reactivity between human and dog proteins

Some antibodies that target clinically important proteins cross-react between human and canine organisms. Several, including human anti-cancer antibodies, can bind to the canine versions of their target proteins and retain some functionality [128,189]. To evaluate the specificity of our antibodies for canine PD-1, we transfected HEK293 cells with plasmids encoding either canine or human PD-1, prepared cell lysates and detected respective proteins using PD1-1.1 and PD1-2.1 in Western Blot. A commercially available anti-human PD-1 antibody served as a positive control for human PD-1 expression. As shown in Figure 2 below, PD1-1.1 and PD1-2.1 recognized the overexpressed canine PD-1 but not the human PD-1, which, in contrast, was detected by the human-specific antibody. We therefore concluded that

the developed antibodies are specific for canine PD-1 and likely do not bind to the conserved regions of the PD-1 amino acid sequence.

Figure 2. Specificity of the developed antibodies against canine and human PD-1. Western blot analysis of HEK293 cells transfected with plasmids encoding either canine or human PD-1. (A) PD1-1.1 antibody specifically detected canine PD-1 but not human PD-1. (B) PD1-2.1 antibody also selectively recognized canine PD-1 without cross-reactivity to human PD-1. (C) A commercially available anti-human PD-1 antibody served as a positive control, showing exclusive binding to human PD-1. The B-actin blots beneath each main blot serve as loading controls, demonstrating equal protein amounts in each sample. The blots have been contrast-enhanced and cropped to display the relevant bands more clearly. Original, unedited blots are provided in Figure S1.
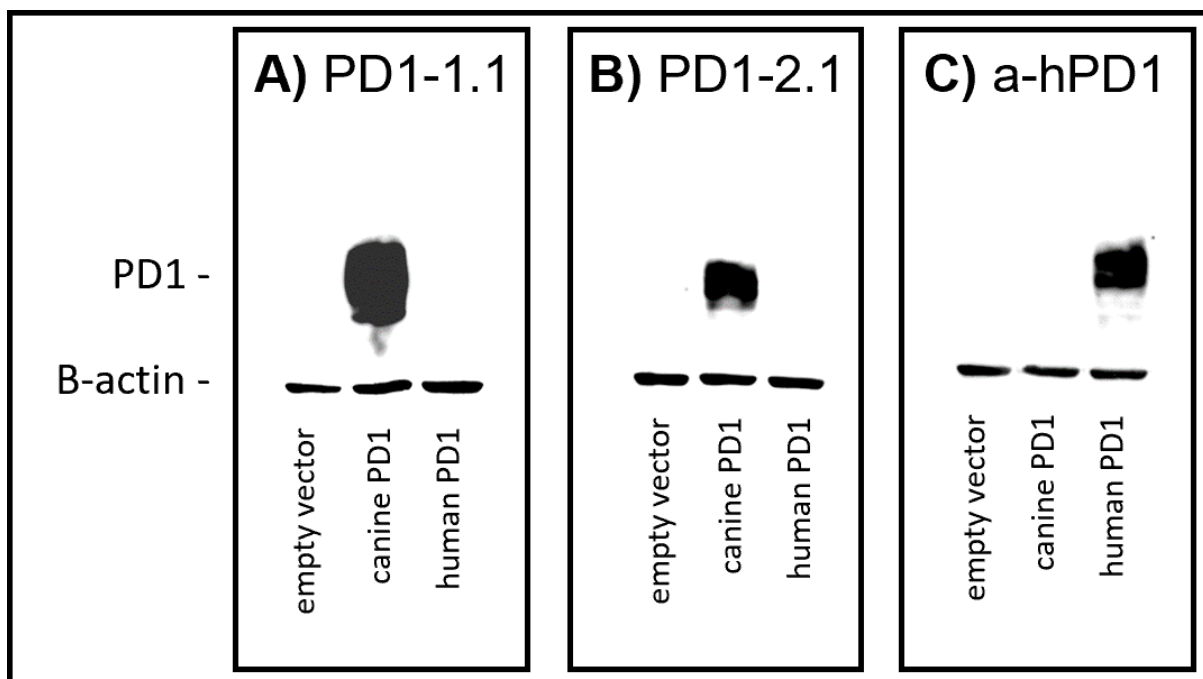
3.2.4 Detection of rcPD-1 in ELISA

Aiming to compare the two mAbs in a quantitative manner, we performed an ELISA. Dilutions of PD1-1.1 and PD1-2.1 mAbs were assayed on a plate coated with recombinant canine PD-1 (rcPD-1). When the results were visualized on a log scale, both antibodies presented characteristic sigmoid curves (Fig. 3), which were used to calculate EC50 values. For the PD1-1.1, the EC50 value was determined to be 6.061 with a 95% confidence interval of 5.388 to 6.818. The R-squared value for the fit was 0.9836. For the PD1-2.1, the EC50 value was 10.16 with a 95% confidence interval of 9.236 to 11.18. The R-squared value for the fit was 0.9886. The lower EC50 value indicates that PD1-1.1 has a higher affinity for the target protein than PD1-2.1. Of note, the signal in ELISA was very high despite the target coating concentration in the lowest

range of the common spectrum. While a high-sensitivity substrate was used to develop the results, this demonstrates very good performance of the tested antibodies in ELISA and possibly a high affinity to canine PD-1 protein in its native state.

Figure 3: Binding curves of monoclonal antibodies PD1-1.1 and PD1-2.1 in ELISA against recombinant canine PD-1. The curves were plotted on a log scale and used to calculate EC50 values. PD1-1.1 showed a higher affinity compared to PD1-2.1. Error bars represent standard deviation from three replicates per datapoint.
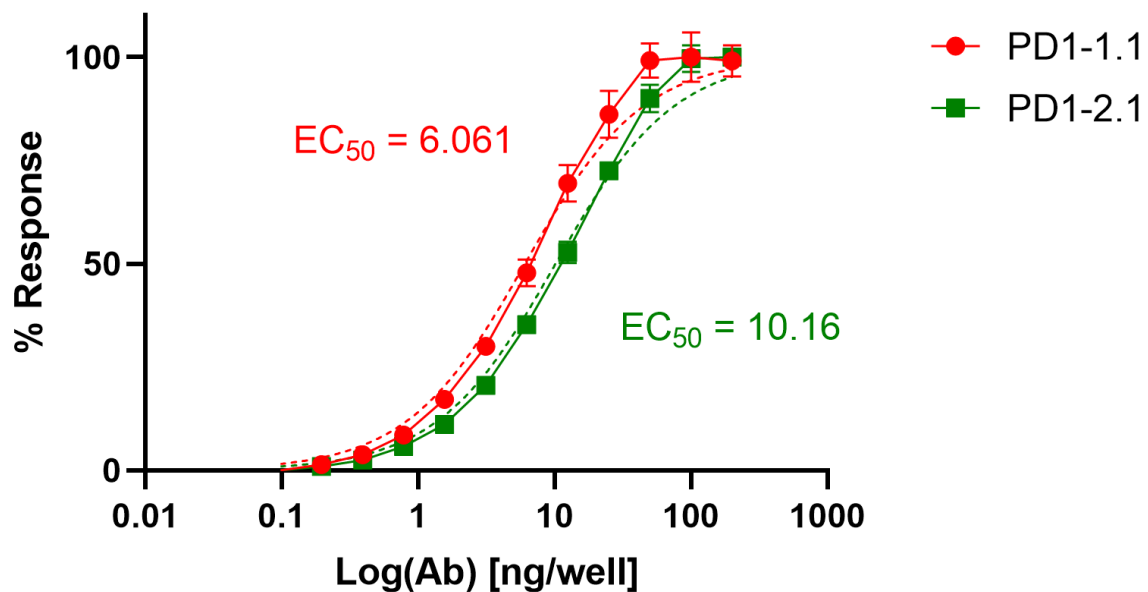
3.2.5 Binding of native canine PD-1 in flow cytometry

Next, we sought to assess the ability of our antibodies to bind cPD-1 in its most natural state, as expressed on live cells. To test this, we transfected U2OS cells with a cPD-1 encoding vector or an empty control vector. We stained the cells with PD1-1.1, PD1-2.1, or an isotype control antibody and analyzed them using flow cytometry (Fig. 4). An isotype control antibody, a non-specific antibody of the same isotype as the primary antibody used in an experiment, serves as a negative control to account for non-specific binding, particularly in assays based on live cells. This control allows us to differentiate specific antibody-antigen interactions from background binding inherent to the antibody class. In this experiment, an isotype control antibody was used to stain cells transfected with the empty vector. Both PD1-1.1 and PD1-2.1 exhibited a shift in signal peaks for cells transfected with the PD-1 as compared to the control cells, indicating specific binding of PD-1. The peaks for PD-1 negative cells stained with

PD1-1.1 and PD1-2.1 corresponded with the position of respective isotype control peaks, further indicating specific binding. Notably, PD1-2.1 displayed a higher median fluorescence intensity (MFI) than PD1-1.1, suggesting it may have superior sensitivity to PD-1 in the flow cytometry conditions.

Figure 4: Flow cytometry analysis of PD1-1.1 and PD1-2.1 mAbs binding to cPD-1 expressed on live U2OS cells. U2OS cells were transfected with a cPD-1 encoding vector or an empty vector and then stained with PD1-1.1 (A) or PD1-2.1 (B), and an isotype control antibody. Each plot visualizes cells stained with a tested antibody (magenta), empty vector control (blue) and isotype control (green). (A) The median fluorescence intensity (MFI) for PD1-1.1 was 91.9 (PE-A channel). (B) The MFI for PD1-2.1 was 125 (APC-A channel). Both antibodies detected cPD-1 positive cells but not the negative control cells. The results indicate that both antibodies specifically recognize native cPD-1 expressed on live cells. Note: APC (allophycocyanin) and PE (phycoerythrin) are fluorescent dyes used for labeling antibodies. The '-A' refers to the specific channel on the flow cytometer used to detect the fluorescence signal.
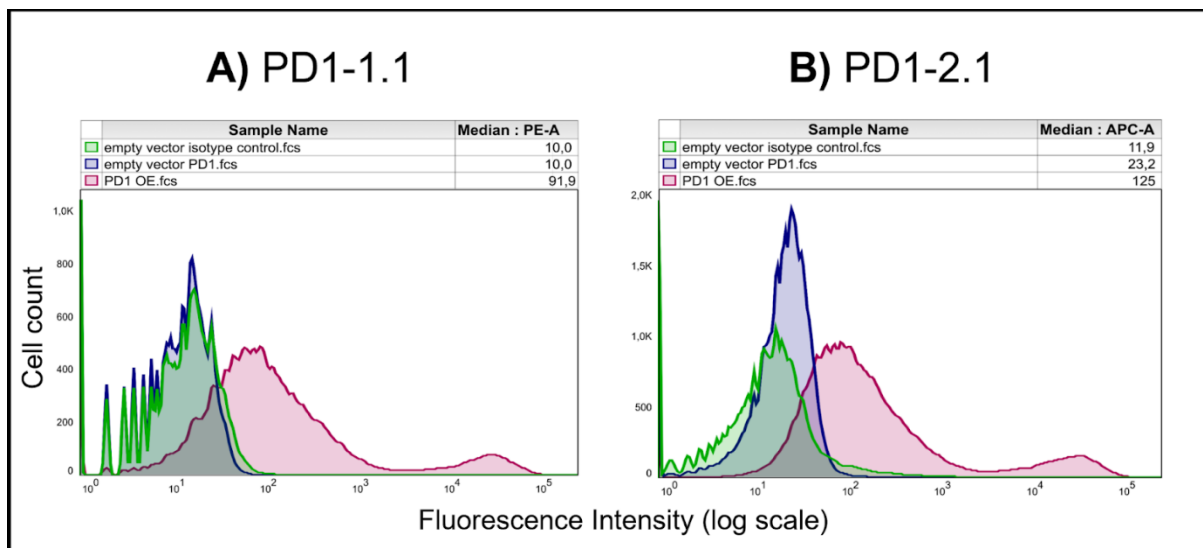
3.2.6 Measuring cPD-1 binding affinity by SPR

Surface Plasmon Resonance (SPR) enables semi-absolute quantitation of protein-ligand interaction. While results always depend on the experimental setup, SPR is a golden standard for assessing the binding potential of therapeutic antibody candidates. We immobilized His-tagged rcPD-1 on dextran chips and assayed PD1-1.1, PD1-2.1 and an isotype control antibody (Fig. 5). Based on the obtained curves, K_a (Association Constant), K_d (Dissociation Constant) and K_D (Equilibrium Dissociation Constant) were computed for each antibody (Tab. 1). KD is a measure of the overall affinity between two interacting molecules in equilibrium and has units of molarity (M). PD1-1.1 and PD1-2.1 displayed sub-nanomolar equilibrium dissociation constant. The isotype control generated no binding signal, thus validating the assay. The SPR analysis revealed the generated mAbs have a very high affinity to canine PD-1, sufficient for further development into therapeutics.

Figure 5: SPR sensorgrams of PD1-1.1 and PD1-2.1 mAbs binding to cPD-1. The sensograms show an increase in signal as the function of time and antibody concentration, indicating the binding between PD-1 immobilized on the sensor surface and the PD1-1.1 (A) PD1-2.1 (B) antibodies; no binding was observed for the isotype control antibody (C). Figure elements by Dr Katarzyna Węgrzyn.
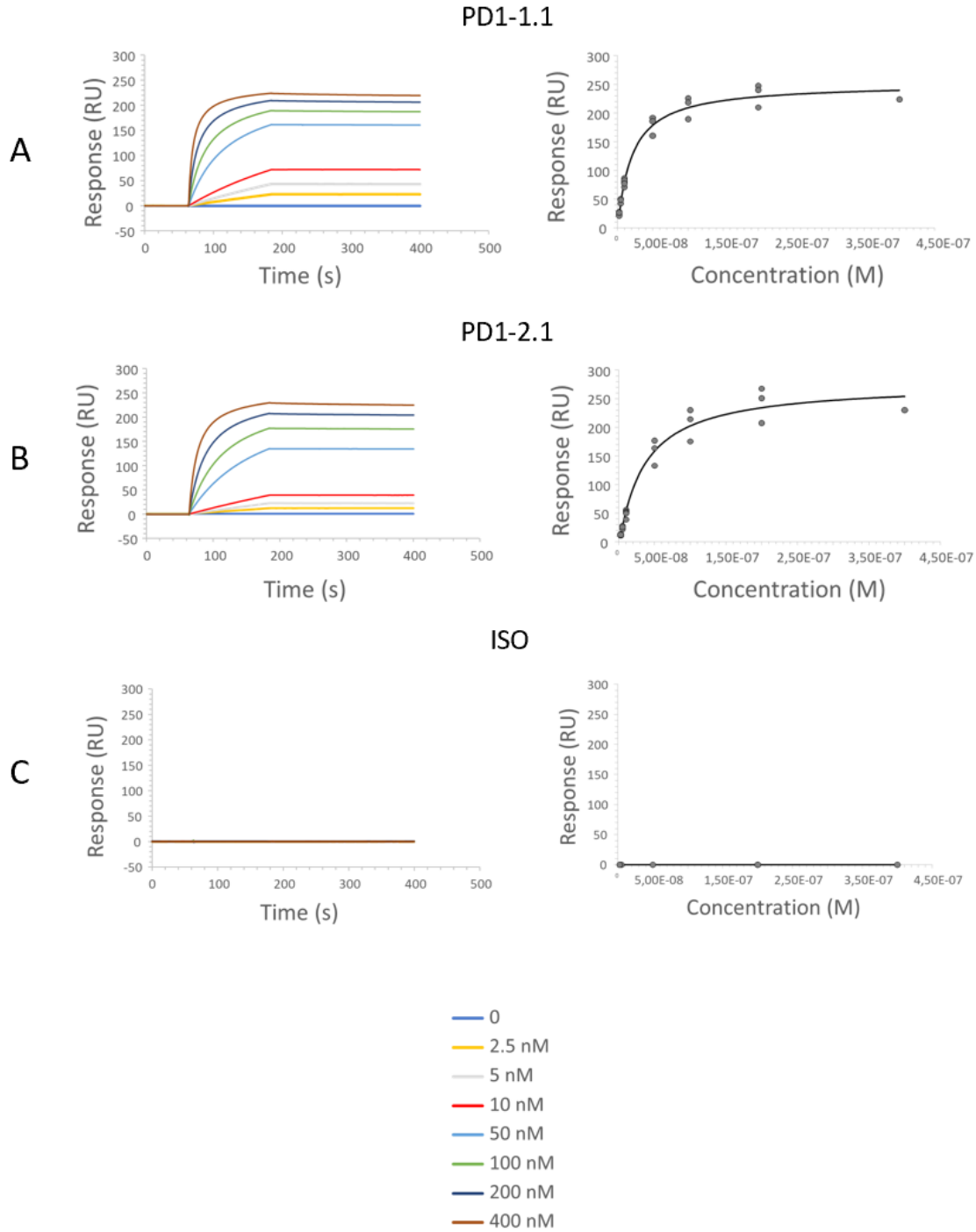
Table 1: Kinetic constants were calculated for each antibody from the obtained SPR data: association rate (Ka), dissociation rate (Kd) and equilibrium dissociation constant (KD); ISO - isotype control antibody; NA - not applicable (no binding detected).

	PD1-1.1	PD1-2.1	ISO
K_a **(1/Ms)**	3.37E+05 (±3.12E+04)	1.75E+05 (±1.91E+04)	NA
K_d **(1/s)**	4.93E-05 (±1.5E-05)	2.36E-05 (±1.43E-05)	NA
K_D **(M)**	1.5E-10 (±6.16E-11)	1.42E-10 (±1.04E-10)	NA

3.2.7 Competitive ELISA for assessing PD-1 checkpoint-blocking potency

The efficacy of immune checkpoint inhibitors, unlike that of many other therapeutic antibodies, depends on their ability to disrupt the interaction between the IC receptor and its ligand of interest. To assess the therapeutic potential of PD1-1.1 and PD1-2.1, we needed to evaluate not only their binding to cPD-1, but also their capacity to prevent cPD-1 from binding to cPD-L1. To this end we used a competitive ELISA assay in which rcPD-1-His was immobilized on the plate and incubated with dilutions of the antibodies under investigation. After washing the plates, rcPD-L1-Fc was added, and its binding was subsequently detected with an anti-human HRP conjugate (Fig. 6). In controls without the tested antibodies, PD-1-PD-L1 binding was entirely unblocked, resulting in the highest signal. Conversely, a reduction in the signal corresponded to successful inhibition of the PD-1-PD-L1 interaction.

Figure 6: PD1-1.1 and PD1-2.1 both inhibit the PD-1/PD-L1 binding in ELISA yet differ in their blocking capacity at the higher concentration. This observation suggests distinct binding sites or mechanisms; IC50 [PD1-1.1] = 0.0002, IC50 [PD1-2.1] = 0.0006; error bars represent standard error of the mean (SEM).
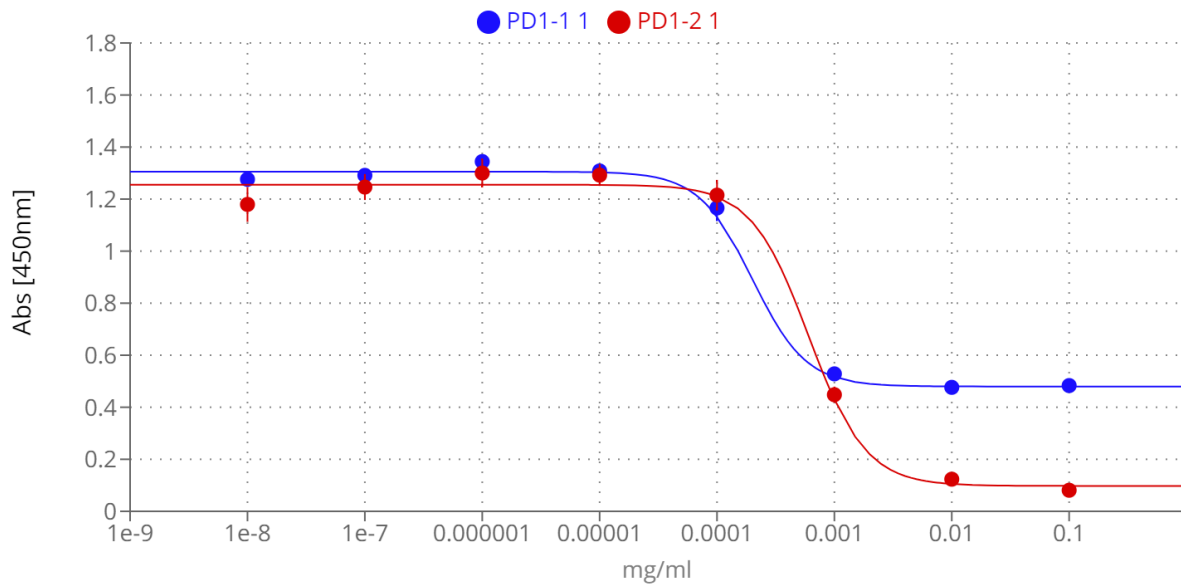
Both PD1-1.1 and PD1-2.1 demonstrated their capability to disrupt the PD-1/PDL-1 interaction. The calculated IC50 value, based on four-parameter logistic regression, was lower for PD1-1.1 (0.0002) compared to PD1-2.1 (0.0006), indicating a higher potency at mid-range concentrations. However, at higher antibody concentrations, only PD1-2.1 exhibited a nearly complete blockade. This was evidenced by a significantly lower 'bottom' plateau in the ELISA curve (~0.1) compared to PD1-1.1 (~0.5). These results suggest that while PD1-1.1 might be slightly more potent at moderate concentrations, PD1-2.1 is far more effective at higher, therapeutically meaningful concentrations of 10-100μg/mL that resemble serum antibody levels in patients undergoing immunotherapy [190–192]. Such differences could stem from the antibodies targeting distinct epitopes on cPD-1 or their specific binding orientation. These findings underscore the importance of considering affinity in the wider context of the specific binding mechanisms.

3.2.8 Activation of IFN-γ secretion in a PBMC-based assay

Having confirmed the PD-1/PD-L1 blocking properties of developed antibodies in ELISA, we strived to validate this functionality in a cell-based assay. To this end, we purified peripheral blood mononuclear cells (PBMC) fraction of whole blood from

canine donors. PBMCs naturally include immune cell populations expressing PD-1 and PD-L1. Healthy T-cells which constitute a major part of PBMCs, when exposed to a T-cell receptor (TCR) stimulant Concanavalin A (ConA), which mimics a potent antigen, increase the expression of PD-1 and the secretion of cytokines such as Interferon-gamma (IFN-γ). At the same time, the contact between their PD-1 receptor and PD-L1 ligands of other PBMCs may decrease the rate of this process. The addition of PD-1 blocking antibodies prevents this decrease. Hence, the measurement of IFN-γ secretion from ConA-stimulated PBMCs is often considered a proxy for the PD-1 blocking capacity of an antibody. In our assay PBMCs obtained from healthy dogs were cultured, either unstimulated (baseline signal), stimulated to ConA (5µg/ml; positive control) or exposed to combinations of ConA with the tested antibodies or isotype control antibody (all antibodies - 10µg/ml) for 72h. After that, the conditioned medium from cell culture was tested for the concentration of secreted IFN-γ by ELISA. We calculated the assay results for PBMCs from 5 dogs (Fig. 7A) and normalized them to the isotype control (Fig. 7B) to enable direct comparison. We calculated the mean result by averaging out the normalized results from five blood samples (Fig. 7C). All PBMC samples reacted to Concanavalin A stimulation (positive control), validating their use in the assay. As shown on Fig. 7C below, statistically significant differences between isotype control and antibody treatments have not been found, which can be partially attributed to a low statistical power of the test. This finding contrasts with the blocking observed in the competitive ELISA assay. Notably, PBMCs from one dog (#4 - dark green) reacted in the way that would be expected based on the prior ELISA, with signal higher for test antibodies than isotype control. For details of the analysis and possible explanations see the discussion and supplement.

Figure 7: The ability of antibodies to block PD-1 was evaluated in a PBMC-based assay. Peripheral blood mononuclear cells (PBMC) were isolated from blood of canine donors and are a fraction high in immune cells. In the assay, the blocking antibodies counteract inhibition of T-cells, resulting in increased secretion of IFN-γ. A) The mean and standard deviation based on duplicate measurements for each sample are presented. B) The data were normalized against the signal from the isotype control. C) The averaged data from PBMC samples taken from five dogs. IFN-γ secretion markedly increased upon exposure to PD1-1.1 and PD1-2.1 in PBMCs of one dog, but no statistically significant difference was found between isotype control and the characterized antibodies (Kruskal-Wallis and Dunn's post-hoc tests). Asterisks indicate statistical significance based on p-value thresholds: $*p < 0.05$, $**p < 0.01$, $***p < 0.001$. IFN-γ - interferon gamma, Abs - absorbance, ConA - Concanavalin A.
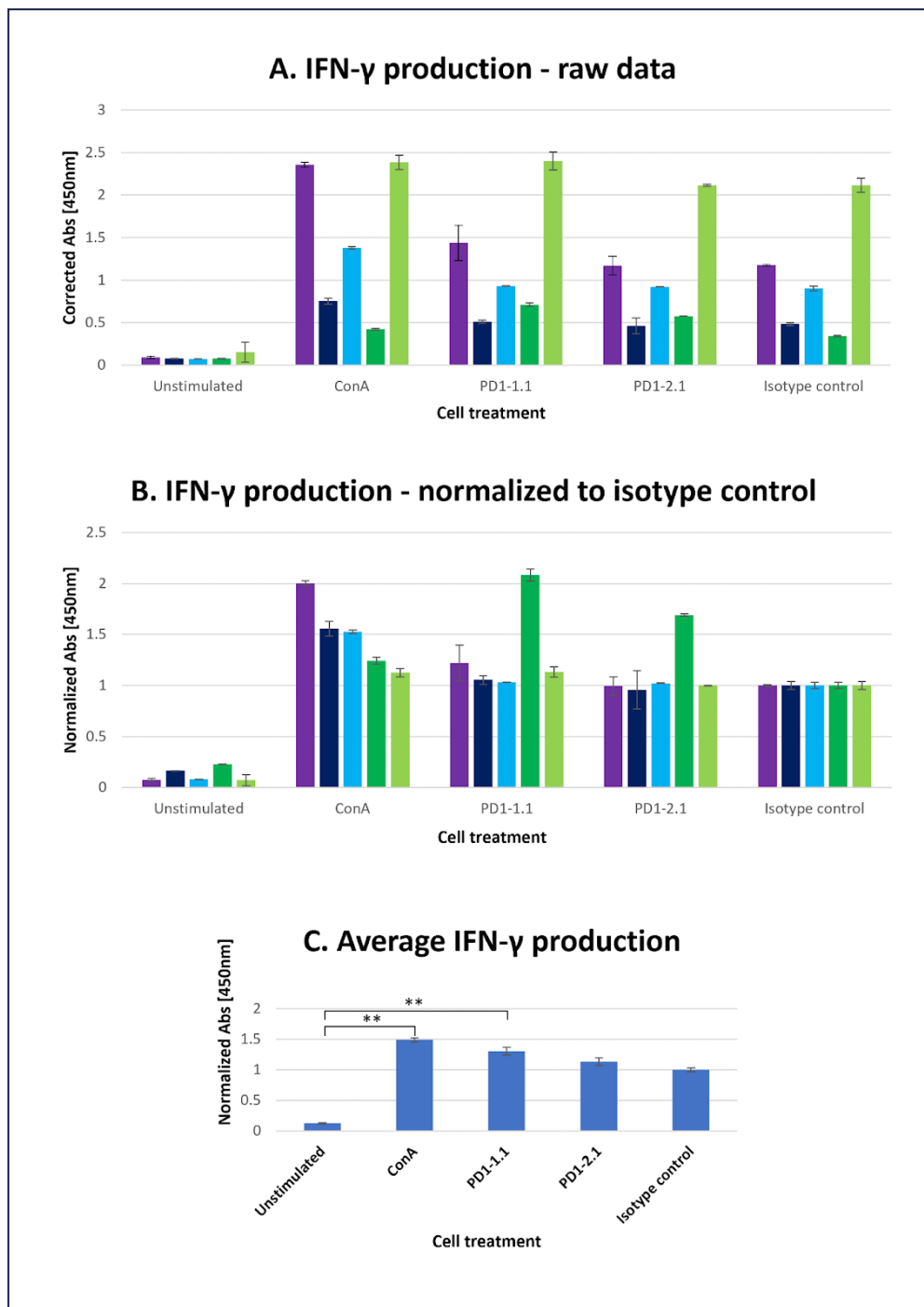
3.2.9 PD1-1.1 but not PD1-2.1 is suitable for cPD-1 detection in IHC

One of the clinically important molecular assays is the immunohistochemical (IHC) staining of cancer-affected tissues. We performed IHC staining of a tonsil lymphoid tissue sample with both antibodies and found that PD1-1.1 stained cell clusters with natural cPD-1 expression (Fig. 8 below). Meanwhile, staining with PD1-2.1 could not be optimized to generate replicable results, hence we concluded only PD1-1.1 is suitable for detection of cPD-1 in IHC. In fact, we have successfully used the PD1-1.1 for an IHC analysis of clinical samples in a prior publication [186].

Figure 8: PD1-1.1 detects cPD-1-positive cell clusters in the IHC staining of a canine tonsil tissue; magnification is 100x-400x and brown color marks the positively stained cells.
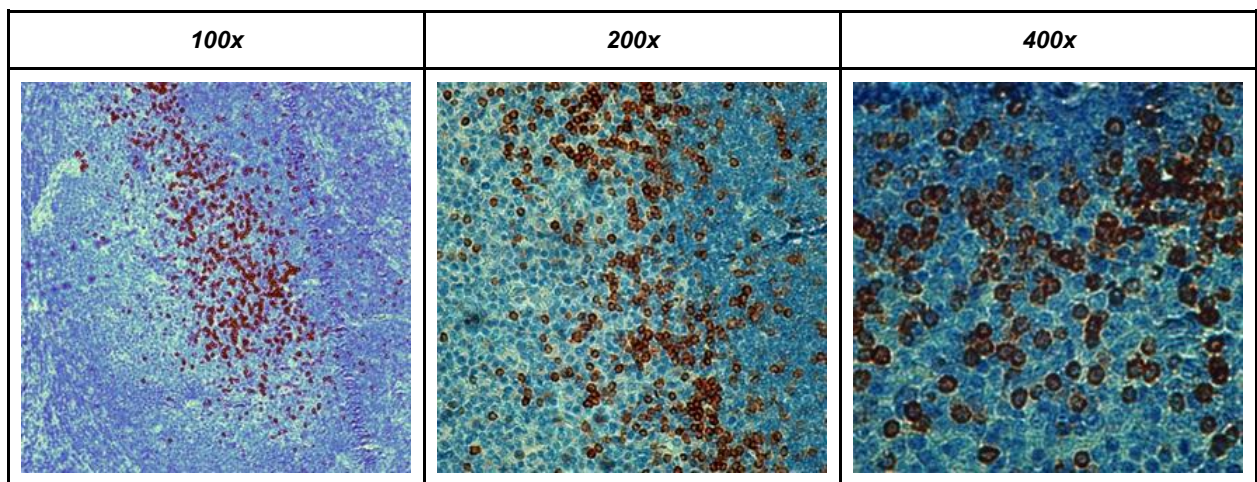
3.2.10 The antibodies detect cPD-1+ cells in immunocytochemistry

To investigate the binding of the PD1-1.1 and PD1-2.1 antibodies to PD-1+ cells in detail, we performed immunocytochemistry, an immunofluorescent (IF) cell staining of U2OS cells with stable cPD-1 overexpression and those transfected with an empty vector. We incubated these cells with either PD1-1.1 or PD1-2.1. Next, we detected the bound antibodies with a fluorescently labeled secondary antibody and observed the fixed cells under a confocal microscope. The results of the immunofluorescent staining were displayed on Figure 9. For both PD1-1.1 (9A) and PD1-2.1 (9B), only the cells transfected with canine PD-1 generated a strong green light signal, indicating that they bound the antibodies. This result demonstrated the binding specificity of both antibodies and their suitability for IF staining experiments.

Figure 9: Immunofluorescent staining of U2OS cells to assess the binding specificity of PD1-1.1 and PD1-2.1 antibodies. U2OS cells with stable PD-1 overexpression and those transfected with an empty vector were incubated with either PD1-1.1 (Panel A) or PD1-2.1 (Panel B) antibodies. Bound antibodies were detected with fluorescently labeled secondary antibody (green), and the cell nuclei were stained with DAPI (blue). Each panel consists of two rows corresponding to cells transfected with an empty vector (top row) and cells with PD-1 overexpression (bottom row). The three columns display images of DAPI-stained nuclei (left), antibody staining (middle), and merged images (right). The green signal is exclusively present in PD-1 overexpressing cells, indicating the binding specificity of both antibodies to PD-1. Figure elements provided by Katarzyna Dziubek.
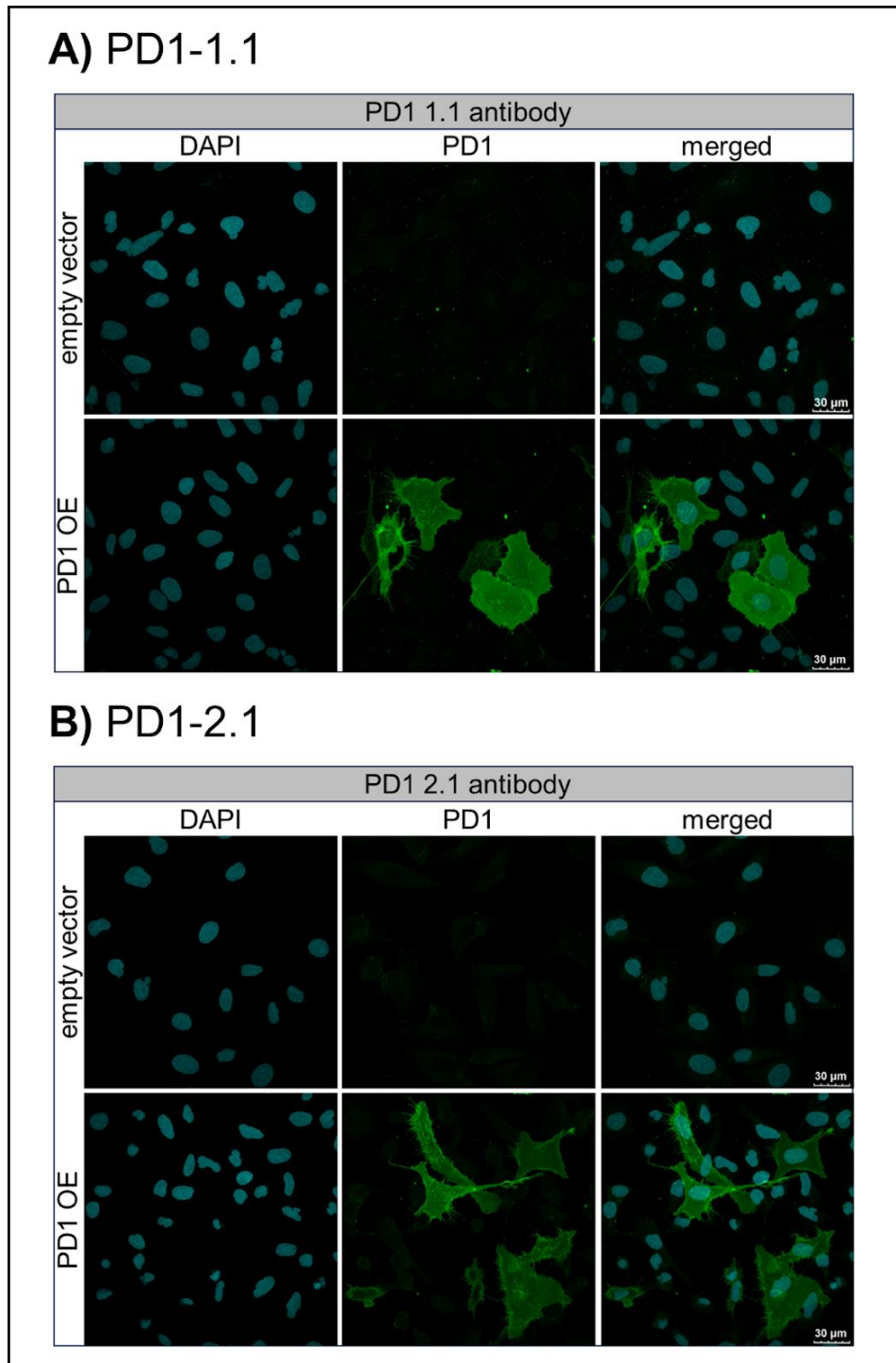
3.2.11 Modeling the cPD-1 epitopes for PD1-1.1 and PD1-2.1

The two antibodies displayed very similar affinity by SPR, yet different PD-1/PD-L1 blocking characteristics and varying performance in other assays. To delineate the respective epitopes of the two antibodies, we initially employed various epitope prediction tools such as Discotope, BepiPred, AbAdapt, EpiPred, and IEDB Epitope Prediction. However, they were not able to narrow down the range of possible epitopes. Epitope mapping through Hydrogen-Deuterium Exchange Mass Spectrometry (HDX-MS) was also attempted for PD1-1.1 without success, due to the epitope region's resistance to proteases. This led us to develop a more targeted approach. We modeled the structures of the PD1-1.1 and PD1-2.1 variable domains as well as the structure of the canine PD-1. Subsequently, we performed docking of variable domains to canine PD-1. For each antibody we chose the top most probable binding model (Fig. 10) and analyzed which residues form the antibody-target interface. The putative PD-1 epitopes - residues participating in the protein-protein interface - were mapped on to the sequence and structure of the PD-1 protein (Fig. 11). The antibody residues participating in the interface belonged to CDR regions. Additionally, we initiated the development of another epitope mapping method, aimed at in vitro validation, described in the supplementary results section.

Figure 10. Top binding poses of PD1-1.1 and PD1-2.1 were identified and visualized with 'mesh' and 'cartoon' projections. Cyan – heavy chain, magenta – light chain, green – canine PD-1.
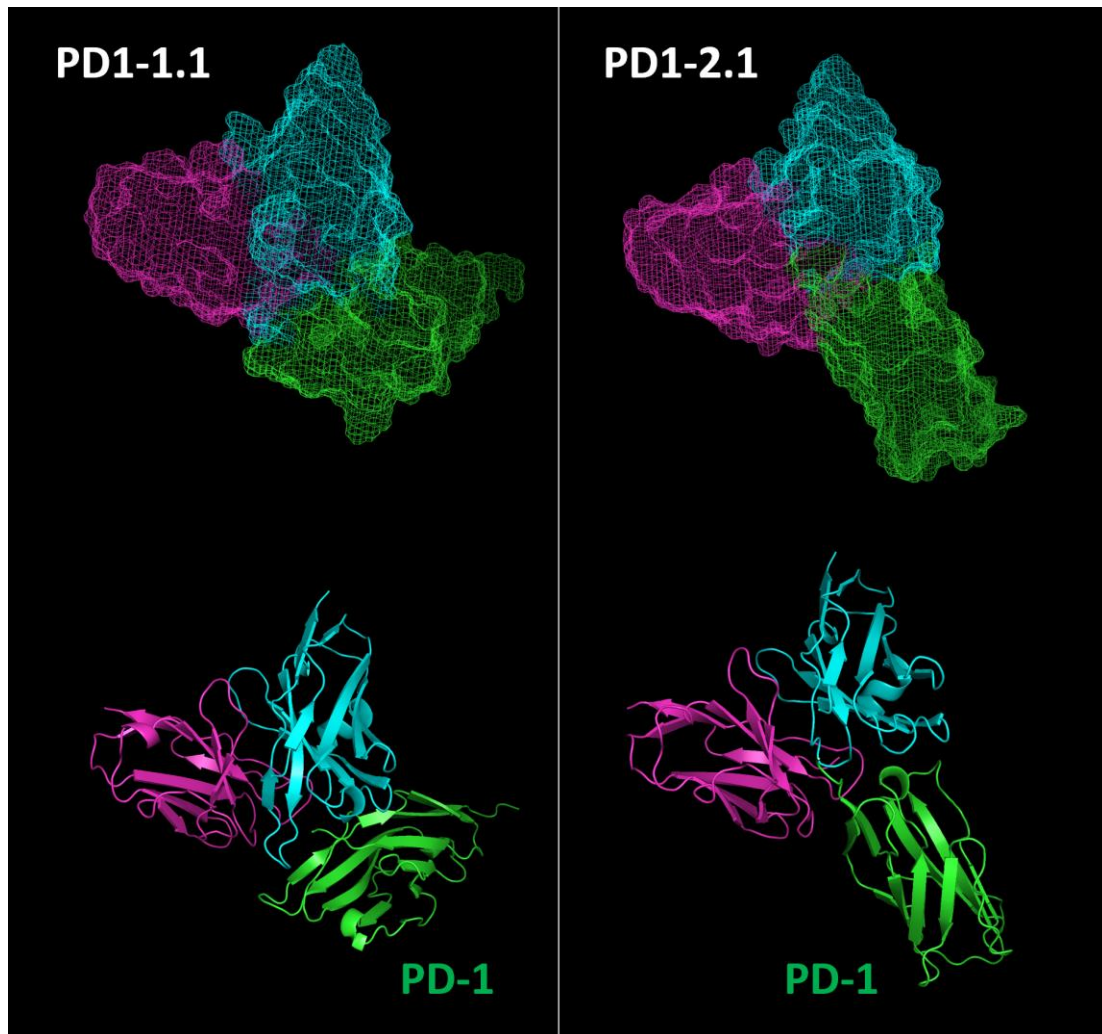
Figure 11. Putative epitopes of PD1-1.1 and PD1-2.1 on canine PD-1 (cPD-1) were identified by molecular modeling and docking. Receptor residues participating in the protein-protein interaction were visualized on the cPD-1 sequence and surface for PD1-1.1 (A) and PD1-2.1 (B). <mark style="background-color:green">Green</mark> – residues participating in the interface; <mark style="background-color:magenta">magenta</mark> – interface residues contributing hydrogen/disulphide bonds, salt bridges or covalent links. Additionally, the cPD-1 regions corresponding to the human PD-1 interaction sites for PD-L1 [193], Nivolumab (Nivo, [194]) and Pembrolizumab (Pembro, [195]) were marked with <mark style="background-color:red">red</mark> (C), <mark style="background-color:cyan">cyan</mark> and <mark style="background-color:yellow">yellow</mark> (D), respectively.
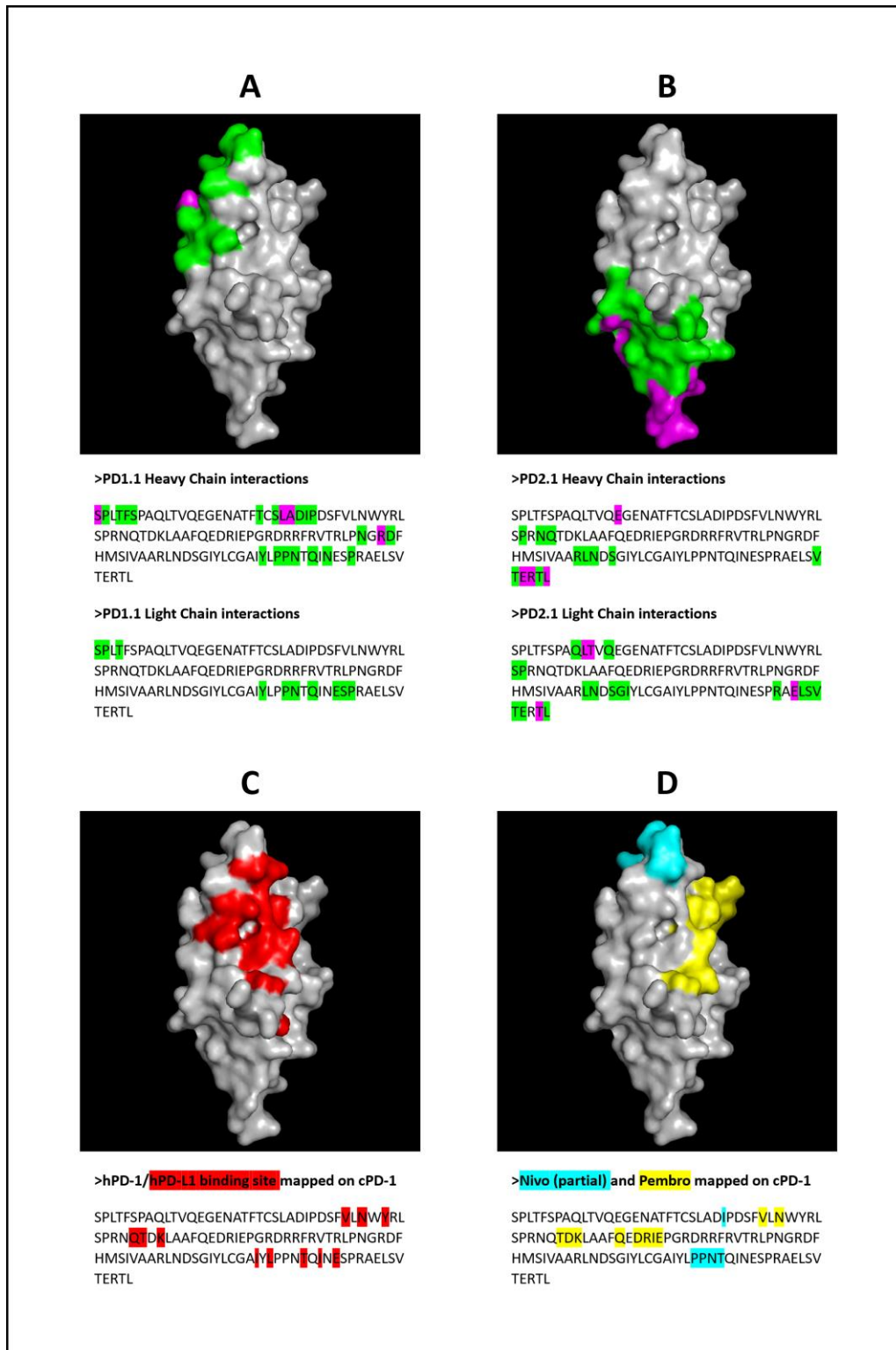
3.3 Discussion

Here, we introduce two monoclonal antibodies (mAbs) against canine PD-1 - PD1-1.1 and PD1-2.1 - to address an unmet need for immune checkpoint blockers in canine oncology. We join the pioneering efforts by Coy [109] and Nemoto [185,196] as the third group to report such antibodies, yet the first to conduct a comprehensive evaluation across the key molecular assays. Uniquely, by utilizing surface plasmon resonance (SPR), we found that both antibodies have high affinity for PD-1, with sub-nanomolar KD values. This characteristic nominates them as suitable candidates for therapeutic development. To evaluate their PD-1-inhibitory dynamics, we developed a novel competitive ELISA assay. Here, PD1-2.1 demonstrated superior blocking activity over PD1-1.1, despite comparable target affinity of both mAbs in SPR. Interestingly, the mAbs exhibited similar IC50 values within lower concentration ranges, but at the higher range PD1-1.1 reached a plateau. Meanwhile, PD1-2.1 continued to decrease the signal, achieving a nearly complete PD-1 blockade at a concentration mimicking therapeutic antibody levels in blood. The superior blocking activity of PD1-2.1 stands in contrast with its inferior binding in a classic PD-1 binding ELISA. This discrepancy underscores the importance of evaluating functional capabilities in tandem with the affinity metrics.

Both our mAbs recognized canine but not human PD-1 in WB. Further, they were functional and specific in flow cytometry (FC), and immunocytochemistry (IC) assays. However, only PD1-1.1 was effective in immunohistochemical staining (IHC). The functional divergence between the two mAbs may be attributed to different epitopes, possibly involving post-translational modifications [197].

Coy et al. similarly characterized two mAbs against PD-1, which were functional in WB, FC, and additionally detected CD4+ and CD8+ T-cells from healthy dog blood in FC [109]. Nemoto et al. also validated two anti-PD-1 mAbs in FC against PD-1 overexpressed in a cell line and induced in PBMCs [185]. They also detected PD-1 in WB. Of note, in their work, the WB results showed bold secondary bands in negative control cells. Further discussion on this finding might be insightful. Their FC-based assays yielded inconclusive results, likely attributable to the specific experimental setup. Functionality in IHC or IC was not tested by the other groups.

In initial Western blots against naturally expressed and recombinant PD-1 both our antibodies demonstrated weak signal. To overcome this limitation, in subsequent WB and IC experiments we utilized cell lines overexpressing canine PD-1 (U2OS and HEK293), similarly as Coy (CHO cells) and Nemoto (NRK cells) [109,185]. These observations suggest that our antibodies target conformational epitopes.

Epitope modeling for PD1-1.1 and PD1-2.1 identified non-continuous, conformational putative epitopes. This feature renders antibodies suitable for therapeutic applications at the cost of weaker performance in molecular assays involving denaturation. The two epitopes were located differently, with both slightly overlapping with the putative PD-L1 binding site as predicted by alignment with human PD-1. In this context it's noteworthy, that the two human anti-PD-1 antibodies Pembrolizumab and Nivolumab also possess different PD-1 epitopes. While the Pembrolizumab epitope closely aligns with the PD-L1 ligand binding site, the Nivolumab epitope does so to a lesser extent [195,194,193]. Yet, both are effective PD-1 blockers. This observation highlights the complexity of the receptor blocking mechanisms.

Efforts to evaluate the ability of our mAbs to activate T-cells in an assay based on peripheral blood mononuclear cells (PBMC) produced inconclusive results, potentially confounded by high inter-donor variability and undisclosed medical histories of the blood donors. Unexpectedly, some PBMC samples stimulated with Concanavalin A (ConA) alone exhibited higher signal than those treated with ConA and the isotype control, which puts the assay mechanism in question. Curiously, a similar issue was observed in the paper by Coy, where addition of isotype control to activated PBMCs significantly lowered the signal [109]. Unlike us, Coy et al. detected statistically significant upregulation of IFN-γ secretion upon treatment with both their mAbs. Nemoto et al. similarly to us observed inconsistent results between dogs [185]. They have seen more positive trends than us, though the visualization of results did not allow for the assessment of statistical significance. The current lack of standardization and repeating artifacts of a PBMC IFN-γ assay appear to limit its usefulness. For an in-depth discussion, please refer to the supplementary materials.

The unique strength of the work by Coy et al. was their dis-inhibition test of one mAb, where ConA-activated PBMCs were 'inhibited' with either recombinant cPD-L1 or cPD-L1-overexpressing cells [109]. In the latter assay, IFN-γ production by PBMCs was

unequivocally inhibited and one of the mAbs partially reversed this inhibition, with a statistically significant effect. Impressively, they have repeated this experiment for both mAbs while using tumor explant cultures as PBMC suppressors. Here, both antibodies reversed the tumor's inhibitory impact. They have additionally demonstrated increased proliferation and IFN-γ secretion in tumor-infiltrating lymphocytes extracted from cancer tissues and treated with the PD-1 antibodies.

In an important contribution, Igase et al., building upon the foundational work of Nemoto et al., advanced the field by taking their antibody characterization into a clinical setting [196]. In collaboration with Nexvet and Zenoaq companies, they re-engineered 4F12-E6 - a previously characterized monoclonal antibody - into a chimeric and a fully caninized form. This antibody exhibited promising results in flow cytometry and PBMC IFN-γ secretion assays, despite some anomalies and the lack of isotype control in the latter. Crucially, their work culminated in an animal trial. The treatment led to a statistically significant decrease in overall survival when compared to historical controls. Although this bold study suffered from methodological issues and the interpretation of trial results invites careful scrutiny (please refer to the supplement), it stands as an important attempt at translating lab bench developments to the bedside. We are actively progressing toward the caninization of our antibodies with the aid of specialized techniques, a crucial step toward the ultimate goal of clinical trials.

Our antibodies against canine PD-1 stand out as comprehensively characterized and uniquely versatile across diverse molecular assays. PD1-1.1 excels in diagnostic applications, whereas PD1-2.1 shows greater promise as a potential therapeutic. Further research is warranted to validate the potential of developed antibodies in both domains.

3.4 Future perspectives

3.4.1 Receptor or ligand - which one to block?

The sequence of PD-L1 - the prevalent PD-1 ligand - is more conserved than the PD-1 sequence (76% vs 66% identity, respectively). This corroborates the fact that human anti-PD-L1 therapeutics Avelumab and Atezolizumab have been found to block canine PD-1 - PD-L1 interaction [128]. However, PD-1, with its less conserved sequence, necessitated the development of canine-specific antibodies.

While targeting PD-1 may be more therapeutically effective in some clinical settings [198], targeting PD-L1 may be associated with fewer adverse reactions [199].

Importantly, both PD-1 ligands have been found to also engage other receptors [200,201]. Consequently, the biological impact of ligand blockade is related to modified signaling downstream of multiple receptors, rather than just PD-1.

On the other hand, a recent study in the field of autoimmune alleviation has illuminated a new mechanism: blocking the CD80 receptor can effectively redirect its ligand, PD-L1, to interact more preferentially with its alternative receptor, PD-1 [202]. This process amplifies the agonistic effect on PD-1, leading to immunosuppression. Extrapolating from this, it is plausible to hypothesize that inhibiting PD-1 could conversely lead to a heightened agonistic effect on CD80. Furthermore, this process could possibly influence the activation of hitherto unidentified receptors for the PD-L1 and PD-L2 ligands.

The potential for undesired receptor modulation could contribute to the mechanisms behind hyperprogression observed in patients undergoing ICB immunotherapy. The biological and clinical differences resulting from receptor and ligand blockade remain to become untangled and fully understood. To complete the PD-1 checkpoint toolkit, we are developing canine anti-PD-L1 mAbs.

3.4.2 The importance of PD-L2

In this study, we analyzed the blocking property of antibodies regarding the PD-1/PD-L1 interaction, while omitting the second known PD-1 ligand: PD-L2. This is a common practice, since PD-L2 expression had long been believed to be restricted to cytokine-

stimulated macrophages and dendritic cells, and to remain insignificant [203]. Since the ICI founding idea was to shield tumor-infiltrating lymphocytes from the cancer-expressed IC ligands, PD-L2 seemed irrelevant. However, light has been shed on the importance of immune checkpoint interactions between immune cell subtypes such as regulatory T-cells (TREGs), tumor-associated macrophages (TAMs), dendritic cells (DCs) and cytotoxic T-lymphocytes [204–206]. Additionally, it was demonstrated that PD-L2 is expressed in stromal, immune and tumor cells, may bind PD-1 with higher affinity than PD-L1 and constitutes an essential immunotherapy target [207–209]. Despite that, PD-L2 remains largely outside the research spotlight. In humans PD-L2 is known to bind PD-1 through a different mechanism than PD-L1 does, potentially making it affected differently by the IC inhibitors [210]. Hence, the conclusions of this study cannot be extrapolated to PD1/PD-L2 interactions. The inhibition of PD-1/PD-L1 axis should not be thought of as a general PD-1 blockade in the context of this and further studies.

3.4.3 Novel immune checkpoint targets

Finally, current research into immune checkpoints is no longer limited to the PD-1 receptor and T-cells [97,211]. Questions arise about the multi-layer network of interactions between all ICs and all immune cell types. Recently, it has become apparent that alternative splicing of IC proteins adds to the already complex picture [212–215]. We predict that monoclonal antibodies specific to IC splice variants and post-translationally modified forms will emerge as a new, more targeted generation of ICI therapeutics [197,216].

3.5 Methods

3.5.1 Generation of anti-canine PD-1 monoclonal antibodies

Initially, a year was devoted to the development of a canine PD-1 antibody using phage display techniques. This approach would have resulted in a low-immunogenic product owing to the fully canine amino acid sequences in the library. Although the same phage library had previously been used with success for another target, it did not succeed with the current one, despite extensive troubleshooting. This experience precipitated the switch in study subject to the characterization of hybridoma-derived antibodies supplied by our collaborators.

Canonical PD-1 protein sequences were obtained from Ensembl for human, dog, mouse, Norwegian rat, and rabbit. The canine sequence was compared to others with Protein Blast. The highest similarity score was found between canine and human protein variants, followed by rabbit, rat and mouse. The mouse sequence was least similar, rendering the mouse the best model for raising antibodies against human PD-1. Development of high-affinity antibodies against the target protein would be less probable in a species that produces a nearly identical protein naturally [179].

The antibody generation and production were carried out Moravian Biotechnology Ltd. (Brno, Czech Republic) under the animal license number 14828/2010–17210 falling under European Union law. The process was performed as we previously described [186]. Briefly, Balb/c mice were immunized with a recombinant protein fusing the complete canine PD-1 sequence and a his-tag (Sino Biological). Upon reaching high antibody titer in serum the mice were sacrificed, splenocytes were collected, and subsequently fused with SP2 mouse myeloma cells. Conditioned media from the culture of individual hybridoma clones were screened for recognition of recombinant canine PD-1 with a human Fc-tag (Sino Biological). Two best binders, coming from clones cAb1910 and cAb1911, were chosen for further study and named PD1-1.1 and PD1-2.1, respectively. For the experimental assays, the antibodies were purified by Fast protein liquid chromatography (FPLC; Cytiva ACTA) on protein A columns (GE Healthcare), eluted with high salt and cleared on desalting columns (Zeba Spin). Antibody aliquots were stored in PBS at a concentration approximating 1mg/L, with or

without (for cell-based assays) 0,1% sodium azide as a preservative. All aliquots were stored frozen at -20°C.

Prior to the characterization of the hybridoma-derived antibodies supplied by our collaborators, approximately a year was devoted to the development of a canine PD-1 antibody using phage display techniques. This approach would have resulted in a product with a fully canine amino acid sequence. However, despite extensive efforts and rigorous troubleshooting, these attempts did not yield a functional product. This experience precipitated the switch in study subject.

3.5.2 Antibody isotyping

The antibodies were isotyped with a Pierce Rapid Antibody Isotyping Kit (Thermo Scientific, #26179) according to the manufacturer's protocol.

3.5.3 Test

The sequences of PD1-1.1 and PD1-2.1 light and heavy chains were obtained by hybridoma sequencing using the 'Cloning Hybridoma cDNA by RACE protocol' by Bradbury [217]. The sequences were kindly provided by Prof. Ted Hupp.

3.5.4 Cell culture

U-2 OS [U2OS] human osteosarcoma cell line was purchased from Elabscience (#CL-0236). Cells were cultured in modified McCoy's 5A medium (Gibco, #16600082) supplemented with 10% FBS (Gibco, #10500064) and 100UI/ml Penicillin-Streptomycin (Gibco, #15140122). Cells were grown in a humidified atmosphere supplemented with 5% CO_2 at 37°C. The U2OS line was chosen for its reliable growth in our laboratory.

3.5.5 Stable PD-1+/- cell lines

To create a stable expression of recombinant protein $2*10^5$ cells were seeded per well of a 6-well plate 24 hours before transfection. The transfection was performed using 6.75µl of Attractene transfection reagent (Qiagen, #301005) mixed with 1.8µg of pcDNA 3.1 plasmid vector encoding either an empty vector or canine PD-1 (Thermo Scientific). To create stable cell lines, cell culture media were replaced with selection

media containing antibiotics 24 hours after the transfection. Control cells transfected with an empty vector were treated with 100 µg/ml Hygromycin B (Gibco, #10687010), while PD1-overexpressing cells were selected using 400 µg/ml Geneticin (Roche, #G418-RO) for 2 weeks. The transfected cell lines used in the final experiments were generated and provided by Katarzyna Dziubek. Preliminary experimental work also included transfected cell lines generated by the author.

3.5.6 Protein isolation and western blotting

U2OS cells were washed two times with PBS and lysed with CelLytic™ M (Sigma-Aldrich, #C2978) mixed with a manufacturer recommended amount of protease inhibitors (Sigma-Aldrich, #P8340-1ML). Lysates were incubated on ice for 20 minutes and centrifuged for 15 minutes at 14,000 x g at 4°C. Next, samples were denatured by boiling for 5 minutes at 95°C in reducing conditions. Subsequently, 30µg of total protein was separated by SDS-PAGE, where samples were run along a PageRuler Plus Prestained 10-180kDa protein ladder (Thermo Scientific, #26616). The separated proteins were transferred to a nitrocellulose blotting membrane (Amersham Protran) using a wet blotting system (Bio-Rad). The membranes were blocked for 1 hour at RT in 5% skimmed milk diluted in 0.1% Tween-20 in Tris-buffered saline (TBST). Subsequently, membranes were incubated overnight with 1:1000 dilution of either PD1-1.1 or PD1-2.1 antibody, washed three times with TBST and incubated for 1 hour at RT with 1:5000 dilution of HRP-conjugated anti-mouse secondary antibody (Abcam, #ab6728). To reprobe the membranes for ß-actin, Restore Plus Western Blot Stripping Buffer (Thermo Scientific, #46430) was used. Following three more washes with TBST, membranes were visualized using ECL substrate (Westar Antares, Cyanagen) and imaged with ChemiDoc imaging system (Bio-Rad). Initial work on the western blot optimization for antibodies in question was undertaken by the author, involving extensive trials and adjustments over a six-month period. This foundational work informed the subsequent decision to use transfected cell lines overexpressing PD-1, an approach successfully implemented by Katarzyna Dziubek for the visualized experiment. Data analysis and interpretation were completed by the author.

3.5.7 Species specificity by western blot

To assess the cross-reactivity of the characterized antibodies with human PD-1, HEK293 cells, which naturally do not exhibit considerable PD-1 expression, were transfected with either a human PD-1 expression vector containing V5 and Twin-Strep tags (V5-TS-PD1) or the canine PD-1 expression vector. Transfection, cell harvesting, and Western Blotting were performed as previously described. The PD1-1.1 and PD1-2.1 antibodies were tested against the lysates containing PD-1 from both species. Additionally, an antibody against human PD-1 was used as a positive control for the presence of hPD-1 (eBioscience, #14-2798-82). All antibodies were used at a dilution of 1:1000. The experimental design was planned by the author, executed by Katarzyna Dziubek, and analyzed by the author.

3.5.8 PD-1 binding ELISA

A 96-well assay plate (ThermoFisher/Nunc, #442404) was coated overnight at 4°C with 9.4μg of rcPD-1 protein (approximately 98ng per well; Sino Biological, #70109-D08H) diluted in PBS (0.25mg/mL). The plate was washed with PBST (PBS with Tween-20 at 0,1%). All washes were performed three times with 400μl PBST/well. Next, the plate surface was blocked with a blocking buffer (BB) consisting of 3% BSA (Sigma-Aldrich, #A3059) in PBST for 1h. All incubations were performed at room temperature. Serial dilutions of the tested antibodies were prepared in BB and transferred to the assay plate at 100μl/well for a 1-hour incubation. Upon a wash, an HRP-conjugated rabbit polyclonal anti-mouse detection antibody (Agilent/Dako, #P0260; discontinued) diluted in BB was added at 100μl per well. After the final wash, 150μl of TMB (Merck, #ES022) was added, the plate was incubated in darkness at RT with shaking for 30min. Subsequently, absorbance was measured at 650nm using a Varioskan LUX multimode microplate reader (ThermoFisher). Data was pre-processed in Microsoft Excel to subtract blank values and compute the means and standard deviation. The EC50 values were computed, and final results visualized using GraphPad Prism.

3.5.9 Flow cytometry (FC)

Cells were trypsinized, washed two times with PBS and stained for 30 minutes protected from light at RT with 1:500 dilution of either PD1-1.1 labeled with PE

(Abcam, #ab102918) or PD1-2.1 conjugated with APC (Abcam, #ab201807). The antibodies were conjugated with fluorophores earlier as described in the manufacturer's protocols. Staining with isotype control antibody (BioLegend, #400263) conjugated with PE or APC fluorophore was used as a negative control. Subsequently, cells were washed two times with PBS and analyzed with BD FACSAria II cell sorter (BD Biosciences). Results were analyzed with FlowJo v10.8.1 flow cytometry analysis software (BD Biosciences) with implementation of doublet discrimination. The experiment was performed exclusively by Katarzyna Dziubek. Implications of the data were interpreted by the author.

3.5.10 Surface plasmon resonance (SPR)

The affinity of the PD1-1.1 and PD1-2.1 to cPD-1 was assessed by surface plasmon resonance (SPR) using a Biacore T200 (GE Healthcare) instrument as described in the manufacturer's manual. A HEK-produced recombinant canine PD-1 (rcPD-1; 17.7 kDa) protein, residue Met1-Leu169, with a C-terminal His-tag was purchased from Sino Biological (#70109-D08H). Protein purity was > 85 % as determined by SDS-PAGE, and the protein was formulated by lyophilization from sterile PBS, pH 7.4. rcPD-1 was reconstituted in sterile water (at a concentration of 0.25mg/mL) and diluted in HBS-EP (150 mM NaCl, 10 mM HEPES pH 7.4, 3 mM EDTA, 0.05% Surfactant P20). The same buffer was used as a running buffer for further analysis. cPD-1 was immobilized on CM5 Series S Sensor Chips (Cytiva) using amine-coupling chemistry at a density of 330RU on flow cell 2 and flow cell 1 was left blank to serve as a reference surface. Ultra-LEAF™ Purified Mouse IgG2a antibody was used as an isotype control (Biolegend, #400263). Both PD1-1.1 and PD1-2.1 solutions but not the isotype control contained 0.02% sodium azide. A Tycho instrument (Nanotemper) was used to confirm the stability of tested antibodies in the given buffer and temperature. Analyte weights were predicted based on the amino acid sequence: PD1-1.1 - 146.33kDa, PD1-2.1 - 145.93kDa, isotype control - estimated as 146kDa considering the same species and isotype [218]. An approximate molecular weight of 146kDa was used for all calculations. To collect kinetic binding data, the analytes in the running buffer were injected into the flow cells at concentrations of 0, 2.5, 5, 10, 50, 100, 200, and 400 nM. The flow rate was 30 µl/min, injection volume was 120 µl and the temperature was stabilized at 25°C. The sensor chip surface was regenerated with 10

mM glycine pH=1.5. Results were analyzed using Biacore T200 Evaluation Software 3.1 (GE Healthcare). The results are presented as sensorgrams obtained after subtracting the signal from the reference cell and the signal after buffer injection. SPR optimization and final experimental work were performed in collaboration with Dr Katarzyna Węgrzyn.

3.5.11 Blocking ELISA

To test the capacity of the PD1.1 and PD2.1 antibodies to block the therapeutically important binding between canine PD-1 receptor and PD-L1 ligand, an ELISA assay was developed and optimized. The recombinant canine PD-1 protein (rcPD-1) with a C-terminal polyhistidine tag (Sino Biological, #70109-D08H) and recombinant canine PD-L1 (rcPD-L1) extracellular domain (ECD) with a C-terminal Fc-tag (Sino biological, #70110-D02H) lyophilized from PBS with protectants were reconstituted in sterile water according to the manufacturer's instruction, reaching 0,25mg/mL protein concentration. Aliquots were prepared containing 6,25µg of protein each, and were stored at -20*C. Both proteins were originally produced in HEK293 cells. The eukaryotic expression system is crucial for the post-translational modifications (PTMs) of these proteins, such as glycosylation, which affect the protein characteristics and binding. While some researchers use variants of these proteins produced in bacterial expression systems for their low cost, we do not consider data on the PD-1/PD-L1 interaction and its blocking reliable, if obtained using bacterial protein products. F96 Maxisorp Nunc Immuno plate (Thermo Scientific, #442404) was coated overnight at 4*C with 100µl of coating solution per well, containing 125ng or rcPD-1 per well (1,25µg/mL) in PBS (in-house) as a coating buffer. The plate was washed 3x with 400µl PBST (PBS + Tween-20 at 0,01%) and blocked with a blocking buffer (BB). BB consisted of 3% Bovine Serum Albumin (BSA, protease free, essentially globulin free, Sigma, #A3059-100G) in PBST. Upon 90min of blocking, the samples were loaded at 100µl. The perimeter rows of the plate were not used and were filled with an equal volume of PBS on this and further stages to avoid temperature gradient affecting all the processes. Ultrasensitive TMB substrate (Merck, #ES022-500ML) was brought to room temperature. Samples were prepared by serial dilutions in BB, starting from azide-preserved antibody stocks in PBS at original concentrations of 1mg/mL for PD1.1 and 1.1mg/mL for PD2.1. Controls were loaded with BB. Upon 60min of

incubation at room temperature (RT) with the plate covered, another wash followed (all washes were done in the same way), the plate was dried upside down on a paper towel, and 100µl of rcPD-L1 dilution was added to all wells, except the „background signal" control and the perimeter rows. PD-L1 was diluted in BB at the concentration of 7,81 µg/mL (781ng/well). After 1h incubation at RT and a wash, a detection antibody was applied at 100µl/well, 1:500 concentration. This secondary antibody was a mouse anti-human-IgG1 antibody conjugated to horseradish peroxidase (HRP; Invitrogen, #A10648), meant to detect the Fc-tag and hence the PD-L1 that remained bound to the PD-1, whenever the PD-1 binding site was not blocked by the tested antibodies. After a 1h incubation and a wash, TMB substrate was added at 100µl to all wells, and the plate was put on a plate shaker for 50min. Next, 100ul of a STOP solution (0.16M sulfuric acid) was added to all wells, and the yellow reaction product was measured by absorbance of the 450nm wavelength using Varioskan Lux (Thermo Scientific) reader and Skanit RE 6.0.1 software. Results were calculated in Microsoft Excel. The curve plot and IC50 values were obtained with an AAT Bioquest IC50 Calculator [219], after subtracting the background signal.

3.5.12 Tissue collection

Fresh blood was obtained from 8 dogs that were euthanized for reasons unrelated to this study. All tissue collection procedures were performed under the approval and guidance of the Veterinary Ethics Research Committee (Institutional Care and Use Committee; project number 96/21) at The Royal (Dick) School of Veterinary Studies, University of Edinburgh. Details regarding the blood donors can be found in Table 3.

Table 3. Details on the canine donors of blood used for PBMC extraction.

Number	Sex	Age	Breed	Health Status
1	male	1 year	Beagle	Healthy
2	female	11 months	Beagle	Healthy
3	male	1 year	Beagle	Healthy
4	male	10 months	Beagle	Healthy
5	female	11 months	Beagle	Healthy
6	male	14 months	Beagle	Healthy
7	female	13 months	Beagle	Healthy
8	female	1 year	Beagle	Healthy

3.5.13 PBMC culture and treatment

PBMC fraction was separated by density gradient centrifugation using Lymphoprep reagent and SepMate-15 tubes (STEMCELL, #07851 and #85415) according to the manufacturer's protocol. The cells were centrifuged, resuspended in RPMI-1640 medium with 10% FBS and Pen-Strep antibiotic mix, and seeded at the initial concentration of 10^5 cells/well, 50µl/well, on a 96-well culture plate. The cells from each animal were grown either exposed to no additional factors, Concanavalin A (ConA; 5µg/ml; ThermoFisher, #00-4978-03), or ConA and one of the three antibodies at 10µg/ml: PD1-1.1, PD1-2.1, isotype control (Biolegend, #401509). The culture lasted 72h, after which the plate was centrifuged. The conditioned medium from each well was harvested and transferred to a prepared ELISA plate in the next step.

3.5.14 PBMC secretion of IFN-γ by ELISA

The Quantikine Canine IFN-γ Immunoassay kit (R&D Systems. #CAIF00), which applies a sandwich enzyme immunoassay technique, was utilized in this study to quantify IFN-γ. The kit was used in accordance with the manufacturer's protocol. Briefly, the provided canine IFN-γ standard was reconstituted and two-fold serial

dilution was prepared, starting at a concentration of 4000 pg/mL, to generate the standard curve. Following the preparation of capture antibody-coated wells, the prepared samples and standard solutions were added. This step was followed by an incubation period. Subsequently, the wells were washed to remove unbound substances. Then, a detector antibody against canine IFN-γ conjugated with biotin was added. The detector antibody binds to the antigen already captured by the first antibody, effectively sandwiching the antigen between the capture antibody and the detector antibody. After another incubation period, another wash followed. The wells were then treated with Streptavidin-HRP (Horseradish Peroxidase), which binds to the Biotin Conjugate, forming an antigen-antibody-enzyme complex. This was followed by an additional incubation and washing phase. The Substrate Solution, which reacts with HRP, resulting in a color change, was then added. The reaction was stopped by adding the Stop Solution, which halts color development. The solution's absorbance was measured at a wavelength of 450 nm with a correction at 570 nm. In four cases the reader noted signal overflow, resulting in missing data; those PBMC samples were rejected, leaving PBMC samples from 5 dogs in the analysis. The mean and standard deviation were calculated for experimental duplicates. The averaged signal was normalized through dividing by the signal from isotype control wells of each respective PBMC sample. Preliminary tests, which ruled out the use of frozen PBMCs and Promega Cell Titer Glo-based proliferation assay, were performed by the author, with Dr. Maciej Parys conducting the experiment in the refined setup. The author is responsible for the data analysis, interpretation, and figure generation.

3.5.15 PBMC secretion of IFN-γ - statistical analysis

Significant differences in signal between treatment groups were sought. The t-test was initially considered for this analysis. However, the t-test assumes that the data is normally distributed, and upon evaluation using the Shapiro-Wilk test, it was determined that the data was not normally distributed for some of the treatment groups. Consequently, the Kruskal-Wallis non-parametric test, which does not assume normal distribution, was performed using GraphPad Prism software and revealed a significant difference to be present among some of the treatment groups. To identify these groups, a post-hoc analysis was conducted using Dunn's multiple comparisons test, which adjusts the p-values for multiple comparisons, reducing the risk of false

positive results. Despite these efforts to employ robust statistical methods, the analysis yielded some unexpected results. Differences were observed between certain treatment groups, but some comparisons that appeared to show biologically meaningful differences did not reach statistical significance. Working with small sample sizes presents challenges, as it diminishes the statistical power of conventional analyses. Consequently, it is essential to interpret results by considering both statistical significance and biological relevance.

3.5.16 Immunohistochemistry

Immunohistochemistry (IHC) was performed on FFPE tissue sections using the Leica Bond Research Detection Kit (Leica Biosystems), according to the standard manufacturer's protocol. Staining was performed on a BOND-RX Multiplex IHC autostainer (Leica Biosystems), with the following settings: sample preparation - 'bake and dewax', staining - 'routine EnVision mouse', HIER protocol - 'HIER 20 min with ER1'. The PD-1 antibody was used at a 1:100 dilution (10µg/mL). IHC images were kindly generated by the Royal (Dick) School of Veterinary Studies imaging facility.

3.5.17 Immunocytochemistry and confocal microscopy

800,000 cells were seeded on 18mm coverslips in a 6-well plate and incubated for 24 hours. Subsequently, cells were fixed with 4% paraformaldehyde for 15 minutes, washed three times with PBS and permeabilized with 0.1% Triton X-100 for 10 minutes. Slides were blocked with 10% goat serum for 1 hour and stained for 1 hour with 100µl of either PD1-1.1 or PD1-2.1 antibodies diluted 1:100 in 0.1% goat serum. Slides were washed five times in 0.1% PBST, 2 minutes each time and incubated for 1 hour protected from light with 100µl of 1:500 dilution of Alexa FluorTM 488 secondary antibody (Invitrogen, #A32723). Subsequently, samples were washed five times with PBST, mounted with ProLong™ Diamond Antifade Mountant with DAPI (Invitrogen, #P36966) and left overnight to dry protected from light. Imaging was performed with Olympus Fluoview FV3000 confocal laser scanning microscope using 63x oil immersion lens. All images were acquired using the same settings for laser power, voltage and gain. Initial experimental groundwork was carried out by the author, and the final experiment utilizing a confocal microscope was conducted by Katarzyna Dziubek.

3.5.18 PD-1 epitope modeling for PD1-1.1 and PD1-2.1

The variable domains of both antibodies were modeled with the antibody-specific AbodyBuilder2 tool [220]. The canine PD-1 sequence was obtained from Ensembl and was identical to the UniProt sequence (A0A8I3PL99). It is important to note that the Ensembl and UniProt annotations of the canine PD-1 gene were modified when this study was undergoing. The (E2RPS2_CANLF) variant used in some earlier analyses was recalled; additionally, another, longer and differing canine PD-1 sequence available at UniProt ID (A0A8I3PR61) which might be preferable for further studies. However, the three sequences do not differ in the extracellular Ig-like region that was analyzed and modeled in this study. The sequence was divided into domains through ClustalO alignment [221] to the human PD-1 sequence, richly annotated on UniProt (Q15116). Additionally, the canine PD-1 domains were validated with InterPro [222]. The identified extracellular, Ig-like receptor domain was submitted for modelling with Phyre2 [223]. Each antibody domain was docked to the PD-1 receptor domain using ClusPro2.0 [224,225] in the antibody mode with masking of non-CDR regions. For each antibody domain, binding models were ranked by the corresponding cluster sizes, and the top most-probable binding model was chosen. Such obtained model was re-exported to PDB file in PyMol [226], to contain a single-object with three chain labels (L,H, and A for light chain, heavy chain and PD-1). The PDB file was analyzed with PISA [227] to identify the key interface residues. Results were visualized in PyMol.

.

3.6 Supplementary materials

3.6.1 Supplementary figures

Figure S1. Western blots corresponding to the results shown in Figure 2 are displayed without cropping or contrast adjustments. These blots confirm the specificity of the PD1-1.1 (A), PD1-2.1 (B), and anti-human PD-1 (C) antibodies in detecting canine and human PD-1 proteins, respectively.
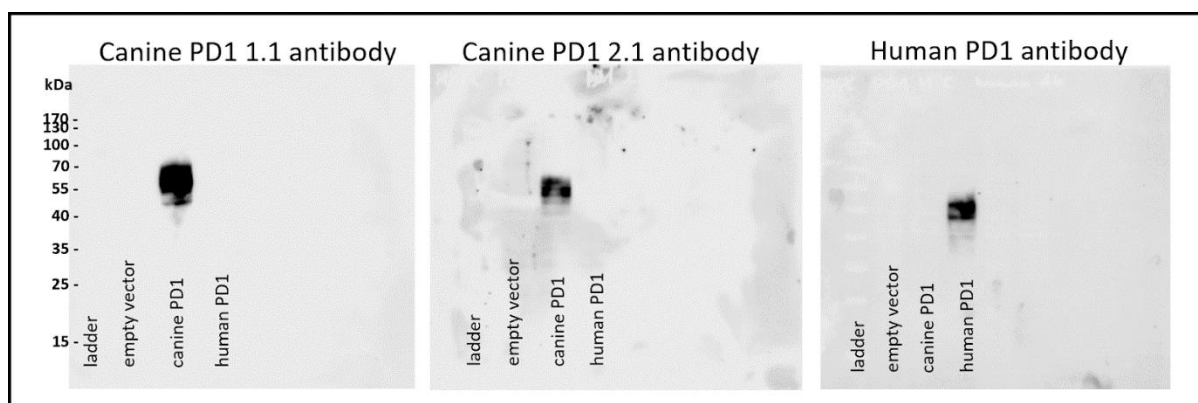
3.6.2 Supplementary results

3.6.2.1 PD1-1.1 epitope mapping by Protein Ligand Interaction Fingerprints (PLIF)

To supplement the in silico prediction of the PD-1 epitopes for our antibodies, we prototyped another epitope mapping method, aimed at laboratory validation. Here, we started by epitope modeling with the Protein Ligand Interaction Fingerprints (PLIF) method. We focused on the PD1-1.1 monoclonal mAb first and modeled its binding to the cPD-1 extracellular domain. Results of multiple prediction rounds highlighted two epitope candidate regions (Fig. S2-S4). For laboratory validation, we focused on two continuous motifs that repeatedly featured in the predictions: cPD1 residues (D61, S62) and (Q83, E84, D85).

Figure S2. Epitope modeling for PD1-1.1 by the Protein Ligand Interaction Fingerprints (PLIF) method. PLIF was applied to model the interactions between cPD-1 and the PD1-1.1 antibody leading to the identification of two candidate epitopes repeatedly appearing in the simulations. Out of those regions, two short sequences were chosen for further validation, based on their prevalence and continuous character. Figure courtesy of Dr Umesh Kalathiya.
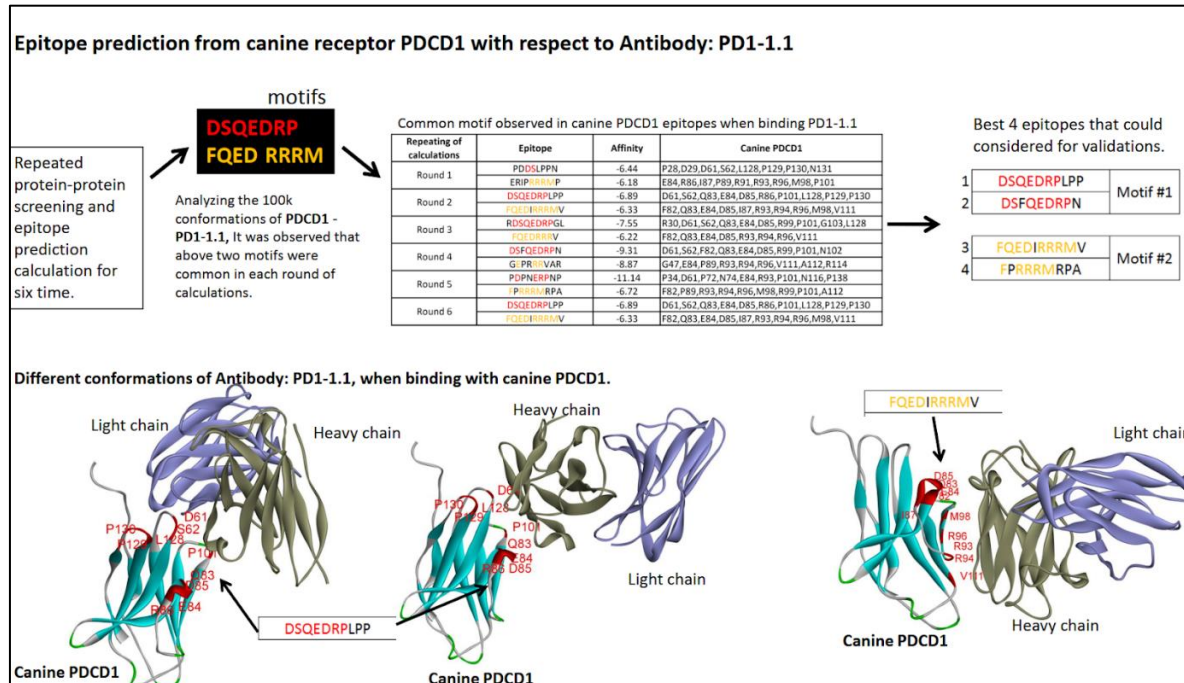
Figure S3: Top four epitope candidates identified for PD1-1.1 by PLIF were mapped on the cPD-1 sequence and compared to the PISA-identified epitope. For PLIF, the green highlight denotes epitope residues; for PISA, the green highlight denotes interface residues, pink - interface residues forming bonds.

Figure S4: Top four epitope candidates identified for PD1-1.1 by PLIF were mapped on the cPD-1 structure and compared to the PISA-identified epitope. For PLIF, the red highlight denotes epitope residues; for PISA, the pink highlight denotes interface residues and the red one denotes the residues forming bonds.
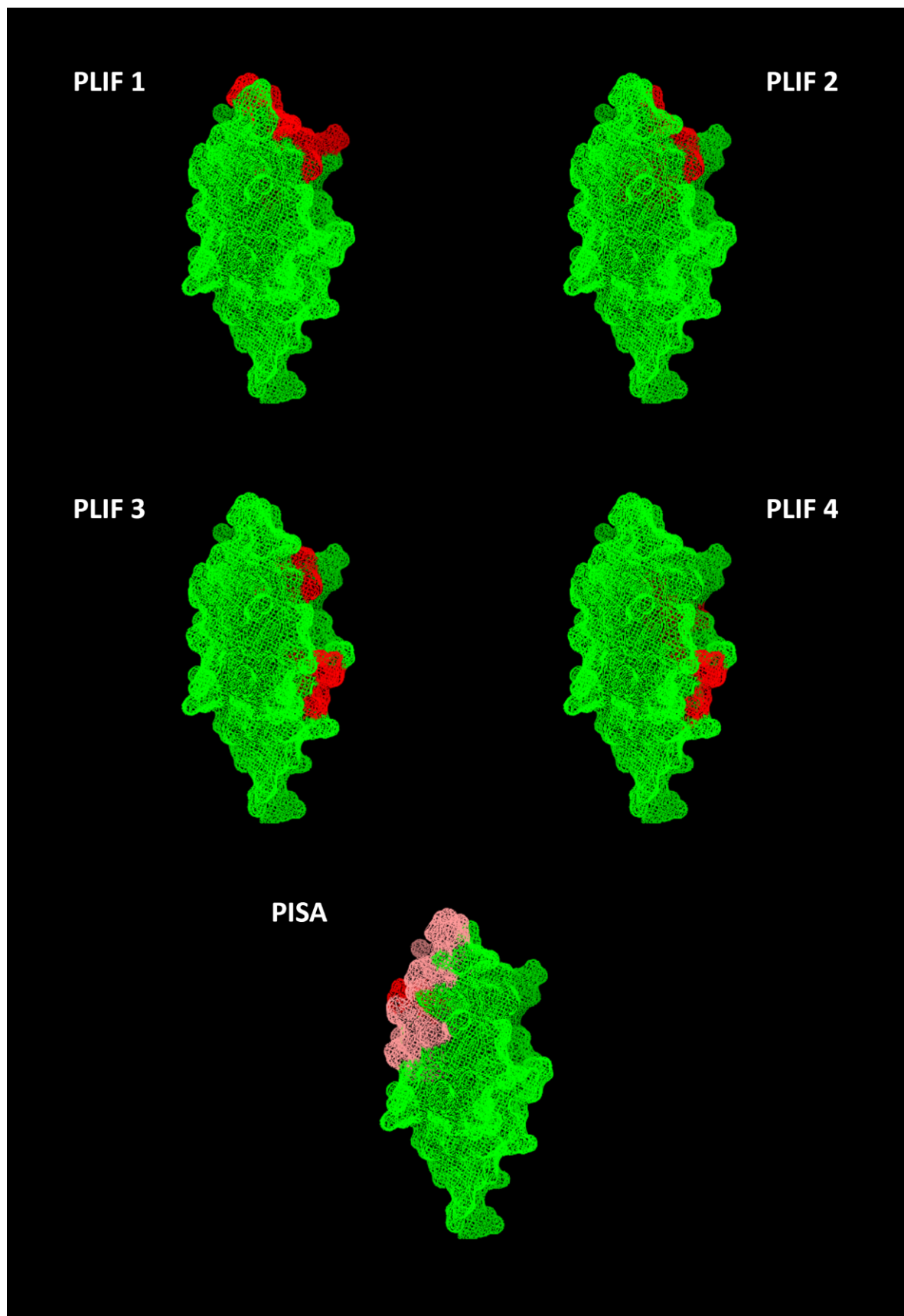
3.6.2.2 PLIF-based epitope validation

Based on the PLIF results, we designed three genetic constructs encoding versions of a cPD-1 protein sequence (Tab. S1). One encoded wild-type cPD-1 for positive control; in the other two, we replaced amino acids of the putative binding sites with Alanine residues. The constructs additionally encode poly-Histidine tags for positive control of each respective protein expression.

Table S1: Canine PD-1 constructs for PD1-1.1 mAb epitope mapping; orange - signal peptide, green - His-tag, red - predicted epitope motif sites, black highlight: introduced mutations.

Mutation	Construct sequence
WT (Uniprot: E2RPS2_CANLF)	MGSRRGPWPLVWAVLQLGWWPGWLLDSPHHHHHHDRPWSPLTFSPAQLTVQE GENATFTCSLADIPDSFVLNWYRLSPRNQTDKLAAFQEDRIEPGRDRRFRVMRLP NGRDFHMSIVAARLNDSGIYLCGAIYLPPNTQINESPRAELSVTERTLEPPTQSPSP PPRLSGQLQGGLVIGVTSVLVGVLLLLLLTWVLAAVFPRATRGACVCGSEDEPLKEG PDAAPVFTLDYGELDFQWREKTPEPPAPCAPEQTEYATIVFPGRPASPGRRASAS SLQGAQPPSPEDGPGLWPL
61-62 mutant	MGSRRGPWPLVWAVLQLGWWPGWLLDSPHHHHHHDRPWSPLTFSPAQLTVQE GENATFTCSLADIPAAFVLNWYRLSPRNQTDKLAAFQEDRIEPGRDRRFRVMRLP NGRDFHMSIVAARLNDSGIYLCGAIYLPPNTQINESPRAELSVTERTLEPPTQSPSP PPRLSGQLQGGLVIGVTSVLVGVLLLLLLTWVLAAVFPRATRGACVCGSEDEPLKEG PDAAPVFTLDYGELDFQWREKTPEPPAPCAPEQTEYATIVFPGRPASPGRRASAS SLQGAQPPSPEDGPGLWPL
83-85 mutant	MGSRRGPWPLVWAVLQLGWWPGWLLDSPHHHHHHDRPWSPLTFSPAQLTVQE GENATFTCSLADIPDSFVLNWYRLSPRNQTDKLAAFAAARIEPGRDRRFRVMRLP NGRDFHMSIVAARLNDSGIYLCGAIYLPPNTQINESPRAELSVTERTLEPPTQSPSP PPRLSGQLQGGLVIGVTSVLVGVLLLLLLTWVLAAVFPRATRGACVCGSEDEPLKEG PDAAPVFTLDYGELDFQWREKTPEPPAPCAPEQTEYATIVFPGRPASPGRRASAS SLQGAQPPSPEDGPGLWPL

The constructs were cloned into expression plasmids. The plasmids were multiplied in *E.coli* culture and highly purified. Those plasmids will be transiently transfected into U2OS cells. After 72h the cells will be lysed and analyzed by WB and ELISA for the binding of anti-PD-1 antibodies. The expression of all protein constructs will be validated with the anti-His antibody. While WB allows for a qualitative assessment of the size of the protein bound by the antibody, ELISA allows for a quantitative assessment, and most importantly, provides non-reducing conditions, which seem to be important for the binding of tested antibodies, as evidenced in the previous assays.

While this approach promises biological validation of the epitope prediction, it is not without risk. The introduced mutations might affect the folding of various protein regions, leading to the disruption of epitopes whether or not they were correctly

predicted. Homology modeling is not suitable for assessing the effect of such point mutations (sbg.bio.ic.ac.uk/phyre2/html/help.cgi?id=help/faq#mutations). Tools designed for such predictions predominantly focus on single mutations only and pre-analyzed mutation databases focus on human proteins. The results of introduced mutations and hence experimental outcomes do not guarantee correct epitope annotation.

3.6.3 Supplementary methods

3.6.3.1 PD1-1.1 epitope modeling by PLIF prediction (supplementary)

Molecular dynamics simulation of PD1-1.1 mAb binding to cPD-1 was performed using Protein-Ligand Interaction Fingerprints (PLIF) method, based on the sequence of cPD-1 Ig-like domain (UniProt: tr|E2RPS2|31-143), and PD1-1.1 heavy and light variable domains. The structures were modeled based on the following templates: cPD-1 - human PD-1 (PDB 5wt9, 71.78% sequence identity), variable light (VL) chain - neutralizing antibody to murine norovirus (PDB: 4NCC, 97.17% identity), variable heavy (VH) - neutralizing antibody 8G12 (PDB: 4PLK, 85.47% identity). Molecular docking identified top putative epitope sites. Between these sites, two continuous motifs were chosen for targeted mutations: PD-1 amino acids 61-62 (D61, S62) and 83-85 (Q83, E84, D85). The preparatory steps were spearheaded by the author, and the molecular modeling was conducted by Dr Umesh Kalathiya.

3.6.3.2 PD1-1.1 PLIF-based epitope validation plan (supplementary)

Three genetic constructs were designed, all encoding the complete cPD-1 sequence with an N-terminal 6xHis tag introduced in between the signal peptide and the protein chain (Table 2). The tag was introduced to enable the detection of each protein construct expression. His-tag was chosen for its exceptionally small size, thanks to which it rarely affects protein function. The tag was inserted 4 residues after the signal peptide to not disrupt the efficiency of its cleavage, as predicted using SignalP-5.0 [228]. The N-terminal tag location was chosen for its extracellular location. One construct encoded wildtype cPD-1 to be used as a positive control. The two remaining ones had mutations introduced into the putative epitope motifs. In each one, a single motif was disrupted by a substitution of its amino acids to Alanine residues. All three constructs were cloned into pTwist CMV Puro vectors, multiplied in *E.coli* culture

grown in LB medium containing selective concentration of Ampicillin and purified with a PureLink HiPure Plasmid Filter Maxiprep Kit (ThermoFisher #K210016). Plasmids dissolved in the TE buffer were quantified with a NanoReady Nanodrop-like instrument (LifeReal).

The plasmids holding three constructs will be used to transiently transfect U2OS cells using Lipofectamine 2000 transfection reagent (#11668019, Invitrogen) according to the manufacturer's recommendations. Upon 3 days of culture, cells will be lysed with CelLytic M buffer (Sigma-Aldrich) and the lysate will be subjected to Western Blot. The three lysates will be tested against three antibodies on Western Blot. First, the expression of the tagged cPD-1 constructs will be assessed in all cases by Anti-Histidine Tag antibody (ThermoFisher, #MA5-33032). Next, PD1-1.1 and PD1-2.1 antibodies will be tested for binding all three constructs. The WT PD-1 lysate will serve as a positive control. Additionally, the samples will be run against the same antibodies in ELISA to enable a more quantitative and sensitive analysis, considering the previous performance of the antibodies in these assays

3.6.4 Supplementary comments

3.6.4.1 The challenges of the PBMC-based IFN secretion assay

There were several issues encountered with our PBMC PD-1 blockade assay that merit discussion. First, we observed substantial heterogeneity in the immune responses of PBMCs to the test antibodies PD1-1.1 and PD1-2.1. While one dog's PBMCs showed a strong response consistent with our previous ELISA results, this outcome was an outlier, with most dogs showing no discernible response. Due to the varying medical histories and treatments of these dogs (information not disclosed to us), we could not control for potential factors that might influence the immune state of the PBMCs. These factors could potentially affect activation or exhaustion of lymphocytes, proportion of immune cell populations, expression of PD-1 and PD-L1, inflammation or immune suppression. Although the ConA control validated that the T-cells in the PBMC samples were capable of activation and IFN-gamma production, it could not account for all the possible complex immune states of the PBMC population. Thus, we acknowledge that the results may not be generalizable.

Second, we noted an unexpected result where the signal from PBMCs treated with ConA alone was higher than that of ConA combined with any of the antibodies. This finding contradicts the expected outcome based on the assay mechanism. Under theoretical expectations, PBMCs activated with ConA alone should produce a signal similar to those treated with both ConA and the isotype control, while PBMCs treated with PD-1 blocking antibodies should display an elevated signal due to the removal of immune inhibition. It is conceivable that PBMCs treated with blocking antibodies might not display an enhanced signal compared to ConA alone if the antibodies are not effective blockers or if there is an insufficient level of PD-L1 expression in the PBMCs to permit PD-1 blocking. However, that fails to explain why the signal for all antibodies was even lower than for ConA. This discrepancy may be attributed to several factors:

- Non-specific binding of antibodies: the antibodies may have non-specifically bound to PBMC components, potentially altering the immune response.

- Fc receptor interactions: the tested antibodies could interact with Fc receptors on immune cells, modulating immune responses. As murine antibodies were used in the assay along canine cells, cross-species reactivity further complicated these interactions.

- Mixed PBMC population: while the assay and its interpretation focus on cytotoxic T-cells, a dominating constituent of PBMC fraction, the presence of various other immune cell types, including T cells, B cells, NK cells, monocytes, and dendritic cells, may impact the overall immune response.

- Monocyte differentiation into macrophages: cultured primary monocytes can differentiate into macrophages in 5-10 days [229]; hypothetically, monocytes present in the PBMC fraction could partially differentiate into macrophages during the experimental period. Macrophages could influence T-cell activation through cytokine production and the pro-inflammatory (M1) or anti-inflammatory (M2) effects. Macrophages are known to be reprogrammed by interactions with Fc antibody sections [230].

In summary, while the PBMC-based IFN-gamma assay aims to simulate a more realistic immune environment than simpler in vitro assays, the lack of standardization limits its interpretability. A more controlled approach could involve isolating cytotoxic

114

T-cells followed by adding recombinant PD-L1 for standardized inhibition, or co-isolating T-cells and PD-L1 expressing cells. The cells could be isolated by magnetic or flow cytometry-based cell sorting. Reliability could potentially be increased by assessing the T-cell activation through a flow cytometry analysis of surface activation markers or cytokine levels within fixed and permeabilized cells. Investigation of the Fc receptor interactions with murine antibodies in the test, and of the potential monocyte and macrophage impact on the assay, while labor intensive, could be informative for future studies involving murine or partially caninized antibodies in canine cancer trials.

Finally, one limitation specific to our assay was found late. For practical reasons, we employed one isotype control antibody of IgG2 isotype specifically, while PD1-1.1 and PD1-2.1 were of IgG2a and IgG2b subtypes, respectively. While the a/b difference may not be relevant in most molecular assays, it could have an impact on an immune cell-based assay. In this context, the key distinction between IgG2a and IgG2b lies in their ability to engage the immune system differently. Specifically, IgG2a is generally considered more pro-inflammatory due to its enhanced ability to interact with Fc receptors and activate immune cells, whereas IgG2b is less potent in this regard. Although the exact interaction between murine isotypes and canine Fc receptors is uncertain, we hypothesize that they could bind differentially. In such a case, results for PD1-1.1 would remain comparable to the isotype control but those for PD1-2.1 less so. Consequently, the experiment should be repeated with improved controls.

3.6.4.2 Blocking ELISA development

To test the capacity of the PD1.1 and PD2.1 antibodies to block the therapeutically important binding between canine PD-1 receptor and PD-L1 ligand, an ELISA assay was developed and optimized. This inconspicuous assay took hundreds of hours and a trip overseas to obtain a viable result.

The recombinant canine PD-1 protein (rcPD-1) with a C-terminal polyhistidine tag (Sino Biological, #70109-D08H) and recombinant canine PD-L1 (rcPD-L1) extracellular domain (ECD) with a C-terminal Fc-tag (Sino biological, #70110-D02H) lyophilized from PBS with protectants were reconstituted in sterile water according to the manufacturer's instruction, reaching 0,25mg/mL protein concentration. Aliquots were prepared containing 6,25ug of protein each, and were stored at -20*C. Both

proteins were originally produced in HEK293 cells. The eukaryotic expression system is crucial for the human-specific post-translational modifications (PTMs) of these proteins, such as glycosylation, which may affect the protein characteristics and binding capacity. While some researchers use variants of these proteins produced in bacterial expression system for their low cost, we do not consider data on the PD-1/PD-L1 interaction and its blocking reliable, if obtained using bacterial protein products.

F96 Maxisorp Nunc Immuno plate (Thermo Scientific, #442404) was coated overnight at 4*C with 100ul of coating solution per well, containing 125ng or rcPD-1 per well (1,25ug/mL, 2 aliquots of 6,25ug in 10mL) in PBS (in-house) as a coating buffer. The plate was washed 3x with 400ul PBST (PBS + Tween-20 at 0,01%) and blocked with a blocking buffer (BB). BB consisted of 3% Bovine Serum Albumin (BSA, protease free, essentially globulin free, Sigma, #A3059-100G) in PBST. Upon 90min of blocking, the samples were loaded at 100ul. The perimeter rows of the plate were not used and were filled with an equal volume of PBS on this and further stages to avoid temperature gradient affecting all the processes. Ultrasensitive TMB substrate (Merck, #ES022-500ML) was brought to room temperature. Samples were prepared by serial dilutions in BB, starting from azide-preserved antibody stocks in PBS at original concentrations of 1mg/mL for PD1.1 and 1.1mg/mL for PD2.1. Controls were loaded with BB. Upon 60min of incubation at room temperature (RT) with the plate covered, another wash followed (all washes done in the same way), the plate was dried upside down on a paper towel, and 100ul of rcPD-L1 dilution was added to all wells, except the „background signal" control on the left and the perimeter rows. PD-L1 was diluted in BB at the concentration of 7,81 ug/mL, effectively 781ng/well (8 aliquots in 6400ul of buffer). After 1h incubation at RT and a wash, a detection antibody was applied at 100ul/well, 1:500 concentration. This secondary antibody was a mouse anti-human-IgG1 antibody conjugated to horseradish peroxidase (HRP; Invitrogen, #A10648), meant to detect the Fc-tag and hence the PD-L1 that remained bound to the PD-1, whenever the PD-1 binding site was not blocked by the tested antibodies. After a 1h incubation and a wash, room-temperature TMB substrate was added at 100ul to all wells, and the plate was put on a plate shaker for 50min. Then, 100ul of STOP solution (0.16M sulfuric acid) was added to all wells, and the yellow reaction product was measured by absorbance of the 450nm wavelength using Varioskan Lux (Thermo

Scientific) reader and Skanit RE 6.0.1 software. Results were calculated in Excel and visualized in GraphPad. The curve plots were obtained by subtracting the „background noise" control, aka the control of unspecific secondary ab binding.

3.6.4.2.1 Prior optimization

At first, lack of signal was an issue, resolved by ordering a new batch of PD-1 protein and increasing the concentration of PD-L1. The signal, as measured with TMB reaction catalyzed by HRP, was still low, below the absorbance value of 0.3 after applying the STOP solution (which increases the absorbance approximately 3x). The optimization revealed the signal can't be increased by changing the detection antibody conjugate but can be increased by higher PD-L1 concentrations. However, the amount of this reagent available was limited. Hence, further optimization ensued. Nunc Maxisorp and Costar high binding (#3922 white; transferred to transparent for readout) plates were compared, with no meaningful output difference in ELISA using PBS PD-1 coating. Bicarbonate buffer at pH 8,6 and PBS (phosphate-buffered saline) at pH 7,4 were compared as a coating buffer. Surprisingly, PBS coating led to a higher final signal (234% for Nunc, 317% for Costar), putatively through a better PD-1 binding. There was 164% difference between two batches of PD-L1 and 136% difference between batches of the secondary detection antibody. The TMB reagents available in the laboratory differed by 170% in a test setup. The best options from the optimization were used for the later experiment, along with coating ON rather than for 1h, decreased detergent concentration (PBS-Tween at 0,01% rather than 0,05-0,5%) and maximum recommended secondary antibody concentration (1:500, from 1:500-1:2000 range), to ensure the best PD-1/PD-L1 binding and detection signal. While the use of ECL (Enhanced Chemiluminescence, a luminol-based substrate for HRP) rather than TMB can achieve up to 10x the sensitivity, we chose to use TMB+STOP, as it provides a precise endpoint measurement of a product from up to 50min incubation, proportionate to the amount of HRP on the bound detection antibody. ECL method, on the other hand, measures luminance at a given point in time. This causes a risk: each well with a different HRP amount has a different reaction dynamic and uses up the substrate at a different rate. ECL substrate may become depleted by a high HRP concentration, or the reaction may slow down for other reasons, with time, while it does not slow down in wells containing less HRP. A „burning out" of the reaction can be

often seen in Western Blots with a high target amount. If measurement of ECL ELISA is not performed at the optimal time, the relationship between the signal from different wells may not be accurate in proportion to the amount of the detected target. ECL provides sensitivity at the cost of reliability.

3.6.4.2.2 Future improvements to assay development

Assuming sufficient reagents, consumables and well calibrated multichannel pipettes are available, the following is a recommended way to perform such assays, to obtain an accurate comparison of two or more antibodies. First, optimize. The time and reagent cost are nothing compared to struggles caused by trying to save them.

Perform a PD-1/PD-L1 binding ELISA, similar as above, but with no test antibodies. Remember not to use the plate's perimeter wells – fill them with PBS. Prepare PD-1 serial dilutions and coat a plate overnight in such a way that each row will have a different PD-1 concentration. Prepare PD-L1 dilutions, starting from as high concentration as possible. After default blocking and washing, add PD-L1 to the plate in such a way, that each column has a different PD-L1 concentration. After blocking, detect with the default detection antibody concentration and TMB. Use timer to add TMB to subsequent columns (with a multi-channel pipette) in regular intervals (10 seconds between the columns suggested) so that the STOP solution can be later added in the same manner and in the same time intervals; this is especially important if the incubation time is short and ensures all wells have the same incubation time leading to results that can be reliably compared.

After analyzing the results choose a combination of PD-1 and PD-L1 concentration that is near the maximum signal plateau, no further, but does not exceed the reliable measurement range in the preferred time frame (for instance, in case of TMB, in a few minutes of development, does not exceed absorbance of 0.7 (before STOP) or 2.5 (after STOP) and that is also financially viable to use in further assays.

Consider testing a few best concentrations in an additional ELISA focused on the unspecific binding. If background noise is considerable, choose the combination with the highest signal-to-noise ratio. If the assay is meant to be used often, run an ELISA testing different secondary antibody concentrations in terms of signal and signal-to-noise ratio. Only if this approach does not yield satisfactory signal strength, or yields

too high of a background signal, proceed to optimizing factors such as the type of the plate, the coating buffer and time, the timing of all incubations, wash and blocking buffer parameters, wash number.

Finally, when the assay is optimized, perform it in the following way for accuracy. While the plate is undergoing blocking, prepare your dilutions of all samples and controls, in excess. Prepare a U-bottom low-attachment non-assay dilution 96 well plate and transfer the samples to the plate in slight excess. When the assay plate is washed, transfer the prepared samples from the dilution plate to the assay plate, using a multichannel pipette. This way, all samples are loaded within approximately one minute, while careful loading of the samples directly to the assay plate may take 10 minutes or more. Direct loading might mean the samples for two compared antibodies, or for some dilution steps, may be separated by several minutes in the time of loading. Considering the following incubation lasting 1h or so, this is a considerable difference. It may not affect the results if the analyzed interaction saturates quickly, but this is not guaranteed. Additionally, if a mistake is made when loading the dilution plate, it is possible to correct, while it's not if the assay plate was loaded incorrectly. Furthermore, there is no concern about the assay plate drying up, which is not recommended, but may happen with prolonged loading. Apply this method to all the samples you need to load on the assay plate, which are not uniformly added to all the wells from reservoir (such as a detection antibody).

If additional reliability is wanted, spread out the replicates of the same samples throughout the plate rather than clustering them all together, to demonstrate the results do not come from a well effect (technical bias of the reader or other). Avoid the use of perimeter rows of the plate if temperature gradient may have any impact on the assay. This is even more important in developing cell-based assays.

3.6.5 Supplementary literature review

3.6.5.1 Critical analysis of the findings in the Igase et al. publication

We would like to acknowledge that pioneering research cannot be held to the same strict standard as studies following the already beaten path. Having stated that, there is an array of debatable features to the article in question [196].

The 'anomalies' alluded to regarding the PBMC IFN secretion assay pertain to the fact that the caninized antibody against PD-1, meant to activate T-cells and increase IFN secretion, appeared to suppress it instead in PBMCs from donor B. Additionally, in donor C cells it appeared as if the antibody had a slight negative effect that was countered by the addition of PD-L1. These findings - unlike in donor A - contradict the expected outcomes.

The caninized, chimeric and rodent antibodies were not directly compared in the same PBMC assay, a surprising choice. Despite the absence of such quantitative comparison, the authors later assert that "both antibodies had binding affinity to PD-1 and an inhibitory effect on PD-1/PD-L1 interaction to the same extent as the original rodent antibody".

The study mentioned the use of an isotype control antibody, though its development process remained unclear. The PBMC assay results, however, did not include this control, a departure from the previous paper on the original rat antibody. This omission casts doubts over the study's findings. An isotype control highlights the non-specific influence of the immunoglobulin presence on cells - or lack thereof. Considering such influence has been observed in other studies, the absence of appropriate control makes it hard to ascribe the assay outcomes solely to specific antibody binding and PD-1 blockade.

Strikingly, while the treatment with anti-PD-1 antibody (both types) of stage IV OMM patients led to a statistically significant decrease in overall survival (OS) and statistically non-significant decrease in progression-free survival (PFS), these findings were misconstrued as evidence of successful treatment: "Although historical comparison of median OS should be viewed with caution, it indicates that treatment with the anti-PD-1 antibody could extend survival in dogs with advanced OMM". To the authors' defense, based on the available data, the new antibodies could possibly be nearing the efficacy of the contemporary treatments used in the control group. However, the effectiveness of these treatments compared to a placebo remains uncertain, and the results do not indicate benefit. Moreover, the high-cost, novel antibody treatment should outperform older methods to warrant its further development.

Of note, a distinction between the caninized and chimeric antibody wasn't highlighted in the clinical trial's analysis. Our computations for dogs in the trial showed considerably longer mean OS and marginally shorter mean PFS for the caninized treatment cohort. Yet, these effects were not statistically significant in a survival analysis (data not shown). Such comparison however may not be meaningful considering the unmatched, small populations of both cohorts.

Of particular interest is the authors' choice to use canine IgG Fc chain A for creation of the chimeric and caninized antibody. Type A chain is known as a functional equivalent of human IgG2 [231]. The choice seems consistent with the IgG2a type of the original rat antibody, but contrasts with the Fc type of human ICB therapeutics - Nivolumab and Pembrolizumab - which are both of IgG4 (dog D) type. Crucially, IgG4 does not induce antibody-dependent cellular cytotoxicity (ADCC). ADCC mechanism is counterproductive for antibodies meant to act through a receptor blockade. What's worse, ADCC can be detrimental: the very lymphocytes that require ICB assistance to kill tumors, can become targets for destruction through ADCC. In ADCC the antibody bound to a cell attracts cytotoxic destruction of the 'tagged' cell. IgG2 (dog A) is far less potent at inducing ADCC than IgG1 (dog B) and IgG3 (dog C), but it appears somewhat capable of triggering ADCC through a FcR-gamma 1 interaction. This is especially disconcerting considering the intention of the authors to use the antibodies in live patients, as a replacement for standard treatment, in the trial described later. To the authors' credit, IgG2 avoids the possibility of Fab arm exchange, which is a known risk with human IgG4, and possibly with the canine IgG-A by extension. Fab arm exchange can cause adverse effects, although not as likely as the T-cell targeted cytotoxicity.

Commendable is the authors' effort to develop a pioneering test for anti-drug antibodies (ADAs) in dogs. This preliminary test found two patients displayed such an immune reaction to the antibody; both cases were treated with a caninized antibody variant, not chimeric. A comparison to the original rat antibody was not possible. Yet, authors concerningly conclude "these results revealed that our engineered antibodies have lower immunogenicity in dogs".

Focusing on one of the two cases that developed ADAs, patient 24 underwent 5 bi-weekly drug administrations, adding up to 70 days. The peak ADA level was observed

on day 70 (same as case 27) and coincided with the lowest level of drug in the serum since the beginning of the treatment. Yet, the authors saw no correlation between ADAs and potential drops in drug serum levels, a conclusion drawn from these two instances. Case 24 patient showed disease progression on the same checkup, the treatment was apparently not continued on day 70 - the PFS was 70 days and OS - 90 days.

It's worth noting that generating ADAs takes weeks, potentially even longer in severely ill patients. Moreover, cancers at advanced stages were present in all patients, which - together with the oncological pre-treatments - could affect the ability of the immune system to mount a strong immune response to the foreign antibodies (or cancer).

Interestingly, on a spider plot displaying changes in tumor burden of 24 dogs, approximately a third of them presented with extremely fast progression upon treatment initiation, which could possibly be indicative of treatment-induced hyperprogression. This risk, known for ICB antibodies, was neither assessed based on pre-treatment tumor burden dynamics, nor discussed.

While the authors were open about the exploratory nature of the trial, it is worth highlighting that the majority of patients have undergone diverse pre-treatments, which could affect the outcomes of subsequent immunotherapy. Additionally, the relatively short follow up period of mostly terminally ill patients was not sufficient for assessing the - often delayed - immunotherapy adverse effects. The comparison of trial results to historical reference controls was a necessary compromise, and a small sample size precluded statistical robustness. Additionally, some concurrent treatments were accepted in the trial, including tyrosine kinase inhibitor toceranib, which could contribute to the observed side effects, and cyclophosphamide - an immunosuppressant that could prevent immune-related adverse effects. Consequently, no definitive conclusions can be drawn, other than that the antibodies aren't universally harmful.

Despite these limitations, it's important to acknowledge that canine antibody trials for cancer are relatively new. This study, therefore, serves as a steppingstone that opens up avenues for further investigations to improve both methodology and patient outcomes.

"If you do something right the first time, then it's not hard enough."

- Danny MacAskill
Scottish trials cyclist

4. CANINIZED ANTIBODIES: STRATEGIES FOR PROTEIN DEIMMUNIZATION

4.1 Introduction

The previously developed and characterized antibodies targeting canine PD-1 have shown potential as immunotherapeutic candidates. However, they were generated using murine hybridoma technology, resulting in their amino acid sequences being distinctively murine. While the antibody structures are highly conserved across the animal kingdom, and sequences are conserved within the antibody class of a particular species, the interspecies variations are clinically significant. Injecting murine proteins into dogs or humans can trigger an immune reaction, largely mediated by ADAs - anti-drug antibodies [232]. This response can neutralize the therapeutic antibody, shorten its half-life in circulation, and compromise its efficacy, diverting the immune system's focus from the disease to the drug. Moreover, it can lead to long-term sensitization, introducing a risk of severe allergic reactions with repeated administration. Given that antibody treatments involve multiple cycles delivered over several weeks or months, the immunogenicity of murine antibodies makes them unsuitable as human or canine therapeutics.

Furthermore, interspecies differences might lead to unpredictable interactions between the antibody's Fc region and the host's Fc receptors. Proper control over these interactions is essential for treatment safety and efficacy. While some antibody therapeutics activate effector functions such as Antibody-Dependent Cellular Cytotoxicity (ADCC), Antibody-Dependent Cellular Phagocytosis (ADCP), or Complement-Dependent Cytotoxicity (CDC) via Fc receptor interactions, the checkpoint inhibitor antibodies must remain inert in this aspect to avoid immune cell destruction (elaborated in Chapter 3 Supplement). The Fc interactions are also increasingly acknowledged as factors influencing adverse effects [230]. Therefore, it is imperative that therapeutic antibodies have well-characterized, and often synthetically engineered, Fc region sequences.

Due to aforementioned factors, the previously developed antibodies required caninization: a modification of their amino acid sequences that would make them resemble naturally occurring canine antibodies. To set the stage for a detailed discussion on antibody engineering in this project, it is essential to first delve into the structural intricacies of antibodies.

4.1.1 The anatomy and utility of therapeutic antibodies

Immunoglobulins, commonly referred to as antibodies, are glycoproteins produced by the adaptive immune system to neutralize foreign agents. The "Y" structure of an antibody is composed of two identical light chains and two identical heavy chains (Fig 1). Each chain can be divided into a variable domain (V) and a constant domain (C). The variable domain derives its name from its sequence being less conserved among different antibodies. This is because each V domain sequence hosts three complementarity-determining regions (CDRs), interspersed by four structural framework regions (FRs; Fig. 1-2). CDRs are highly unique amino acid sequences that form the specific 'key' designed to fit a unique 'lock' or antigen. In contrast, FRs are more conserved regions that provide a structural scaffold to support the CDRs.

More broadly, the "Y" structure has two arms containing antigen-binding regions that confer specificity to the antigen, and a stem known as the Fc region. The acronym "Fc" stands for "Fragment, crystallizable," and describes the part of the antibody that interacts with immune cells and other components of the immune system, such as complement proteins.

Each of the two antigen-binding regions, located at the tips of the "Y" shape, comprises one V domain from light and heavy chain each. It is the combination of the CDRs from both chains that forms a paratope – the antibody part that specifically recognizes the epitope – a particular pattern on the antigen. While the CDRs are always separated by FRs in the linear amino acid sequence, the three-dimensional protein folding brings them together (Fig. 2).

Figure 1: A detailed representation of an IgG antibody's 3D structure. Each antibody is composed of two identical light chains (depicted in yellow and orange) and two identical heavy chains (depicted in blue and cyan). Every chain has distinct regions: a variable domain (shown in saturated colors) and a constant domain (in pale colors). The heavy chain's constant domain is notably longer than the light chain's. On the left is a 'cartoon' representation, and on the right is a 'surface' rendering of the same antibody. The PD1-2.1 model was constructed using Swiss Model [233]. Most of the work in this chapter focuses on the variable domain pair of the light and heavy chain, located at the tips of the 'Y' structure.
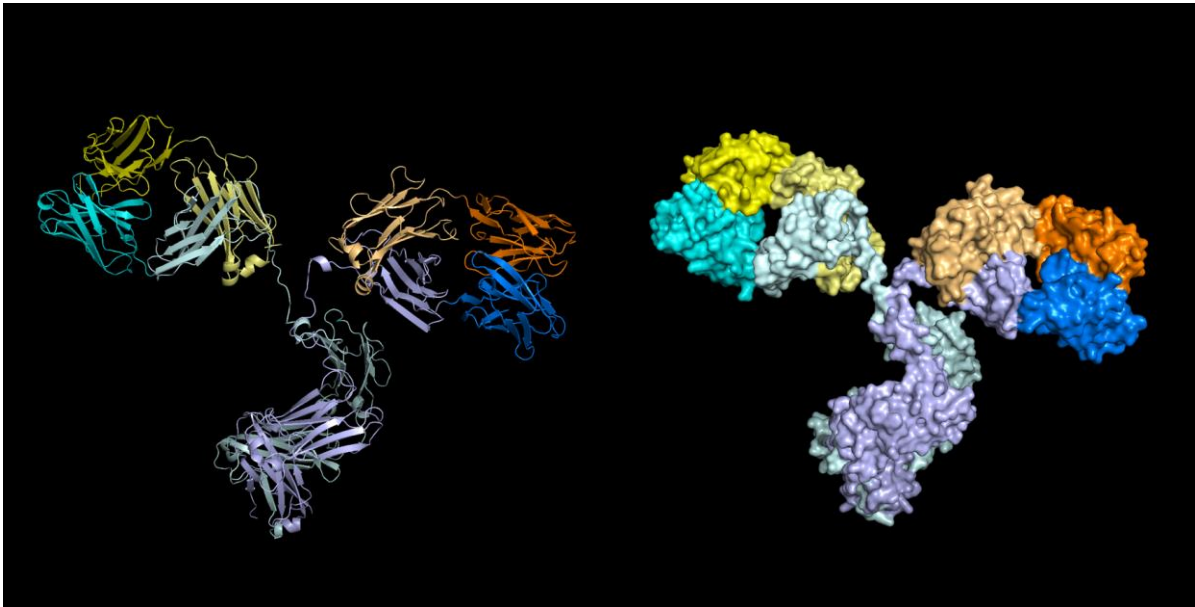
Figure 2: Variable domains and their Complementarity Determining Regions (CDRs). A) Heavy and light chain variable domains represented in blue and orange, respectively, are visualized on the PD1-2.1 antibody structure. B) Three CDRs are present within the variable domain of each chain. Heavy chain CDRs 1-3 depicted in magenta, cyan, and orange; light chain CDRs 1-3 in red, green, and yellow, respectively. C) A rotated view of the antibody from B, highlighting the combined paratope formed by the six CDRs of two chains coming together.
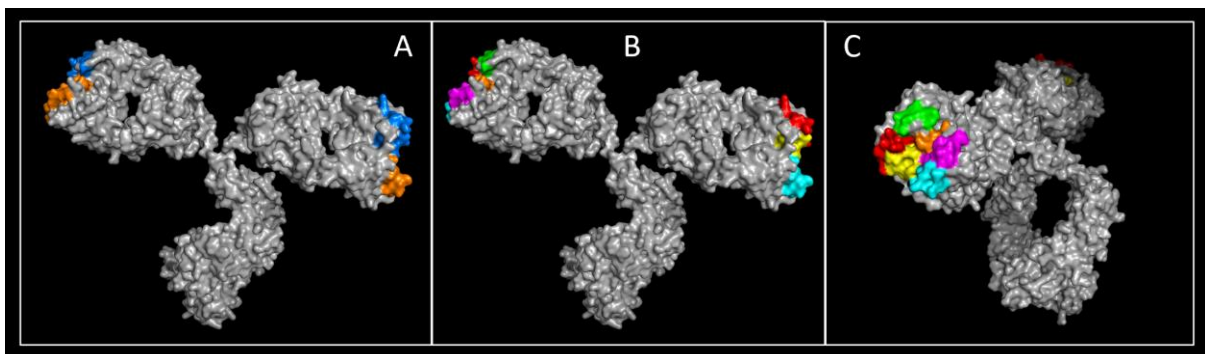
Although all human, murine and canine antibodies have a "Y"-shaped structure, they can be divided into classes, also known as isotypes, based on some structural variations. For instance, an IgM class antibody forms a pentamer, comprising five basic "Y" units held together, while an IgA exists primarily as a dimer. IgG, IgA, IgM, IgE, and IgD classes are distinguished in humans, but homologous classes exist in other species as well, with certain species-specific variations.

Therapeutically, antibodies are primarily derived from the IgG class which offers favorable pharmacokinetic properties such as long half-life, allowing for sustained therapeutic activity and less frequent dosing. Within the IgG class, there are further subtypes, known as IgG1, IgG2, IgG3, and IgG4, distinguished by slight differences in the Fc and hinge regions.

IgG1 and IgG4 subclasses are the most common choices for therapeutic antibodies. IgG1 is typically selected when robust effector functions such as complement activation or ADCC are required. Examples include Rituximab and Trastuzumab, which target cancer cells and recruit natural killer cells via their Fc regions to selectively destroy malignant cells. In contrast, IgG4 is favored when minimal effector functions are desired, as is the case with immune checkpoint inhibitors like Nivolumab and Pembrolizumab. These antibodies target immune cells and block their immune-inhibitory receptors without initiating other immunological effects. However, the choice of the exact antibody class is guided by weighing various desired features with consideration to modern protein engineering abilities. Case in point, Atezolizumab, another immune checkpoint blocker, belongs to the IgG1 subclass, made possible by Fc region engineering, where the introduced N297A mutation disables glycosylation of this residue. Aglycosylation of position 297 effectively eliminates the unwanted ADCC/CDC potential [234].

4.1.2 Antibody speciation

Speciation is a process of modifying antibodies to resemble natural antibodies of the target species. It is crucial for optimizing the safety and efficacy of antibody-based treatment. Speciation is most often described with the human-centric 'humanization' term, referring to adapting rodent antibodies for human use. As virtually all developments in speciation were made in the context of human antibodies, the terms are often used interchangeably. Later in the project, 'caninization' term will be used as the aim was to speciate murine antibodies into canine therapeutics.

4.1.2.1 Chimerization of antibodies

The creation of a chimeric antibody is usually the prelude to the speciation process. Variable domains of the original antibody are combined with the constant domains (Fc region) of the target species to marry antigen specificity with patient-compatible effector functions. As the constant region constitutes approximately 66% of the antibody, this process replaces the bulk of the rodent-specific sequence [235]. However, a substantial rodent component remains in the form of variable domains' frameworks. Chimeric antibodies are sometimes used therapeutically. One successful example is Rituximab, the first monoclonal antibody approved for the treatment of cancer, targeting CD20 in lymphoma, leukemia and non-cancer diseases. This chimeric mAb is considered one of the essential medications [236]. Still, chimeric antibodies are assumed to be more immunogenic and less suited for therapeutic use than fully humanized ones [235]. This is why full speciation is the golden standard of de-immunizing antibodies. Full speciation, a much more challenging process, modifies the variable domains of the established chimera to further reduce the rodent sequence content.

4.1.2.2 For and against speciation

Some researchers have questioned the value of humanizing (speciating) therapeutic antibodies. It was reported that in some antibody formats extensive sequence engineering may introduce protein aggregation, increasing immunogenicity [237]. Others argued that the requirement for humanization slows down the progress in therapeutic development, while the process is only necessary for some antibodies [238]. The key argument against speciation is that many fully humanized antibodies

still elicit anti-mAb responses and other adverse reactions [239]. It is also suggested that complete de-immunization of mAbs is not possible or practical due to the nature of their key regions - CDRs - which elicit immune response too [240]. Moreover, humanization may introduce new immunogenic epitopes. Germline immunoglobulin sequences have often been used as humanization templates. Germline sequences refer to the original, unaltered DNA sequences encoding antibodies before they undergo V(D)J recombination and somatic hypermutation. However, germline sequences do not adequately represent the recombined sequences of antibodies found in circulation [239]. An alternative approach is to search for templates in libraries of expressed immunoglobulin sequences. This, however, risks using dysfunctional sequences or those obtained through sequencing errors. Most importantly, naturally recombined immunoglobulins of one individual may be immunogenic to another [235]. Finally, while a decreased immunogenicity of chimeric antibodies as compared to their rodent originators is well documented, the putative superiority of fully humanized mAbs over chimeric ones is a topic of a long-standing and unsettled debate [241–244]. Some evidence suggests that other approaches - not involving antibody sequence humanization - could be more helpful at inducing the treatment tolerance in the patient [245]. Nevertheless, full speciation is currently considered the golden standard for antibodies aiming at approval as therapeutics. The key approaches to speciation are listed below.

4.1.2.3 CDR Grafting

CDR grafting involves transferring the CDRs from the original antibody onto a host-specific scaffold of frameworks. This approach has been used in developing well-known therapeutics such as Trastuzumab [235]. However, it often requires 'back-mutation' of several residues to the original rodent ones, in order to correct the structure and regain the target affinity. The identification of key residues to back-mutate represents the most difficult and unpredictable step in the process, requiring extensive experimentation or in vitro screening of large variant libraries. Early designs of CDR-grafted antibodies used fixed, well characterized human immunoglobulin templates. With the accumulation of data, it became possible to choose templates from germline sequences or expressed antibody repertoires based on homology to the engineered sequence. Yet another approach is to cluster the known human (target)

immunoglobulin sequences and prepare consensus sequences for each cluster, which can serve as templates [235].

4.1.2.4 Framework Shuffling

Framework shuffling involves identifying multiple framework sequences from the target species that are structurally similar to the original (rodent) antibody's frameworks. These human frameworks are then mixed and matched in various combinations with the original CDR sequences to create a diverse set of new variable regions. These combinations form a library of synthesized genes, which are then expressed to produce full-length antibody constructs. The library is then screened for antibodies that maintain antigen affinity while minimizing the murine sequence content, a process that is both time-consuming and resource intensive [235].

4.1.2.5 Resurfacing (veneering)

In the resurfacing technique, the variable domains of an antibody are treated as 3D structures with distinct internal and external components. The solvent-exposed amino acid residues on the external surface, identified through structural modeling or crystallography, are the most likely to interact with the host's immune system (Fig. 3). These surface-exposed residues are specifically altered to correspond with residues commonly found in the host species, thus reducing immunogenicity. Meanwhile, the CDRs remain unmodified to preserve the antibody's specificity and affinity. This minimalist approach is particularly attractive as it avoids modifying protein core residues, many of which are crucial for the correct interaction and positioning of the heavy and light domains. Yet, it is not clear whether resurfaced antibodies may generate immunogenicity when degraded into fragments [235].

Figure 3: Solvent accessibility of the PD1-2.1 antibody's variable domain set as approximated by PyMol.
The color gradient represents residue solvent exposure, transitioning from blue (low) through green and yellow to red (high). A) Mesh projection; B) 'Spheres' projection, where each individual residue is represented as a colored sphere. This illustration emphasizes the surface-exposed residues, which are pivotal for the resurfacing technique of mitigating immunogenicity. The visualization does not account for the fact some residues may in fact be buried within the protein structure when the variable domain is combined with the constant domain.
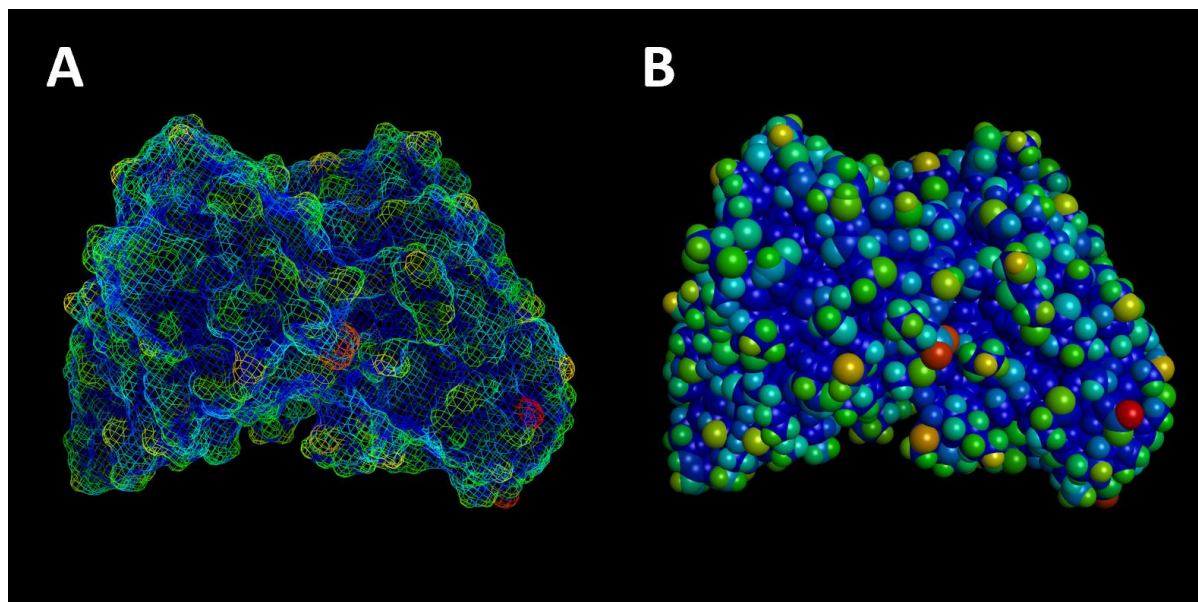
4.1.2.6 Key considerations

Due to the highly conserved antibody structure, variable domain templates for light and heavy chain engineering can generally be taken from different original antibodies. This has been crucial for the antibody engineering field, since identifying the natural light-heavy chain pairs contained in the individual antibody clones has long presented a major technical challenge [246,247].

However, the residues of FRs may still play important roles in determining the antibody characteristics [248,249]. Vernier zone residues are specific amino acids located in the FR regions immediately adjacent to the CDRs that modulate the antibody's binding affinity. Vernier zone residues can make direct contact with the antigen, affect the stability or flexibility of the antibody and the CDR structural loops, all indirectly affecting target binding. Modifications to these residues can significantly impact the antibody's functional characteristics [249]. The packing angle is another critical parameter that defines the spatial orientation between the variable heavy (VH) and variable light (VL) domains of an antibody, and it has significant implications for antigen-binding affinity. Approximately 13 residues at the VH/VL interface have a substantial impact on the

packing angle. Since a substantial portion of the non-CDR residues of VH and VL regions influence the antibody-antigen interaction, speciation of an antibody is hardly a 'copy-and-paste' project. Rather, it is a process of trial-and-error optimization.

4.1.2.7 Antibody numbering schemes

Antibody numbering schemes facilitate the identification and comparison of the variable regions in different antibodies [249,250]. The most prevalent numbering schemes include IMGT, Kabat, Chothia, Martin (also known as Enhanced Chothia or AbM) and were visualized on Fig. 4.

Kabat, one of the earliest systems, defines positions where insertions and deletions are allowed in CDRs and FRs, annotating any extra amino acids with letters [251]. Based on a small original dataset, Kabat has limited flexibility and doesn't consider the 3D topology of the antibody domains.

IMGT, on the other hand, offers greater applicability. It numbers residues from 1 to 128 based on a V-gene sequence alignment and accommodates insertions only between positions 111 and 112 for CDR3 sequences exceeding 13 amino acids [252].

Chothia is a structure-based scheme, developed by aligning crystal structures of variable regions. This scheme is well-suited for capturing the 3D attributes of the antibody hypervariable regions [253].

Martin (AbM), an updated Chothia scheme, includes corrections based on both sequence and structure datasets, in result recognizing greater sequence variability. The upgrades make AbM versatile, especially for analyzing sequences with unconventional CDR lengths and possible deletions [254].

Other, less popular schemes have also been described [255,256]. Several computational tools were developed to aid in CDR loop prediction and numbering scheme application. These include ABlooper [257], SCALOP [258], ANARCI [259] and AbySis [260] as well as several fully commercial platforms.

The choice of an antibody numbering scheme often hinges on the specific research goals. Sequence-based schemes like Kabat and IMGT are better suited for general applications. In contrast, structure-centric schemes like Chothia and Martin are

preferred for engineering efforts rooted in a deep understanding of antibody topology. However, due to its momentum, some antibody engineering projects still opt for the Kabat scheme.

Figure 4: Depiction of the CDR region definitions according to the widely-recognized antibody numbering schemes: Chothia, AbM, Kabat, IMGT, and AbySis 'Contact'. The figure also highlights the full range of residues that can potentially be classified as CDR parts. Sequences without coloration are structural frameworks. The sequence visualized is from the heavy variable domain of a proprietary canine antibody.

4.1.2.8 The challenges of speciation

While the methods described above offer a blueprint for antibody speciation, it's crucial to emphasize that the process is far from straightforward. Diverse tools and information sets are helpful at this undertaking such as crystallographic structures of the given antibody class or the antibody-antigen complex, precise assessments of the interacting residues, complete germline sequences, canonical CDR classes, and immunogenicity prediction tools such as NetMHC [261]. At the time of this project, most of such information was missing or incomplete for the canine species. While various software were made available to aid antibody humanization [262], they were not compatible with the canine species. Hence, in this project we prototyped experimental approaches to canine speciation. The subsequent section will explore the landscape of 'caninized' antibodies developed by others.

4.1.3 Caninized antibodies

A PubMed search for the US and UK spelling of 'caninized/canineized/dogized' returned just 19 results, including studies of 6 caninized antibodies/sets. Additional internet searches revealed a further 6 items. Below they are summarized in Table 1 - The Well Studied, The Controversial, and The Enigmas.

Two caninization approaches were briefly shared in the literature (by Gearing and Bergeron [263,264]) and Lokivetmab was by far the most well-studied caninized antibody [232]. To the best of our knowledge, 11 fully canine antibodies, antibody sets, or scFv fragments were revealed to date, of which 6 did not suffer severe issues (Tab. 1). Two antibodies were targeting PD-1: one remains an enigma known solely from a single case study, and the other comes from a study with concerning irregularities which were discussed in Chapter 3. Notwithstanding, the latter one was patented in the USA (US10280223B2, expiration 2036) as was one more anti-canine PD-1 mAb by Intervet company (US10711061B2, expiration 2034). To our best understanding, at the time of this project's initiation there were no reliably characterized caninized antibodies against PD-1 and no anti-cancer caninized antibodies in clinical use.

Interesting is the case of two caninized antibodies that were at one point approved in the USA and Canada for treating canine lymphomas: Blontress/AT-004, targeting CD20 and Tactress/AT-005 targeting CD52, both owned by Aratana Therapeutics. Their efficacy proved unsatisfactory. As the company (under)stated in 2015, 'Recent scientific studies suggest that AT-004 and AT-005 are not as specific to the targets as expected' [265]. In the investor-focused product update, they comment further: "Aratana has been aggressive in its pursuit of truly innovative therapies for pets, and we have been remarkably successful from a regulatory perspective (...). The ability to take such a disciplined approach is an attractive attribute of the pet therapeutics opportunity." It is hard to disagree that repeatedly performing clinical trials without fully elucidated antibody targets is an aggressive practice. Yet, regulatory success does not treat cancer. The anti-lymphoma efficacy of these mAbs was not as seen for analogic treatments in human patients. In well-controlled studies, Tactress did not improve progression-free survival in its target population - the T-cell lymphoma patients [87]. Currently, Lokivetmab and Bedinvetmab, both appearing to be owned by

Zoetis, seem to be the only two widely approved caninized therapeutic antibodies. Their therapeutic use is for conditions other than cancer.

Interestingly, Gearing et al., who have published their 'PETization' approach to caninizing anti-NGF antibodies in collaboration with Nexvet (subsequently acquired by Zoetis), have also developed a similar felinized antibody for use in cats [266]. This antibody appears to be the only felinized one described in scientific literature. Importantly, the list presented here does not focus on chimeric and other recombinant antibodies developed in veterinary research [267]. Although not supported by scientific literature, it's worth noting that several companies reportedly hold patents for anti-NGF mAbs intended for use in dogs [268].

What's also noteworthy in the context of canine clinical trials is one exceptional study, in which mogamulizumab - a humanized anti-CCR4 antibody – was trialed in dogs with advanced prostate cancer [269]. Remarkably, the drug was well-tolerated despite being administered multiple times. Several factors could contribute to this unexpected tolerability, including patient characteristics and the co-administration of Piroxicam, an anti-inflammatory medication. While this case raises the intriguing possibility that humanized antibodies could potentially be well-tolerated in dogs, caution is warranted. Canine immunoglobulins differ from the human ones, and comprehensive research on the safety of humanized antibodies in dogs is lacking.

Considering the factors discussed above, we perceived a high, unmet need for antibodies that would be designed to target canine immune checkpoints in cancer, comprehensively characterized and fully caninized.

Table 1: The Well Studied, The Controversial, and The Enigmas – a review of caninized antibodies.

Ab/set name	Type	Condition	Target	Format	Maker	Refs	Limitations	Notes
ca-4F12-E6	Caninized	cancers	PD-1	Ab	Nemoto, 2020 /Nexvet (Australia)	[185,196]	Design and study issues described earlier	Followed 'PETization' approach
MP001	Caninized	cancers	PD-1	Ab	Biocytogen (China)	[270]	Virtually undescribed	Known solely form a single **case study**
NV-01 /Ranevetmab	Caninized	pain	NGF	Ab	Gearing, 2013 /Nexvet (Australia)	[263]	-	Introduced 'PETization' approach; **small trial**
Bedinvetmab	Caninized	pain in osteoarthritis	NGF	Ab	Zoetis (USA)	[271,272]	-	**Two "field study" trials,** approval EMA 2020, FDA 2023
Lokivetmab /Cytopoint	Caninized	allergic dermatitis	IL-31	Ab	Zoetis (USA)	[232]	-	**Numerous clinical trials;** approval USDA 2016, EMA 2017
can225IgG	*Chimeric*	cancers	EGFR (human)	Ab	Singer, 2014	[273,274]	Mislabelled as caninized	Chimeric version of cetuximab, capitalizes on high human-dog protein homology
-	Caninized	cancers	CTLA-4	scFv	Mason, 2021	[275]	-	Developed using a canine immunoglobulin phage library
-	Caninized	-	CTLA-4	Ab set	Bergeron, 2014	[264]	-	Research, not therapeutic oriented; described a speciation method
Tactress /AT-005	Caninized	T-cell lymphoma	CD52	Ab	Aratana Therapeutics (USA)	[87,265]	Lack of specificity, failed trials; no peer-reviewed data	**Did not improve progression-free survival in clinical trials**
Blontuvetmab	Caninized	-	CD20 (MS4A1)	Ab	-	[276]	Undescribed	Described as biosimilar
-	Caninized	B-cell lymphoma	CD20	scFv	Jain, 2016	[277]	-	Developed using a canine immunoglobulin phage library
Blontress /AT-004	Caninized	B-cell lymphoma	CD20	Ab	Aratana Therapeutics (USA)	[87,265]	Lack of specificity, no peer-reviewed data	-

136

4.2 Results

4.2.1 Generating a chimeric antibody

First, we needed to establish whether our antibodies could be recombined while retaining their target affinity. We started with the approach well-established in humanization: generating a chimeric antibody. PD1-1.1 antibody was selected for this purpose, as it appeared to be more versatile than PD1-2.1 at this stage of the parallel antibody characterization project. Both clones had already been sequenced and isotyped (chapter 3) as IgG2 with kappa light chains.

We identified the murine LV/HV sequences of PD1-1.1 and combined them with canine constant domains. For the heavy chain constant region, we chose the canine gamma D chain for its lack of immune effector activity [264]. For the light chain constant region, we picked a canine lambda constant, based on in its prevalence in dogs [278]. The sequences employed in the project are detailed in the methods section.

Additionally, we set out to test a novel antibody expression method. In our prior work with CD20 antibody engineering, we found that co-transfecting cells with separate vectors for the light and heavy chains necessitates considerable optimization. We thus decided to utilize a bicistronic vector, co-expressing both chains under a single promoter [49,279]. We hypothesized this should result in a nearly equal production of both chains. Another advantage of this approach was the construct's compatibility with recombinant viral vectors which we were considering as an experimental treatment delivery method. Vectors based on adeno-associated viruses (AAV), with IgG constructs of similar design, have been tested with encouraging results [280]. They could be used to elicit local, in vivo antibody expression, thus bypassing the various limitations of biotechnological drug production and administration.

To test the antibody's engineering potential and the viability of our expression system, we designed a genetic construct with heavy and light chains separated by a self-cleaving linker. The linker consisted of a Thosea asigna virus (TaV) 2A peptide [281,282] and an additional N-terminal linker sequence for improved cleavage efficiency [283,284]. We transfected the prepared plasmid vectors into mammalian cell

cultures to produce the antibody and assessed the purified product via ELISA and SPR.

4.2.2 Chimeric antibody retained activity in ELISA

This chimeric antibody product was tested in ELISA against recombinant canine PD-1 (Fig. 5). The antibody successfully bound to its target. A quantitative comparison of potency with the original murine antibody was not possible in this setup. The chimeric and originator antibodies differed in their Fc regions, necessitating the use of an anti-canine and anti-murine detection antibodies, respectively. To compare the two, we next performed an SPR analysis.

Figure 5: Chimeric version of the PD1-1.1 antibody binds canine PD-1 in ELISA. Anti-murine detection Ab was used for the murine PD1-1.1 detection, and an anti-canine detection Ab for the remaining two. The plate was coated with recombinant canine PD-1 at 200ng/well. Error bars represent standard deviation of a triplicate (not visible due to low values).
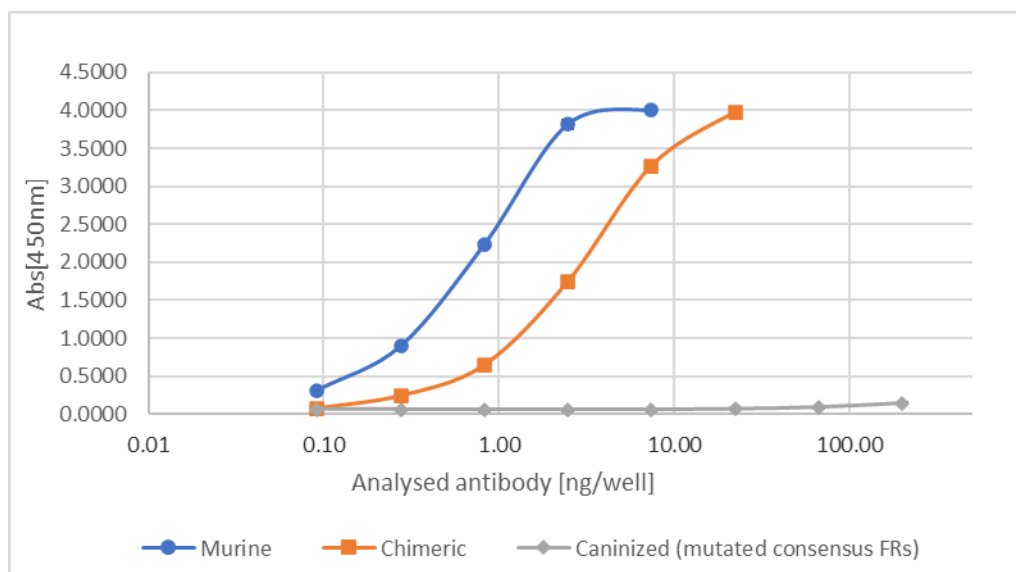
4.2.3 Chimeric antibody retained activity in SPR

Enough chimeric antibody was produced to perform a single kinetics SPR run at 20nM concentration (Fig. 6). The resulting data was not enough to calculate the KD and quantitatively compare the antibodies. However, the result demonstrated the chimeric antibody was actively binding PD-1 with potency in the same order of magnitude as the original PD1.1. Some difference could be expected considering the different

production, purification and storage methods for the murine hybridoma and canine recombined antibodies.

Figure 6: Chimeric version of the PD1-1.1 antibody binds canine PD-1 in SPR. The plot demonstrates chimeric antibody binding to PD-1 with comparable strength to its parent molecule PD1-1.1. Ab chimera – the chimeric variant of PD1-1.1, Buffer – negative control run, ISO – isotype control antibody.
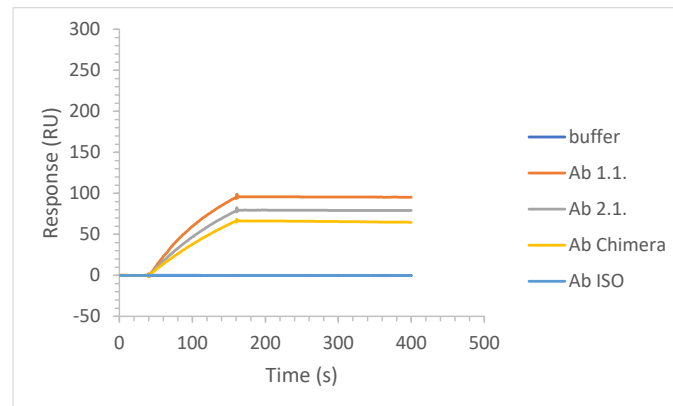
Based on the basic chimera characterization we concluded that we successfully designed and produced a canine-murine chimeric antibody based on PD1-1.1. PD1-1.1 mAb was well suited for cloning and protein engineering, traits likely extending to PD1-2.1. Furthermore, we found our bicistronic vector design and expression method were functional and suitable for further use in the project.

4.2.4 Consensus-based antibody caninization

The next objective was to fully caninize the antibody variable domains. In the beginning stage of this project, we only had a very limited dataset of expressed canine antibody sequences at our disposal. Due to that limitation, caninization based on the sequence homology to naturally expressed antibodies did not appear attractive. Considering the contemporary limitations in the description of canine immunoglobulin germline sequences, we did not prioritize the germline method either. Instead, the approach we were tasked with testing first was a consensus-based one (Fig. 7). Here, we analyzed a small proprietary dataset of canine HV/kappa/lambda sequences kindly shared by Prof. Ted Hupp. For each of the FRs we generated a consensus sequence - a set of top most common residues. Additionally, several back-mutations were introduced to these sequences.

PD1-1.1 sequence was analyzed to define the CDRs, which were then combined with canine mutated consensus frameworks to form new, recombinant LV and HV domains. The variable domains were subsequently combined with canine constant chains as before, except this time we changed the light constant domain from lambda to kappa type. It was not known whether canine FR sequences differ between kappa and lambda chain types. Hence, we assumed using the kappa sequence matching the original murine type might increase the likelihood of success. The antibody construct was designed, expressed and purified as before. The product was tested in ELISA like before. This time, however, no activity was detected. The caninized antibody was successfully expressed but did not retain its affinity to rcPD-1 (Fig. 5).

While antibody speciation is an iterative process, the failure of the consensus approach could be explained by the oversimplified treatment of the canine Ig repertoire diversity. Here, the consensus sequences were generated for heavy/kappa/lambda chains based on all the sequences from the respective lists. Those sequences may have belonged to different subtypes within each chain type. In other words, similar, yet biologically distinct sequence groups were averaged into a single output sequence. Additionally, this approach resembled the 'fixed template' approach, in which the homology level between the input sequence and the speciation template is not considered. An improved approach could cluster the available canine sequences, align the murine antibody of interest to the resultant clusters, and generate a consensus for the top homologous cluster specifically. This consensus would serve as a caninization template. This approach would stand a better chance of success, as the generated cluster consensus would be matched by homology and would provide a better representation of real canine Ig sequences. However, clustering would require a dataset larger than was available at the time.

Any consensus-based approach poses a risk shared by averaging data in general: it could average diverse real sequences into a single one that does not exist in reality. Such a process would be agnostic of residue combinations allowed or disallowed by the antibody biophysics, and the result could be dysfunctional or immunogenic. The consensus-based caninization was not a suitable method, so we next embarked on a journey into more complex speciation approaches.

Figure 7: Consensus-based framework caninization. Consensus sequences were computed for canine FR 1-4 of heavy/lambda/kappa types, and compared to the FRs from the original, murine antibody. Based on the repertoire of amino acid residues present at each position in the canine dataset as well as the chemical character of residues, arbitrary back-mutations were introduced.

Light chains

	FR1	FR2	FR3	FR4
Consensus - lambda - dog	AQSVLTQPASVSGSLGQRVTISC	WYQ-QLPGTGPRTLIY	GVPDRFSGSRSGNTATLTISGLQAEDEADYC	FGGGTHLTVLG
Consensus - kappa - dog	DIVMTQTPLSLSVSPGEPASISC	WFRQKPGQSPQRLIY	GVPDRFSGSGSGTDFTLRISRVEADDAGVYYC	FGQGTKLEIK
Mutated consensus - kappa - dog	QIVLTQSPASLSVSPGEKVTITC	WFQQKPGQSPKLLIY	GVPDRFSGSGSGTDFSLTISRVEAEDAATYYC	FGQGTKLEIK
PD1-1.1 - mouse	QIVLTQSPAIMSASPGEKVTITC	WFQQKPGTSPKLWIY	GVPARFSGSGSGTSYSLTISRMEAEDAATYYC	FGGGTKLEIK

Heavy chains

	FR1	FR2	FR3	FR4
Consensus - dog	EVQLVESGGDLVKPGGSLRLSCVAS	WVRQAPGKGLQWVA	YADAVKGRFTISRDNAKNTLYLQMNSLRAEDTAVYYCAK	WGQGTLVTVSS
Mutated consensus - dog	EVQLQESGPDLVKPGASLKLSCVAS	WVRQSPGKGLEWVG	YNDAVKGRFTLYDNSKSTLYLQLNSLTSDDTAVYYCTR	WGQGTSVTVSS
PD1-1.1 - mouse	EVQLQQSGPELVKPGASVKISCKAS	WVKQSHGKSLEWIG	YNQNFKRKATLTVDNSSSTAYMELRSLTSDDSAVYYCTR	WGQGTSVTVSS

Colour scheme:

Dog consensus conflicted with murine sequence, but murine residue was present in canine sequence logo, back-mutation to murine was performed.

Dog consensus conflicted with murine sequence, but murine residue was present in the canine library, back-mutation to murine was performed.

Dog consensus conflicted with murine sequence, but the amino acids were considered chemically similar in this context.

Dog consensus conflicted with murine sequence, resolved by back-mutation to murine.

Dog consensus conflicted with murine sequence, not resolved.

No conflict.

141

4.2.5 The new approach to caninizing

In a new approach, we switched focus to the PD1-2.1 antibody, as it became apparent it had superior PD-1 blocking capabilities compared to PD1-1.1. Next, we conceived and tested several caninization methods in parallel. For some, it was necessary to first develop a comprehensive library of canine Ig sequences.

4.2.6 Canine immunoglobulin database I

Initially, we developed a library combining Ig sequences from various sources. These included a seminal publication by Braganza et al. [285], searches in NCBI and AbySis databases and our MiXCR analysis of various published canine RNAseq datasets [285]. The input data for MiXCR analysis included in-house sequencing of blood samples from septic dogs as well as canine immunoglobulin sequencing published by Hwang et al. [286] and Aresu et al. [287].

Dedicated to the extraction of the most reliable sequences, we consulted MiXCR tool authors who advised us that the most reliable approach would involve repertoire sequencing utilizing unique molecular identifiers, submitting all samples in replicates and only picking sequences detected in all replicates. Since this was not possible, we applied a more stringent requirement. Only sequences that were repeated in at least two different samples were retained. This meant that the retained sequences had to be present in at least two different animals. While this limited the number of available sequences by orders of magnitude, it ensured we only worked with real, common and likely versatile sequences as templates for therapeutic antibody engineering. We found several other sources of canine bulk and Ig-targeted sequencing data that we could use for sequence extraction. These, however, originated from canine lymphoma patients, and in our view, sequences obtained from mutation-prone, dysregulated cancer cells would not provide a good platform for designing reliable, therapeutic antibodies. The final library encompassed a total of 1607 non-redundant canine immunoglobulin sequences.

4.2.7 Canine immunoglobulin database II

To obtain a broader set of canine Ig sequences, we performed long-read sequencing of a plasmid library encoding canine antibodies (Tab 2). Upon inspecting the individual

reads we attempted a reference-free Ig sequence extraction based on unique library features. The reference-free method was chosen because it allows for extracting antibody chains that do not align with known germline reference sequences. This was important, because those reference sequences for canine model were likely incomplete and the missing germline data could lead to the omission of many real Ig sequences. Moreover, a recent benchmarking study demonstrated that even in the human model, recovered antibody repertoires differed massively depending on the employed tool and a source of germline reference [288].

Unfortunately, due to the diversity of sequences in the library this approach demonstrated poor sequence recovery. We then turned to a reference-based approach. An extensive bioinformatic pipeline was developed to handle, clean and process the multi-gigabyte sequencing files and to extract the complete, productive LV and HV sequences. The 'unproductive' status indicates that a chain sequence is unlikely to result in a functional antibody due to factors like a disrupted reading frame, premature stop codons or unsuccessful V(D)J recombination. 'Unproductive' sequences are not useful for applications requiring functional antibodies. However, a risk of misclassifying a sequence as 'not productive' exists, especially as the classification tools rely on the known germline sequences. As this project aimed to build a resource of highly reliable sequences that could be used to construct functional antibodies and train artificial intelligence models, the limiting yet stringent approach was appropriate.

Table 2: The numbers of unique, productive canine antibody variable domain sequences extracted from the long-read plasmid library sequencing.

Chain Type	Unique Sequences Extracted
Heavy	272,535
Light kappa	79,545
Light lambda	81,881

For each of the three chain types, we characterized the diversity of its FRs and CDRs in the library, including only the productive chains and excluding those containing any ambiguous residue positions (Tab. 3).

Table 3: Unique sequence counts for each FR and CDR type in the Heavy, Light Kappa and Light Lamba chains from the sequenced dataset. Only productive sequences with no ambiguous residues were considered. The FR and CDR borders were identified according to the IMGT scheme.

	CDR1	CDR2	CDR3	FR1	FR2	FR3	FR4
Heavy	17496	43831	95479	9851	21613	84948	4058
Kappa	2920	303	9643	2219	4604	13624	652
Lambda	9832	1720	25250	10032	12238	22693	665

4.2.8 Advanced caninization

Building upon the previous efforts, we devised nine caninization techniques utilizing the combined two canine immunoglobulin libraries established earlier, hereafter referred to as the "library". With each technique we constructed one light and one heavy chain. Although these light and heavy chains could be combined freely, for the initial evaluation we paired the L/H chains originating from the same method. The specific caninization methods are detailed below and the caninized constructs were described in Tab. 4 and Fig. 9.

4.2.8.1 Method 1: fixed functional scaffold

This method employed scaffolds from a light and heavy chain pair proven to produce a functional antibody when expressed together. While our research indicated that the consensus sequences of functional scFv chains did not deviate from the consensus of chains from our naive canine library, a consensus analysis does not provide complete insights. Additionally, ensuring the appropriate light-chain pairing remains non-trivial. Hence, we gathered a set of chain pairs from functional scFvs generated in past projects by phage display of our canine library. These pairs were effectively expressed and bound to their respective targets. PD1-2.1 chains were aligned with this set. The top two homologous scFvs were CD20 binders from a prior publication [49]. Intriguingly, these were the only scFvs in the set with the preferred kappa light chains, akin to the murine PD1-2.1. It's generally believed that the constant region of the light antibody chain determines its kappa/lambda classification. However, our alignment suggests the variable segment might also differ between kappa and lambda. The two scFvs only varied in their light chain sequence. Given that in one instance the light chain wasn't involved in target binding and in the other, the light chain had an atypical sequence - indicated by the AbySis software's inability to pinpoint its

FRs/CDRs - we chose to graft the PD1-2.1 CDRs onto both. This resulted in two caninized variants: PD21_CA_M1A and PD21_CA_M1B.

4.2.8.2 Method 2: resurfacing

In this approach, we computed the solvent exposure of the amino acids of each chain, based on the sequence (AbySis, [260]) and modeled structure (GETAREA, [289]). Solvent-Accessible Surface Area (SASA) or Accessible Surface Area (ASA) describes the portion of a molecule accessible to a solvent, defining its most externally exposed surface. For resurfacing, we selected the more conservative AbySis ASA estimate, tailored to antibodies. Utilizing AbySis, we pinpointed amino acid residues disallowed for a canine antibody. If a residue was determined to be both exposed and disallowed, we altered it to the most chemically analogous of the permissible ones. Given that the murine sequence contained a stretch of three residues absent in the canine references, we excised it for the PD21_CA_M2A caninized construct. However, we also designed a more conservative PD21_CA_M2B which retained these extraneous residues.

4.2.8.3 Method 3: substitution of disallowed amino acid residues

Here, we performed a substitution of residues disallowed for a canine antibody, as assessed by AbySis based on its – limited – canine reference sequence repertoire. Substitution was performed as in resurfacing, albeit for all problematic residues irrespective of their exposed or buried character. This produced a variant named PD21_CA_M3.

4.2.8.4 Method 4: matching individual frameworks from the expressed repertoire

Making use of our extensive, combined library of expressed, productive canine immunoglobulin sequences, we performed a search for analogues of the six framework sequences from PD1-2.1. Heavy chain frameworks were aligned to the 'heavy' sub-library, and light chain frameworks – to the 'kappa' sub-library. Murine frameworks were replaced with the top canine matches. This produced a variant named PD21_CA_M4.

4.2.8.5 Method 5: CDR grafting based on the alignment or the entire chain

Similarly, as in the previous method, we used the canine sequence library to perform an alignment, albeit this time we searched for the entire heavy chain and entire light chain in the respective sub-libraries. For each PD1-2.1 chain, CDRs were grafted on to a scaffold made of the four frameworks from the top alignment hit. This produced a variant named PD21_CA_M5.

4.2.8.6 Method 6: CDR grafting based on a FR scaffold alignment

It could be argued that the match-and-mix framework substitution approach, as demonstrated in method 4, could inadvertently combine incompatible frameworks. On the other hand, the entire chain alignment in method 5 might be perceived as too broad of a search criterion. With this in mind, in method 6, we aimed to identify the most suitable all-frameworks scaffold match between the PD1-2.1 chains and the library. For this purpose, we executed local Blast searches using both soft and hard masking of the CDR residues, excluding them from alignment or both alignment and hit scoring, respectively. Regardless of the masking method used, the top match for both the light and heavy chain consistently mirrored the results from method 5. Consequently, no variant was prepared using this method.

4.2.8.7 Method 7: CDR grafting to a scaffold based on CDR3 similarity

Typically, the third CDR of each antibody chain is the most distinctive, with HCDR3 undergoing the most recombination to achieve maximal diversity. Given the importance of HCDR3 and LCDR3 in antibody binding, we focused our search on chains in the library with the closest matches to these CDRs. The best matching chains then served as scaffolds for PD1-2.1 CDR grafting. This produced a variant named PD21_CA_M7.

4.2.8.8 Method 8: CDR grafting based on the CDR set alignment

In this approach, methodologically analogous to method 6, we focused the alignment on the set of CDRs from PD1-2.1 antibody. Despite the framework masking, once again the top matches were identical to those in method 5. No variant was created with this method for the antibody in question.

4.2.8.9 Method 9: germline-based speciation

Despite limited data for the canines, we decided to test the approach based on the canine germline immunoglobulin sequences. These were sourced from IMGT and manually curated, then aligned with PD1-2.1 frameworks. This produced a variant named PD21_CA_M9.

4.2.9 In silico construct evaluation

To assess the caninization techniques and the derived antibody constructs, we performed a set of in silico analyses. For each antibody, we modeled the combination of light and heavy chains domains with ABodyBuilder2 [220]. To uncover the potential sequence liabilities inherent to antibodies, we employed ABodyBuilder-ML [290]. Maintaining the structural integrity of our antibodies post-caninization was paramount. Thus, we compared each caninized construct with its original murine counterpart in PyMol [226]. Using the Root Mean Square Deviation (RMSD) metric, we measured the atomic differences between the 3D structures, both for the global structure and for the CDR set specifically. The next stage was to understand how each antibody construct might interact with the PD-1 receptor. We used ClusPro2.0 [224,225] to dock each construct on to the previously obtained PD-1 receptor domain structure (Chapter 3). In this approach 10e9 positions of the ligand in relation to the receptor were scored with the Piper algorithm [291] and the top 10e3 were chosen, which were subsequently clustered into binding models. The obtained models were ranked based on their cluster sizes. From these, we chose the top most probable binding model for each construct. This model was examined with Prodigy [292], providing a binding affinity prediction. The results of this deep dive were presented in Tab. 4.

Given the absence of standardized methods to predict the successful creation of functional, caninized antibody constructs, we sought metrics to evaluate and select our top constructs for subsequent expression and lab testing. The original murine antibodies, PD1-1.1 and PD1-2.1, which were comprehensively characterized using lab techniques in Chapter 3, were employed as positive controls. For negative controls, we turned to the caninized variants of the PD1-1.1 antibody, developed earlier in our study, which showed no target binding. PD1-1.1 and its caninized variants were evaluated with the same methods as the PD1-2.1 family of variants.

Table 4: In silico evaluation of caninized antibody constructs. The table details the Root Mean Square Deviation (RMSD) values for each construct, highlighting structural deviations in comparison to the original murine antibody, both on a global scale and specifically within the Complementarity Determining Regions (CDRs). Predicted binding affinities are also provided. The original murine antibodies, PD1-1.1 and PD1-2.1, serve as positive controls, whereas the V2 and V3 caninized variants of PD1-1.1, which did not demonstrate target binding previously, are used as negative controls. Kd - dissociation constant, a parameter describing the affinity of a molecule for its binding partner; the lower the Kd, the stronger the affinity.

Variant ID	Origin	Predicted Kd [M]	RMSD – global [Å]	RMSD – CDRs [Å]
PD1-2.1_OG	**Original murine 2.1 antibody**	**2.8e-09**	**n/a**	**n/a**
PD21_CA_M1A	Functional scFv, Light Chain 7	1.3e-09	1.657	1.562
PD21_CA_M1B	Functional scFv, Light Chain 3	7.6e-09	1.481	1.476
PD21_CA_M2A	Resurfacing with superfluous part of Heavy Chain removed	9.6e-08	1.253	1.187
PD21_CA_M2B	Resurfacing with superfluous part of Heavy Chain retained	2.3e-07	1.135	1.011
PD21_CA_M3	AbySis speciation of disallowed residues	1.0e-08	1.893	1.220
PD21_CA_M4	Individual framework search in the library	1.2e-08	1.172	1.102
PD21_CA_M5	Entire chain search in the library	5.5e-09	1.377	1.195
PD21_CA_M7	CDR3 search in the library	3.6e-10	1.334	1.152
PD21_CA_M9	Germline	7.5e-10	1.209	1.099
PD1-1.1_OG	**Original murine 1.1 antibody**	**8.9e-08**	**n/a**	**n/a**
PD11_CA_V2	Consensus framework sequences	5.7e-09	1.698	1.970
PD11_CA_V3	Consensus framework sequences modified	6.1e-08	1.477	1.973

Regrettably, the relative affinity score predicted at the end of our analytical process did not discern between the high-performing murine binders and the ineffective V2 and V3 PD1-1.1 caninized antibodies. For the murine antibodies, the absolute predicted Kd values did not align with the experimentally determined ones either. We next turned to the predicted sequence liabilities that could affect antibody functionality, but they didn't seem to clarify the binding discrepancy (Tab. S1-S2). The global structure RMSD didn't provide clarity either. Yet, it was evident that the CDR RMSD distance approached 2 ångström for the ineffective constructs. In contrast, the CDR RMSD ranged from 1.011 to 1.562 ångström for the new PD1-2.1 constructs caninized with more advanced methods. Considering the key role of CDR structure for the binding parameters and acknowledging an inherent level of variability in structural predictions, we hypothesized that a CDR RMSD nearing 1 may be informative of successful caninization, while the value nearing 2 may predict disruption to the binding capacity. Visual inspection of the models for PD1-1.1 murine antibody and its non-binding caninized variants (Fig. 8) suggested caninization disrupted the paratope by

introducing steric obstructions to the formerly vacant binding pockets formed by the murine CDRs. This observation bolstered our confidence in using CDR RMSD metric to evaluate caninized constructs.

Figure 8: Structural visualization of the PD1-1.1 murine antibody variable domain and its caninized variants. (A) The variable domain of the original PD1-1.1 murine antibody. (B) The V2 caninized variant of PD1-1.1. (C) The V3 caninized variant of PD1-1.1. (D) Superimposition of the original and caninized structures, highlighting steric obstructions introduced by caninization into the binding pockets formed by CDRs. On each panel the more saturated color highlights the CDR-made antibody paratope. This visual evidence supports the value of the CDR RMSD metric in assessing caninized constructs.
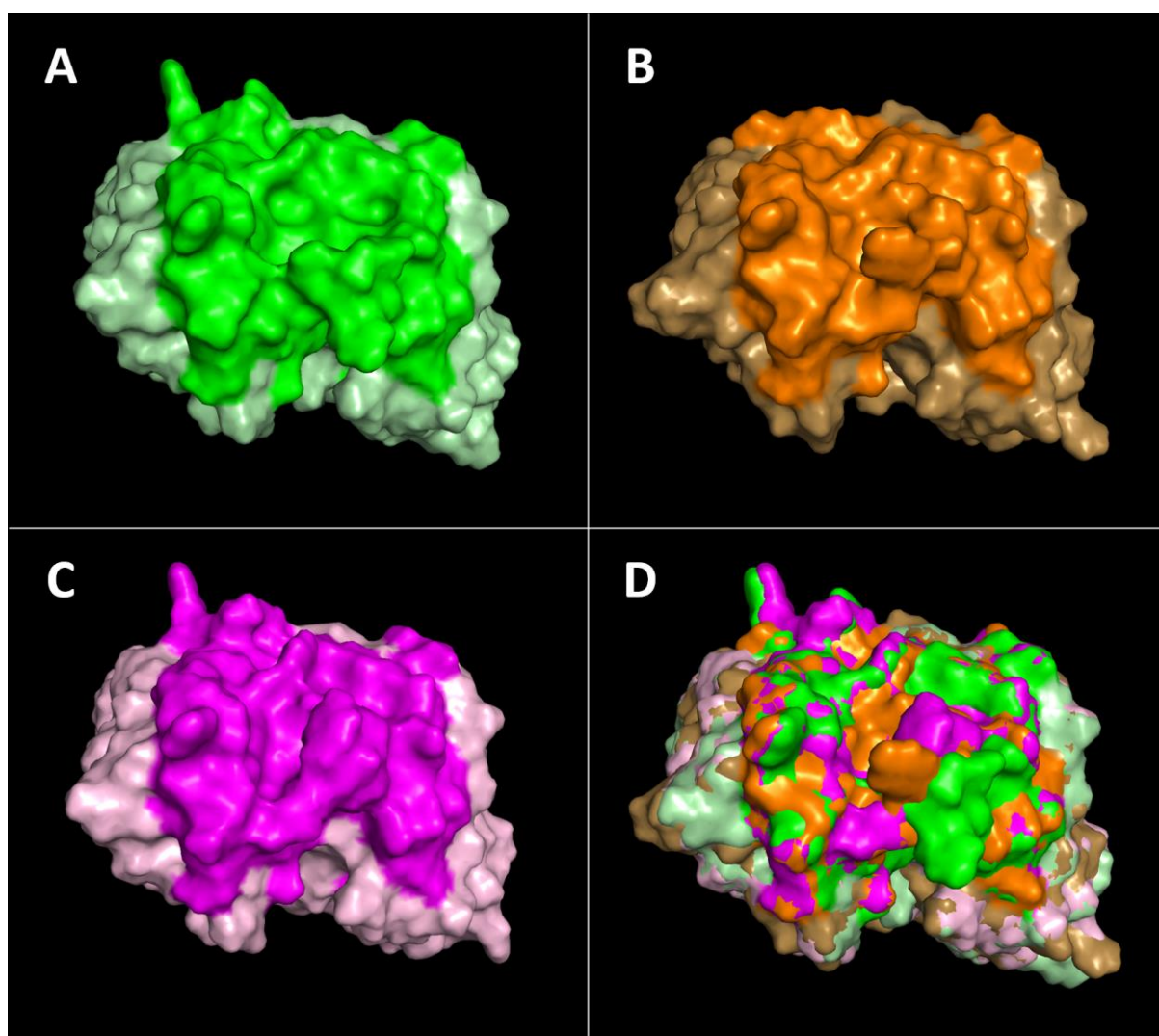
Consequently, PD21_CA_M2B, PD21_CA_M9, and PD21_CA_M4 emerged as the most promising caninized constructs, exhibiting CDR RMSD of 1.011, 1.099, and 1.102, respectively (Fig. 9).

Figure 9: Structural visualization of the PD1-2.1 murine antibody variable domain (PD21_OG) alongside its three top caninized variants. The paratope of PD1-2.1 is highlighted in pea green for ease of comparison. Upon visual inspection, the paratope appears to be well-preserved in the caninized variants.
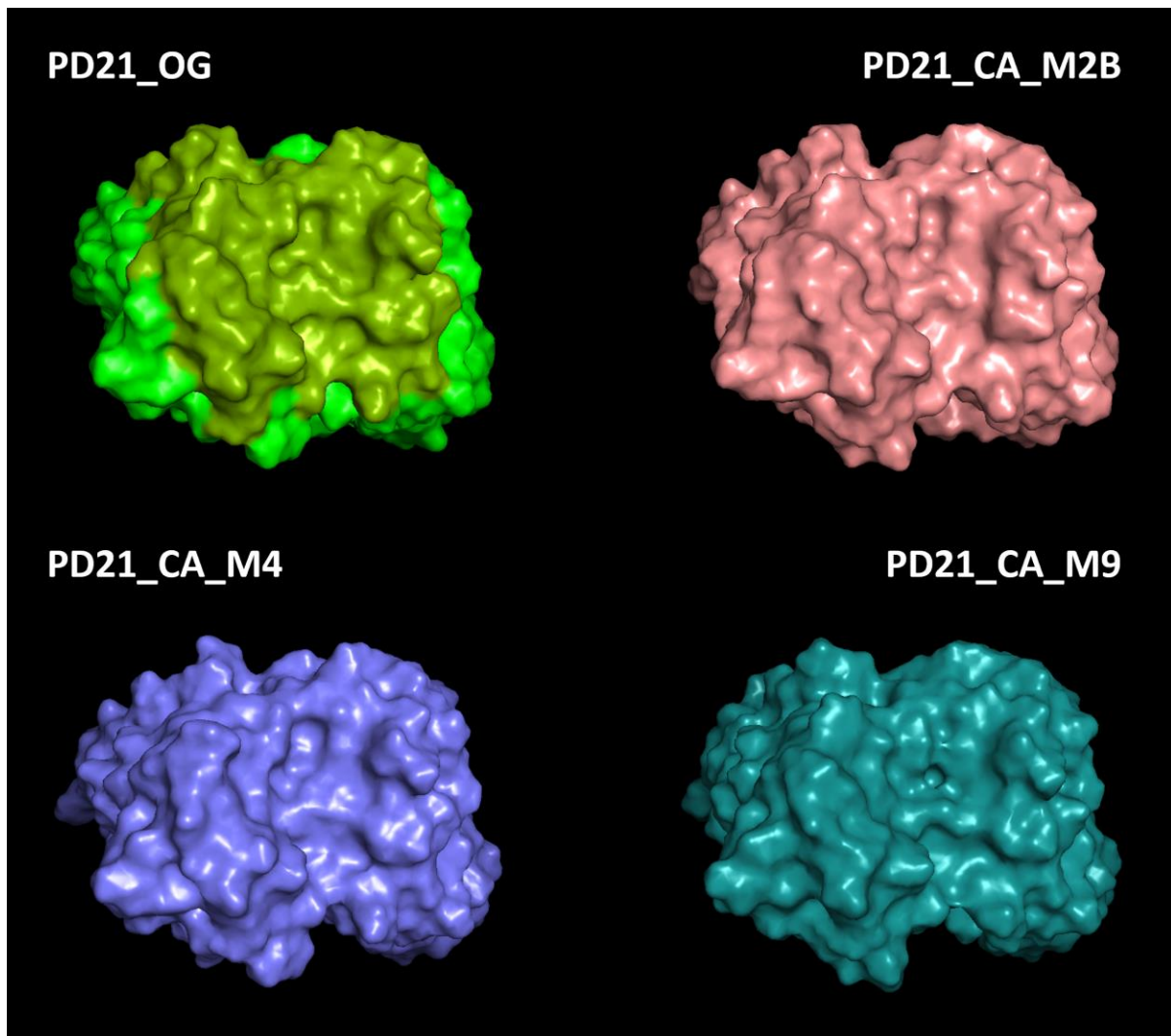
The top position secured by the more conservative of the two resurfacing variants was understandable given the minimal modifications introduced. The outcome for the germline-caninized variant was pleasantly surprising, given the scarcity of canine germline data and the pronounced sequence disparity between the original and the substituted sequences. We were also pleased to observe the match-and-mix framework method, derived from our canine library, concluded the top tier but not the entirety of promising constructs. The affirmed potential of this approach is key because even if the resurfaced and germline-caninized variants become successfully expressed and bind to PD-1, they might not appear as natural to the canine immune system as the PD21_CA_M4 might.

4.3 Discussion

4.3.1 Summary

This work introduces anti-cancer drug candidates to veterinary oncology and valuable resources to the underexplored realm of canine antibodies and their speciation. First, we developed a functional chimeric antibody against canine PD-1, alongside an efficient antibody expression system. To enable further antibody engineering, we established an expansive library of natural, pre-evaluated, and productive canine immunoglobulin sequences, suitable for the forthcoming protein engineering and machine learning endeavours. To facilitate the library generation, we developed a bioinformatics pipeline for analyzing exceptionally vast immunoglobulin sequencing datasets. Building upon these advancements, we introduced several methods of antibody caninization that have not been attempted before. Through trial and error, we identified promising metrics for choosing the best theoretical antibody constructs. In the project's culmination, we generated caninized antibody variants and identified those that best retained the key structural features. The top-scoring antibodies will undergo further validation in laboratory assays. Pending successful outcomes, these candidates will advance to therapeutic trials, marking a pivotal step towards innovative cancer treatments for dogs.

4.3.2 Future work

4.3.2.1 Expression and transfection

Top candidates will be expressed using single chain encoding vectors. This approach will allow the expression of various light and heavy chain pairings. These vectors will be transiently transfected into mammalian cells for antibody production.

4.3.2.2 Conditioned medium analysis

The conditioned medium containing caninized antibody variants will be tested with ELISA. ELISA will be most appropriate given the susceptibility of our antibodies' PD-1 to degradation in reducing conditions. Testing the conditioned medium is beneficial because various purification methods may decrease antibody activity thus obfuscating the results, and purification methods can be optimized at later stages. The results will

enable us to screen out constructs that were effectively expressed and maintained the ability to bind cPD-1.

4.3.2.3 Post-purification evaluation

Results from Chapter 3 demonstrated that the affinity of receptor-blocking antibodies as measured by ELISA isn't directly indicative of their blocking capacity. Hence, after the purification, antibody samples of defined concentration will undergo a blocking ELISA developed in Chapter 3. This will allow for a quantitative comparison of their therapeutic mechanism. Additionally, the affinity of novel antibodies will be compared to the original murine antibody using SPR, providing the absolute affinity values.

4.3.2.4 Refinements and affinity maturation

Should certain candidates exhibit suboptimal binding, back-mutations to the Vernier zone residues will be introduced. The modified constructs will undergo another expression and assessment cycle. Depending on outcomes, affinity maturation methodologies may be used to enhance antibody performance.

4.3.2.5 Developability assessment

The Bioluminate software (Schrodinger) or similar will be used to gauge the developability of candidates. Developability encompasses the biophysical and biochemical properties of an antibody that predict its suitability for successful progression from discovery to a therapeutic product. Key considerations include the antibody's solubility (especially at high concentrations to prevent aggregation) and its inherent stability under diverse conditions (to resist denaturation or degradation). The previously characterized variations in post-translational modifications, such as glycosylation, can also impact the antibody's performance and should be consistently monitored. Another important feature of an antibody is its isoelectric point (IEP) - the pH at which the antibody has no net electrical charge. IEP depends on the charged amino acids of the antibody sequence and broadly affects its pharmacokinetic properties. Identified liabilities may be addressed through targeted mutations. A cost-effective way to introduce them into the vectors could employ PCR techniques.

4.3.2.6 Fc region engineering

In the uncharted realm of canine immunotherapeutics, potential for treatment-associated disease hyperprogression demands exploration. As described earlier, some literature suggests a connection between hyperprogression and Fc-macrophage interactions, encouraging Fc region engineering. The caninized antibodies utilize a canine IgG-D heavy chain, which is a human IgG4 equivalent. IgG4 type may be prone to fab arm exchange - a potentially liability which can also be countered with stabilizing mutations to the antibody Fc sequence.

4.3.2.7 Validation and supplementary assessments

The developed antibodies will be used for immunoprecipitation from a cell lysate coupled with Mass Spectrometry analysis. This will ensure their binding is specific to the PD-1 protein. Additional evaluations could comprise fluorescent microscopy to monitor antibody internalization and RNA sequencing paired with pathway enrichment to detect potential agonistic behaviours.

4.3.2.8 Optimizing the expression system

Our novel expression system employing a single vector with a single promoter for the expression of both antibody chains was successfully used for antibody production. However, to produce the chosen antibodies in cell cultures at higher scale, a single vector with separate promoters for both chains could be constructed for potential improvement in antibody yield [293]. If higher yield would be desired, optimization of heavy and light chain signal peptides could be included in the future work, choosing the most appropriate ones for the given expression system [294]. Regarding the self-cleaving peptide linkers, the cleavage efficacy varies depending on the peptide type and the exact construct, with incomplete cleavage leading to lower yield and expression of fusion proteins that may impact cell vitality [295]. It remains to be tested whether our vector design could be used for large-scale antibody production.

4.3.3 Limitations and improvements

4.3.3.1 The PacBio sequencing library

It is important to note that due to the exclusion of incomplete sequences, the reference-based extraction, and the germline-based productivity-oriented filtering, the canine Ig library data reported here is only a subset of the available antibody repertoire. Moreover, the sequencing protocol was not aimed at exhausting the diversity of the library. The reported numbers should not be treated as an absolute measure of the true diversity of antibody repertoires contained in the employed libraries.

The PacBio long-read plasmid sequencing involves multiple rounds of sequencing per plasmid, with a consensus provided as the output. The results of this process are considered reliable. However, construction of phage display libraries relies on PCR methods, which are often error prone. Consequently, some mutations may be present in a small subset of sequences from the library. Hence, the real diversity of the sequence repertoire may be somewhat lower than it appears to be. For protein engineering, it may be advisable to avoid any highly unusual sequences, as they may contain errors or present a higher risk of immunogenicity.

4.3.3.2 In silico antibody assessment

The affinity prediction of our antibodies did not align with the experimentally obtained results. Specifically, it failed to identify non-binding caninized variants. The failure may be related to structure modelling tools relying too heavily on homology modelling and underestimating the deviation of artificial constructs from the classic antibody structure. A plethora of modelling methods are available, both generalist (e.g., Phyre2, Swiss Fold, AlphaFold) and antibody-specific (e.g., ABodyBuilder2, IgFold), that are founded on different machine learning, homology modelling, and other algorithms. It remains to be tested whether these could lead to improved results. Alternatively, other docking methods (Rosetta, Zdock) and affinity prediction methods could be explored [296]. Future research might refine a method for predicting caninized antibody binding, enhancing the in silico scoring of the construct variants.

4.3.3.3 Structure-based template search

In this study, we utilized sequence-based searches of our library to identify templates homologous to the original murine antibody. Shifting to a structure-focused search could potentially yield even more suitable templates. Such an approach, however, would necessitate identifying the most dependable CDR modelling method for our library. This method would then be employed to model the extensive array of variable domains from our library - a massive undertaking in itself. Finally, a method like Foldseek would have to be integrated in the pipeline for structural search [297].

4.3.3.4 Software development

We are considering encoding the developed methods into an intuitive program simplifying the generation and evaluation of speciated antibody constructs irrespective of the species of interest. It must be acknowledged though that antibody engineering remains a highly empirical field requiring domain knowledge and tailored approach. Moreover, one could question the longevity of methods discussed here, considering the rapid developments in the area of deep learning, 'protein language' research and generative artificial intelligence (AI) technologies. The landscape of AI in proteomic engineering has been described in the supplementary discussion section. Considering the rapid development in this field, it is rational to work on systems that will be compatible with future AI capabilities. Alongside our caninizing methods, we are considering the development of a canine-specific antibody sequence AI model.

4.4 Methods

4.4.1 Designing the chimeric construct

The genetic sequences of the 2 murine antibodies were kindly provided by Prof. Ted Hupp. A murine heavy constant chain of PD1-1.1 mAb was replaced with a canine heavy gamma D amino acid sequence (GenBank: AAL35304.1), and murine kappa light constant chain was replaced by a canine kappa light sequence (NCBI: XP_532962.3) [298]. The construct was designed containing a light leader peptide, light chain, self-cleavage sequence, heavy leader peptide, heavy chain and stop codon. The self-cleavage sequence was Thosea asigna virus (TaV) 2A peptide [281,282] with a GSG linker added at the N-terminus (GSGEGRGSLLTCGDVEENPGP) to increase cleavage efficiency [283]. Uniquely, the chimeric antibody used two different leader peptides - the original murine leader peptides for the L and H chain. Further, caninized, constructs used human IL-2 leader (MYRMQLLSCIALSLALVTNS) peptides, which serve to provide secretion of the protein product outside the human cells, especially in HEK cells which we originally intended to use.

4.4.2 Antibody expression and production

For each engineered construct, the codons were optimized for human or hamster expression with the GeneArt tool (Invitrogen), for HEK and CHO expression systems respectively. The engineered sequence was synthesized and cloned into a pcDNA3.1(+) expression vector containing the Kozak consensus sequence (ACCAUGG) for improved expression. The vector was transfected into HEK or CHO cells for mAb production and purified as described for the original antibody in the previous chapter. The difference was the purification resin, chosen appropriately for the Fc region of each antibody, as proteins A and G most commonly used in purification have different affinity to the various heavy constant chain types.

4.4.3 ELISA

ELISA was performed as described in the previous chapter. However, to detect the recombinant antibodies with a canine Fc region, an anti-dog antibody-HRP conjugate was used (Sigma, #A6792).

4.4.4 Surface Plasmon Resonance (SPR)

SPR was performed as described in the previous chapter.

4.4.5 Consensus-based caninization

The murine antibody variable sequences were divided into FRs and CDRs using AbySis tool suite [260]. Martin's (AbM) antibody numbering scheme was chosen for its updated and structure-conscious character. A small dataset of canine Ig sequences was contributed by Prof. Ted Hupp, which originated from an exploratory, shallow, short-read sequencing of a canine Ig phage display library (pending publication). The sequences, apparently divided by the Kabat scheme, were concatenated, cleaned, and divided by AbM scheme like before. Unknown residues ('X') were substituted with the most likely amino acid based on an NCBI BlastP search [299]. Each framework type set was aligned with Clustal Omega [300] and the consensus sequences were generated with Jalview software [301]. Additionally, a sequence logo was generated for each FR using WebLogo tool [302] to visualize the diversity of top common residues at each position. Sequence logos were not visualized in the thesis but guided the back-mutations.

4.4.6 Septic dogs sequencing dataset

The data from RNA sequencing of blood samples from eight septic dogs treated in the R(D)SVS was generated in another project and kindly provided for this analysis by Dr Maciej Parys.

4.4.7 Creation of the canine immunoglobulin (Ig) library I

Whenever we obtained published sequences that included an unidentified residue ('X') it was substituted by the most likely amino acid based on an NCBI BlastP search. RNA

sequencing datasets analyzed with MiXCR were cleaned manually using BioEdit [303]. All data combined was dereplicated using JalView [301].

4.4.8   Creation of the canine immunoglobulin library II

Canine immunoglobulin plasmid libraries were kindly provided by Prof. Ted Hupp, including a light chain holding, a heavy chain holding and a combined scFv library. The libraries were generated using pooled spleen samples of several dogs, a process awaiting publication. The libraries were sequenced using long-read technology (PacBio) as described in the guidelines further below. The sequencing was performed in collaboration with Dr Małgorzata Lisowska. All data analysis was performed by the author.

Initially, the sequencing reads were inspected with SnapGene viewer software (Dotmatics). The reference-free extraction approach used sequence tags such as PelB, Myc and others to define immunoglobulin sequence start and end. Next, a proprietary reference-based bioinformatic pipeline was developed for raw data pre-processing sequence extraction. The pipeline cleaned the dataset, fixed sequences broken by the linear readouts of circular plasmids and employed both simple and sub-string dereplication of sequences. This ensured the maximum number of unique, complete canine Ig sequences could be extracted while limiting files to a size suitable for further processing. The pipeline next performed a reference-based HV, LV kappa and LV lambda sequence extraction and employed the IMGT/HighV-QUEST algorithm for the identification of putative 'productive' sequences [304]. The analysis was performed using the in-house Mephisto computational cluster.

4.4.9   The new approach to caninizing methods

AbM residue numbering scheme was used as a default in this project, and a proprietary method of defining CDRs was used for caninization. AbySis suite was used for antibody chain analysis, amino acid substitutions, and solvent exposure assessment [260]. Canine germline sequences were sourced from the IMGT repository and manually curated [252]. Local NCBI Blast installation was used for sequence alignment and scoring. BLOSUM62 scoring matrix was used. This matrix assigns numerical values to pairs of amino acids, reflecting their likelihood of alignment due to evolutionary constraints or functional similarities. While antibody-

specific matrices are also being developed [305], the analysis predominantly focused on the structural FR regions which are conserved due to their role in maintaining antibody integrity. BLOSUM62 offered a balanced approach for aligning moderately similar sequences. All computations were performed on the Mephisto cluster.

4.4.10 In silico evaluation of the caninized antibody constructs

For each antibody the variable domains were modeled with ABodyBuilder2 [220]. Potential sequence liabilities were analyzed in silico with the ABodyBuilder-ML [290]. Each construct was structurally aligned to its corresponding murine antibody in PyMol [226]. The Root Mean Square Deviation (RMSD) - a measure of atomic deviation between two structures - was used to assess the structural similarity between the original and caninized molecules. For each caninized variant RMSD was computed for the global structure and for all CDRs as defined with the proprietary method used in this project.

The canine PD-1 sequence was obtained from Ensembl as described in Chapter 3, and divided into domains through ClustalO alignment [221] to the human PD-1 sequence, richly annotated on UniProt (Q15116). Additionally, the identified canine PD-1 domains were validated with InterPro [222]. The extracellular, Ig-like receptor domain was submitted for modeling with Phyre2 [223].

Each antibody construct was docked to the PD-1 receptor using ClusPro2.0 [224,225], using the antibody mode without non-CDR masking. It was previously found that masking does not improve the accuracy of downstream affinity prediction (data not shown). For each antibody domain, binding models were ranked by the corresponding cluster sizes, and the top most-probable binding model was chosen. Such a model was re-exported to a PDB file in PyMol so as to contain a single object with three chain labels (L,H, and A for light chain, heavy chain and PD-1), thus enabling the next step. The PDB file was analyzed with Prodigy [292] to perform affinity prediction. Results were visualized in PyMol.

4.4.11 PacBio Phage Plasmid Library Sequencing

The sequencing of plasmids contained in the library was performed in collaboration with Dr Małgorzata Lisowska. The bioinformatic analysis, extraction of the antibody

sequences and assembly of a canine sequence library was performed solely by the author. Below is the general instruction for PacBio long-read RNA sequencing of a library of plasmids encoding immunoglobulin fragments or other sequences of similar size. Some details (like volume and concentration of the sample) are specific to the sequencing laboratory.

PacBio basics

Pacific Biosciences (PacBio) offers a unique sequencing technology that enables high-fidelity, long-read, reasonably deep sequencing. While the reads number is orders of magnitude lower than with the top Illumina options, in PacBio each read is a complete, high-quality sequence, while on Illumina and similar machines, high number of reads needs to be aligned together to generate one complete sequence. Moreover, such an assembly may not be completely confident in certain applications like ours.

The provider

The following is based on the guidance from Leiden University Medical Center (LUMC) in Netherlands. which I've identified as the best provider upon contacting all European sites offering such a service. The specialists from LUMC were helpful, and the service was significantly cheaper than elsewhere at the time. Professionalism is the main advantage of this lab over competition; their service is the most complete (including size selection), the contact is (achievable! Unlike a certain company in Scotland) quick, and the service is flexible: it is possible to add more SMRT cells for increased depth after obtaining the first results batch; they can also take different sample volumes/concentrations; they are the only provider happy to perform plasmid linearization before the analysis. Moreover, they were resistant to delays caused by Covid-19 pandemic, which were very severe elsewhere (especially in UK). On top of this, LUMC uses Sequel II machine, which is the best one at the time of writing. For a helpful introduction to plasmid linearization visit Addgene (addgene.org/protocols/restriction-digest/) and for advice on analyzing DNA by gel electrophoresis consult this guide (eu.idtdna.com/pages/education/decoded/article/running-agarose-and-polyacrylamide-gels).

How to order the service:

Contact them, and they surely will be happy to help! The procedure involves registering an account in their ordering system (at https://lgtc.nl/order/client_client.php?action=add). This requires a billing name and address, needed to receive an official quote and sample submission form.

The general approach

Assuming the plasmid is relatively short (PacBio can sequence 20kb and more; our common plasmids with antibody chain inserts shall be 4-6kb), we can produce the phage/plasmids in the bacteria, extract DNA with a kit and sequence entire plasmids. This approach is especially good if the percentage of empty or truncated plasmids in the library is low. This allows us to avoid any potential amplification bias and polymerase-related mutations, which is key, as:

1. we need to trust the sequences 100% if they are to be used in labor-intensive and costly antibody engineering and validation
2. single, unusual amino acids can be key information for this purpose (and could easily be errors in case of PCR)

Since the diversity of our phage library was expected to be much higher than the coverage available with PacBio, it only makes sense to run one sample of library on one SMRT sequencing cell. In this case we don't have to worry about adding any adapters/barcodes (neither with whole plasmid, nor with PCR amplification approach; otherwise, this would be done through overhangs on primers). Adding more samples to SMRT cells does not make sense, adding more SMRT cells does – but it costs more and is described further below.

Other approaches

The three approaches to chose from are:
- amplify the plasmid library in bacteria, linearize and sequence – best for quality results; be careful when choosing the enzymes for linearizing - since the exact sequences of the fragments of interest are unknown, there is a risk of losing some to possible cut sites within the sequences. This method is described in detail later below.

161

- amplify the plasmid library in a bacterial culture and cut out fragments of interest – best if the majority of plasmids are empty, since it saves wasteful sequencing. LUMC offers superior option – size selection on their side. However, there is a double risk of restriction-destruction of valuable sequences.

- amplify the fragment of interest by PCR – okay when lower quality is acceptable; **STILL** top-fidelity, proof-reading, hot-start polymerases are necessary such as Kappa HiFi or Fusion Ultra. Additionally, the cycle number has to be kept low (no more than 20) to avoid introducing errors and chimeras. If necessary, run PCR replicates instead of increased cycles to increase the product quantity. Consider adding UMIs to PCR, they mark each amplification product with a unique identifier (random few nucleotides), to differentiate between replicate sequences actually obtained from the replicates in the library vs replicates resulting from PCR bias. For a PCR product of the ScFv size, the required DNA quantity would be 500ng or more.

Steps (approach 1)

- Amplify your library in the bacterial culture with appropriate antibiotics
- Extract plasmids with any quality kit (not phenol-chloroform – the residue will prevent sequencing from working)
- With plasmids of our length aim for **at very least 1 ug** DNA (one microgram). **Aim for 5 ug** if possible. Volume is not too important as they are able to concentrate or dilute the sample, but it would be great if you can manage at least 50ul of 100ng/ul plasmid. Higher concentration is more than welcome.
- Check the purity of the product.
  a. Either Bioanalyzer or Tape Station is required to confirm that the majority of the sample is the full-length sequence, not some smaller products.
  b. Quantitate DNA with both NanoDrop and Qubit, compare the results. They should both show an amount in excess of the number required. As for NanoDrop, the 260:280 ratio of 1.8-2.0 and a 260:230 ratio of 2.0-2.2 are acceptable.
  c. In general, the sample has to be:
     - dsDNA (ssDNA is not compatible)
     - free of contamination with RNA

162

- or insoluble material

- not exposed to high temperatures or extremes of pH

- have been eluted and stored in a neutral, buffered solution, preferably QIAGEN EB Buffer with no EDTA. Avoid storing samples in unbuffered solutions, RNase-free water or AE Buffer.

- have not been vortexed or shaken, as this can cause shearing of the DNA.

- have not been exposed to intercalating fluorescent dyes or ultraviolet radiation.

- does not contain denaturants (such as guanidinium salts or phenol), divalent metal cations (such as Mg2+) or detergents (such as SDS or Triton-X100).

- does not contain contamination from the original organism/tissue (not applicable to phage; haeme, humic acid, polyphenols, etc.).

- **Linearize the plasmid by digesting it with an appropriate restriction enzyme.** In our case NotI **OR** NcoI should be good (based on the library creation scheme available to me). We are not trying to cut out the ScFv fragment, just linearize the plasmid. The size here does not affect the price or coverage. You can linearize the plasmid at whatever site you would like. The data you receive is generated on multiple passes of the sequence so all bases will supposedly have the same quality score independent of their position within the molecule. This step could be omitted for some very large plasmids as they are sheared by mechanical forces during the procedure anyway.

- Cutting out the ScFv sequence could only make sense if there are a lot of empty plasmids. In such a case though, the Leiden lab offers size selection (to remove empty or truncated plasmid**;** this is already included in the total library prep costs!). It is performed on a Blue Pippin device as a part of the service. The downside is that a lot of material is lost during the size selection step, so in such a case at least 5ug (five micrograms) of DNA is required as a starting amount. Alternatively (not recommended – again, avoid UV irradiation!), you could:

  a. cut out the ScFv fragment sequence by using two enzymes; It doesn't matter if the enzyme generates sticky or blunt ends, as overhangs will be removed at the beginning of the library prep.

163

<ol type="b" start="2">
run the sample on agarose gel appropriate for the size difference you want to separate
excise the correct band from the gel under UV; when cutting bands out of gel, never use EtBr. Use Sybr-Safe or Sybr-Gold instead. EtBr is unacceptable, other dyes are not validated and may prevent correct sequencing!
clean up the DNA with Qiagen Gel Extraction Kit /deactivate the enzyme
re-quantify
submit such DNA as a sample

- After linearization you need to remove/deactivate the restriction enzyme – you can just use any column-based plasmid prep kit (confirm with the enzyme manufacturers instruction).
- Ship the sample to the Leiden laboratory and they'll take care of the library prep and sequencing. If we were to assume 1.3MLN unique sequences in the library (that's just the diversity of HCDR3 reportedly), and if the sample quality is good, we can get between 1-2x coverage of the library (theoretical maximum on Sequel II is 2.5 MLN reads).
- Ordering an additional SMRT cell is possible with LUMC and cheaper than the original service cost – this can be used to get more coverage, or to choose sequences duplicated in both runs for antibody engineering with more confidence. On the other hand, our diversity is likely much higher than coverage, so each run sequences a subset of sequences and these subsets may not be sufficiently overlapping – so this would exclude most sequences unnecessarily.

4.5 Supplementary materials

4.5.1 Supplementary discussion

4.5.1.1 *The landscape of AI-aided proteomic engineering*

In the rapidly evolving landscape of AI-assisted protein and antibody design, several breakthroughs stand out [306–312]. Bimekizumab, the first antibody drug proclaimed to be designed with AI aid, was brought to market at accelerated speed. OpenAI's GPT-2 architecture has been adapted by Bayreuth University to create ProtGPT2,

which can generate protein sequences like those found in nature, whereas the ProGen deep-learning model has been trained on an extensive dataset to produce functional protein sequences across diverse families. The ChimeraX ESMFold tool uses AI for protein structure prediction, complementing traditional methods with confidence levels for each prediction. AlphaFold from DeepMind revolutionized protein structure prediction by achieving an unprecedented level of accuracy, capable of predicting structures for nearly the entire human proteome and extending its database to include around 200 million predicted protein structures from multiple species. RoseTTAFold Diffusion (RFdiffusion) takes structure prediction a step further by combining denoising tasks to create new and functional protein backbones. Denoising refers to the process of adding random variations to known protein structures and then training the model to remove these variations, thereby helping it learn the essential features of functional proteins. In antibody-specific applications, pAb and DeepAb use deep learning methods to predict antibody structures, outperforming traditional methods that rely on grafting pieces of previously solved structures. They also introduce novel scoring metrics and interpretable attention mechanisms to further refine the engineering process. Interpretable attention mechanisms allow researchers to see which specific residues the model focuses on, thereby making the prediction process transparent and providing insights into key features that influence antibody binding affinity. Lastly, IgFold combines pre-trained language models and graph networks for the rapid prediction of complex antibody structures. Here, graph models serve as a way to map out the interactions between different parts of the protein, treating these parts as points (nodes) and the interactions between them as connections (edges), which helps in making complex predictions about antibody behaviour and structure.

Still, AI's potential is currently limited by our understanding of proteins. Effective feature engineering is crucial in AI models, and without a comprehensive domain knowledge, there's a ceiling to AI's proficiency. In this context it is worth noting that our understanding of antibodies is still evolving. For instance, constant antibody chains are commonly overlooked in their role in defining antibody affinity, despite some evidence suggesting otherwise [313,314]. Computational methods can generate promising candidates but often require empirical validation and fine-tuning, especially in complex biological systems where not all variables can be accounted for computationally. A hybrid approach which will marry empirical methods with machine

learning, especially in protein design and deimmunization, is likely the most effective path.

4.5.2 Supplementary tables

Table S1. Potential liabilities identified in the sequence of the PD1-1.1 mAb and its caninized variants.

Ab	Chain	Position (AbM)	AA	Liability
PD11_OG	H	72A	N	N-linked glycosylation (NXS/T X not P)
	H	72B	S	N-linked glycosylation (NXS/T X not P)
	H	72C	S	N-linked glycosylation (NXS/T X not P)
	H	34	M	Met oxidation (M)
	H	100D	M	Met oxidation (M)
	L	33	M	Met oxidation (M)
	L	78	M	Met oxidation (M)
	H	103	W	Trp oxidation (W)
	L	35	W	Trp oxidation (W)
	L	47	W	Trp oxidation (W)
PD11_CA_V2	H	34	M	Met oxidation (M)
	H	100D	M	Met oxidation (M)
	L	33	M	Met oxidation (M)
	H	103	W	Trp oxidation (W)
	L	35	W	Trp oxidation (W)
PD11_CA_V3	H	72A	N	N-linked glycosylation (NXS/T X not P)
	H	72B	S	N-linked glycosylation (NXS/T X not P)
	H	72C	S	N-linked glycosylation (NXS/T X not P)
	H	34	M	Met oxidation (M)
	H	100D	M	Met oxidation (M)
	L	33	M	Met oxidation (M)
	H	103	W	Trp oxidation (W)
	L	35	W	Trp oxidation (W)
	L	47	W	Trp oxidation (W)

Table S2. Potential liabilities identified in the sequence of the PD1-2.1 mAb and its caninized variants.

Ab	Chain	Position (AbM)	AA	Liability
PD21_OG	H	22	C	Unpaired Cys (C)
	H	92	C	Unpaired Cys (C)
	L	88	C	Unpaired Cys (C)
	H	34	M	Met oxidation (M)
	H	36	W	Trp oxidation (W)
	L	35	W	Trp oxidation (W)
	L	38	E	Lysine Glycation (KE KD EK ED)
	L	39	K	Lysine Glycation (KE KD EK ED)
PD21_CA_M1A	H	34	M	Met oxidation (M)
	L	4	M	Met oxidation (M)
	H	103	W	Trp oxidation (W)
	L	35	W	Trp oxidation (W)
	H	53	N	Asn deamidation (NG NS NT)
	H	54	T	Asn deamidation (NG NS NT)
PD21_CA_M1B	H	34	M	Met oxidation (M)
	L	4	M	Met oxidation (M)
	H	103	W	Trp oxidation (W)
	L	35	W	Trp oxidation (W)
	H	53	N	Asn deamidation (NG NS NT)
	H	54	T	Asn deamidation (NG NS NT)
PD21_CA_M2A	H	34	M	Met oxidation (M)
	H	103	W	Trp oxidation (W)
	L	35	W	Trp oxidation (W)
	H	53	N	Asn deamidation (NG NS NT)
	H	54	T	Asn deamidation (NG NS NT)
PD21_CA_M2B	H	22	C	Unpaired Cys (C)
	H	92	C	Unpaired Cys (C)
	L	88	C	Unpaired Cys (C)
	H	34	M	Met oxidation (M)
	H	36	W	Trp oxidation (W)
	L	35	W	Trp oxidation (W)
	L	38	E	Lysine Glycation (KE KD EK ED)
	L	39	K	Lysine Glycation (KE KD EK ED)
PD21_CA_M3	H	34	M	Met oxidation (M)
	H	103	W	Trp oxidation (W)
	L	35	W	Trp oxidation (W)
	H	53	N	Asn deamidation (NG NS NT)
	H	54	T	Asn deamidation (NG NS NT)
PD21_CA_M4	H	34	M	Met oxidation (M)
	L	4	M	Met oxidation (M)
	H	103	W	Trp oxidation (W)

	L	35	W	Trp oxidation (W)
	H	53	N	Asn deamidation (NG NS NT)
	H	54	T	Asn deamidation (NG NS NT)
PD21_CA_M5	H	34	M	Met oxidation (M)
	L	4	M	Met oxidation (M)
	H	103	W	Trp oxidation (W)
	L	35	W	Trp oxidation (W)
	H	53	N	Asn deamidation (NG NS NT)
	H	54	T	Asn deamidation (NG NS NT)
PD21_CA_M7	H	34	M	Met oxidation (M)
	L	4	M	Met oxidation (M)
	H	103	W	Trp oxidation (W)
	L	35	W	Trp oxidation (W)
	H	53	N	Asn deamidation (NG NS NT)
	H	54	T	Asn deamidation (NG NS NT)
PD21_CA_M9	H	22	C	Unpaired Cys (C)
	H	92	C	Unpaired Cys (C)
	L	88	C	Unpaired Cys (C)
	H	34	M	Met oxidation (M)
	L	4	M	Met oxidation (M)
	H	36	W	Trp oxidation (W)
	L	35	W	Trp oxidation (W)
	L	38	E	Lysine Glycation (KE KD EK ED)
	L	39	K	Lysine Glycation (KE KD EK ED)

5. CONCLUSIONS AND IMPLICATIONS

5.1 Summary

Throughout this thesis, each experimental chapter delved into the significance, strengths, and limitations of its findings. When viewed individually, these findings provide valuable insights into specific areas of study. Synthesized, they converge into a robust toolkit. This toolkit advances the field of comparative oncology, while offering meaningful contributions to the immunology of both humans and canines. What follows is a consolidated overview of the three primary investigations.

In the inaugural experimental chapter, we set out to reveal the previously unexplored landscape of immune checkpoint (IC) expression in canine cancers. We characterized 44 ICs in 14 canine cancer types, significantly enriching the body of knowledge in canine oncology. To draw parallels with human cancers, we developed a method of contrasting comprehensive IC expression patterns, dubbed IC signatures. This method, when applied to human gene expression data, revealed distinct signatures tied to different cancer types. Notably, our analysis spotlighted heterogeneity among individual patients, hinting at the posibility of personalized treatment, and avenues for research into immunotherapy resistance. Our comparative approach identified remarkable signature similarities between canine and human cancers, especially in brain cancers and certain sarcomas. This finding enables strategic selection of cancer types to serve as models in comparative oncology immunotherapy studies.

In the subsequent chapter, we introduced and characterized two antibodies against the canine PD-1 immune checkpoint. As the pair successfully covered most common laboratory immunoassays, we effectively provided new, validated research reagents to accelerate canine immunology research. The high affinity, checkpoint-blocking attributes, and overall robust profiles additionally position those antibodies as potential veterinary therapeutics.

In the culminating chapter we navigated the complexities of caninizing (de-immunizing) our antibodies. We validated a novel, streamlined antibody production method, and generated a functional chimeric antibody. Through an iterative process, we refined the sequence of the most effective blocking antibody to create a fully caninized construct. This task necessitated the creation of novel methods and the

assembly of a canine antibody sequence database, both of which stand as precious assets for future canine research. Our caninized antibodies demonstrated promising characteristics in computational evaluation. The top scoring variants await laboratory validation, which might pave the way towards canine clinical trials.

Individually, these studies carve niches in their respective domains. Combined, they make a significant dent in the field of comparative oncology. The molecules, datasets, and methods developed here come together as a canine research toolkit poised to amplify advancements at the intersection of human and canine immunology, protein engineering, and cancer treatment. We are optimistic that these resources will narrow the divide between the promise of the canine research model and its translational application. It is our hope that they will also serve other researchers, blooming with collaborative discoveries.

5.2 Winds of change

Canine cancer research, despite its significance, often remains under-acknowledged. While academia is typically viewed as a place of innovation and questioning of the established norms, it is far from immune to dusty dogmas. Even James P. Allison, the father of immune checkpoint therapy, faced significant skepticism and pushback when unveiling his revolutionary findings [45]. Even sadder was the fate of this year's Nobelists, to whom we owe the rapid development of mRNA vaccines against COVID-19. However, the tide is turning for dogs: an increasing number of research labs, consortia, and prestigious institutions are channeling their focus, commitment, and sheer expertise into canine research. The global momentum in canine oncology was recently highlighted in a comprehensive review by Amy K. LeBlanc and Christina N. Mazcko [83]. Gradually, this area of study is earning the acclaim it rightfully deserves.

5.3 Unmet needs in canine research

During the course of this research, several unaddressed needs became evident, highlighting opportunities for future study:

Checkpoint Blockade Assays: PBMC-based assays for evaluating antibodies against the PD-1/PD-L1 interaction show variability due to blood donor differences.

This highlights the need for standardized methods. Commercially available assays, like Promega #J1250 used in our other study [315], provide solutions for human PD-1/PD-L1 evaluation using engineered cells. Developing similar assays tailored for dogs, especially across various immune checkpoints, would be beneficial.

Single-Cell Analysis: the field would benefit from single-cell sequencing studies, the results of which could be used to build reference data for applications like Cibersort. While some teams do apply Cibersort to canine transcriptomic data [138], they are forced to use reference gene signatures originating from human samples. Such analyses would benefit in accuracy from the availability of canine-specific reference data.

Antibody Crystallography: antibody engineering projects often rely on precise protein structures obtained by protein crystallography; in this approach, a structure of a novel sequence can be predicted based on a similar, previously analyzed antibody which becomes a template. Canine antibodies are not identical to human ones, but at the moment have to be modeled based on human templates, as no canine antibodies feature in the PDB database. Crystallographic data of any canine antibodies could lead to better results.

Antibody Cross-Reactivity: the lack of antibodies against a particular target in an unusual research species can sometimes be addressed with cross-reactive antibodies, which bind the same target in more than one species. For this reason, antibodies are occasionally characterized in respect to a few species. However, these usually are limited to humans, monkeys, rodents, and occasionally farm animals. Addition of canine proteins to these tests would be a low-cost but high-impact contribution enabling new studies without the burden of antibody development specifically for a particular project.

Transcriptome Annotation: as reported earlier, inconsistencies were found in the canine reference genome used in the transcriptomic study earlier. Ensemble database was notified, and improvements in annotation can have influence on the accuracy of downstream studies. For instance, one of the IC genes in the aforementioned study had no detectable expression. This may be a difference between human and canine cancers just as well as a mis-annotation of the respective gene.

Data Quality and Ethical Considerations: the veterinary research community must place greater emphasis on thorough data management and description [316]. Adequate patient and sample metadata should accompany sequencing studies, making it possible to link this metadata with individual samples in shared datasets. Some studies within this thesis followed these guidelines. However, the inconsistent quality of sequencing and lack of methodological transparency remain major concerns. Inadequate dataset descriptions make downstream analyses exceedingly difficult, requiring time-consuming detective work and additional data pre-processing. Moreover, different sequencing protocols can introduce bias, necessitating full disclosure to allow for informed data integration. Suboptimal data management can lead to the inferior quality of results or exclusion of samples and entire studies, effectively reducing the statistical power of subsequent analyses. There is often a disconnect between those writing the publication and ordering the sequencing, those executing it, and those performing the analysis. This fragmented approach seemingly leads to important information being lost, especially when researchers see no immediate benefit in adequate data management and adherence to reproducibility guidelines. As in other fields, additional incentives may be necessary to ensure these best practices are followed. However, the obligation to maximize the utility of data generated in publicly funded studies is both ethical and pragmatic. Failure to provide comprehensive methodological and dataset information diminishes the opportunity for new insights. For researchers wishing to conduct similar analyses, the lack of well-described and open data necessitates repeating studies. This repetition is wasteful, consuming not just time and effort but also tangible resources and assets such as electricity, lab materials, precious samples and even animal lives. In an increasingly data-driven world, breakthroughs often lie in well-curated datasets. Yet, the importance of big data and the considerable effort required of bioinformaticians to process such data are often underestimated. To further advance the field, we shall encourage the continuation of high-quality transcriptomic studies that utilize state-of-the-art sequencing technologies and practice transparent data sharing. This will build upon the meaningful progress that has already been made.

These areas represent the current limitations and the directions in which future efforts could be particularly impactful.

5.4 The complex network of immune checkpoints

Traditional approaches relying on the quantification of individual immune checkpoints offer an incomplete picture of the tumor environment. By employing comprehensive gene signatures and dimensionality reduction techniques, this work transcends conventional methods. Yet, we must acknowledge the multilayered complexity of the immune checkpoint network that extends to depths still uncharted, as exemplified below.

To start with, multiple ICs are capable of binding to more than one partner. Some ligands, such as CD80 and CD86, can bind multiple receptors - both stimulatory (CD28) and inhibitory (CTLA-4) [131]. Another example is TIGIT, competing with CD226 for a PVR ligand [317] or PD-L1 - an inhibitory ligand of PD-1 demonstrated to also interact with B7-1 [318]. Others, like VISTA, appear to act both as a ligand and as a receptor [319]. NKG2A forms an inhibitory receptor as a heterodimer with CD94 [320].

Alternative splicing further diversifies the IC landscape by generating various protein variants, such as a soluble PD-1 receptor [212,321], soluble PD-L1 ligand correlating with cancer prognosis [214,322], alternative PD-L1 splice form producing non-coding RNA that promotes lung adenocarcinoma progression [215] or SLAMF6 splice isoforms balancing the T-cell Effector Functions through their antagonistic roles [213].

Adding another layer of complexity, certain IC receptors - traditionally considered characteristic of immune cells - are also expressed on cancer cells. Specifically, PD-1 and TIGIT have been expressed by cancerous cells, though their roles in this context remain unclear [323,324]. In another intriguing twist, some proteins, such as SIGLEC-3 (CD33), serve as immune checkpoints during viral infections and simultaneously modulate immune-related proteins relevant for cancer [325]. This adds a fascinating dimension when considering the interplay between cancer and microbiology, which we will unearth later in this work.

Moreover, the field of cancer immunotherapy has traditionally been T-cell centric, even though evidence suggests that in certain cancers, other immune cell types like B-cells are responsible for the response to immunotherapy. The most recognized checkpoint,

PD-1, is commonly perceived and represented as a T-cell receptor. However, T-cells only express high levels of PD-1 under specific conditions, and B-cells can also express PD-1, as well as play prominent and multi-faceted roles in the tumor microenvironment [326–328]. Yet, B-cells are still commonly relegated to the 'Cinderella' role of antibody production, relevant mainly for therapeutic antibody production or vaccination. In another example, Neutrophils are not only important for response to immunotherapy, but can also eliminate tumor cells on their own in some experiments [329–331]. This undue focus on T-cells demonstrates the tendency within biomedicine to adhere to existing dogmas. A growing body of recent literature is highlighting the important roles played by diverse immune cell types in cancer immunotherapy.

Three additional factors contribute to the complexities of studying this field. First, the phenomenon of trogocytosis - the exchange of membrane fragments, including surface receptors, between both tumor cells themselves and between immune and tumor cells. This process disrupts the straightforward relationship between transcript and protein levels in the cell, a relationship often co-studied in multi-omic analyses [332]. Second, immune checkpoints (ICs) are not solitary entities. Numerous other proteins interact with or regulate them, complicating our understanding of immune responses. Additionally, the term 'immune checkpoint' is being applied increasingly broadly, which begs the question: what truly constitutes an IC? Lastly, the varied aliases used by different authors to refer to the same ICs make it difficult to grasp the whole picture based on literature. Extracting the clinically relevant information from the tumor immune checkpoint landscapes will likely require automated algorithms capable of synthesizing complex data into human-readable tumor status descriptions.

5.5 Field horizons

Within two decades since the seminal immunotherapy papers on CTLA-4 and PD-1 by Allison and Honjo, we have seen remarkable developments. The immune inhibition hypothesis was validated, therapeutics against the identified targets were developed and approved, leading to many lives being saved. The Nobel prize was awarded for these findings. Subsequently, dozens of further proteins were identified as ICs, their interactions were characterized with more nuance and complexity, and finally their

splicing variants are being explored. The immune checkpoints went from a hypothesis to an entire field of its own, with several layers of its complexity currently known. Considering this relatively fast progression from bench to bedside and the life-changing impact of ICB treatments, there is hope that comprehensive characterization of immune checkpoint networks will bring about even bigger improvement in clinical care if not cancer detection and prevention.
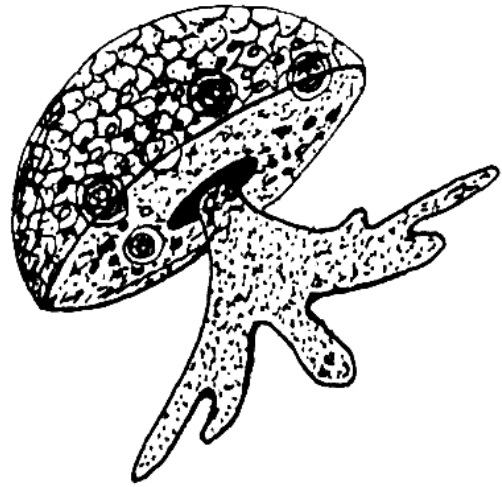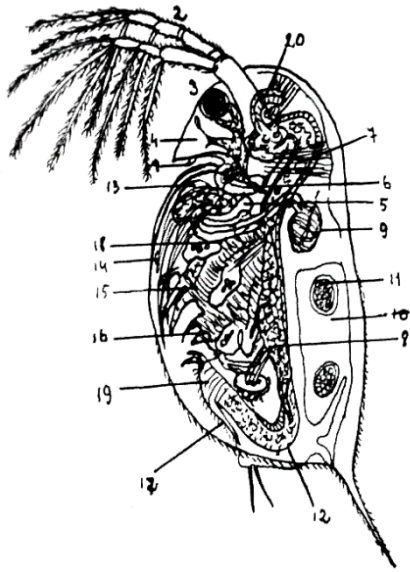
6. PERSPECTIVES

As the great, late scientist Freeman Dyson wrote in regard to the fellow mathematicians, *"some (…) are birds, others are frogs. Birds fly high in the air and survey broad vistas of mathematics out to the far horizon. They delight in concepts that unify our thinking and bring together diverse problems from different parts of the landscape. Frogs live in the mud below and see only the flowers that grow nearby. They delight in the details of particular objects, and they solve problems one at a time. (…) The world of mathematics is both broad and deep, and we need birds and frogs working together to explore it."* [333]. Having wrapped up the findings of this thesis, I would like to take off from the pond to the sky and ponder some broader aspects of immunotherapy and cancer research.

6.1 Elephant in the room

My background in biopharmaceutical antibody development has given me a unique perspective on both the challenges and opportunities in immunotherapy. Creating and consistently supplying therapeutic antibodies that meet rigorous safety standards is a monumental task. It consumes specialized resources and requires orchestrated effort of numerous experts and large teams, all contributing to the extraordinary costs that are inevitably passed onto healthcare systems and patients.

While the treatment costs are expected to decrease as patents expire and development costs are recouped with profit, even some old and relatively unsophisticated therapies, like doxorubicin, remain prohibitively expensive in many high-income countries. The situation is even more dire in low-income countries; of the top 20 cancer medicines considered essential by oncologists, only one is universally available, as cited in a recent study [334]. Regarding immunotherapy specifically, in middle-income countries, accessing treatments like Pembrolizumab often results in 'catastrophic expenditure,' defined as healthcare costs exceeding 40% of a family's post-subsistence income.

This alarming reality highlights a pressing, yet seldom discussed need to explore alternative forms of immune checkpoint modulation that don't rely on antibodies or biological drugs. Such approaches could simplify the drug development, production, storage, and administration processes, thereby making life-saving treatments more affordable, accessible and democratic. This reality underscores the need to reconsider

our approach to cancer treatment development. Scientific and technological advancements, while undoubtedly crucial and impressive, should not be pursued at the expense of making treatment unattainable for most patients. Therefore, in addition to focusing on innovative solutions, the field should prioritize the development of accessible, equitable, and sustainable therapies.

6.2 Going small

One suggested alternative for simpler immune modulation is IC-blocking peptides, like those we have recently described [315]. A team from the Jagiellonian University has also very recently described pAC65, an already patented, PD-L1 targeting macrocyclic peptide capable of blocking the PD-1/PD-L1 with equivalent potency to the FDA-approved antibodies [335]. While peptides related to pAC65 have been described as yielding favorable outcomes in clinical trials, it is essential to clarify that these were studies evaluating basic safety and pharmacological properties in healthy volunteers, rather than therapeutic trials [336,337].

While peptides consist of amino acids - the same building blocks as antibodies - unlike antibodies they can be produced synthetically, with methods such as solid-phase peptide synthesis [338]. This eliminates the need for bioreactors and the associated risks, including contamination from infectious agents, simplifying both production and purification. These benefits could potentially result in a more reliable supply and lower costs.

Moreover, the smaller size of peptides could enhance tissue penetration, crucial for treating solid tumors. Such tumors are often characterized by densely packed epithelial cells, shielded by extracellular matrix (ECM) proteins and have limited vascular access, all impeding drug delivery [339–341]. Uneven tumor penetration by therapeutics, including antibodies, may result in limited response to therapy, and potentially, selection of resistant cells [339,342].

While ICB peptides show promise both in silico and in vitro, therapeutic applications appear distant. One challenge is their inherent instability in blood; a plethora of serum components can inactivate them, including extracellular peptidases. This instability would likely necessitate multiple re-administrations daily, contrasting sharply with the

time between antibody intravenous administrations measured in weeks [343]. Furthermore, peptides may be susceptible to unspecific binding, leading to a high probability of off-target effects in the complex labyrinth of blood vessels with various cell types.

The research on ICB peptides is rife with limitations that need addressing for realistic therapeutic applications. For instance, the concentrations of peptides effective in cellular assays can be so high as to alter the very consistency of the culture medium, posing questions about their physiological relevance. Surprisingly, many of these peptides are published without wet-lab validation, remaining theoretical constructs rather than biological drugs. Typically, they are not evaluated for activity after exposure to blood serum, a critical step. The promise of peptide-based immunotherapies will remain unrealized unless researchers rigorously assess their efficacy and safety. Methods such as competitive ELISA, cell viability and PBMC assays can offer insight into the peptides' capability to block ICs of immune cells, while ensuring safety of the healthy cells.

Despite the challenges, peptides may still hold untapped therapeutic potential if integrated with advanced drug delivery systems. For example, sustained-release peptide polymers could be deposited into the tumor site, assuring therapeutic drug concentration with increased specificity [344]. Alternatively, a more sophisticated approach could involve cycling the release of various peptides in sync with emerging insights into the molecular and chronobiological cycles occurring in cancers, an approach that seems promising in other treatment modalities [345–348]. Such strategies could make treatment personalization more realistic than existing forms of immunotherapy.

While the prospects of peptide-based therapies are exciting, it's worth considering whether small-molecule drugs could outpace them in becoming viable alternatives to antibodies. Small molecules, despite their limitations in directly blocking interactions between large proteins, could act at earlier stages to affect protein conformation. Small molecule drugs offer advantages like better oral bioavailability, good stability in blood, and superior tissue penetration. Compounds like CA-170, a small molecule inhibitor targeting both PD-L1 and VISTA checkpoints, are noteworthy in this context [349]. This arena is where the rapidly developing fields of computational drug design and

molecular modeling combined with deep learning protein folding algorithms are set to shine.

6.3 Going large

Perhaps antibodies hold more promise as specialized molecular agents with advanced functionalities. Fundamental improvements in antibody design are being explored, including aspects like pH-dependent behavior for targeting antigens in cancer-specific environments. This is particularly pertinent since local acidity in tumors can profoundly influence both the bioactivity and distribution of antibodies, ultimately affecting their clinical efficacy [350]. Another area for enhancement is the study of protein glycosylation, which impacts both the antibodies themselves and their target antigens. Furthermore, antibodies can be engineered for protease resistance to prevent their degradation by tumor-associated or microbial proteases, thereby enhancing their efficacy [351,352]. As the field advances, antibodies are being conceived as molecular bots with ambitious functionalities. For instance, pH-sensitive design allows for more precise cancer targeting [353]. The development of bispecific antibodies can facilitate more targeted immune checkpoint blockade [354] and make antibodies act as cell engagers that bring immune cells into proximity with cancer-specific targets [355]. Additionally, antibodies are being engineered to carry therapeutic cargos like silencing RNA [356,357] or cytotoxic agents. Furthermore, efforts are underway to improve the efficiency of antibody production. Notable approaches include the production of antibodies in hen eggs, a technique successfully demonstrated by our colleagues at the Roslin Institute [358]. An alternative approach aims to bypass the antibody manufacturing step altogether through therapeutic antibody gene transfer, using vectors such as the Sendai virus, which can be chosen or engineered for the required tissue- or cancer-specific tropism [359,360]. It is conceivable that a combination of aforementioned technologies and functionalities could have an exponential effect, leading to completely novel treatment opportunities, lowering the amount of the drug needed or the cost and justifying the costs. However, these advances do not appear to be close to clinical application and alternative approaches are needed in the meantime.

6.4 The garden of earthly microbes: microflora and its role in immunotherapy

Bacteria

Following a reignited interest in research on human microbial flora, the entrepreneurial space started filling up with startups wanting to capitalize on these developments, somewhat lacking science to back them up at first. However, more than a temporary boom, human-hosted microbes are here to stay. Unimaginable until the last decade, those "commensal" gut bacteria of our bodies, long believed to benefit from our hospitality with a neutral effect on us, turn out to do as much as influence the oncogenesis and the outcomes of cancer immunotherapy [361]. As for the gut microflora, the largest part of the human microbiome, there is a body of research on its interaction with various diets and its impact on assimilation of various substances - these bacteria are no longer anonymous. However, with such substantial impact in severe disease, we might need to reevaluate our diets even more than we did till now, especially in terms of the preservatives consumed, processed foods and disease prevention.

Moreover, rare reports of microbial genetic material found in the sequencing results of human tissues can no longer be dismissed by default as cases of equipment contamination. This is following a buildup of evidence for unique, cancer-specific microbial communities taking up residence in the tumor environment [362]. Poore et. al. go so far as to call their findings a "cancer's second genome," that is "redefining clonal evolution as a multispecies process" [363]. Some of the cancer's very own microbiomes, like in the case of pancreatic ductal adenocarcinoma (PDA), drive cancer-protective immune suppression [364].

Caudovirales

In the coming years, I anticipate that bacteriophages - the viruses attacking bacteria - will also find their way into mainstream cancer research - extending beyond their current uses as laboratory tools or protein carriers. Bacteriophages were already used experimentally against cancer, resulting in reprogramming the macrophages from the M2 tumor-supportive to M1 phenotype, which effected neutrophils to act against

cancer [365]. However, one can imagine the application of phages specifically for modulating the composition of individual microbiomes as a supportive strategy in cancer treatment. The most prevalent quasi-alive entities on Earth, 'predators' and 'parasites' of bacteria, another layer of microbial complexity, will certainly have their time in the spotlight once we gain the understanding of bacteria in cancer and face a limit of knowledge once again.

Retroviridae wanted - neither dead nor alive

Another fascinating possibility is the use of our genome's residual retroviruses to tag cancer cells as targets for immunotherapy-activated immune cells [366]. Since the dawn of Homo sapiens, our ancestors' bodies have been invaded by retroviruses - a class of RNA viruses capable of inserting their genetic material into the host's DNA [367]. Gradually, these exogenous progenitors merged with the human genome, transforming into endogenous retroviruses (ERVs). Those ERVs descended into what many have dismissively dubbed "junk DNA" - seemingly non-coding sections that constitute most of our genetic material [368]. Retroviral components alone are believed to make up to 8% of our DNA [369]. It might seem like these viral relics merely serve as reminders of ancient evolutionary events, with a few exceptions adapted to serve beneficial functions. However, recent research shows that ERVs have not merely descended into the shadow to lay dormant. In certain instances of dysregulated cellular control, as in cancer, ERVs can reawake, leading to the presentation of novel antigens. The human immune system, recognizing these viral antigens as foreign, could be rallied against such 'marked' cancerous cells. This mechanism could be leveraged by intentionally inducing ERV expression or utilizing drugs that enhance the immune response to these ERV-derived proteins. Such 'tagging' of malignant cells could potentially augment the body's intrinsic cancer-fighting capability or provide new targets for antibody-based therapeutics [370], particularly in those cancers that evade immune detection by down-regulating other tumor markers or shedding them from the cellular membrane. ERVs have also been linked to aging, where they appear to both become resurrected by cellular senescence and elicit it in younger cells [371]. Age is closely linked to cancer development, and retroviruses, outside their potential new role, may also contribute to tumorigenesis [372,373]. Due to this last property, ERVs may have more potential as targets for human-made immunotherapy, be it antibody-

or cell-based, rather than as artificially induced tags for immune cells. ERVs, once adversaries, not classified in any kingdom of life, may turn from forgotten foes into allies in a stunning showcase of evolutionary complexity in the interplay with human ingenuity.

The dark matter

The retroviral companions discussed earlier, intriguing as they are, represent just the tip of the iceberg - the iceberg here being the secrets of the seemingly well researched human genome. Within the realm of genomics, 'dark matter' refers to sections of DNA sequence that remain unreadable with contemporary technology. While not directly linked to immunotherapy at this point, this 'dark matter' is likely concealing genes, mutations, and regulatory elements critical for cancer and other diseases [374,375]. Further, unknown genomic sequences corresponding to certain transcripts affect the accuracy of RNAseq - one of the central tools in cancer research [376]. There are two main culprits behind this predicament. Firstly, the chemical make-up of some genomic regions, especially unusual levels of guanine-cytosine (GC), can throw a wrench in the standard sequencing protocols [377]. Secondly, regions rich in repeats of various lengths, ranging from short tandem repeats to gene duplications, have been making the accurate assembly of sequencing reads into a genomic sequence an impossible task. These challenges are increasingly solvable with newer, more robust and long-read sequencing methods [375]. And just as these hidden genes have been leading bird researchers on wild goose chases [378,379], we can anticipate some surprising findings in *Homo sapiens* too, following the broader availability of a robust sequencing technology. We may be on the edge of a renaissance in genomics, which would naturally boost the related 'omics' fields. It seems the time might just be ripe for *Human Genome Project vol. II*.

Fungi

In a fascinating turn of events, an old concept — linking cancer with fungi, a notion dating back to 1909 or earlier — has recently experienced a significant resurgence ([380,381] and a private archive). Once considered an outlandish theory in the modern era, this notion has just gained ground, and a lot of it. High profile papers detected intratumoral fungi, not only present, but involved in the cancer mechanisms [382–384].

In one example, the fungal presence appeared to promote the already mentioned PDA [385]. Fungi, one of the most mysterious yet indispensable groups of organisms [386], have already revolutionized medicine and biotechnology once, starting from the age of Penicillin, and its folk application long before Pasteur. They might just revolutionize our understanding of cancers.

Omnia vivunt, omnia inter se conexa

While we may be alone in the universe (or not? [387]), we are very much not alone on Earth, and the interactions between _Eukaryota_, _Prokaryota_ and _Viridae_ are a constant source of fascinating insights. With many groundbreaking publications in this field popping up like mushrooms just now, and the factors behind individual microbiome differences largely unknown, it is an incredibly promising and exciting space to observe. This revolution serves as a reminder of the intricate complexity and unexpected utility concealed within our biology. The human propensity to repeatedly ascribe wastefulness to nature and to underestimate 'lesser' creatures - from dark DNA to the appendix to the microbial flora - remains one of the grand mysteries of biology.

6.5 Biodiversity for biomedicine

I would be remiss to overlook the profound lessons on the interplay between biodiversity and medicine that I acquired during my PhD course. Most of the current drugs, especially in the realm of oncology, are either directly sourced from living organisms, inspired by these organisms, or are derivatives of such molecules [388]. Even though we seem to be running out of effective antibiotics and have seemingly plucked most low-hanging fruits of anticancer compounds [389], Nature continues to provide a plethora of secondary metabolites produced by diverse life forms including plants, animals, fungi and bacteria [390]. As genomic and proteomic methods refine, we are increasingly able to unearth these substances. As we described in the past, concurrent advances in biotechnology pave the way for production of these compounds in quantities ample enough for therapeutic use — a prospect that seemed unrealistic for a long time [391–393]. However, despite our ongoing discovery of new species — some only sighted a handful of times — we, the humans, are causing widespread destruction to their habitats. It's estimated that every day, dozens of

species that we haven't even described yet become extinct. In this way, we're irreparably losing potential discoveries of therapeutic compounds. If not for the pure value and beauty of life and biodiversity, humans need to understand the pressing need to safeguard it for their own survival [394,395].

Local communities residing in untouched natural areas have always accumulated knowledge about the medicinal properties of local plants and other biological materials, often in combination. While these practices are often deemed "alternative medicine", it's important to recognize that many of these treatments have been effective for ages, whereas Western medicine has made its share of spectacular errors. Importantly, modern medicine heavily relies on these ancestral transmissions. However, as local communities are dispossessed of their ancestral lands and traditional lifestyles, the knowledge of the elders sinks to the ground. Additionally, the past exploitation of their knowledge and homelands for financial gains makes them justifiably resistant to sharing. Unethical practices like unauthorized collection of living material in developing countries and patenting medical solutions based on prior knowledge of Indigenous people, collectively known as 'biopiracy,' precipitated legislation meant to protect these nations and ecosystems. However, the implemented measures hinder research as a side effect [396]. The research into natural medicinal compounds must continue. It is vital to ensure the profits not merely benefit countries with major pharmaceutical industries but also aid effective conservation of the harnessed ecosystems. Furthermore, it's paramount to share these benefits with local nations, honoring their cultural heritage in the process.

Despite our apparent knowledge of the world, there remain habitats that are largely uncharted by humans. For instance, the deep-sea realm, home to an array of incredible creatures, is only partially explored. These mysterious depths have been examined through unique projects like the metagenomic sampling expedition led by geneticist Craig Venter aboard his research yacht, the 'Sorcerer II'. Such ventures allow scientists to discover new microbial strains, genes and potentially useful proteins. Yet, tragically, even the most remote of these locations, barely glimpsed by human eyes, bear the scars of our pollution - as demonstrated by the microplastics detected in the Mariana Trench [397–399]. Our reliance on plastic materials does more than litter our world; it introduces harmful, stable and under-researched endocrine-

disrupting compounds (EDCs), into our environment. These include well known ones like Bisphenol A (BPA) and others less unknown [400]. These compounds pose a significant threat to human and wildlife health alike. A massive body of research found links between these compounds and the risk of cancer, diabetes, reproductive and fertility problems, obesity, neurological and other health problems in humans [401–403].

With each day we continue on this path, we inadvertently ingest toxins, obliterate unknown species along with the medicinal potential they hold, and continue to inflict irreparable harm to our ecosystems. Some hope remains that we can cease these destructive habits, curb our reliance on harmful substances and collectively pivot towards a greener, healthier, and more biodiverse future.

6.6 Epilogue

The awe-inspiring complexity, depth, and seemingly boundless interconnectedness in the natural world around us and within us might be as captivating as it is intimidating for someone looking to solve modern medical and humanitarian challenges. I'd like to propose an unexpected source of inspiration from another field of research. As the story has it, in 1677 Anton van Leeuwenhoek, the Dutch creator of the first compound microscope, used his simple tool to examine semen. Since this observation, it has been known that the spermatozoa "moved forward owing to the motion of their tails like that of a snake or an eel swimming in water" - side to side [404]. Thus, the understanding of a fundamental reproductive process, a crucial aspect of biology, was established. Except, after 350 years' worth of assumed wiggling, it turned out the cornerstone of human reproductive biology has been an illusion. It was only when a British mathematician, a Mexican biotechnologist and three engineers took the matter in their own hands, that we collectively learned the sperm cells move - to quote the experts - "like playful otters corkscrewing through water" [405]. Despite the light-hearted description, this finding shattered a long-standing dogma in its field. To use an oversimplified metaphor, what it took, was to look from a different angle.

7. BIBLIOGRAPHY

1. Dagogo-Jack I, Shaw AT. Tumour heterogeneity and resistance to cancer therapies. Nat Rev Clin Oncol. 2018 Feb;15[2]:81–94.

2. Gerlinger M, Rowan AJ, Horswell S, Larkin J, Endesfelder D, Gronroos E, et al. Intratumor Heterogeneity and Branched Evolution Revealed by Multiregion Sequencing. N Engl J Med. 2012 Mar 8;366[10]:883–92.

3. Casás-Selves M, DeGregori J. How Cancer Shapes Evolution and How Evolution Shapes Cancer. Evo Edu Outreach. 2011 Dec;4[4]:624–34.

4. Wortzel I, Dror S, Kenific CM, Lyden D. Exosome-Mediated Metastasis: Communication from a Distance. Developmental Cell. 2019 May;49[3]:347–60.

5. Peinado H, Alečković M, Lavotshkin S, Matei I, Costa-Silva B, Moreno-Bueno G, et al. Melanoma exosomes educate bone marrow progenitor cells toward a pro-metastatic phenotype through MET. Nat Med. 2012 Jun;18[6]:883–91.

6. Hanahan D, Weinberg RA. The Hallmarks of Cancer. Cell. 2000 Jan;100[1]:57–70.

7. Hanahan D, Weinberg RA. Hallmarks of Cancer: The Next Generation. Cell. 2011 Mar;144[5]:646–74.

8. Hanahan D. Hallmarks of Cancer: New Dimensions. Cancer Discovery. 2022 Jan 1;12[1]:31–46.

9. Obenauf AC, Massagué J. Surviving at a Distance: Organ-Specific Metastasis. Trends in Cancer. 2015 Sep;1[1]:76–91.

10. Jones PA, Baylin SB. The Epigenomics of Cancer. Cell. 2007 Feb;128[4]:683–92.

11. Beroukhim R, Mermel CH, Porter D, Wei G, Raychaudhuri S, Donovan J, et al. The landscape of somatic copy-number alteration across human cancers. Nature. 2010 Feb;463[7283]:899–905.

12. Vogelstein B, Papadopoulos N, Velculescu VE, Zhou S, Diaz LA, Kinzler KW. Cancer Genome Landscapes. Science. 2013 Mar 29;339[6127]:1546–58.

13. Cross W, Kovac M, Mustonen V, Temko D, Davis H, Baker AM, et al. The evolutionary landscape of colorectal tumorigenesis. Nat Ecol Evol. 2018 Aug 31;2[10]:1661–72.

14. Nam AS, Chaligne R, Landau DA. Integrating genetic and non-genetic determinants of cancer evolution by single-cell multi-omics. Nat Rev Genet. 2021 Jan;22[1]:3–18.

15. Hynds RE, Vladimirou E, Janes SamM. The secret lives of cancer cell lines. Disease Models & Mechanisms. 2018 Nov 1;11[11]:dmm037366.

16. Gillet JP, Calcagno AM, Varma S, Marino M, Green LJ, Vora MI, et al. Redefining the relevance of established cancer cell lines to the study of

mechanisms of clinical anti-cancer drug resistance. Proc Natl Acad Sci USA. 2011 Nov 15;108[46]:18708–13.

17.   Suarez-Martinez E, Suazo-Sanchez I, Celis-Romero M, Carnero A. 3D and organoid culture in research: physiology, hereditary genetic diseases and cancer. Cell Biosci. 2022 Dec;12[1]:39.

18.   Hirsch C, Schildknecht S. In Vitro Research Reproducibility: Keeping Up High Standards. Front Pharmacol. 2019 Dec 10;10:1484.

19.   O'Donnell JS, Teng MWL, Smyth MJ. Cancer immunoediting and resistance to T cell-based immunotherapy. Nat Rev Clin Oncol. 2019 Mar;16[3]:151–67.

20.   Dujon AM, Boutry J, Tissot S, Lemaître JF, Boddy AM, Gérard AL, et al. Cancer Susceptibility as a Cost of Reproduction and Contributor to Life History Evolution. Front Ecol Evol. 2022 May 9;10:861103.

21.   Boddy AM, Kokko H, Breden F, Wilkinson GS, Aktipis CA. Cancer susceptibility and reproductive trade-offs: a model of the evolution of cancer defences. Phil Trans R Soc B. 2015 Jul 19;370[1673]:20140220.

22.   Rozhok AI, DeGregori J. The three dimensions of somatic evolution: Integrating the role of genetic damage, life-history traits, and aging in carcinogenesis. Evolutionary Applications. 2020 Aug;13[7]:1569–80.

23.   Key TJ, Bradbury KE, Perez-Cornago A, Sinha R, Tsilidis KK, Tsugane S. Diet, nutrition, and cancer risk: what do we know and what is the way forward? BMJ. 2020 Mar 5;m511.

24.   Zhang FF, Cudhea F, Shan Z, Michaud DS, Imamura F, Eom H, et al. Preventable Cancer Burden Associated With Poor Diet in the United States. JNCI Cancer Spectrum. 2019 Jun 1;3[2]:pkz034.

25.   Chang K, Gunter MJ, Rauber F, Levy RB, Huybrechts I, Kliemann N, et al. Ultra-processed food consumption, cancer risk and cancer mortality: a large-scale prospective analysis within the UK Biobank. EClinicalMedicine. 2023 Feb;56:101840.

26.   Laguna JC, Alegret M, Cofán M, Sánchez-Tainta A, Díaz-López A, Martínez-González MA, et al. Simple sugar intake and cancer incidence, cancer mortality and all-cause mortality: A cohort study from the PREDIMED trial. Clinical Nutrition. 2021 Oct;40[10]:5269–77.

27.   Epner M, Yang P, Wagner RW, Cohen L. Understanding the Link between Sugar and Cancer: An Examination of the Preclinical and Clinical Evidence. Cancers. 2022 Dec 8;14[24]:6042.

28.   Harris BHL, Macaulay VM, Harris DA, Klenerman P, Karpe F, Lord SR, et al. Obesity: a perfect storm for carcinogenesis. Cancer Metastasis Rev. 2022 Sep;41[3]:491–515.

29.   Tran KB, Lang JJ, Compton K, Xu R, Acheson AR, Henrikson HJ, et al. The global burden of cancer attributable to risk factors, 2010–19: a systematic analysis for the Global Burden of Disease Study 2019. The Lancet. 2022 Aug;400[10352]:563–91.

30.   Eckerling A, Ricon-Becker I, Sorski L, Sandbank E, Ben-Eliyahu S. Stress and cancer: mechanisms, significance and future directions. Nat Rev Cancer. 2021 Dec;21[12]:767–85.

31.   Kraav SL, Lehto SM, Kauhanen J, Hantunen S, Tolmunen T. Loneliness and social isolation increase cancer incidence in a cohort of Finnish middle-aged men. A longitudinal study. Psychiatry Research. 2021 May;299:113868.

32.   Lynch BM. Sedentary Behavior and Cancer: A Systematic Review of the Literature and Proposed Biological Mechanisms. Cancer Epidemiology, Biomarkers & Prevention. 2010 Nov 1;19[11]:2691–709.

33.   Hermelink R, Leitzmann MF, Markozannes G, Tsilidis K, Pukrop T, Berger F, et al. Sedentary behavior and cancer–an umbrella review and meta-analysis. Eur J Epidemiol. 2022 May;37[5]:447–60.

34.   Vineis P, Alavanja M, Buffler P, Fontham E, Franceschi S, Gao YT, et al. Tobacco and Cancer: Recent Epidemiological Evidence. JNCI Journal of the National Cancer Institute. 2004 Jan 21;96[2]:99–106.

35.   Lee Y. Roles of circadian clocks in cancer pathogenesis and treatment. Exp Mol Med. 2021 Oct;53[10]:1529–38.

36.   Choi YJ, Moskowitz JM, Myung SK, Lee YR, Hong YC. Cellular Phone Use and Risk of Tumors: Systematic Review and Meta-Analysis. IJERPH. 2020 Nov 2;17[21]:8079.

37.   Grell K, Frederiksen K, Schüz J, Cardis E, Armstrong B, Siemiatycki J, et al. The Intracranial Distribution of Gliomas in Relation to Exposure From Mobile Phones: Analyses From the INTERPHONE Study. Am J Epidemiol. 2016 Dec 1;184[11]:818–28.

38.   Huss A, Egger M, Hug K, Huwiler-Müntener K, Röösli M. Source of Funding and Results of Studies of Health Effects of Mobile Phone Use: Systematic Review of Experimental Studies. Environ Health Perspect. 2007 Jan;115[1]:1–4.

39.   Baj J, Dring JC, Czeczelewski M, Kozyra P, Forma A, Flieger J, et al. Derivatives of Plastics as Potential Carcinogenic Factors: The Current State of Knowledge. Cancers. 2022 Sep 24;14[19]:4637.

40.   Park JH, Hong S, Kim OH, Kim CH, Kim J, Kim JW, et al. Polypropylene microplastics promote metastatic features in human breast cancer. Sci Rep. 2023 Apr 17;13[1]:6252.

41.   Erren T, Zeuß D, Steffany F, Meyer-Rochow B. Increase of wildlife cancer: an echo of plastic pollution? Nat Rev Cancer. 2009 Nov;9[11]:842–842.

42.   Anand P, Kunnumakara AB, Sundaram C, Harikumar KB, Tharakan ST, Lai OS, et al. Cancer is a Preventable Disease that Requires Major Lifestyle Changes. Pharm Res. 2008 Sep;25[9]:2097–116.

43.   Baer M, Groth A, Lund AH, Sonne-Hansen K. Creativity as an antidote to research becoming too predictable. The EMBO Journal. 2023 Feb 15;42[4]:e112835.

44.   Hanahan D, Coussens LM. Accessories to the Crime: Functions of Cells Recruited to the Tumor Microenvironment. Cancer Cell. 2012 Mar;21[3]:309–22.

45.   Zang X. 2018 Nobel Prize in medicine awarded to cancer immunotherapy: Immune checkpoint blockade – A personal account. Genes & Diseases. 2018 Dec;5[4]:302–3.

46.   Robert C, Ribas A, Hamid O, Daud A, Wolchok JD, Joshua AM, et al. Durable Complete Response After Discontinuation of Pembrolizumab in Patients With Metastatic Melanoma. JCO. 2018 Jun 10;36[17]:1668–74.

47.   Forsström B, Bisławska Axnäs B, Rockberg J, Danielsson H, Bohlin A, Uhlen M. Dissecting Antibodies with Regards to Linear and Conformational Epitopes. Mantis NJ, editor. PLoS ONE. 2015 Mar 27;10[3]:e0121673.

48.   Jain S, Aresu L, Comazzi S, Shi J, Worrall E, Clayton J, et al. The Development of a Recombinant scFv Monoclonal Antibody Targeting Canine CD20 for Use in Comparative Medicine. Meinl E, editor. PLoS ONE. 2016 Feb 19;11[2]:e0148366.

49.   Uhrik L, Hernychova L, Muller P, Kalathiya U, Lisowska MM, Kocikowski M, et al. Hydrogen deuterium exchange mass spectrometry identifies the dominant paratope in CD20 antigen binding to the NCD1.2 monoclonal antibody. Biochemical Journal. 2021 Jan 15;478[1]:99–120.

50.   Mahler SM, Marquis CP, Brown G, Roberts A, Hoogenboom HR. Cloning and expression of human V-genes derived from phage display libraries as fully assembled human anti-TNF alpha monoclonal antibodies. Immunotechnology. 1997 Mar;3[1]:31–43.

51.   Safdari Y, Farajnia S, Asgharzadeh M, Khalili M. Antibody humanization methods – a review and update. Biotechnology and Genetic Engineering Reviews. 2013 Oct 1;29[2]:175–86.

52.   Frenzel A, Schirrmann T, Hust M. Phage display-derived human antibodies in clinical development and therapy. MAbs. 2016 Jul 14;8[7]:1177–94.

53.   Guo L, Zhang H, Chen B. Nivolumab as Programmed Death-1 (PD-1) Inhibitor for Targeted Immunotherapy in Tumor. J Cancer. 2017;8[3]:410–6.

54.   De Sousa Linhares A, Battin C, Jutz S, Leitner J, Hafner C, Tobias J, et al. Therapeutic PD-L1 antibodies are more effective than PD-1 antibodies in blocking PD-1/PD-L1 signaling. Sci Rep. 2019 Aug 7;9[1]:11472.

55. Juneja VR, McGuire KA, Manguso RT, LaFleur MW, Collins N, Haining WN, et al. PD-L1 on tumor cells is sufficient for immune evasion in immunogenic tumors and inhibits CD8 T cell cytotoxicity. Journal of Experimental Medicine. 2017 Apr 3;214[4]:895–904.

56. Aguilar EJ, Ricciuti B, Gainor JF, Kehl KL, Kravets S, Dahlberg S, et al. Outcomes to first-line pembrolizumab in patients with non-small-cell lung cancer and very high PD-L1 expression. Annals of Oncology. 2019 Oct;30[10]:1653–9.

57. Frelaut M, Le Tourneau C, Borcoman E. Hyperprogression under Immunotherapy. IJMS. 2019 May 30;20[11]:2674.

58. Ghisoni E, Wicky A, Bouchaab H, Imbimbo M, Delyon J, Gautron Moura B, et al. Late-onset and long-lasting immune-related adverse events from immune checkpoint-inhibitors: An overlooked aspect in immunotherapy. European Journal of Cancer. 2021 May;149:153–64.

59. Robert C. A decade of immune-checkpoint inhibitors in cancer therapy. Nat Commun. 2020 Jul 30;11[1]:3801.

60. Couey MA, Bell RB, Patel AA, Romba MC, Crittenden MR, Curti BD, et al. Delayed immune-related events (DIRE) after discontinuation of immunotherapy: diagnostic hazard of autoimmunity at a distance. j immunotherapy cancer. 2019 Dec;7[1]:165.

61. Kocikowski M, Dziubek K, Parys M. Hyperprogression Under Immune Checkpoint-Based Immunotherapy—Current Understanding, The Role of PD-1/PD-L1 Tumour-Intrinsic Signalling, Future Directions and a Potential Large Animal Model. Cancers. 2020 Mar 27;12[4]:804.

62. Champiat S, Dercle L, Ammari S, Massard C, Hollebecque A, Postel-Vinay S, et al. Hyperprogressive Disease Is a New Pattern of Progression in Cancer Patients Treated by Anti-PD-1/PD-L1. Clinical Cancer Research. 2017 Apr 15;23[8]:1920–8.

63. Raedler LA. Opdivo (Nivolumab): Second PD-1 Inhibitor Receives FDA Approval for Unresectable or Metastatic Melanoma. Am Health Drug Benefits. 2015 Mar;8[Spec Feature]:180–3.

64. EMA. European Medicines Agency. [cited 2023 Sep 3]. European Medicines Agency. Available from: https://www.ema.europa.eu/en

65. Pilard C, Ancion M, Delvenne P, Jerusalem G, Hubert P, Herfs M. Cancer immunotherapy: it's time to better predict patients' response. Br J Cancer. 2021 Sep 28;125[7]:927–38.

66. Cristescu R, Mogg R, Ayers M, Albright A, Murphy E, Yearley J, et al. Pan-tumor genomic biomarkers for PD-1 checkpoint blockade–based immunotherapy. Science. 2018 Oct 12;362[6411]:eaar3593.

67. Patel SP, Kurzrock R. PD-L1 Expression as a Predictive Biomarker in Cancer Immunotherapy. Molecular Cancer Therapeutics. 2015 Apr 1;14[4]:847–56.

68.   Auslander N, Zhang G, Lee JS, Frederick DT, Miao B, Moll T, et al. Robust prediction of response to immune checkpoint blockade therapy in metastatic melanoma. Nat Med. 2018 Oct;24[10]:1545–9.

69.   Hegde PS, Chen DS. Top 10 Challenges in Cancer Immunotherapy. Immunity. 2020 Jan;52[1]:17–35.

70.   Jentzsch V, Osipenko L, Scannell JW, Hickman JA. Costs and Causes of Oncology Drug Attrition With the Example of Insulin-Like Growth Factor-1 Receptor Inhibitors. JAMA Netw Open. 2023 Jul 28;6[7]:e2324977.

71.   Park JS, Withers SS, Modiano JF, Kent MS, Chen M, Luna JI, et al. Canine cancer immunotherapy studies: linking mouse and human. j immunotherapy cancer. 2016 Dec;4[1]:97.

72.   Schreiber RD, Old LJ, Smyth MJ. Cancer Immunoediting: Integrating Immunity's Roles in Cancer Suppression and Promotion. Science. 2011 Mar 25;331[6024]:1565–70.

73.   Routy B, Le Chatelier E, Derosa L, Duong CPM, Alou MT, Daillère R, et al. Gut microbiome influences efficacy of PD-1–based immunotherapy against epithelial tumors. Science. 2018 Jan 5;359[6371]:91–7.

74.   Richmond A, Su Y. Mouse xenograft models vs GEM models for human cancer therapeutics. Disease Models & Mechanisms. 2008 Sep 26;1[2–3]:78–82.

75.   Mak IW, Evaniew N, Ghert M. Lost in translation: animal models and clinical trials in cancer treatment. Am J Transl Res. 2014;6[2]:114–8.

76.   Van Der Worp HB, Howells DW, Sena ES, Porritt MJ, Rewell S, O'Collins V, et al. Can Animal Models of Disease Reliably Inform Human Studies? PLoS Med. 2010 Mar 30;7[3]:e1000245.

77.   Hansen K, Khanna C. Spontaneous and genetically engineered animal models. European Journal of Cancer. 2004 Apr;40[6]:858–80.

78.   Khanna C, Lindblad-Toh K, Vail D, London C, Bergman P, Barber L, et al. The dog as a cancer model. Nat Biotechnol. 2006 Sep 1;24[9]:1065–6.

79.   Ostrander EA, Wang GD, Larson G, vonHoldt BM, Davis BW, Jagannathan V, et al. Dog10K: an international sequencing effort to advance studies of canine domestication, phenotypes and health. National Science Review. 2019 Jul 1;6[4]:810–24.

80.   Dow S. A Role for Dogs in Advancing Cancer Immunotherapy Research. Front Immunol. 2020 Jan 17;10:2935.

81.   Cekanova M, Rathore K. Animal models and therapeutic molecular targets of cancer: utility and limitations. DDDT. 2014 Oct;1911.

82.   Davis BW, Ostrander EA. Domestic Dogs and Cancer Research: A Breed-Based Genomics Approach. ILAR Journal. 2014 Jan 1;55[1]:59–68.

83.   LeBlanc AK, Mazcko CN. Improving human cancer therapy through the evaluation of pet dogs. Nat Rev Cancer. 2020 Dec;20[12]:727–42.

84.   Paoloni M, Davis S, Lana S, Withrow S, Sangiorgi L, Picci P, et al. Canine tumor cross-species genomics uncovers targets linked to osteosarcoma progression. BMC Genomics. 2009;10[1]:625.

85.   Dobson JM. Breed-Predispositions to Cancer in Pedigree Dogs. ISRN Veterinary Science. 2013 Jan 17;2013:1–23.

86.   Baioni E, Scanziani E, Vincenti MC, Leschiera M, Bozzetta E, Pezzolato M, et al. Estimating canine cancer incidence: findings from a population-based tumour registry in northwestern Italy. BMC Vet Res. 2017 Dec;13[1]:203.

87.   Klingemann H. Immunotherapy for Dogs: Running Behind Humans. Front Immunol. 2018 Feb 5;9:133.

88.   Cannarozzi G, Schneider A, Gonnet G. A Phylogenomic Study of Human, Dog, and Mouse. Bourne PE, editor. PLoS Comput Biol. 2007 Jan 5;3[1]:e2.

89.   Martin J, Ponstingl H, Lefranc MP, Archer J, Sargan D, Bradley A. Comprehensive annotation and evolutionary insights into the canine (Canis lupus familiaris) antigen receptor loci. Immunogenetics. 2018 Apr;70[4]:223–36.

90.   Vilà C, Savolainen P, Maldonado JE, Amorim IR, Rice JE, Honeycutt RL, et al. Multiple and Ancient Origins of the Domestic Dog. Science. 1997 Jun 13;276[5319]:1687–9.

91.   Schleidt WM, Shalter MD. Dogs And Mankind: Coevolution on the Move – An Update. HEB. 2018 Mar 25;33[1]:15–38.

92.   Thalmann O, Perri AR. Paleogenomic Inferences of Dog Domestication. In: Lindqvist C, Rajora OP, editors. Paleogenomics [Internet]. Cham: Springer International Publishing; 2018 [cited 2023 Sep 3]. p. 273–306. [Population Genomics]. Available from: https://link.springer.com/10.1007/13836_2018_27

93.   Tacon P, Pardoe C. Dogs make us human. Nature Aust. 2002 Jan 1;27.

94.   Wang G dong, Zhai W, Yang H chuan, Fan R xi, Cao X, Zhong L, et al. The genomics of selection in dogs and the parallel evolution between dogs and humans. Nat Commun. 2013 May 14;4[1]:1860.

95.   Son KH, Aldonza MBD, Nam AR, Lee KH, Lee JW, Shin KJ, et al. Integrative mapping of the dog epigenome: Reference annotation for comparative intertissue and cross-species studies. Sci Adv. 2023 Jul 7;9[27]:eade3399.

96.   Driscoll CA, Clutton-Brock J, Kitchener AC, O'Brien SJ. The Taming of the Cat. Sci Am. 2009 Jun;300[6]:68–75.

97.   Marin-Acevedo JA, Dholaria B, Soyano AE, Knutson KL, Chumsri S, Lou Y. Next generation of immune checkpoint therapy in cancer: new developments and challenges. J Hematol Oncol. 2018 Dec;11[1]:39.

98. Sun N, Luo Y, Zheng B, Zhang Z, Zhang C, Zhang Z, et al. A novel immune checkpoints-based signature to predict prognosis and response to immunotherapy in lung adenocarcinoma. J Transl Med. 2022 Dec;20[1]:332.

99. Zhen Z, Shen Z, Sun P. Dissecting the Role of Immune Checkpoint Regulation Patterns in Tumor Microenvironment and Prognosis of Gastric Cancer. Front Genet. 2022 Apr 19;13:853648.

100. Kang SY, Heo YJ, Kwon GY, Lee J, Park SH, Kim KM. Five-gene signature for the prediction of response to immune checkpoint inhibitors in patients with gastric and urothelial carcinomas. Pathology - Research and Practice. 2023 Jan;241:154233.

101. Wang YQ, Zhang Y, Jiang W, Chen YP, Xu SY, Liu N, et al. Development and validation of an immune checkpoint-based signature to predict prognosis in nasopharyngeal carcinoma using computational pathology analysis. j immunotherapy cancer. 2019 Dec;7[1]:298.

102. Tu L, Guan R, Yang H, Zhou Y, Hong W, Ma L, et al. Assessment of the expression of the immune checkpoint molecules PD-1, CTLA4, TIM-3 and LAG-3 across different cancers in relation to treatment response, tumor-infiltrating immune cells and survival. Int J Cancer. 2020 Jul 15;147[2]:423–39.

103. Shayan G, Srivastava R, Li J, Schmitt N, Kane LP, Ferris RL. Adaptive resistance to anti-PD1 therapy by Tim-3 upregulation is mediated by the PI3K-Akt pathway in head and neck cancer. Oncoimmunology. 2017;6[1]:e1261779.

104. Koyama S, Akbay EA, Li YY, Herter-Sprie GS, Buczkowski KA, Richards WG, et al. Adaptive resistance to therapeutic PD-1 blockade is associated with upregulation of alternative immune checkpoints. Nat Commun. 2016 Feb 17;7[1]:10501.

105. The ICGC/TCGA Pan-Cancer Analysis of Whole Genomes Consortium, Aaltonen LA, Abascal F, Abeshouse A, Aburatani H, Adams DJ, et al. Pan-cancer analysis of whole genomes. Nature. 2020 Feb 6;578[7793]:82–93.

106. Tissue expression of FGL1 - Summary - The Human Protein Atlas [Internet]. [cited 2023 Sep 3]. Available from: https://www.proteinatlas.org/ENSG00000104760-FGL1/tissue#rna_expression

107. Kim AMJ, Nemeth MR, Lim SO. 4-1BB: A promising target for cancer immunotherapy. Front Oncol. 2022 Sep 14;12:968360.

108. Deleuze A, Saout J, Dugay F, Peyronnet B, Mathieu R, Verhoest G, et al. Immunotherapy in Renal Cell Carcinoma: The Future Is Now. IJMS. 2020 Apr 5;21[7]:2532.

109. Coy J, Caldwell A, Chow L, Guth A, Dow S. PD-1 expression by canine T cells and functional effects of PD-1 blockade: Canine PD-1 antibodies. Vet Comp Oncol. 2017 Dec;15[4]:1487–502.

110. Scharf VF, Farese JP, Coomer AR, Milner RJ, Taylor DP, Salute ME, et al. Effect of bevacizumab on angiogenesis and growth of canine osteosarcoma cells xenografted in athymic mice. ajvr. 2013 May;74[5]:771–8.

111. Maekawa N, Konnai S, Nishimura M, Kagawa Y, Takagi S, Hosoya K, et al. PD-L1 immunohistochemistry for canine cancers and clinical benefit of anti-PD-L1 antibody in dogs with pulmonary metastatic oral malignant melanoma. npj Precis Onc. 2021 Feb 12;5[1]:10.

112. Chand D, Dhawan D, Sankin A, Ren X, Lin J, Schoenberg M, et al. Immune Checkpoint B7x (B7-H4/B7S1/VTCN1) is Over Expressed in Spontaneous Canine Bladder Cancer: The First Report and its Implications in a Preclinical Model. BLC. 2019 Jan 31;5[1]:63–71.

113. Aresu L, Marconato L, Martini V, Fanelli A, Licenziato L, Foiani G, et al. Prognostic Value of PD-L1, PD-1 and CD8A in Canine Diffuse Large B-Cell Lymphoma Detected by RNAscope. Veterinary Sciences. 2021 Jun 29;8[7]:120.

114. Porcellato I, Brachelente C, Cappelli K, Menchetti L, Silvestri S, Sforna M, et al. FoxP3, CTLA-4, and IDO in Canine Melanocytic Tumors. Vet Pathol. 2021 Jan;58[1]:42–52.

115. Murakami K, Miyatake S, Miyamae J, Saeki K, Shinya M, Akashi N, et al. Expression profile of immunoregulatory factors in canine tumors. Veterinary Immunology and Immunopathology. 2022 Nov;253:110505.

116. Creelan BC, Antonia SJ. The NKG2A immune checkpoint — a new direction in cancer immunotherapy. Nat Rev Clin Oncol. 2019 May;16[5]:277–8.

117. Cazzetta V, Bruni E, Terzoli S, Carenza C, Franzese S, Piazza R, et al. NKG2A expression identifies a subset of human Vδ2 T cells exerting the highest antitumor effector functions. Cell Reports. 2021 Oct;37[3]:109871.

118. Van Velzen M, Laman JD, KleinJan A, Poot A, Osterhaus ADME, Verjans GMGM. Neuron-Interacting Satellite Glial Cells in Human Trigeminal Ganglia Have an APC Phenotype. The Journal of Immunology. 2009 Aug 15;183[4]:2456–61.

119. Wang L, Zhang Q, Chen W, Shan B, Ding Y, Zhang G, et al. B7-H3 is Overexpressed in Patients Suffering Osteosarcoma and Associated with Tumor Aggressiveness and Metastasis. Marie PJ, editor. PLoS ONE. 2013 Aug 5;8[8]:e70689.

120. Blank CU, Haanen JB, Ribas A, Schumacher TN. The "cancer immunogram." Science. 2016 May 6;352[6286]:658–60.

121. Smith JB, Stashwick C, Powell DJ. B7-H4 as a potential target for immunotherapy for gynecologic cancers: A closer look. Gynecologic Oncology. 2014 Jul;134[1]:181–9.

122. Tringler B, Liu W, Corral L, Torkko KC, Enomoto T, Davidson S, et al. B7-H4 overexpression in ovarian tumors. Gynecologic Oncology. 2006 Jan;100[1]:44–52.

123.   Wang L, Yang C, Liu X bo, Wang L, Kang F biao. B7-H4 overexpression contributes to poor prognosis and drug-resistance in triple-negative breast cancer. Cancer Cell Int. 2018 Dec;18[1]:100.

124.   Han S, Li Y, Zhang J, Liu L, Chen Q, Qian Q, et al. Roles of immune inhibitory molecule B7-H4 in cervical cancer. Oncology Reports. 2017 Mar;37[4]:2308–16.

125.   Tringler B, Zhuo S, Pilkington G, Torkko KC, Singh M, Lucia MS, et al. B7-H4 Is Highly Expressed in Ductal and Lobular Breast Cancer. Clinical Cancer Research. 2005 Mar 1;11[5]:1842–8.

126.   Mersana Therapeutics. A Phase 1, First-in-human, Dose Escalation and Expansion, Multicenter Study of XMT-1660 in Participants With Solid Tumors [Internet]. clinicaltrials.gov; 2023 Aug [cited 2023 Sep 1]. Report No.: NCT05377996. Available from: https://clinicaltrials.gov/study/NCT05377996

127.   Beavis PA, Milenkovski N, Henderson MA, John LB, Allard B, Loi S, et al. Adenosine Receptor 2A Blockade Increases the Efficacy of Anti–PD-1 through Enhanced Antitumor T-cell Responses. Cancer Immunology Research. 2015 May 1;3[5]:506–17.

128.   Pantelyushin S, Ranninger E, Guerrera D, Hutter G, Maake C, Markkanen E, et al. Cross-Reactivity and Functionality of Approved Human Immune Checkpoint Blockers in Dogs. Cancers. 2021 Feb 13;13[4]:785.

129.   Reches A, Ophir Y, Stein N, Kol I, Isaacson B, Charpak Amikam Y, et al. Nectin4 is a novel TIGIT ligand which combines checkpoint inhibition and tumor specificity. J Immunother Cancer. 2020 Jun;8[1]:e000266.

130.   Nocentini G, Ronchetti S, Petrillo MG, Riccardi C. Pharmacological modulation of GITRL/GITR system: therapeutic perspectives: GITRL/GITR system: therapeutic perspectives. British Journal of Pharmacology. 2012 Apr;165[7]:2089–99.

131.   Sansom DM. CD28, CTLA-4 and their ligands: who does what and to whom?: The effects of CD28 and CTLA-4 ligands. Immunology. 2000 Oct;101[2]:169–77.

132.   Nicolet BP, Salerno F, Wolkers MC. Visualizing the life of mRNA in T cells. Biochemical Society Transactions. 2017 Apr 15;45[2]:563–70.

133.   Mattei F, Andreone S, Spadaro F, Noto F, Tinari A, Falchi M, et al. Trogocytosis in innate immunity to cancer is an intimate relationship with unexpected outcomes. iScience. 2022 Oct;25[10]:105110.

134.   O'Neill JR, Mayordomo MY, Mitulović G, Al Shboul S, Bedran G, Faktor J, et al. Multi-omics integration in Esophageal Adenocarcinoma reveals therapeutic targets and EAC-specific regulation of protein abundances [Internet]. Genetic and Genomic Medicine; 2022 Nov [cited 2023 Sep 3]. Available from: http://medrxiv.org/lookup/doi/10.1101/2022.11.24.22281691

135.   Taher L, Beck J, Liu W, Roolf C, Soller JT, Rütgen BC, et al. Comparative High-Resolution Transcriptome Sequencing of Lymphoma Cell Lines and de novo

Lymphomas Reveals Cell-Line-Specific Pathway Dysregulation. Sci Rep. 2018 Apr 19;8[1]:6279.

136.   Harris LJ, Hughes KL, Ehrhart EJ, Labadie JD, Yoshimoto J, Avery AC. Canine CD4+ T-cell lymphoma identified by flow cytometry exhibits a consistent histomorphology and gene expression profile. Vet Comp Oncol. 2019 Sep;17[3]:253–64.

137.   ICDC [Internet]. [cited 2023 Sep 3]. Available from: https://caninecommons.cancer.gov/#/study/NCATS-COP01

138.   Amin SB, Anderson KJ, Boudreau CE, Martinez-Ledesma E, Kocakavuk E, Johnson KC, et al. Comparative Molecular Life History of Spontaneous Canine and Human Gliomas. Cancer Cell. 2020 Feb;37[2]:243-257.e7.

139.   Megquier K, Turner-Maier J, Swofford R, Kim JH, Sarver AL, Wang C, et al. Comparative Genomics Reveals Shared Mutational Landscape in Canine Hemangiosarcoma and Human Angiosarcoma. Molecular Cancer Research. 2019 Dec 1;17[12]:2410–21.

140.   Gorden BH, Kim JH, Sarver AL, Frantz AM, Breen M, Lindblad-Toh K, et al. Identification of Three Molecular and Functional Subtypes in Canine Hemangiosarcoma through Gene Expression Profiling and Progenitor Cell Characterization. The American Journal of Pathology. 2014 Apr;184[4]:985–95.

141.   Dhawan D, Hahn NM, Ramos-Vara JA, Knapp DW. Naturally-occurring canine invasive urothelial carcinoma harbors luminal and basal transcriptional subtypes found in human muscle invasive bladder cancer. Knowles MA, editor. PLoS Genet. 2018 Aug 8;14[8]:e1007571.

142.   Kim KK, Seung BJ, Kim D, Park HM, Lee S, Song DW, et al. Whole-exome and whole-transcriptome sequencing of canine mammary gland tumors. Sci Data. 2019 Aug 14;6[1]:147.

143.   Scott MC, Temiz NA, Sarver AE, LaRue RS, Rathe SK, Varshney J, et al. Comparative Transcriptome Analysis Quantifies Immune Cell Transcript Levels, Metastatic Progression, and Survival in Osteosarcoma. Cancer Research. 2018 Jan 15;78[2]:326–37.

144.   Peralta S, McCleary-Wheeler AL, Duhamel GE, Heikinheimo K, Grenier JK. Ultra-frequent *HRAS* p.Q61R somatic mutation in canine acanthomatous ameloblastoma reveals pathogenic similarities with human ameloblastoma. Vet Comp Oncol. 2019 Sep;17[3]:439–45.

145.   Capodanno Y, Buishand FO, Pang LY, Kirpensteijn J, Mol JA, Elders R, et al. Transcriptomic analysis by RNA sequencing characterises malignant progression of canine insulinoma from normal tissue to metastatic disease. Sci Rep. 2020 Jul 14;10[1]:11581.

146.   Grenier JK, Foureman PA, Sloma EA, Miller AD. RNA-seq transcriptome analysis of formalin fixed, paraffin-embedded canine meningioma. Thamm D, editor. PLoS ONE. 2017 Oct 26;12[10]:e0187150.

147.   Guscetti F, Nassiri S, Beebe E, Rito Brandao I, Graf R, Markkanen E. Molecular homology between canine spontaneous oral squamous cell carcinomas and human head-and-neck squamous cell carcinomas reveals disease drivers and therapeutic vulnerabilities. Neoplasia. 2020 Dec;22[12]:778–88.

148.   Thiemeyer H, Taher L, Schille JT, Harder L, Hungerbuehler SO, Mischke R, et al. Suitability of ultrasound-guided fine-needle aspiration biopsy for transcriptome sequencing of the canine prostate. Sci Rep. 2019 Sep 13;9[1]:13216.

149.   FastQC [Internet]. 2015. Available from: https://qubeshub.org/resources/fastqc

150.   Ewels P, Magnusson M, Lundin S, Käller M. MultiQC: summarize analysis results for multiple tools and samples in a single report. Bioinformatics. 2016 Oct 1;32[19]:3047–8.

151.   Bray NL, Pimentel H, Melsted P, Pachter L. Near-optimal probabilistic RNA-seq quantification. Nat Biotechnol. 2016 May;34[5]:525–7.

152.   Lawrence M, Huber W, Pagès H, Aboyoun P, Carlson M, Gentleman R, et al. Software for Computing and Annotating Genomic Ranges. Prlic A, editor. PLoS Comput Biol. 2013 Aug 8;9[8]:e1003118.

153.   Soneson C, Love MI, Robinson MD. Differential analyses for RNA-seq: transcript-level estimates improve gene-level inferences. F1000Res. 2015 Dec 30;4:1521.

154.   Love MI, Huber W, Anders S. Moderated estimation of fold change and dispersion for RNA-seq data with DESeq2. Genome Biol. 2014 Dec;15[12]:550.

155.   Wickham H. ggplot2: Elegant Graphics for Data Analysis [Internet]. New York, NY: Springer; 2009 [cited 2023 Sep 3]. Available from: https://link.springer.com/10.1007/978-0-387-98141-3

156.   Garnier S, Ross N, BoB Rudis, Filipovic-Pierucci A, Galili T, Timelyportfolio, et al. sjmgarnier/viridis: CRAN release v0.6.3 [Internet]. Zenodo; 2023 [cited 2023 Sep 3]. Available from: https://zenodo.org/record/4679423

157.   O'Connell P, Hyslop S, Blake MK, Godbehere S, Amalfitano A, Aldhamen YA. SLAMF7 Signaling Reprograms T Cells toward Exhaustion in the Tumor Microenvironment. The Journal of Immunology. 2021 Jan 1;206[1]:193–205.

158.   Danaher P, Warren S, Dennis L, D'Amico L, White A, Disis ML, et al. Gene expression markers of Tumor Infiltrating Leukocytes. j immunotherapy cancer. 2017 Dec;5[1]:18.

159.   Uhlén M, Fagerberg L, Hallström BM, Lindskog C, Oksvold P, Mardinoglu A, et al. Tissue-based map of the human proteome. Science. 2015 Jan 23;347[6220]:1260419.

160.   Jensen LJ, Kuhn M, Stark M, Chaffron S, Creevey C, Muller J, et al. STRING 8--a global view on proteins and their functional interactions in 630 organisms. Nucleic Acids Research. 2009 Jan 1;37[Database]:D412–6.

161.   Hubbard ME, Arnold S, Bin Zahid A, McPheeters M, Gerard O'Sullivan M, Tabaran AF, et al. Naturally Occurring Canine Glioma as a Model for Novel Therapeutics. Cancer Investigation. 2018 Sep 14;36[8]:415–23.

162.   Ammons DT, Guth A, Rozental AJ, Kurihara J, Marolf AJ, Chow L, et al. Reprogramming the Canine Glioma Microenvironment with Tumor Vaccination plus Oral Losartan and Propranolol Induces Objective Responses. Cancer Research Communications. 2022 Dec 19;2[12]:1657–67.

163.   Boudreau CE, Najem H, Ott M, Horbinski C, Fang D, DeRay CM, et al. Intratumoral Delivery of STING Agonist Results in Clinical Responses in Canine Glioblastoma. Clinical Cancer Research. 2021 Oct 15;27[20]:5528–35.

164.   Koehler JW, Miller AD, Miller CR, Porter B, Aldape K, Beck J, et al. A Revised Diagnostic Classification of Canine Glioma: Towards Validation of the Canine Glioma Patient as a Naturally Occurring Preclinical Model for Human Glioma. Journal of Neuropathology & Experimental Neurology. 2018 Nov 1;77[11]:1039–54.

165.   Olin M, Ampudia-Mesias E, Pennell C, Sarver A, Chen C, Moertel C, et al. Treatment Combining CD200 Immune Checkpoint Inhibitor and Tumor-Lysate Vaccination after Surgery for Pet Dogs with High-Grade Glioma. Cancers. 2019 Jan 24;11[2]:137.

166.   Yu MW, Quail DF. Immunotherapy for Glioblastoma: Current Progress and Challenges. Front Immunol. 2021 May 13;12:676301.

167.   Lim M, Xia Y, Bettegowda C, Weller M. Current state of immunotherapy for glioblastoma. Nat Rev Clin Oncol. 2018 Jul;15[7]:422–42.

168.   Kamran N, Calinescu A, Candolfi M, Chandran M, Mineharu Y, Asad AS, et al. Recent advances and future of immunotherapy for glioblastoma. Expert Opinion on Biological Therapy. 2016 Oct 2;16[10]:1245–64.

169.   Khasraw M, Reardon DA, Weller M, Sampson JH. PD-1 Inhibitors: Do they have a Future in the Treatment of Glioblastoma? Clinical Cancer Research. 2020 Oct 15;26[20]:5287–96.

170.   Gromeier M, Brown MC, Zhang G, Lin X, Chen Y, Wei Z, et al. Very low mutation burden is a feature of inflamed recurrent glioblastomas responsive to cancer immunotherapy. Nat Commun. 2021 Jan 13;12[1]:352.

171.   Brown MC, Ashley DM, Khasraw M. Low tumor mutational burden and immunotherapy in gliomas. Trends in Cancer. 2022 May;8[5]:345–6.

172.   Bod L, Kye YC, Shi J, Torlai Triglia E, Schnell A, Fessler J, et al. B-cell-specific checkpoint molecules that regulate anti-tumour immunity. Nature. 2023 Jul 13;619[7969]:348–56.

173.   Lim JX, Lai CY, Mallett GE, McDonald D, Hulme G, Laba S, et al. Programmed cell death-1 receptor-mediated regulation of Tbet $^+$ NK1.1 $^-$ innate lymphoid cells within the tumor microenvironment. Proc Natl Acad Sci USA. 2023 May 2;120[18]:e2216587120.

174.   Tissue expression of SIRPA - Summary - The Human Protein Atlas [Internet]. [cited 2023 Sep 3]. Available from: https://www.proteinatlas.org/ENSG00000198053-SIRPA/tissue

175.   The Human Protein Atlas [Internet]. [cited 2023 Sep 3]. Available from: https://www.proteinatlas.org/

176.   Hu J, Xiao Q, Dong M, Guo D, Wu X, Wang B. Glioblastoma Immunotherapy Targeting the Innate Immune Checkpoint CD47-SIRPα Axis. Front Immunol. 2020 Nov 27;11:593219.

177.   Hutter G, Theruvath J, Graef CM, Zhang M, Schoen MK, Manz EM, et al. Microglia are effector cells of CD47-SIRPα antiphagocytic axis disruption against glioblastoma. Proc Natl Acad Sci USA. 2019 Jan 15;116[3]:997–1006.

178.   Kuo TC, Chen A, Harrabi O, Sockolosky JT, Zhang A, Sangalang E, et al. Targeting the myeloid checkpoint receptor SIRPα potentiates innate and adaptive immune responses to promote anti-tumor activity. J Hematol Oncol. 2020 Dec;13[1]:160.

179.   Sim J, Sockolosky JT, Sangalang E, Izquierdo S, Pedersen D, Harriman W, et al. Discovery of high affinity, pan-allelic, and pan-mammalian reactive antibodies against the myeloid checkpoint receptor SIRPα. mAbs. 2019 Aug 18;11[6]:1036–52.

180.   Maekawa N, Konnai S, Ikebuchi R, Okagawa T, Adachi M, Takagi S, et al. Expression of PD-L1 on Canine Tumor Cells and Enhancement of IFN-γ Production from Tumor-Infiltrating Cells by PD-L1 Blockade. Shiku H, editor. PLoS ONE. 2014 Jun 10;9[6]:e98415.

181.   Maekawa N, Konnai S, Okagawa T, Nishimori A, Ikebuchi R, Izumi Y, et al. Immunohistochemical Analysis of PD-L1 Expression in Canine Malignant Cancers and PD-1 Expression on Lymphocytes in Canine Oral Melanoma. Shiku H, editor. PLoS ONE. 2016 Jun 8;11[6]:e0157176.

182.   Choi JW, Withers SS, Chang H, Spanier JA, De La Trinidad VL, Panesar H, et al. Development of canine PD-1/PD-L1 specific monoclonal antibodies and amplification of canine T cell function. Ho M, editor. PLoS ONE. 2020 Jul 2;15[7]:e0235518.

183.   Maekawa N, Konnai S, Takagi S, Kagawa Y, Okagawa T, Nishimori A, et al. A canine chimeric monoclonal antibody targeting PD-L1 and its clinical efficacy in canine oral malignant melanoma or undifferentiated sarcoma. Sci Rep. 2017 Aug 21;7[1]:8951.

184.   Oh W, Kim AMJ, Dhawan D, Kirkham PM, Ostafe R, Franco J, et al. Development of an Anti-canine PD-L1 Antibody and Caninized PD-L1 Mouse

Model as Translational Research Tools for the Study of Immunotherapy in Humans. Cancer Research Communications. 2023 May 15;3[5]:860–73.

185.   Nemoto Y, Shosu K, Okuda M, Noguchi S, Mizuno T. Development and characterization of monoclonal antibodies against canine PD-1 and PD-L1. Veterinary Immunology and Immunopathology. 2018 Apr;198:19–25.

186.   Minoli L, Licenziato L, Kocikowski M, Cino M, Dziubek K, Iussich S, et al. Development of Monoclonal Antibodies Targeting Canine PD-L1 and PD-1 and Their Clinical Relevance in Canine Apocrine Gland Anal Sac Adenocarcinoma. Cancers. 2022 Dec 14;14[24]:6188.

187.   Bradbury ARM, Trinklein ND, Thie H, Wilkinson IC, Tandon AK, Anderson S, et al. When monoclonal antibodies are not monospecific: Hybridomas frequently express additional functional variable regions. mAbs. 2018 May 19;10[4]:539–46.

188.   Spira G, Yuan R, Paizi M, Weisendal M, Casadevall A. Simultaneous expression of kappa and lambda light chains in a murine IgG3 anti-Cryptococcus neoformans hybridoma cell line. Hybridoma. 1994 Dec;13[6]:531–5.

189.   Ciftci O, Müller LM, Jäggle LM, Lehmann C, Kneilmann C, Stierstorfer B, et al. Cross-reactivity of human monoclonal antibodies with canine peripheral blood mononuclear cells. Veterinary Immunology and Immunopathology. 2023 May;259:110578.

190.   Nugue G, Bidart M, Arlotto M, Mousseau M, Berger F, Pelletier L. Monitoring Monoclonal Antibody Delivery in Oncology: The Example of Bevacizumab. Rota R, editor. PLoS ONE. 2013 Aug 12;8[8]:e72021.

191.   Watanabe E, Nishida O, Kakihana Y, Odani M, Okamura T, Harada T, et al. Pharmacokinetics, Pharmacodynamics, and Safety of Nivolumab in Patients With Sepsis-Induced Immunosuppression: A Multicenter, Open-Label Phase 1/2 Study. Shock. 2020 Jun;53[6]:686–94.

192.   Sureda M, Mata JJ, Catalán A, Escudero V, Martínez-Navarro E, Rebollo J. Therapeutic drug monitoring of nivolumab in routine clinical practice. A pilot study. Farm Hosp. 2020 Apr 17;44[3]:81–6.

193.   Zak KM, Kitel R, Przetocka S, Golik P, Guzik K, Musielak B, et al. Structure of the Complex of Human Programmed Death 1, PD-1, and Its Ligand PD-L1. Structure. 2015 Dec 1;23[12]:2341–8.

194.   Tan S, Zhang H, Chai Y, Song H, Tong Z, Wang Q, et al. An unexpected N-terminal loop in PD-1 dominates binding by nivolumab. Nat Commun. 2017 Feb 6;8[1]:14369.

195.   Na Z, Yeo SP, Bharath SR, Bowler MW, Balıkçi E, Wang CI, et al. Structural basis for blocking PD-1-mediated immune suppression by therapeutic antibody pembrolizumab. Cell Res. 2017 Jan;27[1]:147–50.

196.   Igase M, Nemoto Y, Itamoto K, Tani K, Nakaichi M, Sakurai M, et al. A pilot clinical study of the therapeutic antibody against canine PD-1 for advanced spontaneous cancers in dogs. Sci Rep. 2020 Oct 27;10[1]:18311.

197.   Sun L, Li CW, Chung EM, Yang R, Kim YS, Park AH, et al. Targeting Glycosylated PD-1 Induces Potent Antitumor Immunity. Cancer Research. 2020 Jun 1;80[11]:2298–310.

198.   Banna GL, Cantale O, Bersanelli M, Del Re M, Friedlaender A, Cortellini A, et al. Are anti-PD1 and anti-PD-L1 alike? The non-small-cell lung cancer paradigm. Oncol Rev [Internet]. 2020 Jul 21 [cited 2023 Sep 3];14[2]. Available from: https://www.frontierspartnerships.org/articles/10.4081/oncol.2020.490

199.   Sonpavde GP, Grivas P, Lin Y, Hennessy D, Hunt JD. Immune-related adverse events with PD-1 versus PD-L1 inhibitors: a meta-analysis of 8730 patients from clinical trials. Future Oncology. 2021 Jul;17[19]:2545–58.

200.   Butte MJ, Keir ME, Phamduy TB, Sharpe AH, Freeman GJ. Programmed Death-1 Ligand 1 Interacts Specifically with the B7-1 Costimulatory Molecule to Inhibit T Cell Responses. Immunity. 2007 Jul;27[1]:111–22.

201.   Xiao Y, Yu S, Zhu B, Bedoret D, Bu X, Francisco LM, et al. RGMb is a novel binding partner for PD-L2 and its engagement with PD-L2 promotes respiratory tolerance. Journal of Experimental Medicine. 2014 May 5;211[5]:943–59.

202.   Sugiura D, Okazaki IM, Maeda TK, Maruhashi T, Shimizu K, Arakaki R, et al. PD-1 agonism by anti-CD80 inhibits T cell activation and alleviates autoimmunity. Nat Immunol. 2022 Mar;23[3]:399–410.

203.   Kwok G, Yau TCC, Chiu JW, Tse E, Kwong YL. Pembrolizumab (Keytruda). Human Vaccines & Immunotherapeutics. 2016 Nov;12[11]:2777–89.

204.   Whiteside TL. The tumor microenvironment and its role in promoting tumor growth. Oncogene. 2008 Oct 6;27[45]:5904–12.

205.   Lin Y, Xu J, Lan H. Tumor-associated macrophages in tumor metastasis: biological roles and clinical therapeutic applications. J Hematol Oncol. 2019 Dec;12[1]:76.

206.   Li C, Jiang P, Wei S, Xu X, Wang J. Regulatory T cells in tumor microenvironment: new mechanisms, potential therapeutic strategies and future prospects. Mol Cancer. 2020 Dec;19[1]:116.

207.   Yearley JH, Gibson C, Yu N, Moon C, Murphy E, Juco J, et al. PD-L2 Expression in Human Tumors: Relevance to Anti-PD-1 Therapy in Cancer. Clinical Cancer Research. 2017 Jun 15;23[12]:3158–67.

208.   Solinas C, Aiello M, Rozali E, Lambertini M, Willard-Gallo K, Migliori E. Programmed cell death-ligand 2: A neglected but important target in the immune response to cancer? Translational Oncology. 2020 Oct;13[10]:100811.

209.   Miao YR, Thakkar KN, Qian J, Kariolis MS, Huang W, Nandagopal S, et al. Neutralization of PD-L2 is Essential for Overcoming Immune Checkpoint Blockade Resistance in Ovarian Cancer. Clinical Cancer Research. 2021 Aug 1;27[15]:4435–48.

210.   Ghiotto M, Gauthier L, Serriari N, Pastor S, Truneh A, Nunes JA, et al. PD-L1 and PD-L2 differ in their molecular mechanisms of interaction with PD-1. International Immunology. 2010 Aug 1;22[8]:651–60.

211.   Donini C, D'Ambrosio L, Grignani G, Aglietta M, Sangiolo D. Next generation immune-checkpoints for cancer therapy. J Thorac Dis. 2018 May;10[S13]:S1581–601.

212.   Nielsen C, Ohm-Laursen L, Barington T, Husby S, Lillevang ST. Alternative splice variants of the human PD-1 gene. Cellular Immunology. 2005 Jun;235[2]:109–16.

213.   Hajaj E, Zisman E, Tzaban S, Merims S, Cohen J, Klein S, et al. Alternative Splicing of the Inhibitory Immune Checkpoint Receptor SLAMF6 Generates a Dominant Positive Form, Boosting T-cell Effector Functions. Cancer Immunology Research. 2021 Jun 1;9[6]:637–50.

214.   Hassounah NB, Malladi VS, Huang Y, Freeman SS, Beauchamp EM, Koyama S, et al. Identification and characterization of an alternative cancer-derived PD-L1 splice variant. Cancer Immunol Immunother. 2019 Mar;68[3]:407–20.

215.   Qu S, Jiao Z, Lu G, Yao B, Wang T, Rong W, et al. PD-L1 lncRNA splice isoform promotes lung adenocarcinoma progression via enhancing c-Myc activity. Genome Biol. 2021 Dec;22[1]:104.

216.   Oku T, Ando Y, Ogura M, Tsuji T. Development of Splice Variant-Specific Monoclonal Antibodies Against Human α3 Integrin. Monoclonal Antibodies in Immunodiagnosis and Immunotherapy. 2016 Feb;35[1]:12–7.

217.   Bradbury A. Cloning Hybridoma cDNA by RACE. In: Antibody Engineering.

218.   Stothard P. The Sequence Manipulation Suite: JavaScript Programs for Analyzing and Formatting Protein and DNA Sequences. BioTechniques. 2000 Jun;28[6]:1102–4.

219.   AAT Bioquest Inc. IC50 Calculator [Internet]. 2023. Available from: https://www.aatbio.com/tools/ic50-calculator

220.   Abanades B, Wong WK, Boyles F, Georges G, Bujotzek A, Deane CM. ImmuneBuilder: Deep-Learning models for predicting the structures of immune proteins. Commun Biol. 2023 May 29;6[1]:1–8.

221.   Sievers F, Wilm A, Dineen D, Gibson TJ, Karplus K, Li W, et al. Fast, scalable generation of high-quality protein multiple sequence alignments using Clustal Omega. Mol Syst Biol. 2011 Oct 11;7:539.

222. InterPro in 2022 | Nucleic Acids Research | Oxford Academic [Internet]. [cited 2023 Sep 30]. Available from: https://academic.oup.com/nar/article/51/D1/D418/6814474

223. Kelley LA, Mezulis S, Yates CM, Wass MN, Sternberg MJE. The Phyre2 web portal for protein modeling, prediction and analysis. Nat Protoc. 2015 Jun;10[6]:845–58.

224. Vajda S, Yueh C, Beglov D, Bohnuud T, Mottarella SE, Xia B, et al. New additions to the ClusPro server motivated by CAPRI. Proteins. 2017 Mar;85[3]:435–44.

225. Brenke R, Hall DR, Chuang GY, Comeau SR, Bohnuud T, Beglov D, et al. Application of asymmetric statistical potentials to antibody-protein docking. Bioinformatics. 2012 Oct 15;28[20]:2608–14.

226. Brunger AT, Wells JA. Warren L. DeLano 21 June 1972–3 November 2009. Nat Struct Mol Biol. 2009 Dec;16[12]:1202–3.

227. Krissinel E, Henrick K. Inference of macromolecular assemblies from crystalline state. J Mol Biol. 2007 Sep 21;372[3]:774–97.

228. SignalP 5.0 improves signal peptide predictions using deep neural networks | Nature Biotechnology [Internet]. [cited 2023 Sep 3]. Available from: https://www.nature.com/articles/s41587-019-0036-z

229. Smith SR, Schaaf K, Rajabalee N, Wagner F, Duverger A, Kutsch O, et al. The phosphatase PPM1A controls monocyte-to-macrophage differentiation. Sci Rep. 2018 Jan 17;8[1]:902.

230. Lo Russo G, Moro M, Sommariva M, Cancila V, Boeri M, Centonze G, et al. Antibody–Fc/FcR Interaction on Macrophages as a Mechanism for Hyperprogressive Disease in Non–small Cell Lung Cancer Subsequent to PD-1/PD-L1 Blockade. Clinical Cancer Research. 2019 Feb 1;25[3]:989–99.

231. Bergeron LM, McCandless EE, Dunham S, Dunkle B, Zhu Y, Shelly J, et al. Comparative functional characterization of canine IgG subclasses. Veterinary Immunology and Immunopathology. 2014 Jan;157[1–2]:31–41.

232. Michels GM, Walsh KF, Kryda KA, Mahabir SP, Walters RR, Hoevers JD, et al. A blinded, randomized, placebo-controlled trial of the safety of lokivetmab (ZTS-00103289), a caninized anti-canine IL-31 monoclonal antibody in client-owned dogs with atopic dermatitis. Veterinary Dermatology. 2016;27[6]:505-e136.

233. Waterhouse A, Bertoni M, Bienert S, Studer G, Tauriello G, Gumienny R, et al. SWISS-MODEL: homology modelling of protein structures and complexes. Nucleic Acids Res. 2018 Jul 2;46[W1]:W296–303.

234. Li M, Zhao R, Chen J, Tian W, Xia C, Liu X, et al. Next generation of anti-PD-L1 Atezolizumab with enhanced anti-tumor efficacy in vivo. Sci Rep. 2021 Mar 11;11:5774.

235.   Lo BKC. Antibody Engineering [Internet]. Vol. 248. New Jersey: Humana Press; 2003 [cited 2023 Sep 17]. Available from: http://link.springer.com/10.1385/1592596665

236.   World Health Organization. World Health Organization model list of essential medicines: 21st list 2019 [Internet]. World Health Organization; 2019 [cited 2023 Sep 17]. Report No.: WHO/MVP/EMP/IAU/2019.06. Available from: https://apps.who.int/iris/handle/10665/325771

237.   Rossotti MA, Bélanger K, Henry KA, Tanha J. Immunogenicity and humanization of single-domain antibodies. The FEBS Journal. 2022;289[14]:4304–27.

238.   Getts DR, Getts MT, McCarthy DP, Chastain EM, Miller SD. Have we overestimated the benefit of human(ized) antibodies? MAbs. 2010;2[6]:682–94.

239.   Beirão BCB. THE DEVELOPMENT OF ANTIBODIES AGAINST THE CANINE CSF-1R.

240.   Harding FA, Stickler MM, Razo J, DuBridge R. The immunogenicity of humanized and fully human antibodies. mAbs. 2010 May 1;2[3]:256–65.

241.   Clark M. Antibody humanization: a case of the "Emperor's new clothes"? Immunol Today. 2000 Aug;21[8]:397–402.

242.   Abhinandan KR, Martin ACR. Analyzing the "Degree of Humanness" of Antibody Sequences. Journal of Molecular Biology. 2007 Jun 8;369[3]:852–62.

243.   Gao SH, Huang K, Tu H, Adler AS. Monoclonal antibody humanness score and its applications. BMC Biotechnol. 2013 Jul 5;13:55.

244.   Doevendans E, Schellekens H. Immunogenicity of Innovative and Biosimilar Monoclonal Antibodies. Antibodies. 2019 Mar;8[1]:21.

245.   Waldmann H. Human monoclonal antibodies: the residual challenge of antibody immunogenicity. Methods Mol Biol. 2014;1060:1–8.

246.   Devulapally PR, Bürger J, Mielke T, Konthur Z, Lehrach H, Yaspo ML, et al. Simple paired heavy- and light-chain antibody repertoire sequencing using endoplasmic reticulum microsomes. Genome Medicine. 2018 Apr 27;10[1]:34.

247.   DeKosky BJ, Kojima T, Rodin A, Charab W, Ippolito GC, Ellington AD, et al. In-depth determination and analysis of the human paired heavy- and light-chain antibody repertoire. Nat Med. 2015 Jan;21[1]:86–91.

248.   Abhinandan KR, Martin ACR. Analysis and prediction of VH/VL packing in antibodies. Protein Eng Des Sel. 2010 Sep;23[9]:689–97.

249.   Dondelinger M, Filée P, Sauvage E, Quinting B, Muyldermans S, Galleni M, et al. Understanding the Significance and Implications of Antibody Numbering and Antigen-Binding Surface/Residue Definition. Frontiers in Immunology [Internet].

2018 [cited 2023 Sep 17];9. Available from: https://www.frontiersin.org/articles/10.3389/fimmu.2018.02278

250. Antibody numbering schemes and CDR definitions [Internet]. [cited 2023 Sep 17]. Available from: https://pipebio.com/blog/antibody-numbering

251. Kabat EA, Wu TT, Bilofsky H. Sequences of immunoglobulin chains: tabulation and analysis of amino acid sequences of precursors, V-regions, C-regions, J-chain and 2-microglobulins. National Institute of Health; 1979.

252. IMGT Index [Internet]. [cited 2023 Sep 17]. Available from: https://www.imgt.org/IMGTindex/numbering.php

253. Chothia C, Lesk AM. Canonical structures for the hypervariable regions of immunoglobulins. J Mol Biol. 1987 Aug 20;196[4]:901–17.

254. bioinf.org.uk - Prof. Andrew C.R. Martin's group at UCL [Internet]. [cited 2023 Sep 17]. Available from: http://www.bioinf.org.uk/abs/info.html

255. Honegger A, Plückthun A. Yet another numbering scheme for immunoglobulin variable domains: an automatic modeling and analysis tool. J Mol Biol. 2001 Jun 8;309[3]:657–70.

256. Vattekatte AM, Shinada NK, Narwani TJ, Noël F, Bertrand O, Meyniel JP, et al. Discrete analysis of camelid variable domains: sequences, structures, and in-silico structure prediction. PeerJ. 2020 Mar 6;8:e8408.

257. ABlooper: fast accurate antibody CDR loop structure prediction with accuracy estimation | Bioinformatics | Oxford Academic [Internet]. [cited 2023 Sep 17]. Available from: https://academic.oup.com/bioinformatics/article/38/7/1877/6517780

258. Wong WK, Georges G, Ros F, Kelm S, Lewis AP, Taddese B, et al. SCALOP: sequence-based antibody canonical loop structure annotation. Bioinformatics. 2019 May 15;35[10]:1774–6.

259. Dunbar J, Deane CM. ANARCI: antigen receptor numbering and receptor classification. Bioinformatics. 2016 Jan 15;32[2]:298–300.

260. Swindells MB, Porter CT, Couch M, Hurst J, Abhinandan KR, Nielsen JH, et al. abYsis: Integrated Antibody Sequence and Structure-Management, Analysis, and Prediction. J Mol Biol. 2017 Feb 3;429[3]:356–64.

261. Lundegaard C, Lamberth K, Harndahl M, Buus S, Lund O, Nielsen M. NetMHC-3.0: accurate web accessible predictions of human, mouse and monkey MHC class I affinities for peptides of length 8-11. Nucleic Acids Res. 2008 Jul 1;36[Web Server issue]:W509-512.

262. Prihoda D, Maamary J, Waight A, Juan V, Fayadat-Dilman L, Svozil D, et al. BioPhi: A platform for antibody design, humanization, and humanness evaluation based on natural antibody repertoires and deep learning. MAbs. 2022;14[1]:2020203.

263.   Gearing DP, Virtue ER, Gearing RP, Drew AC. A fully caninised anti-NGF monoclonal antibody for pain relief in dogs. BMC Vet Res. 2013 Nov 9;9:226.

264.   Bergeron LM, McCandless EE, Dunham S, Dunkle B, Zhu Y, Shelly J, et al. Comparative functional characterization of canine IgG subclasses. Vet Immunol Immunopathol. 2014 Jan 15;157[1–2]:31–41.

265.   Aratana Therapeutics Provides Product Updates [Internet]. Aratana Therapeutics - InvestorRoom. [cited 2023 Sep 4]. Available from: https://www.aratana.com

266.   Gearing DP, Huebner M, Virtue ER, Knight K, Hansen P, Lascelles BDX, et al. In Vitro and In Vivo Characterization of a Fully Felinized Therapeutic Anti-Nerve Growth Factor Monoclonal Antibody for the Treatment of Pain in Cats. J Vet Intern Med. 2016 Jul;30[4]:1129–37.

267.   Bustamante-Córdova L, Melgoza-González EA, Hernández J. Recombinant Antibodies in Veterinary Medicine: An Update. Front Vet Sci. 2018 Jul 27;5:175.

268.   Enomoto M, Mantyh PW, Murrell J, Innes JF, Lascelles BDX. Anti-nerve growth factor monoclonal antibodies for the control of pain in dogs and cats. Veterinary Record. 2019;184[1]:23–23.

269.   Maeda S, Motegi T, Iio A, Kaji K, Goto-Koshino Y, Eto S, et al. Anti-CCR4 treatment depletes regulatory T cells and leads to clinical activity in a canine model of advanced prostate cancer. J Immunother Cancer. 2022 Jan 31;10[2]:e003731.

270.   Xu S, Xie J, Wang S, Tang N, Feng J, Su Y, et al. Reversing stage III oral adenocarcinoma in a dog treated with anti-canine PD-1 therapeutic antibody: a case report. Frontiers in Veterinary Science [Internet]. 2023 [cited 2023 Sep 4];10. Available from: https://www.frontiersin.org/articles/10.3389/fvets.2023.1144869

271.   Krautmann M, Walters R, Cole P, Tena J, Bergeron LM, Messamore J, et al. Laboratory safety evaluation of bedinvetmab, a canine anti-nerve growth factor monoclonal antibody, in dogs. The Veterinary Journal. 2021 Oct 1;276:105733.

272.   Corral MJ, Moyaert H, Fernandes T, Escalada M, Kira S Tena J, Walters RR, et al. A prospective, randomized, blinded, placebo-controlled multisite clinical study of bedinvetmab, a canine monoclonal antibody targeting nerve growth factor, in dogs with osteoarthritis. Veterinary Anaesthesia and Analgesia. 2021 Nov 1;48[6]:943–55.

273.   Singer J, Fazekas J, Wang W, Weichselbaumer M, Matz M, Mader A, et al. Generation of a canine anti-EGFR (ErbB-1) antibody for passive immunotherapy in dog cancer patients. Mol Cancer Ther. 2014 Jul;13[7]:1777–90.

274.   Fazekas-Singer J, Berroterán-Infante N, Rami-Mark C, Dumanic M, Matz M, Willmann M, et al. Development of a radiolabeled caninized anti-EGFR antibody for comparative oncology trials. Oncotarget. 2017 Sep 15;8[47]:83128–41.

275.   Mason NJ, Chester N, Xiong A, Rotolo A, Wu Y, Yoshimoto S, et al. Development of a fully canine anti-canine CTLA4 monoclonal antibody for comparative translational research in dogs with spontaneous tumors. mAbs. 2021 Jan 1;13[1]:2004638.

276.   Anti-Canine MS4A1 Recombinant Antibody (Blontuvetmab) - Creative Biolabs [Internet]. [cited 2023 Sep 14]. Available from: https://www.creativebiolabs.net/Blontuvetmab-67643.htm

277.   Jain S, Aresu L, Comazzi S, Shi J, Worrall E, Clayton J, et al. The Development of a Recombinant scFv Monoclonal Antibody Targeting Canine CD20 for Use in Comparative Medicine. PLoS One. 2016;11[2]:e0148366.

278.   Arun SS, Breuer W, Hermanns W. Immunohistochemical Examination of Light-chain Expression (Λ/ k Ratio) in Canine, Feline, Equine, Bovine and Porcine Plasma Cells. Journal of Veterinary Medicine Series A. 1996 Feb 12;43[1–10]:573–6.

279.   Gion WR, Davis-Taber RA, Regier DA, Fung E, Medina L, Santora LC, et al. Expression of antibodies using single open reading frame (sORF) vector design. MAbs. 2013 Jul 1;5[4]:595–607.

280.   Fuchs SP, Martinez-Navio JM, Gao G, Desrosiers RC. Recombinant AAV Vectors for Enhanced Expression of Authentic IgG. PLoS One. 2016 Jun 22;11[6]:e0158009.

281.   Ju HL, Calvisi DF, Moon H, Baek S, Ribback S, Dombrowski F, et al. Transgenic mouse model expressing P53R172H, luciferase, EGFP, and KRASG12D in a single open reading frame for live imaging of tumor. Sci Rep. 2015 Jan 27;5:8053.

282.   Platisa J, Vasan G, Yang A, Pieribone VA. Directed Evolution of Key Residues in Fluorescent Protein Inverses the Polarity of Voltage Sensitivity in the Genetically Encoded Indicator ArcLight. ACS Chem Neurosci. 2017 Mar 15;8[3]:513–23.

283.   Szymczak-Workman AL, Vignali KM, Vignali DAA. Design and Construction of 2A Peptide-Linked Multicistronic Vectors. Cold Spring Harb Protoc. 2012 Feb 1;2012[2]:pdb.ip067876.

284.   Chng J, Wang T, Nian R, Lau A, Hoi KM, Ho SC, et al. Cleavage efficient 2A peptides for high level monoclonal antibody expression in CHO cells. mAbs. 2015 Mar 4;7[2]:403–12.

285.   Braganza A, Wallace K, Pell L, Parrish CR, Siegel DL, Mason NJ. Generation and validation of canine single chain variable fragment phage display libraries. Veterinary Immunology and Immunopathology. 2011 Jan 1;139[1]:27–40.

286.   Hwang MH, Darzentas N, Bienzle D, Moore PF, Morrison J, Keller SM. Characterization of the canine immunoglobulin heavy chain repertoire by next generation sequencing. Vet Immunol Immunopathol. 2018 Aug;202:181–90.

287. Aresu L, Ferraresso S, Marconato L, Cascione L, Napoli S, Gaudio E, et al. New molecular and therapeutic insights into canine diffuse large B-cell lymphoma elucidates the role of the dog as a model for human disease. Haematologica. 2019 Jun;104[6]:e256–9.

288. Smakaj E, Babrak L, Ohlin M, Shugay M, Briney B, Tosoni D, et al. Benchmarking immunoinformatic tools for the analysis of antibody repertoire sequences. Bioinformatics (Oxford, England). 2019 Dec 24;36.

289. Fraczkiewicz R, Braun W. Exact and Efficient Analytical Calculation of the Accessible Surface Areas and Their Gradients for Macromolecules. JOURNAL OF COMPUTATIONAL CHEMISTRY. 19[3].

290. Leem J, Dunbar J, Georges G, Shi J, Deane CM. ABodyBuilder: Automated antibody structure prediction with data–driven accuracy estimation. mAbs. 2016 Oct 2;8[7]:1259–68.

291. Kozakov D, Brenke R, Comeau SR, Vajda S. PIPER: an FFT-based protein docking program with pairwise potentials. Proteins. 2006 Nov 1;65[2]:392–406.

292. Xue LC, Rodrigues JP, Kastritis PL, Bonvin AM, Vangone A. PRODIGY: a web server for predicting the binding affinity of protein–protein complexes. Bioinformatics. 2016 Dec 1;32[23]:3676–8.

293. Kim KJ, Kim HE, Lee KH, Han W, Yi MJ, Jeong J, et al. Two-promoter vector is highly efficient for overproduction of protein complexes. Protein Sci. 2004 Jun;13[6]:1698–703.

294. Haryadi R, Ho S, Kok YJ, Pu HX, Zheng L, Pereira NA, et al. Optimization of Heavy Chain and Light Chain Signal Peptides for High Level Expression of Therapeutic Antibodies in CHO Cells. PLoS One. 2015 Feb 23;10[2]:e0116878.

295. Liu Z, Chen O, Wall JBJ, Zheng M, Zhou Y, Wang L, et al. Systematic comparison of 2A peptides for cloning multi-genes in a polycistronic vector. Sci Rep. 2017 May 19;7:2193.

296. Guest JD, Vreven T, Zhou J, Moal I, Jeliazkov JR, Gray JJ, et al. An expanded benchmark for antibody-antigen docking and affinity prediction reveals insights into antibody recognition determinants. Structure. 2021 Jun;29[6]:606-621.e5.

297. Kempen M van, Kim SS, Tumescheit C, Mirdita M, Söding J, Steinegger M. Foldseek: fast and accurate protein structure search [Internet]. bioRxiv; 2022 [cited 2023 Oct 4]. p. 2022.02.07.479398. Available from: https://www.biorxiv.org/content/10.1101/2022.02.07.479398v2

298. Tang L, Sampson C, Dreitz MJ, McCall C. Cloning and characterization of cDNAs encoding four different canine immunoglobulin gamma chains. Vet Immunol Immunopathol. 2001 Aug 10;80[3–4]:259–70.

299. Sayers EW, Bolton EE, Brister JR, Canese K, Chan J, Comeau DC, et al. Database resources of the National Center for Biotechnology Information. Nucleic Acids Res. 2021 Dec 1;50[D1]:D20–6.

300. Sievers F, Wilm A, Dineen D, Gibson TJ, Karplus K, Li W, et al. Fast, scalable generation of high-quality protein multiple sequence alignments using Clustal Omega. Mol Syst Biol. 2011 Oct 11;7:539.

301. Waterhouse AM, Procter JB, Martin DMA, Clamp M, Barton GJ. Jalview Version 2—a multiple sequence alignment editor and analysis workbench. Bioinformatics. 2009 May 1;25[9]:1189–91.

302. Crooks GE, Hon G, Chandonia JM, Brenner SE. WebLogo: A Sequence Logo Generator.

303. Dagona AG. BioEdit: a user-friendly biological sequence alignment editor and analysis program for Windows 95/98/NT. Nucleic acids symposium series [Internet]. 1999 Jan 1 [cited 2023 Sep 19]; Available from: https://www.academia.edu/2034992/BioEdit_a_user_friendly_biological_sequence _alignment_editor_and_analysis_program_for_Windows_95_98_NT

304. Brochet X, Lefranc MP, Giudicelli V. IMGT/V-QUEST: the highly customized and integrated system for IG and TR standardized V-J and V-D-J sequence analysis. Nucleic Acids Res. 2008 Jul 1;36[Web Server issue]:W503-508.

305. Mirsky A, Kazandjian L, Anisimova M. Antibody-Specific Model of Amino Acid Substitution for Immunological Inferences from Alignments of Antibody Sequences. Mol Biol Evol. 2015 Mar;32[3]:806–19.

306. PhD AZ. Forbes. [cited 2023 Sep 3]. AI In Big Pharma: The First Antibody Designed Using AI In The Clinic. Available from: https://www.forbes.com/sites/alexzhavoronkov/2022/12/21/ai-in-big-pharma-the-first-antibody-designed-using-ai-in-the-clinic/

307. GPT Language Model Spells Out New Proteins - IEEE Spectrum [Internet]. [cited 2023 Sep 3]. Available from: https://spectrum.ieee.org/gpt-2-language-model-proteins

308. Madani A, Krause B, Greene ER, Subramanian S, Mohr BP, Holton JM, et al. Large language models generate functional protein sequences across diverse families. Nat Biotechnol. 2023 Aug;41[8]:1099–106.

309. Ruffolo JA, Chu LS, Mahajan SP, Gray JJ. Fast, accurate antibody structure prediction from deep learning on massive set of natural antibodies [Internet]. bioRxiv; 2022 [cited 2023 Sep 3]. p. 2022.04.20.488972. Available from: https://www.biorxiv.org/content/10.1101/2022.04.20.488972v1

310. Ruffolo JA, Sulam J, Gray JJ. Antibody structure prediction using interpretable deep learning. Patterns. 2022 Feb;3[2]:100406.

311. Watson JL, Juergens D, Bennett NR, Trippe BL, Yim J, Eisenach HE, et al. Broadly applicable and accurate protein design by integrating structure prediction

networks and diffusion generative models [Internet]. bioRxiv; 2022 [cited 2023 Sep 3]. p. 2022.12.09.519842. Available from: https://www.biorxiv.org/content/10.1101/2022.12.09.519842v1

312. AlphaFold and beyond. Nat Methods. 2023 Feb;20[2]:163–163.

313. Janda A, Bowen A, Greenspan NS, Casadevall A. Ig Constant Region Effects on Variable Region Structure and Function. Front Microbiol. 2016 Feb 4;7:22.

314. Torres M, Fernaéndez-Fuentes N, Fiser A, Casadevall A. The Immunoglobulin Heavy Chain Constant Region Affects Kinetic and Thermodynamic Parameters of Antibody Variable Region Interactions with Antigen *. Journal of Biological Chemistry. 2007 May 4;282[18]:13917–27.

315. Bojko M, Węgrzyn K, Sikorska E, Kocikowski M, Parys M, Battin C, et al. Design, synthesis and biological evaluation of PD-1 derived peptides as inhibitors of PD-1/PD-L1 complex formation for cancer therapy. Bioorganic Chemistry. 2022 Nov;128:106047.

316. Wilson G, Bryan J, Cranston K, Kitzes J, Nederbragt L, Teal TK. Good enough practices in scientific computing. Ouellette F, editor. PLoS Comput Biol. 2017 Jun 22;13[6]:e1005510.

317. Chiang EY, Mellman I. TIGIT-CD226-PVR axis: advancing immune checkpoint blockade for cancer immunotherapy. J Immunother Cancer. 2022 Apr;10[4]:e004711.

318. Butte MJ, Peña-Cruz V, Kim MJ, Freeman GJ, Sharpe AH. Interaction of human PD-L1 and B7-1. Molecular Immunology. 2008 Aug;45[13]:3567–72.

319. Flies DB, Han X, Higuchi T, Zheng L, Sun J, Ye JJ, et al. Coinhibitory receptor PD-1H preferentially suppresses CD4+ T cell–mediated immunity. J Clin Invest. 2014 May 1;124[5]:1966–75.

320. Brooks AG, Posch PE, Scorzelli CJ, Borrego F, Coligan JE. NKG2A Complexed with CD94 Defines a Novel Inhibitory Natural Killer Cell Receptor. The Journal of Experimental Medicine. 1997 Feb 17;185[4]:795–800.

321. Ponce De León C, Lorite P, López-Casado MÁ, Barro F, Palomeque T, Torres MI. Significance of PD1 Alternative Splicing in Celiac Disease as a Novel Source for Diagnostic and Therapeutic Target. Front Immunol. 2021 Jun 16;12:678400.

322. Ding L, Odunsi K. RNA Splicing and Immune-Checkpoint Inhibition. Phimister EG, editor. N Engl J Med. 2021 Nov 4;385[19]:1807–9.

323. Yao H, Wang H, Li C, Fang JY, Xu J. Cancer Cell-Intrinsic PD-1 and Implications in Combinatorial Immunotherapy. Front Immunol. 2018 Jul 30;9:1774.

324. Zhou XM, Li WQ, Wu YH, Han L, Cao XG, Yang XM, et al. Intrinsic Expression of Immune Checkpoint Molecule TIGIT Could Help Tumor Growth in vivo by Suppressing the Function of NK and CD8+ T Cells. Front Immunol. 2018 Nov 29;9:2821.

325. Tsai TY, Huang MT, Sung PS, Peng CY, Tao MH, Yang HI, et al. SIGLEC-3 (CD33) serves as an immune checkpoint receptor for HBV infection. Journal of Clinical Investigation. 2021 Jun 1;131[11]:e141965.

326. Fridman WH, Petitprez F, Meylan M, Chen TWW, Sun CM, Roumenina LT, et al. B cells and cancer: To B or not to B? Journal of Experimental Medicine. 2021 Jan 4;218[1]:e20200851.

327. Laumont CM, Nelson BH. B cells in the tumor microenvironment: Multi-faceted organizers, regulators, and effectors of anti-tumor immunity. Cancer Cell. 2023 Mar;41[3]:466–89.

328. Thibult ML, Mamessier E, Gertner-Dardenne J, Pastor S, Just-Landi S, Xerri L, et al. PD-1 is a novel regulator of human B-cell activation. International Immunology. 2013 Feb;25[2]:129–37.

329. Albanesi M, Mancardi DA, Jönsson F, Iannascoli B, Fiette L, Di Santo JP, et al. Neutrophils mediate antibody-induced antitumor effects in mice. Blood. 2013 Oct 31;122[18]:3160–4.

330. Neutrophils Are Critical to the Effectiveness of Cancer Immunotherapy. Cancer Discovery. 2023 Jun 2;13[6]:1285.

331. Gungabeesoon J, Gort-Freitas NA, Kiss M, Bolli E, Messemaker M, Siwicki M, et al. A neutrophil response linked to tumor control in immunotherapy. Cell. 2023 Mar;186[7]:1448-1464.e20.

332. Shin JH, Jeong J, Maher SE, Lee HW, Lim J, Bothwell ALM. Colon cancer cells acquire immune regulatory molecules from tumor-infiltrating lymphocytes by trogocytosis. Proc Natl Acad Sci USA. 2021 Nov 30;118[48]:e2110241118.

333. Dyson FJ. Birds and frogs in mathematics and physics. Phys-Usp. 2010 Nov 15;53[8]:825–34.

334. Fundytus A, Sengar M, Lombe D, Hopman W, Jalink M, Gyawali B, et al. Access to cancer medicines deemed essential by oncologists in 82 countries: an international, cross-sectional survey. The Lancet Oncology. 2021 Oct;22[10]:1367–77.

335. Rodriguez I, Kocik-Krol J, Skalniak L, Musielak B, Wisniewska A, Ciesiołkiewicz A, et al. Structural and biological characterization of pAC65, a macrocyclic peptide that blocks PD-L1 with equivalent potency to the FDA-approved antibodies. Molecular Cancer [Internet]. 2023 [cited 2023 Sep 14];22[1]. Available from: https://link.springer.com/epdf/10.1186/s12943-023-01853-4

336. ISRCTN - ISRCTN17572332: Phase I Trial, Quotient code: QSC203717 [Internet]. [cited 2023 Sep 14]. Available from: https://www.isrctn.com/ISRCTN17572332

337. Bristol-Myers Squibb. Randomized, Double-Blinded, Placebo-Controlled, Single Ascending Dose Study to Evaluate the Pharmacokinetics, Safety, Tolerability and Pharmacodynamics of BMS-986189 in Healthy Subjects [Internet].

clinicaltrials.gov; 2018 Feb [cited 2023 Sep 14]. Report No.: NCT02739373. Available from: https://clinicaltrials.gov/study/NCT02739373

338. Coin I, Beyermann M, Bienert M. Solid-phase peptide synthesis: from standard procedures to the synthesis of difficult sequences. Nat Protoc. 2007 Dec;2[12]:3247–56.

339. Minchinton AI, Tannock IF. Drug penetration in solid tumours. Nat Rev Cancer. 2006 Aug;6[8]:583–92.

340. Grantab RH, Tannock IF. Penetration of anticancer drugs through tumour tissue as a function of cellular packing density and interstitial fluid pressure and its modification by bortezomib. BMC Cancer. 2012 Dec;12[1]:214.

341. Choi IK, Strauss R, Richter M, Yun CO, Lieber A. Strategies to Increase Drug Penetration in Solid Tumors. Front Oncol [Internet]. 2013 [cited 2023 Sep 3];3. Available from: http://journal.frontiersin.org/article/10.3389/fonc.2013.00193/abstract

342. Thurber GM, Schmidt MM, Wittrup KD. Antibody tumor penetration: Transport opposed by systemic and antigen-mediated clearance. Advanced Drug Delivery Reviews. 2008 Sep;60[12]:1421–34.

343. Sasikumar PG, Ramachandra M. Small-Molecule Immune Checkpoint Inhibitors Targeting PD-1/PD-L1 and Other Emerging Checkpoint Pathways. BioDrugs. 2018 Oct;32[5]:481–97.

344. Liu N, Zhang R, Shi Q, Jiang H, Zhou Q. Intelligent delivery system targeting PD-1/PD-L1 pathway for cancer immunotherapy. Bioorganic Chemistry. 2023 Jul;136:106550.

345. Patwardhan GA, Marczyk M, Wali VB, Stern DF, Pusztai L, Hatzis C. Treatment scheduling effects on the evolution of drug resistance in heterogeneous cancer cell populations. npj Breast Cancer. 2021 May 26;7[1]:60.

346. Tzamali E, Tzedakis G, Sakkalis V. Modeling How Heterogeneity in Cell Cycle Length Affects Cancer Cell Growth Dynamics in Response to Treatment. Front Oncol. 2020 Sep 10;10:1552.

347. Harris LA, Beik S, Ozawa PMM, Jimenez L, Weaver AM. Modeling heterogeneous tumor growth dynamics and cell–cell interactions at single-cell and cell-population resolution. Current Opinion in Systems Biology. 2019 Oct;17:24–34.

348. Meaney C, Kohandel M, Novruzi A. Temporal optimization of radiation therapy to heterogeneous tumour populations and cancer stem cells. J Math Biol. 2022 Nov;85[5]:51.

349. Sasikumar PG, Sudarshan NS, Adurthi S, Ramachandra RK, Samiulla DS, Lakshminarasimhan A, et al. PD-1 derived CA-170 is an oral immune checkpoint inhibitor that exhibits preclinical anti-tumor efficacy. Commun Biol. 2021 Jun 8;4[1]:699.

350. Huber V, Camisaschi C, Berzi A, Ferro S, Lugini L, Triulzi T, et al. Cancer acidity: An ultimate frontier of tumor immune escape and a novel target of immunomodulation. Semin Cancer Biol. 2017 Apr;43:74–89.

351. Kinder M, Greenplate AR, Grugan KD, Soring KL, Heeringa KA, McCarthy SG, et al. Engineered protease-resistant antibodies with selectable cell-killing functions. J Biol Chem. 2013 Oct 25;288[43]:30843–54.

352. Igawa T, Ishii S, Tachibana T, Maeda A, Higuchi Y, Shimaoka S, et al. Antibody recycling by engineered pH-dependent antigen binding improves the duration of antigen neutralization. Nat Biotechnol. 2010 Nov;28[11]:1203–7.

353. Traxlmayr MW, Lobner E, Hasenhindl C, Stadlmayr G, Oostenbrink C, Rüker F, et al. Construction of pH-sensitive Her2-binding IgG1-Fc by directed evolution. Biotechnol J. 2014 Aug;9[8]:1013–22.

354. Koopmans I, Samplonius DF, Ginkel RJ van, Wierstra PJ, Heskamp S, Bremer E, et al. Abstract 4553: A novel bispecific antibody for EGFR-directed blockade of the PD-1/PD-L1 immune checkpoint. Cancer Research. 2018 Jul 1;78[13_Supplement]:4553.

355. Huehls AM, Coupet TA, Sentman CL. Bispecific T-cell engagers for cancer immunotherapy. Immunol Cell Biol. 2015 Mar;93[3]:290–6.

356. Toloue MM, Ford LP. Antibody targeted siRNA delivery. Methods Mol Biol. 2011;764:123–39.

357. Diamantis N, Banerji U. Antibody-drug conjugates--an emerging class of cancer treatment. Br J Cancer. 2016 Feb 16;114[4]:362–7.

358. Herron LR, Pridans C, Turnbull ML, Smith N, Lillico S, Sherman A, et al. A chicken bioreactor for efficient production of functional cytokines. BMC Biotechnology. 2018 Dec 29;18[1]:82.

359. Marasco WA. Therapeutic antibody gene transfer. Nat Biotechnol. 2005 May;23[5]:551–2.

360. Griesenbach U, McLachlan G, Owaki T, Somerton L, Shu T, Baker A, et al. Validation of recombinant Sendai virus in a non-natural host model. Gene Ther. 2011 Feb;18[2]:182–8.

361. Zitvogel L, Galluzzi L, Viaud S, Vétizou M, Daillère R, Merad M, et al. Cancer and the gut microbiota: An unexpected link. Sci Transl Med [Internet]. 2015 Jan 21 [cited 2023 Sep 3];7[271]. Available from: https://www.science.org/doi/10.1126/scitranslmed.3010473

362. Poore GD, Kopylova E, Zhu Q, Carpenter C, Fraraccio S, Wandro S, et al. Microbiome analyses of blood and tissues suggest cancer diagnostic approach. Nature. 2020 Mar 26;579[7800]:567–74.

363. Sepich-Poore GD, Guccione C, Laplane L, Pradeu T, Curtius K, Knight R. Cancer's second genome: Microbial cancer diagnostics and redefining clonal

evolution as a multispecies process: Humans and their tumors are not aseptic, and the multispecies nature of cancer modulates clinical care and clonal evolution. BioEssays. 2022 May;44[5]:2100252.

364. Pushalkar S, Hundeyin M, Daley D, Zambirinis CP, Kurz E, Mishra A, et al. The Pancreatic Cancer Microbiome Promotes Oncogenesis by Induction of Innate and Adaptive Immune Suppression. Cancer Discovery. 2018 Apr 1;8[4]:403–16.

365. Eriksson F, Tsagozis P, Lundberg K, Parsa R, Mangsbo SM, Persson MAA, et al. Tumor-Specific Bacteriophages Induce Tumor Destruction through Activation of Tumor-Associated Macrophages. The Journal of Immunology. 2009 Mar 1;182[5]:3105–11.

366. Ng KW, Boumelha J, Enfield KSS, Almagro J, Cha H, Pich O, et al. Antibodies against endogenous retroviruses promote lung cancer immunotherapy. Nature. 2023 Apr 20;616[7957]:563–73.

367. Jha AR, Nixon DF, Rosenberg MG, Martin JN, Deeks SG, Hudson RR, et al. Human Endogenous Retrovirus K106 (HERV-K106) Was Infectious after the Emergence of Anatomically Modern Humans. Hendricks M, editor. PLoS ONE. 2011 May 25;6[5]:e20234.

368. Junk DNA - Wikipedia [Internet]. [cited 2023 Sep 3]. Available from: https://en.wikipedia.org/wiki/Junk_DNA

369. Belshaw R, Pereira V, Katzourakis A, Talbot G, Pačes J, Burt A, et al. Long-term reinfection of the human genome by endogenous retroviruses. Proc Natl Acad Sci USA. 2004 Apr 6;101[14]:4894–9.

370. Saini SK, Ørskov AD, Bjerregaard AM, Unnikrishnan A, Holmberg-Thydén S, Borch A, et al. Human endogenous retroviruses form a reservoir of T cell targets in hematological cancers. Nat Commun. 2020 Nov 9;11[1]:5660.

371. Liu X, Liu Z, Wu Z, Ren J, Fan Y, Sun L, et al. Resurrection of endogenous retroviruses during aging reinforces senescence. Cell. 2023 Jan;186[2]:287-304.e26.

372. Jansz N, Faulkner GJ. Endogenous retroviruses in the origins and treatment of cancer. Genome Biol. 2021 May 10;22[1]:147.

373. Vergara Bermejo A, Ragonnaud E, Daradoumis J, Holst P. Cancer Associated Endogenous Retroviruses: Ideal Immune Targets for Adenovirus-Based Immunotherapy. IJMS. 2020 Jul 8;21[14]:4843.

374. Hargreaves AD, Zhou L, Christensen J, Marlétaz F, Liu S, Li F, et al. Genome sequence of a diabetes-prone rodent reveals a mutation hotspot around the ParaHox gene cluster. Proc Natl Acad Sci USA. 2017 Jul 18;114[29]:7677–82.

375. Ebbert MTW, Jensen TD, Jansen-West K, Sens JP, Reddy JS, Ridge PG, et al. Systematic analysis of dark and camouflaged genes reveals disease-relevant genes hiding in plain sight. Genome Biol. 2019 Dec;20[1]:97.

376. Robert C, Watson M. Errors in RNA-Seq quantification affect genes of relevance to human disease. Genome Biol. 2015 Dec;16[1]:177.

377. Chen YC, Liu T, Yu CH, Chiang TY, Hwang CC. Effects of GC Bias in Next-Generation-Sequencing Data on De Novo Genome Assembly. Xu Y, editor. PLoS ONE. 2013 Apr 29;8[4]:e62856.

378. Lovell PV, Wirthlin M, Wilhelm L, Minx P, Lazar NH, Carbone L, et al. Conserved syntenic clusters of protein coding genes are missing in birds. Genome Biol. 2014 Dec;15[12]:565.

379. Hron T, Pajer P, Pačes J, Bartůněk P, Elleder D. Hidden genes in birds. Genome Biol. 2015 Dec;16[1]:164.

380. Mescon H, Eiman JW, Kligman AM. Fungi in human neoplastic tissue. Cancer Res. 1953 May;13[4–5]:318–20.

381. Mescon H, Eiman JW, Kligman AM. Investigation for the presence of fungi in human neoplastic tissues. Am J Pathol. 1951 Aug;27[4]:739–40.

382. Zong Z, Zhou F, Zhang L. The fungal mycobiome: a new hallmark of cancer revealed by pan-cancer analyses. Sig Transduct Target Ther. 2023 Feb 1;8[1]:50.

383. Shiao SL, Kershaw KM, Limon JJ, You S, Yoon J, Ko EY, et al. Commensal bacteria and fungi differentially regulate tumor responses to radiation therapy. Cancer Cell. 2021 Sep;39[9]:1202-1213.e6.

384. Narunsky-Haziza L, Sepich-Poore GD, Livyatan I, Asraf O, Martino C, Nejman D, et al. Pan-cancer analyses reveal cancer-type-specific fungal ecologies and bacteriome interactions. Cell. 2022 Sep;185[20]:3789-3806.e17.

385. Aykut B, Pushalkar S, Chen R, Li Q, Abengozar R, Kim JI, et al. The fungal mycobiome promotes pancreatic oncogenesis via activation of MBL. Nature. 2019 Oct 10;574[7777]:264–7.

386. Blackwell M. The Fungi: 1, 2, 3 … 5.1 million species? American Journal of Botany. 2011 Mar;98[3]:426–38.

387. Yokoo H, Oshima T. Is bacteriophage φX174 DNA a message from an extraterrestrial intelligence? Icarus. 1979 Apr;38[1]:148–53.

388. Newman DJ, Cragg GM. Natural Products as Sources of New Drugs from 1981 to 2014. J Nat Prod. 2016 Mar 25;79[3]:629–61.

389. Davis C, Naci H, Gurpinar E, Poplavska E, Pinto A, Aggarwal A. Availability of evidence of benefits on overall survival and quality of life of cancer drugs approved by European Medicines Agency: retrospective cohort study of drug approvals 2009-13. BMJ. 2017 Oct 4;j4530.

390. Walker AA, Robinson SD, Yeates DK, Jin J, Baumann K, Dobson J, et al. Entomo-venomics: The evolution, biology and biochemistry of insect venoms. Toxicon. 2018 Nov;154:15–27.

391.   Piper R. The Conversation. 2017 [cited 2023 Sep 3]. Drugs from bugs: the next blockbuster medicine could be lurking inside an insect. Available from: http://theconversation.com/drugs-from-bugs-the-next-blockbuster-medicine-could-be-lurking-inside-an-insect-71831

392.   Katz L, Baltz RH. Natural product discovery: past, present, and future. Journal of Industrial Microbiology and Biotechnology. 2016 Mar 1;43[2–3]:155–76.

393.   Kote S, Faktor J, Dapic I, Mayordomo MY, Kocikowski M, Kagansky A, et al. Analysis of venom sac constituents from the solitary, aculeate wasp Cerceris rybyensis. Toxicon. 2019 Nov;169:1–4.

394.   Neergheen-Bhujun V, Awan AT, Baran Y, Bunnefeld N, Chan K, Dela Cruz TE, et al. Biodiversity, drug discovery, and the future of global health: Introducing the biodiversity to biomedicine consortium, a call to action. Journal of Global Health. 2017 Dec;7[2]:020304.

395.   Linhares Y, Kaganski A, Agyare C, Kurnaz IA, Neergheen V, Kolodziejczyk B, et al. Biodiversity: the overlooked source of human health. Trends in Molecular Medicine. 2023 Mar;29[3]:173–87.

396.   Paterson R, Lima N, editors. Bioprospecting: Success, Potential and Constraints [Internet]. Cham: Springer International Publishing; 2017 [cited 2023 Sep 3]. [Topics in Biodiversity and Conservation; vol. 16]. Available from: http://link.springer.com/10.1007/978-3-319-47935-4

397.   Peng X, Chen M, Chen S, Dasgupta S, Xu H, Ta K, et al. Microplastics contaminate the deepest part of the world's ocean. Geochem Persp Let. 2018 Nov;1–5.

398.   Jamieson AJ, Brooks LSR, Reid WDK, Piertney SB, Narayanaswamy BE, Linley TD. Microplastics and synthetic particles ingested by deep-sea amphipods in six of the deepest marine ecosystems on Earth. R Soc open sci. 2019 Feb;6[2]:180667.

399.   Cózar A, Echevarría F, González-Gordillo JI, Irigoien X, Úbeda B, Hernández-León S, et al. Plastic debris in the open ocean. Proc Natl Acad Sci USA. 2014 Jul 15;111[28]:10239–44.

400.   La Merrill MA, Vandenberg LN, Smith MT, Goodson W, Browne P, Patisaul HB, et al. Consensus on the key characteristics of endocrine-disrupting chemicals as a basis for hazard identification. Nat Rev Endocrinol. 2020 Jan;16[1]:45–57.

401.   O'Connor JC, Chapin RE. Critical evaluation of observed adverse effects of endocrine active substances on reproduction and development, the immune system, and the nervous system. Pure and Applied Chemistry. 2003 Jan 1;75[11–12]:2099–123.

402.   Okada H, Tokunaga T, Liu X, Takayanagi S, Matsushima A, Shimohigashi Y. Direct Evidence Revealing Structural Elements Essential for the High Binding Ability of Bisphenol A to Human Estrogen-Related Receptor-γ. Environ Health Perspect. 2008 Jan;116[1]:32–8.

403. Buck Louis GM, Sundaram R, Sweeney AM, Schisterman EF, Maisog J, Kannan K. Urinary bisphenol A, phthalates, and couple fecundity: the Longitudinal Investigation of Fertility and the Environment (LIFE) Study. Fertility and Sterility. 2014 May;101[5]:1359–66.

404. Kempers RD. The Tricentennial of the Discovery of Sperm. Fertility and Sterility. 1976 May;27[5]:603–5.

405. Gadêlha H, Hernández-Herrera P, Montoya F, Darszon A, Corkidi G. Human sperm uses asymmetric and anisotropic flagellar controls to regulate swimming symmetry and cell steering. Sci Adv. 2020 Jul 31;6[31]:eaba5168.

8. APPENDICES

8.1 For the fellow student

8.1.1 Tool idiosyncrasies

In the process of performing this study I have encountered and reported errors in several tools and resources. These included:

Ensembl canine reference genome/transcriptome

As discussed in detail in the supplementary section of my first experimental chapter, I have identified the CPA3 gene locus that appeared to be mis-described, leading to confusing RNAseq results. Caution is advised when interpreting data based on such experiments, and choosing newer reference versions as they appear may be the best choice.

EBI Expression Atlas

For the analysis conducted in my first experimental chapter, I calculated gene expression averages for various cancer types. The data for individual patients were sourced from the International Cancer Genome Project's Pan-Cancer Analysis of Whole Genomes (PCAWG) dataset, which is publicly available on the EBI website. This dataset is offered both at the level of individual cancer types and individual patients. However, I noticed that the website did not indicate whether the provided values for each cancer type were means or medians. Upon further investigation, I found these values to be close to medians, but not exact. For those seeking to conduct similar analyses, it is recommended to calculate your own averages when utilizing this dataset.

PCAtools package in R

For those interested in principal component analysis, I employed both the base R PCA function and functionalities from the PCAtools optional package when working on my initial experimental chapter. While the default calculations from both yielded identical

results, I encountered discrepancies in visualization. Certain plots generated by PCAtools appeared to misrepresent the data and be misalign with plots I crafted using ggplot. Despite delving into the package's source code and exhaustively exploring its functionalities, I was unable to reconcile these inconsistencies. As of this writing, I have yet to receive a response from the package maintainers regarding this issue. Given these experiences, I would advise caution when considering the use of PCAtools, despite its appealing pre-constructed visualization features.

Promega's CellTiter Glo reagent

In the course of my second experimental chapter, I made extensive efforts to quantify lymphocyte proliferation utilizing Promega's CellTiter Glo reagent. Typically, the cells under investigation originated from the PBMC (Peripheral Blood Mononuclear Cells) fraction of blood. Despite rigorously adhering to recommended best practices and undertaking comprehensive optimization, the replicates were consistently displaying extreme variation, rendering any subsequent analysis unfeasible. It's noteworthy that I was not alone in encountering this issue. Although I have in the end received a response from Promega's customer service it did not provide a resolution. This is not to suggest the reagent is of poor quality. Rather, it may not be universally applicable to all cell types, or it may be that PBMCs cannot be reliably plated for such an assay. For additional insights into this issue, you may refer to a discussion on ResearchGate: researchgate.net/post/Horrible_variation_between_replicates_with_Cell_Titer_Glo#view=64ca8ea7880092850f0674f7

Schrodinger's Bioluminate software suite

For my third experimental chapter, I underwent commercial training by Schrodinger company for their software suite, specifically the online version. Afterwards, I tried running their Bioluminate protein engineering software on my computer. While I was able to launch the program, numerous features were either inoperative or led to severe errors. Despite having more than adequate hardware resources, and despite the commendable time investment of Schrodinger's team spanning several weeks, we were not able to make the software fully functional under Windows 10. It's worth noting

that newer versions of the software might not exhibit these issues. Alternatively, the software can be run in Linux environment, where it should be more stable.

8.1.2 Is R for reproducibility?

Stepping into the world of data analysis with R is an exciting journey. As you explore, you will discover many packages providing utilities for specific research branches. However, be aware that while powerful, they are not without their quirks and challenges. They are continuously evolving, which can occasionally lead to painful surprises (see: datacolada.org/95 and datacolada.org/100). As a beginner bioinformatician, I've faced these obstacles, and I hope that sharing some of my notes can help you navigate your own path more smoothly.

One crucial aspect of each scientific analysis is reproducibility. In the context of coding the concept is straightforward: anyone (including your future self) should be able to run your code and achieve the same results. In practice, due to updates and modifications in R and its packages, reproducibility can become an issue. Subtle changes in the behavior of functions can lead to unexpected errors or changes in output. At times, I found myself reinstalling R, RStudio, and all packages manually, or even modifying the code substantially just to keep it functional.

Also, the interaction between different R packages can be tricky. An update required by one package can inadvertently disrupt another, leading to a scenario dubbed 'dependency hell'. This can lead to a cycle of continuous fixing and updating, consuming significant time that could be spent on actual science. Fortunately, there are some strategies and tools to navigate these challenges:

1. Version Control: Make a habit of recording the versions of R and any packages you're using. This will help recreate the same environment if needed in the future. Example code snippet below.
2. R Environment Management: Consider using packages like **renv** in R. **renv** allows you to isolate your project's environment and keeps track of package versions, increasing the reproducibility of your work.
3. Containerization: For more complex projects, tools like Docker or Singularity can provide a way to create a snapshot of your computational environment,

226

though this might be an overkill for simpler projects and for projects in development.

4. Reportedly, R can be replaced with Python in most data analysis applications. If you're contemplating using Python as an alternative, this is what I've learned: Python shares some challenges with R, particularly around package dependencies. But it also offers solutions like virtual environments (**venv** or **conda**) that allow for isolating the environment for each project, and **pip freeze** to capture package version.

```r
#Exporting version information for directly loaded packages and their
dependencies.

# Function to get all dependencies
get_all_dependencies <- function(pkg) {
  deps <- unclass(tools::package_dependencies(pkg, recursive=TRUE))
  return(deps[[1]])
}

# Use the function for your packages
my_packages <- c("ggplot2", "dplyr", "tidyverse")

# Get dependencies
all_deps <- unlist(lapply(my_packages, get_all_dependencies))

# Remove duplicates - reducing redundant operations
unique_deps <- unique(all_deps)

# Get versions for all packages (your packages + dependencies)
all_pkgs <- c(my_packages, unique_deps)

# Initialize a data frame to store package versions
pkg_versions <- data.frame(package=character(), version=character())


# Loop over all packages and get versions;
for (pkg in all_pkgs) {
  version <- ifelse(requireNamespace(pkg, quietly = TRUE),
    tryCatch({
      as.character(packageVersion(pkg))
    }, error=function(e) NA), # Packages with "NA" version = corrupt or
not installed - likely "suggests" class dependency
    "Not installed"
  )

  pkg_versions <- rbind(pkg_versions, data.frame(package=pkg,
version=version))
}


# Remove duplicates based on both package and version
pkg_versions <- pkg_versions[!duplicated(pkg_versions), ]
```

```
# Write the data frame to a CSV file
write.csv(pkg_versions, file="./OUTPUT/20230624_Package_Versions.csv",
row.names=FALSE)
```

I would also like to share some suggestions and experiences from my more experienced colleagues. While each individual has their unique set of preferences and practices, their insights can provide additional perspectives to consider:

- Some have found running R in a Jupyter notebook to be quite helpful. This setup is compatible with a **conda** environment, enabling you to work with a GUI/IDE while keeping your project environment isolated.

- Project Management with **Docker**: Docker can be an effective solution for ensuring replicability of finished projects. However, maintaining a Docker recipe file with updates and new packages can be time-consuming.

- Another suggestion is to limit the number of custom libraries used in an R project to minimize issues and improve reproducibility. However, this is not always feasible, as a scientific project should not waste time on re-writing functions that already exist.

- **Nextflow**: This tool aims to aid in managing and organizing computational workflows. It could be worth exploring, though experiences with it may vary.

- Python and **Conda**: If you consider using Python, you can specify strict versions in a requirements.txt file. However, keep in mind that Conda might not always maintain these older versions. Moreover, the availability of older versions tends to be more reliable with **PyPi/Pip** compared to Conda. When using Conda, also consider the channel precedence when the package version matters.

- There is no perfect solution for ensuring reproducibility, especially for projects in development. One needs to stay vigilant.

As a fellow explorer in the world of data analysis, I offer these insights not as instructions, but as friendly suggestions based on my own experiences. Regardless of whether you choose R or Python, encountering and overcoming these and other challenges apparently is part of the learning process.

8.1.3 Scientific reproduction (not that kind)

Reproducibility is at the very heart of the scientific method. If you would like to learn more about it, you will find a lot of materials online searching for "scientific reproducibility" and "replication crisis". What you will find may be disheartening at first but know that there are people out there who care deeply and work tirelessly to "make science great again". You can connect with some of them through your local scientific reproducibility network or society (ukrn.org/international-networks/) and ReproducibiliTea clubs (reproducibilitea.org/). Another direction worth exploring in this theme is "open research practices". And below you will find some great materials.

<u>Key articles</u>

- Munafò, M., Nosek, B., Bishop, D. *et al.* **A manifesto for reproducible science.** *Nat Hum Behav* **1**, 0021 (2017). Doi: 10.1038/s41562-016-0021
- Ioannidis JP. **Why most published research findings are false.** PLoS Med. 2005 Aug;2(8):e124. Doi: 10.1371/journal.pmed.0020124
- Bishop DV. 2017. **Fallibility in science: Responding to errors in the work of oneself and others.** PeerJ Preprints Doi: 10.7287/peerj.preprints.3486v1
- Madsen RR**. Scientific impact and the quest for visibility.** FEBS J. 2019 Doi: 10.1111/febs.15043
- Kerr NL. **HARKing: hypothesizing after the results are known.** Pers Soc Psychol Rev. 1998;2(3):196-217. doi: 10.1207/s15327957pspr0203_4

<u>Interesting articles</u>

- splice-bio.com/**data-detective-exposes-fraud-and-mistakes-in-leading-clinical-trials/**
- science.org/content/article/**meet-data-thugs-out-expose-shoddy-and-questionable-research**
- science.org/content/article/**more-and-more-scientists-are-preregistering-their-studies-should-you**

Other resources

- online.ucpress.edu/collabra/article/7/1/18684/115927/**Easing-Into-Open-Science-A-Guide-for-Graduate**
- youtube.com/c/**riotscienceclub**
- **Everything Hertz** podcast
- **compare-trials.org** - tracking switched outcomes in clinical trials
- **retractionwatch.com –** tracking scientific publication retractions
- **Dance of the p-values**, youtube.com/watch?v=5OL1RqHrZQ8

Interesting tools

- **Statcheck** - check a paper for errors in statistical reporting https://michelenuijten.shinyapps.io/statcheck-web/
- **P-checker**
  https://shinyapps.org/apps/p-checker/

Best of luck in your journey!

9. PUBLICATIONS AND PRESENTATIONS

The following is a list of scientific publications and international presentations I've authored or contributed to during my doctoral studies. While some of the publications are not directly related to the topic of this thesis, they are included to trace the full arc of my academic journey during this period.

Journal Papers

1. J Robert O'Neill, Marcos Yébenes Mayordomo, Goran Mitulović, Sofian Al Shboul, Georges Bedran, Jakub Faktor, Lenka Hernychova, Lukas Uhrik, Maria Gomez-Herranz, **Mikołaj Kocikowski**, Vicki Save, Bořivoj Vojtěšek, Mark Arends, OCCAMS consortium, Ted Hupp, Javier Alfaro. *Multi-omics integration in Esophageal Adenocarcinoma reveals therapeutic targets and EAC-specific regulation of protein abundances*. medRxiv. doi.org/10.1101/2022.11.24.22281691

2. Minoli L*, Licenziato L, **Kocikowski M***, Cino M, Dziubek K, Iussich S, Fanelli A, Morello E, Martano M, Hupp T, Vojtesek B, Parys M, Aresu L. *Development of Monoclonal Antibodies Targeting Canine PD-L1 and PD-1 and Their Clinical Relevance in Canine Apocrine Gland Anal Sac Adenocarcinoma*. Cancers (Basel). 2022 Dec 14;14(24):6188. doi.org/10.3390/cancers14246188, *These authors contributed equally to this work.

3. Bojko M, Węgrzyn K, Sikorska E, **Kocikowski M**, Parys M, Battin C, Steinberger P, Kogut MM, Winnicki M, Sieradzan AK, Spodzieja M, Rodziewicz-Motowidło S. *Design, synthesis and biological evaluation of PD-1 derived peptides as inhibitors of PD-1/PD-L1 complex formation for cancer therapy*. Bioorg Chem. 2022 Nov;128:106047. doi.org/10.1016/j.bioorg.2022.106047

4. Uhrik, L., Hernychova, L., Muller, P., Kalathiya, U., Lisowska, M. **M., Kocikowski**, M., Parys, M., Faktor, J., Nekulova, M., Nortcliffe, C., Zatloukalova, P., Ruetgen, B., Fahraeus, R., Ball, K. L., Argyle, D. J., Vojtesek, B., & Hupp, T. R. (2021). *Hydrogen deuterium exchange mass spectrometry identifies the dominant paratope in CD20 antigen binding to the NCD1.2 monoclonal antibody*. Biochemical Journal, 478(1), 99–120. doi.org/10.1042/BCJ20200674

5. **Kocikowski, M**., Dziubek, K., & Parys, M. (2020). *Hyperprogression Under Immune Checkpoint-Based Immunotherapy-Current Understanding, The Role of PD-1/PD-L1 Tumour-Intrinsic Signalling, Future Directions and a Potential Large Animal Model*. Cancers, 12(4), Article 4. doi.org/10.3390/cancers12040804

6. Kote, S., Faktor, J., Dapic, I., Mayordomo, M. Y., **Kocikowski, M**., Kagansky, A., Goodlett, D., Vojtesek, B., Hupp, T., Wilcockson, D., & Piper, R. (2019*). Analysis of venom sac constituents from the solitary, aculeate wasp Cerceris rybyensis*. Toxicon, 169, 1–4. doi.org/10.1016/j.toxicon.2019.07.012

Conference Presentations

1. **Kocikowski, M**., (2022*). "Of dogs and men. How canines can help cure human cancers";* Science – Polish Perspectives, University of Oxford, Oxford UK.

Conference Posters

1. **Kocikowski, M**., Dziubek, K., Vojtesek, B., Argyle, D., Hupp, T., & Parys, M. (2020). Abstract 2234: *Development of caninized monoclonal antibodies against PD1*. Cancer Research, 80(16 Supplement), 2234–2234. doi.org/10.1158/1538-7445.AM2020-2234, AACR, virtual, USA.

2. Dziubek, K**., Kocikowski, M**., Vojtesek, B., Argyle, D., Lisowska, M., Hupp, T., & Parys, M. (2020). Abstract 5637: *Investigating tumor intrinsic PD-1/PD-L1 signaling in canine osteosarcoma cell lines as a spontaneous model for human disease*. Cancer Research, 80(16 Supplement), 5637–5637. doi.org/10.1158/1538-7445.AM2020-5637, AACR, virtual, USA.

3. Wang, Y.J., Pietrzak, K., **Kocikowski, M**., Argyle, D., Hupp, T., & Parys, M (2019). Abstract 3972: *Investigation of tumor intrinsic PD1/PD-L1 in canine urothelial carcinomas as a spontaneous translational model for human invasive bladder cancer.* Cancer Research, 79 (13_Supplement): 3972. doi.org/10.1158/1538-7445.AM2019-3972, AACR, Atlanta, USA.

4. **Kocikowski, M.M.**, Hupp, T.R., Argyle, D.J. & Parys, M. (2019). *Dogizing Antibodies Against PD1 and CD20.* Mass Spectrometry School in Biotechnology and Medicine, Dubrovnik, Croatia.

5. **Kocikowski, M**. (2023). *Twins. Immune checkpoint transcription patterns of dog and human brain cancers.* Canvas Spring School, Sobieszewo, Poland.